UNIVERSIDAD AUTÓNOMA DE MADRID
FACULTAD DE CIENCIAS
DEPARTAMENTO DE BIOLOGIA MOLECULAR

Regulation of the Meiotic Cell Cycle by CDK/RINGO Complexes

Edgar Josué Ruiz Medina

Thesis Director:
Dr. Angel Rodríguez Nebreda

Centro Nacional de Investigaciones Oncológicas (CNIO), Madrid

ABBREVIATIONS

CAK	CDK-activating kinase
cAMP	adenosine 3‘,5’-cyclic monophosphate
Cdc	cell division cycle
CDK	cyclin-dependent kinase
CHX	cycloheximide
CPE	cytoplasmic polyadenylation element
CPEB	cytoplasmic polyadenylation element-binding factor
C-terminal; C-terminus	carboxyl-terminal; carboxyl-terminus
Cyc A	cyclin A
Cyc B	cyclin B
GST	glutathione-S-transferase
GVBD	germinal vesicle breakdown
H1K	histone H1 kinase
IP	immunoprecipitation
MAPK	mitogen-activated protein kinase
mBarth	modified Barth
MBP	maltose-binding protein
MEK	MAPK kinase
MPF	maturation-promoting factor
N-terminal; N-terminus	amino-terminal; amino-terminus
PAGE	polyacrylamide gel electrophoresis
PKA	cAMP-dependent protein kinase/protein kinase A
PKB	protein kinase B
PP1	phosphatase 1
PP2A	phosphatase 2A
PP2C	phosphatase 2C
XRINGO	*Xenopus* RINGO

ABSTRACT

Cyclin-dependent kinases (CDKs) are a conserved family of Ser/Thr kinases that perform critical roles in regulating the stepwise progression through the eukaryotic cell cycle. The activity of CDKs is regulated through phosphorylation by CDK-activating kinase (CAK) and most significantly by interaction with cyclins. CDK1 and CDK2 can be also activated by non-cyclin proteins named RINGO/Speedy, which were identified as inducers of the G2/M transition in *Xenopus* oocytes. Further work has supported an important regulatory role for XRINGO in meiotic progression, although it is unclear exactly how XRINGO triggers the activation of CDK1/cyclin B complexes that drive oocyte maturation. Since cyclins contribute significantly to the substrate specificity of CDKs, we have investigated potential differences in the substrate specificity of XRINGO-activated CDK1 and CDK2 and the equivalent CDK-cyclin complexes. We have focused on two CDK substrates, the Wee1 family kinase Myt1 and the phosphatase Cdc25, which regulate M phase entry in *Xenopus* oocytes by controlling CDK1 phosphorylation and dephosphorylation on Thr14 and Tyr15, respectively. We found no significant differences in Cdc25 phosphorylation sites when CDK1 and CDK2 were activated by either XRINGO or cyclins. In contrast, XRINGO-activated CDKs can target a different subset of phosphorylation sites on the regulatory domain of Myt1 than the same CDKs activated by cyclins. In particular, we have identified three Ser (410, 414 and 444) that are major phosphoacceptor sites for CDK/XRINGO but are poorly phosphorylated by CDK/cyclin. Phosphorylation of these Ser by CDK/XRINGO inhibits Myt1 kinase activity. We also show that these Myt1 residues are phosphorylated during XRINGO-induced oocyte maturation and that a non-phosphorylatable Myt1 mutant with the three Ser changed to Ala is resistant to CDK/XRINGO-induced inhibition. Our results demonstrate that XRINGO-activated CDKs have different substrate specificity than the CDK/cyclin complexes. Moreover, we have also identified five sites (Thr453, Ser472, Ser475, Ser492 and Ser504) located in the regulatory domain of Myt1 whose phosphorylation by p90Rsk reduces the affinity of Myt1 for CDK1/cyclin B and which are phosphorylated during progesterone-induced oocyte maturation. We describe a mechanism of Myt1 regulation based on site-specific phosphorylation, which is likely to mediate the induction of G2/M transition in oocytes by the interplay between XRINGO and p90Rsk.

RESUMEN

Las quinasas dependientes de ciclinas (CDKs) son una familia de Ser/Thr quinasas esenciales en la regulación del ciclo celular eucariótico. La actividad enzimática de las CDKs se regula por la fosforilación de su bucle de activación mediada por la proteína-quinasa que activa a las CDKs (CAK) y, principalmente por la interacción con las ciclinas. Las quinasas CDK1 y CDK2 también se pueden activar por las proteínas RINGO/Speedy, las cuales fueron inicialmente identificadas como potentes inductores de la transición G2/M en oocitos de *Xenopus laevis*. Trabajos posteriores demostraron que la proteína XRINGO es un importante regulador de la progresión meiótica, aunque se desconoce cómo la proteína XRINGO induce la activación del complejo CDK1/ciclina B, el cual media la maduración de los oocitos. Dado que las ciclinas participan en el reconocimiento y especificidad de sustratos de las CDKs, hemos investigado posibles diferencias en la especificidad de sustratos entre las CDKs activadas por XRINGO y las CDKs activadas por ciclinas. Nos hemos centrado en dos sustratos conocidos de las CDKs, la proteína-quinasa Myt1 y la fosfatasa Cdc25, proteínas que regulan la entrada en la fase M al controlar la fosforilación y la defosforilización de la proteína-quinasa CDK1 en los residuos Thr14 y Tyr15, respectivamente. No hemos encontrado diferencias significativas en los sitios de fosforilación de Cdc25, cuando XRINGO o las ciclinas activan CDK1 y CDK2. Por el contrario, las CDKs activadas por XRINGO fosforilan el dominio regulador de Myt1 en sitios diferentes a las mismas CDKs activadas por ciclinas. En particular, hemos identificado tres residuos de Ser (410, 414 y 444) que son los principales sitios de fosforilación de los complejos CDK/XRINGO, pero no son fosforilados por los complejos CDK/ciclinas. La fosforilación de estas tres Ser por CDK/XRINGO inhibe la actividad quinasa de Myt1. Además, estos mismos residuos son fosforilados durante la maduración meiótica inducida por XRINGO. También observamos que un mutante con las tres Ser cambiadas a Ala y que no es fosforilado por CDK/XRINGO, hace que la proteína-quinasa Myt1 sea resistente a la inhibición inducida por XRINGO. Nuestros resultados demuestran que las CDKs activadas por XRINGO tienen diferente especificidad de sustrato que los complejos CDK/ciclinas. Por otra parte, también hemos identificado cinco sitios (Thr453, Ser472, Ser475, Ser492 y Ser504) localizados en el dominio regulador de Myt1, cuya fosforilación mediada por p90Rsk reduce la afinidad de Myt1 por el complejo CDK1/ciclina B y estos sitios son fosforilados durante la maduración meiótica inducida por progesterona. También describimos un

mecanismo de regulación de Myt1, el cual está basado en la fosforilación sitio-específica. Es probable que la conexión entre XRINGO y p90Rsk module la inducción de la transición G2/M en oocitos de *Xenopus*.

INTRODUCTION

Organisms consist of cells that multiply through cell division. Before a cell can divide, it must grow in size, duplicate its chromosomes and separate the chromosomes between the two daughter cells, so that each daughter cell receives all the machinery and information necessary to repeat the process (Nurse, 2000). These different processes are coordinated in the cell cycle. The fundamental molecular mechanisms controlling the cell cycle are highly conserved throughout evolution and operate in the same manner in yeast, insects, plants, animals and humans (Tyson and Novak, 2008).

Two major types of cell cycles can be defined: the mitotic cell cycle and the meiotic cell cycle. The mitotic cell cycle, which aims to produce daughter cells with the same number of chromosomes, is the reproduction mode of unicellular organisms and is also necessary for a total mass increase in multicellular organisms. However, sexual reproduction requires the fusion of two germinal cells coming from the two parental cells. In this case there is a necessity to generate daughter cells different from the mother (in terms of DNA information). This is the meiotic cell cycle that results in the reduction of the DNA content of the mother cell by half, leading to the formation of germinal cells or gametes.

1. The Mitotic Cell Cycle

The mitotic cell cycle of eukaryotic cells is conventionally divided into four phases (Fig. 1). In the first phase (G1) the cell grows and prepares to initiate DNA synthesis (S phase), where the chromosomes are duplicated. During the next phase (G2) the cell prepares for division. In mitosis (M) the chromosomes are separated, and the cell divides into two daughter cells. Through this mechanism the daughter cells receive identical sets of chromosomes. After division, the cells stay in G1 phase and the cell cycle is completed. If the extracellular conditions are unfavorable, cells may enter a specialized resting state known as G0, in which they are quiescent and can remain for years. Indeed, some cells known as post-mitotic remain permanently in G0 (e.g. neurons) (Olashaw and Pledger, 2002).

Cell cycle also requires switch-like transitions known as checkpoints at the end of G1, at the onset of S phase and at the entry and the exit of mitosis. The primary checkpoint acts late in G1 and is known as the restriction point (R) (Fig. 1). Once cells have passed this point successfully, they are normally committed to a round of cell division. Other checkpoints in S phase are necessary to activate DNA repair

mechanisms in case of DNA damage and at the G2/M transition to ensure that cells have fully replicated their DNA and that it is undamaged before they enter mitosis. Finally, there are checkpoint control mechanisms within mitosis to ensure that conditions remain suitable for the cell to complete cell division (Harper and Brooks, 2005).

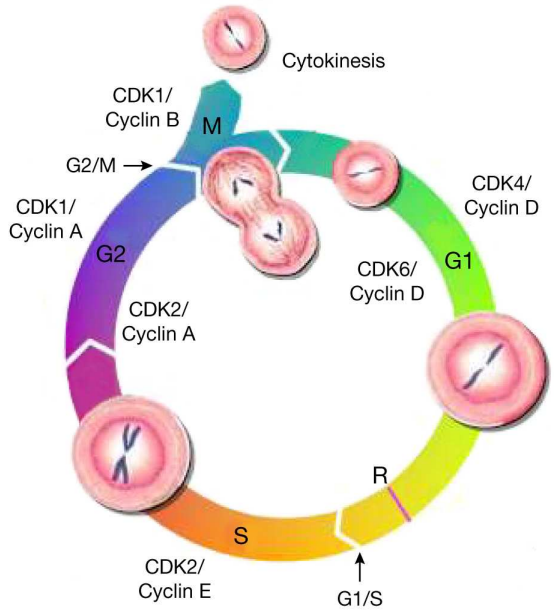

Figure 1 | The Classical Model of Cell Cycle Control. In the currently accepted model based on biochemical evidence, each of the main events that take place during interphase (G1, S and G2) is driven by cyclin-dependent kinases (CDKs) bound to specific cyclins. Cycling cells undergo three major transitions during their cell cycle. The beginning of S phase is marked by the onset of DNA replication, the start of mitosis (M) is accompanied by breakdown of the nuclear envelope and chromosome condensation, whereas segregation of the sister chromatids marks the metaphase-to-anaphase transition.

In a typical human cell that is proliferating, interphase –which includes G1, S and G2 phases- takes about 24 h and only 1 h is necessary for mitosis. Although mitosis is short it can be divided into five stages. During the prophase, chromosomes containing duplicated DNA strands condense, the nuclear envelope breaks down, and the chromosomes, each consisting of a pair of sister chromatids, become attached to the microtubules of the mitotic spindle. In metaphase, the chromosomes align at the equator of the mitotic spindle. During the anaphase, sister chromatids separate and the chromosomes move to the opposite poles of the spindle. Finally in telophase, the chromosomes decondense and the nuclear membrane is reconstituted. The cell is

then divided in two daughter cells by the cytoplasmic division or cytokinesis (Harper and Brooks, 2005).

At the heart of transitions between the different stages of the cell cycle are the cyclin-dependent kinases (CDKs), heterodimeric enzymes with a protein kinase subunit and a protein subunit, called cyclins, which are regulated by various biochemical changes (Malumbres and Barbacid, 2001; Olashaw and Pledger, 2002).

2. The Meiotic Cell Cycle

Meiosis is a specialized type of cell division that generates germ cells (oocytes and sperm cells) with a haploid set of chromosomes. It is the pre-requisite for sexual reproduction, in which two haploid germ cells fuse to form a diploid zygote with recombined parental genetic material (Hochwagen, 2008).

In meiosis, the immature germ cells replicate their DNA and undergo two consecutive specialized cell divisions (M phases), termed meiosis I and meiosis II, in the absence of DNA replication. In meiosis I, homologue chromosomes are separated from each other, reducing the diploid set of chromosomes to haploid. In meiosis II, sister chromatids are separated, similar to mitosis, resulting in haploid mature germ cells ready for fertilization and subsequent embryonic development (Hochwagen, 2008; Marston and Amon, 2004). Like mitotic cell cycles, meiotic cell cycles are divided into four phases: prophase, metaphase, anaphase and telophase. While meiosis II largely resembles a mitotic cell division, in which the single pairs of sister chromatids separate in anaphase II, meiosis I differs in several ways. The first meiotic prophase of oocytes lasts much longer, up to several months or even years, depending on the organism. Prophase is itself divided in several phases termed leptotene, zygotene, pachytene, diplotene and diakinesis. The chromosomes that are separated in meiosis I undergo homologous recombination in prophase I or pachytene, resulting in the exchange of genes between homologous chromosomes. During diplotene, the meiotic maturation of oocytes is arrested, and the oocytes reach their maximal size. Diplotene chromosomes are partially decondensed similar to interphase chromosomes (Hochwagen, 2008). This arrest resembles a G2 arrest, the gap phase between S and M phase of the cell cycle. The resumption of meiosis after stimulation of the oocytes with species-specific inducers of meiosis is comparable to a G2/M transition.

3. CDKs, Cyclins and the Regulation of the Cell Cycle

Cyclin-dependent kinases (CDKs) are proline-directed Ser/Thr protein kinases that play essential roles in the regulation of eukaryotic cell division. CDKs were discovered initially by genetic analysis of the cell cycle in yeast and were found to be a universal hallmark of the eukaryotic cell cycle. It is now clear that CDKs, either directly or indirectly, control the major cell cycle transitions and phases in all eukaryotic organisms (Ekholm and Reed, 2000; Malumbres and Barbacid, 2009).

The mammalian genome has eleven loci encoding CDKs, although only five of them, CDK1, CDK2, CDK3, CDK4 and CDK6 have been directly implicated in driving the cell cycle (Malumbres and Barbacid, 2005). CDK5 is restricted to neuronal tissues and is involved in several aspects of neuronal function. CDK7 partners with cyclin H is both a CDK-activating kinase (CAK), which phosphorylates cell cycle CDKs within the activation segment (T loop), and a component of the general transcription factor TFIIH, which phosphorylates the C-terminal domain of the largest subunit of RNA polymerase II. CDK8 and CDK9 have key roles in the control of transcription by RNA polymerase II. CDK10 and CDK11 are thought to have a role at the G2/M transition, in addition to their roles in regulating transcription (Malumbres, 2005; Malumbres and Barbacid, 2005).

Cyclins were identified as proteins that oscillated through the cell cycle in rapidly cleaving early embryonic cells (reviewed in Murray 2004; Bloom and Cross 2007). All cyclins share an approximately 100 residues long box of high homology, called the cyclin box. This region binds to the N-terminal of CDKs and is required for CDK activation (Bloom and Cross, 2007). Eight type of cyclins have been described that directly affect cell cycle progression, cyclins A1 and A2, cyclins B1, B2 and B3, cyclin C, cyclins D1, D2 and D3, cyclins E1 and E2, cyclin F, cyclins G1 and G2, and cyclin H (reviewed in Malumbres and Barbacid 2005; Wolgemuth 2008).

Concentrations of the cyclins oscillate during the cell cycle by successive rounds of transcription followed by ubiquitin-mediated proteolysis, which results in abrupt inactivation of the associated CDK (Murray, 2004; Sherr and Roberts, 2004). Cyclins are important for ensuring that CDKs are activated at the correct points in the cell cycle, targeted to the correct substrates and localized to the correct subcellular regions (Sherr and Roberts, 2004). Each phase of the cell cycle is characterized by the activation of different CDK/cyclin complexes that phosphorylate and regulate downstream protein substrates (Bloom and Cross, 2007). For instance, mitogenic

signals are first sensed by expression of the D-type cyclins (D1, D2 and D3) that preferentially bind to and activate CDK4 and CDK6 during G1 (Ekholm and Reed, 2000). Activation of these complexes leads to partial inactivation of the pocket proteins, such as Rb, p107 and p130, to allow expression of E-type cyclins (E1 and E2), which bind to and activate CDK2 (Ekholm and Reed, 2000). CDK2/cyclin E complexes further phosphorylate these pocket proteins, leading to their complete inactivation (Olashaw and Pledger, 2002). CDK2 is subsequently activated by cyclin A during the late stages of DNA replication to drive the transition from S phase to mitosis, in G2 phase. Finally, CDK1 is activated by A-type cyclins at the end of interphase to facilitate the onset of mitosis. Following nuclear envelope breakdown, A-type cyclins are degraded, facilitating the formation of the CDK1/cyclin B complexes responsible for driving cells through mitosis (Fig. 1) (Malumbres and Barbacid, 2005).

3.1. Mechanisms of CDK Activation and Inhibition

The enzymatic activity of CDKs is controlled by different processes such as binding of activating cyclin subunits, binding of inhibitory subunits, and both inhibitory and activating phosphorylations (Pavletich, 1999; Radzio-Andzelm et al., 1995). Crystallographic studies of CDKs in different complexes have revealed the mechanisms by which these regulatory processes control the CDK activity.

The structure of monomeric CDK2 shares the same fold as other eukaryotic protein kinases. CDK2 contains an N-terminal lobe, rich in β-sheet structure and a long α-helix containing the highly conserved sequence PSTAIRE, typical of the CDK family and constitutes the main point of interaction with cyclin A, and a larger C-terminal lobe that is primarily α-helical (Fig. 2A). The site for ATP binding and catalysis is located between these two lobes (De Bondt et al., 1993).

The monomeric CDK2 is catalytically inactive due to two major structural constraints (De Bondt et al., 1993). First, the T loop localized in the C-terminal lobe is positioned in front of the catalytic cleft entrance and hence blocks the accessibility of the substrates to the active site. Second, a number of key residues (Lys33 and Asp145) involved in ATP phosphate binding are not correctly positioned. As a result, the phosphotransfer reaction is inhibited because of the improper orientation of ATP phosphates.

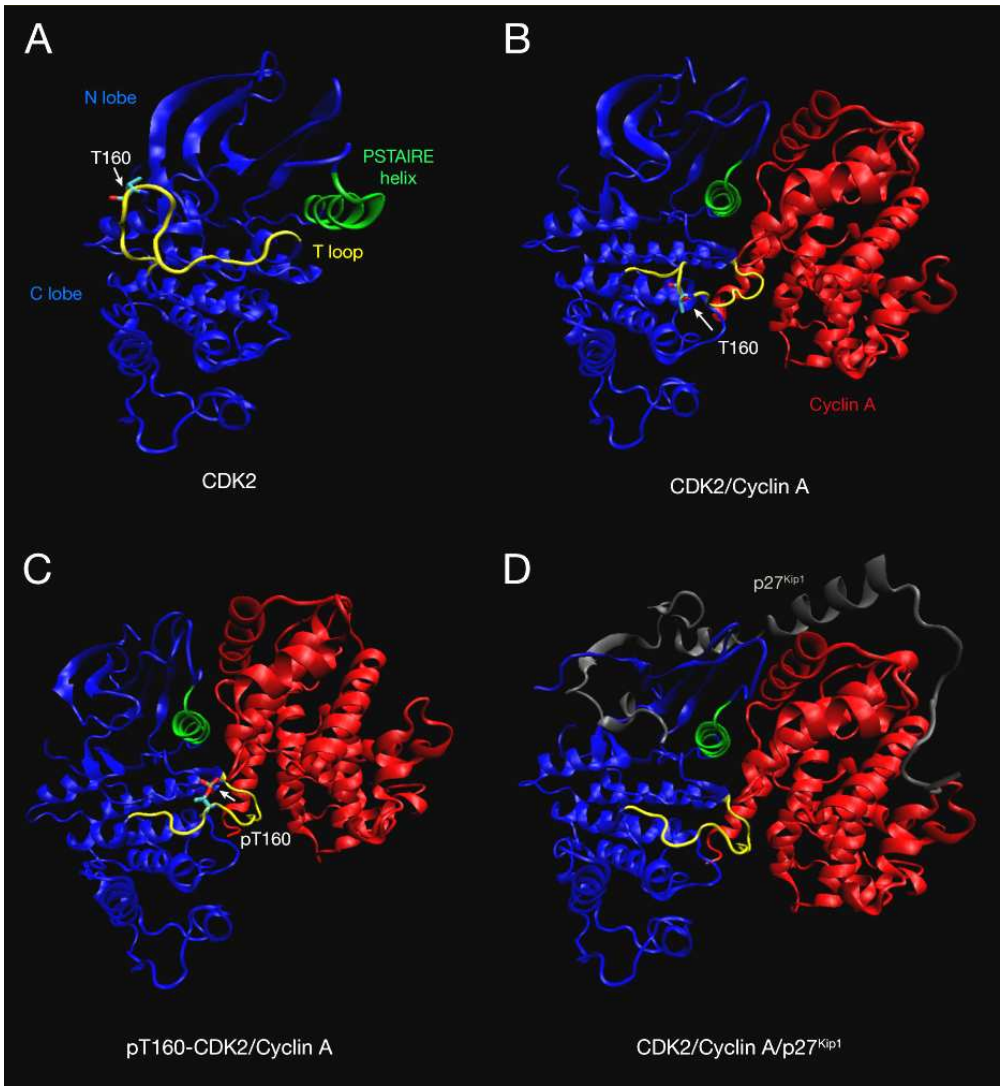

Figure 2 | Structural Basis of CDK Activation. CDK2 structures corresponding to non-activated (A, monomeric CDK2), partially active (B, CDK2/cyclin A complex), fully active (C, phosphorylated CDK2/cyclin A complex), and inhibited (D, CDK2/cyclin A/p27^{KIP1} complex) states. Regions of CDK2 that undergo large conformational changes upon cyclin A binding are highlighted: the PSTAIRE helix is green and the T loop is yellow. Unphosphorylated and phosphorylated Thr160 are indicated.

Activation

Cyclin binding activates the kinase by causing several conformational changes (Jeffrey et al., 1995). Cyclin binding moves the PSTAIRE helix into the catalytic cleft leading to changes in the ATP binding site and enabling the correct positioning of the ATP phosphates for the phosphotransfer reaction. After cyclin binding, the T loop is displaced and the phosphorylation site is exposed (Fig. 2B). Phosphorylation of a conserved Thr (Thr161 in CDK1 and Thr160 in CDK2) by the CAK kinase (CDK7/cyclin H/MAT1 complex) induces the T loop to undergo an additional conformational change. This change is induced by the phosphate group acting as an organizing center in the T

loop (Fig. 2C). The significance of this CDK region is that it is part of the catalytic cleft, and in particular, the putative polypeptide substrate interaction site (Russo et al., 1996b). Phosphorylation completes the reorganization of the substrate binding site and leads to full activation of the CDK (Fig. 2C). Thus, the full activation of CDKs by cyclins requires two events: cyclin binding and T loop phosphorylation.

Inhibition

CDK/cyclin complexes can be inactivated by either cyclin degradation or by phosphatase PP2C-mediated dephosphorylation of the T loop (De Smedt et al., 2002; Hochegger et al., 2008). CDK kinase activity is also regulated by two families of CDK inhibitors (CKIs): INK4 proteins, including $p16^{INK4A}$, $p15^{INK4B}$, $p18^{INK4C}$ and $p19^{INK4D}$, and the Cip and Kip family, composed of $p21^{Cip1}$, $p27^{Kip1}$ and $p57^{Kip2}$ (Olashaw and Pledger, 2002). The mechanism of CDK/cyclin inhibition by CKIs was revealed by crystallographic studies of CDK/cyclin/CKI complexes (Russo et al., 1996a; Russo et al., 1998). The structure of CDK2/cyclin A/$p27^{Kip1}$ demonstrated that $p27^{Kip1}$ binds to both CDK2 and cyclin A and interferes with CDK activity by insertion of a small α-helix into the kinase catalytic cleft, thereby blocking ATP binding. Furthermore, $p27^{Kip1}$ binding rearranges the structure of the catalytic cleft rendering the CDK molecule inactive (Fig. 2D) (Russo et al., 1996a).

In addition, the complexes can be inhibited by inhibitory phosphorylations at two sites near the N-terminus of CDK (Thr14 and Tyr15 in human CDK1). In the three dimensional structure of CDK2, both sites are located at the top of the ATP-binding site (De Bondt et al., 1993). It is suggested that phosphorylation on Thr14 prevents ATP binding (Endicott et al., 1994), whereas that on Tyr15 interferes with phosphate transfer to the substrate owing to its positioning in the ATP binding site on CDK1 (Atherton-Fessler et al., 1993). These inhibitory phosphorylations events are carried out by the kinases Wee1 and Myt1 (Lee et al., 1994; Mueller et al., 1995a; Mueller et al., 1995b). Wee1 specifically phosphorylates Tyr15 (Mueller et al., 1995a), whereas Myt1 phosphorylates both Thr14 and Tyr15, with a stronger affinity for Thr14 (Liu et al., 1997; Mueller et al., 1995b). The dephosphorylation of the inhibitory residues is necessary for the activation of the CDK/cyclin complex and is carried out by Cdc25, a family of dual-specificity phosphatases (Kumagai and Dunphy, 1992). Cdc25 phosphatases act on their protein substrates in a stepwise mechanism, wherein the

enzyme dissociates after dephosphorylation of phospho-Thr and must reassociate for dephosphorylation of phospho-Tyr (Kristjansdottir and Rudolph, 2004).

3.2. RINGO/Speedy Proteins, New CDK Activators

Although cyclins play an important role in cell cycle progression, activation of CDKs does not necessarily require the presence of cyclins. Atypical CDK activators include a new family of proteins named RINGO/Speedy that can activate CDK1 and CDK2 independently of cyclin binding (Gastwirt et al., 2007).

To date five mammalian homologues have been identified. All of the RINGO/Speedy proteins (hereafter referred to as RINGO) contain a conserved central region of about 100 residues that has been referred to as the RINGO core or box (Cheng et al., 2005b; Dinarina et al., 2005), which has 51–67% homology among the family members. The RINGO core is predicted to have an α-helical secondary structure, as it has been reported for the cyclin box, and it is critical for CDK binding and activation (Dinarina et al., 2005). This may account for the ability of both types of proteins to activate CDKs, in spite of their lack of sequence homology.

Mutations in the conserved RINGO core residues abolish CDK2 binding and activation (Cheng et al., 2005b; Dinarina et al., 2005). Indeed, the RINGO core appears to be both necessary and sufficient for CDK activation by RINGO proteins. The residues flanking the conserved core have also been implicated in the function of RINGO proteins. C-terminal truncation mutants of RINGO A can bind to but not activate CDK2, suggesting that this region may be necessary for CDK2 activation. Likewise, the N-terminus may be involved in regulating the expression of RINGO A (Cheng et al., 2005b).

RINGO mRNAs exhibit distinct expression patterns in mouse and human tissues, although all appear to be enriched in testis (Cheng et al., 2005b; Dinarina et al., 2005). Interestingly, no sequences with significant similarities to RINGO proteins have been found in yeast, worms, flies or plants. However, a potential RINGO gene has been identified in the most primitive branching clade of chordates (*Ciona intestinalis*) (Cheng et al., 2005b; Dinarina et al., 2005).

Regarding the specificity, mammalian RINGO family members can bind to and activate CDK1 and CDK2, albeit with different efficiencies, but they neither bind to nor activate CDK4 and CDK6. *In vitro* and overexpression experiments suggest that most

RINGO proteins might bind to and activate CDK2 more efficiently than CDK1 (Cheng et al., 2005b; Dinarina et al., 2005; Karaiskou et al., 2001b; Porter et al., 2002).

Interestingly, the lack of amino acid sequence homology between cyclins and RINGO proteins results in significant differences in their mechanisms of CDK activation. For example, CDK1 and CDK2 activated by RINGO proteins do not require phosphorylation in the activation loop of the CDK (Karaiskou et al., 2001b), which is essential for full activation of these CDKs by cyclins (Espinoza et al., 1996; Kaldis et al., 1996). In fact, RINGO proteins are more efficient CDK activators than cyclins in the absence of the T loop phosphorylation (Cheng et al., 2005a). Consistent with these observations, binding of RINGO A alters the activation loop conformation of CDK2, but in a distinct manner from how cyclin A does so (Cheng et al., 2005a). Furthermore, RINGO-bound CDK2 is a poor substrate for the mammalian CDK-activating kinase that phosphorylates CDK2 on Thr160 (Cheng et al., 2005a).

Biochemical data shows that RINGO proteins also bind to the same region of the CDK molecule as cyclins. *Xenopus* RINGO binding to CDK2 involves residues in the PSTAIRE helix (Ile49 and Arg50) and in the activation loop (Arg150) that are also important for binding to cyclin A (Dinarina et al., 2005).

All mammalian RINGO proteins also bind the CKI $p27^{Kip1}$, but with an inverse efficiency to their ability to bind to CDK1 (Dinarina et al., 2005). The interaction between RINGO A and $p27^{Kip1}$ involves residues 43-128 of $p27^{Kip1}$, which include the CDK binding region (residues 53–93) (Porter et al., 2003). Overexpression of $p27^{Kip1}$ increased the amount of RINGO A detected in CDK2 immunoprecipitates, suggesting the formation of a trimeric complex (Porter et al., 2003). It was proposed that RINGO A expression enhances CDK2-dependent $p27^{Kip1}$ degradation (McAndrew et al., 2007). Another important difference from CDK/cyclin complexes is that RINGO-activated CDK1 and CDK2 are less susceptible to inhibition by both the CKI $p21^{Cip1}$ and by the protein kinase Myt1 (Karaiskou et al., 2001b).

Recently, the substrate specificity of CDKs activated by RINGO has started to be characterized. CDK2/RINGO A shows low enzymatic activity towards conventional CDK2/cyclin A substrates with the consensus site S/TPXK/R (where X is any amino acid). Unlike CDK2/cyclin A, which strongly favors a Lys at the P+3 position of the phospho-acceptor site S/TPXK/R, RINGO A-activated CDK2 displays broader substrate specificity. Using GST-tagged pentapeptide substrates of the form KSPRX, CDK2/RINGO A tolerated all amino acid substitutions at the P+3 position. Thus,

CDK2/RINGO A phosphorylated non-canonical CDK2 substrates, which contained tyrosine and tryptophan, but not lysine in the P+3 position, relatively well compared to CDK2/cyclin A, whereas optimal CDK2 substrates, such as histone H1 or a KSPRK peptide, were phosphorylated poorly (Cheng et al., 2005a).

In the case of substrates like Cdc25 phosphatases, which contain several potential CDK phosphorylation sites, phosphorylation induced by CDK2/RINGO A was almost as efficient as CDK2/cyclin A. Interestingly, phosphopeptide mapping reveled that several Cdc25 sites were phosphorylated by CDK2/RINGO A but not by CDK2/cyclin A (Cheng et al., 2005a). Thus, the potential physiological importance of RINGO-activated CDK2 should not be underestimated by the low *in vitro* activity displayed on conventional CDK substrates.

4. *Xenopus* Oocytes Maturation as a Model System for Studying the Meiotic G2/M Transition

The meiotic maturation of *Xenopus* oocytes is an excellent system to study the mechanisms that regulate M phase entry and progression. Fully grown *Xenopus* oocytes are arrested in a G2-like phase, at prophase in the G2/M boundary of the first meiotic division, and are induced to enter meiosis I by progesterone stimulation in a process called meiotic maturation (Philpott and Yew, 2008). The progression through meiosis can be easily studied because of the oocyte large size which enables an easy manipulation. Another reason why *Xenopus* oocytes represent a good system is that mRNAs, recombinant proteins, antibodies or oligonucleotides can be easily injected into oocytes, thereby allowing overexpression or inactivation of the target proteins (Philpott and Yew, 2008; Smith et al., 1991).

Fully grown oocytes are spherical cells with a diameter of 1.3 mm and a volume of about 1 µl. They display a specific pigmentation pattern, which defines the radial symmetry of the oocyte. The animal hemisphere is dark brown, whereas the vegetal hemisphere is only weakly pigmented. The nucleus of the oocyte, also called the germinal vesicle, has a volume of 40 nl and therefore is about 10^5 times larger than the nucleus of a normal somatic cell (Smith et al., 1991).

The steroid hormone progesterone releases the G2 arrest of the oocyte, which then completes meiosis I, resumes meiosis II and arrests again at the metaphase of meiosis II until fertilization (Fig. 3). The first and second meiotic divisions are highly asymmetrical. At each M phase, a small non-functional polar body containing half of

the genetic material is extruded, resulting in a single mature oocyte. The mature oocytes or eggs remain arrested in metaphase II, once fertilization takes place, meiosis II is completed and the eggs initiate further development (Schmitt and Nebreda, 2002).

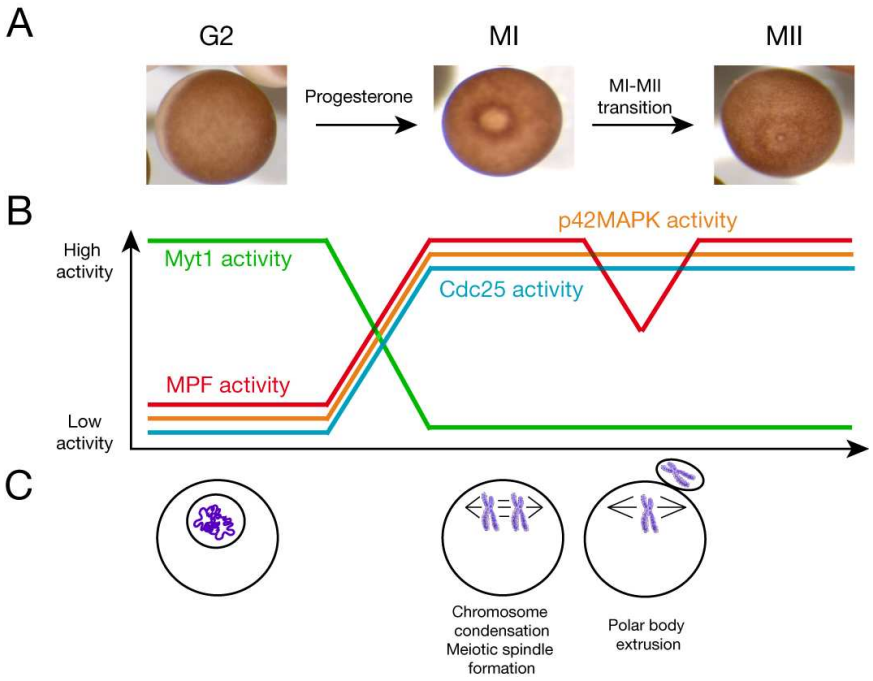

Figure 3 | Dynamics of Cell Cycle Regulators through Meiotic Maturation. (A and B) Fully grown immature *Xenopus* oocytes are arrested at the G2/M border of the meiotic cell cycle. Progesterone overcomes this arrest and causes initiation of oocyte maturation. The oocytes enter meiosis I (MI), as witnessed by the appearance of a white spot on the animal hemisphere due to the breakdown of the germinal vesicle (nuclear envelope), after progesterone stimulation. This is followed by a transient decline in MPF activity and entry into meiosis II (MII), culminating with arrest in metaphase through an activity known as cytostatic factor. Important protein activities crucial for the process of oocyte maturation are indicated. (C) In the diagrams of the oocytes, the membrane of the nucleus (the germinal vesicle containing the replicated DNA) disappear, the chromosomes condense, align in the metaphase spindle and separate in meiosis I, leading to the extrusion of the first polar body.

The induction of oocyte maturation involves a number of morphological and biochemical changes. The most obvious morphological change associated with oocyte maturation is the appearance of a white spot on the animal pole of the oocyte, resulting from the migration of the nucleus to the apex of the pigmented animal pole and disintegration of the nuclear envelope, a process called germinal vesicle breakdown (GVBD) (Fig. 3). Moreover, this event correlates with the rearrangement of cortical pigment granules and depigmentation of the apical pole. GVBD is therefore used as a marker of the entry into meiosis I (Schmitt and Nebreda, 2002). In addition to GVBD, other morphological changes are associated with meiotic maturation. The

chromosomes condense, the meiotic spindle is assembled and the condensed chromosomes align at the first meiotic spindle. The homologous chromosomes then separate, the first polar body is extruded and the oocytes arrest in metaphase of meiosis II due to cytostatic factor (CSF) activity (Schmitt and Nebreda, 2002).

4.1. Signalling Pathways Involved in Oocyte Meiotic Maturation

Biochemical changes during oocyte maturation include changes in the activity of a number of signalling pathways required for the M phase progression that eventually converge to promote dephosphorylation and activation of the maturation-promoting factor or MPF, a key enzymatic activity that regulates the G2/M transition in all eukaryotic cells by phosphorylating a wide range of structural and regulatory proteins (Karaiskou et al., 2001a; Nebreda and Ferby, 2000).

MPF is inactive in S and G2 phases and reaches its maximum activity in each mitotic or meiotic cycle. During the meiotic cell cycle in *Xenopus* oocytes, MPF is first activated at meiosis I, then transiently inactivated between meiosis I and II and finally reactivated at meiosis II (Fig. 3) (Schmitt and Nebreda, 2002).

MPF is a heterodimer kinase composed of a catalytic subunit, the Ser/Thr protein kinase CDK1, and a regulatory subunit, a B-type cyclin (Fig. 4) (review by Nebreda and Ferby, 2000). The activity of MPF is tightly regulated during the cell cycle by post-translational modifications of CDK1 and by synthesis and destruction of cyclin B. In G2-arrested *Xenopus* oocytes, the majority of CDK1 (about 90%) is thought to be monomeric, and some of it might be phosphorylated on the T loop (Thr161) by CAK kinase (De Smedt et al., 2002), but only a small fraction of the CDK1 pool (about 10%) is associated with cyclins B2 and B5 and phosphorylated on Thr161. These preformed CDK1/cyclin B complexes, referred to as pre-MPF, are maintained inactive by phosphorylation of CDK1 on Thr14 and Tyr15. The inhibitory phosphorylations are catalyzed by the protein kinase Myt1 (Liu et al., 1997; Mueller et al., 1995b), whereas dephosphorylation of these residues, which is required to activate CDK1/cyclin B and promote entry into M phase, is catalyzed by the Cdc25 phosphatases (Kumagai and Dunphy, 1992). In late G2 phase, the balance between Myt1 and Cdc25 activities shifts in favor of CDK1 dephosphorylation, resulting in the activation of CDK1/cyclin B complexes and entry into meiosis (Fig. 4). The initial triggering events that reverse the dominance of Myt1 over Cdc25 activity in late G2 phase and lead to CDK1/cyclin B activation are poorly characterized.

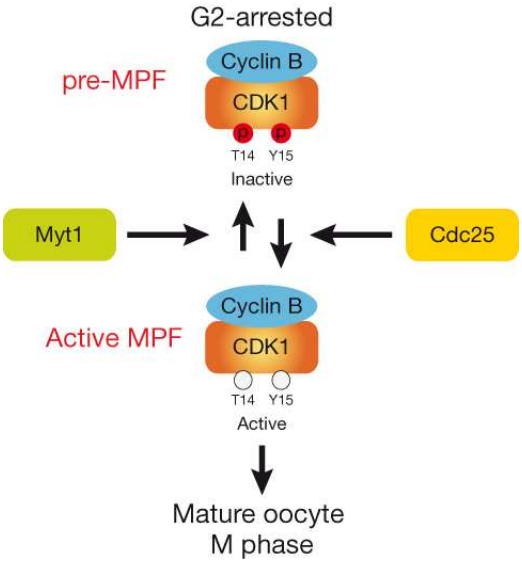

Figure 4 | Activation of MPF is Essential for Entry into M Phase. A key enzymatic activity that regulates the G2/M transition in eukaryotic cells is the maturation-promoting factor (MPF), a complex formed by CDK1 and cyclin B. In G2-arrested oocytes, there is a preformed complex of CDK1/cyclin B, referred to as pre-MPF, which is maintained inactive by phosphorylation of CDK1 on Thr14 and Tyr15. The protein kinase Myt1 is responsible for the inhibitory phosphorylations. These two CDK1 residues are dephosphorylated by the Cdc25 phosphatase, resulting in the activation of CDK1/cyclin B complexes and entry into M phase.

4.1.1. Release from G2 Arrest: Early Events that Trigger Meiotic Maturation

Meiotic resumption from G2 arrest is induced by hormonal stimuli. In *Xenopus* oocytes, maturation is thought to be initiated by the steroid hormone progesterone, which is synthesized and released by follicular cells surrounding the oocyte. Progesterone is now thought to initiate oocyte maturation in non-mammalian vertebrates by binding to a recently identified seven-transmembrane G protein-coupled receptor (GPCR) (Deng et al., 2008; Zhu et al., 2003a; Zhu et al., 2003b), which also has close homologs in mammals. Progesterone binding to its GPCR inhibits adenylyl cyclase in a GTP-dependent, pertussis toxin-sensitive manner (Deng et al., 2008; Zhu et al., 2003a; Zhu et al., 2003b), and decreases the level of cAMP. This, in turn, causes reassociation of the catalytic subunit of cAMP-dependent protein kinase (PKA) with the regulatory subunit, resulting in the reduction of PKA activity and leading to the activation of a putative maturation inducing protein, probably Cdc25 (Duckworth et al., 2002; Shibuya, 2003). The other role of PKA inactivation in oocytes is to promote the synthesis of a small number of proteins necessary for meiotic maturation. Mos and cyclin B are the most potential candidates because they are

synthesized *de novo* after PKA inactivation (Karaiskou et al., 2001a; Nebreda and Ferby, 2000).

Inhibitors of translation, like Cycloheximide (CHX), completely block progesterone-induced meiotic maturation, showing that translation, unlike transcription, is indispensable for meiotic maturation (Bodart et al., 2002). Because the transcriptional process in the oocytes itself is repressed during meiotic maturation, the proteins that are translated from the stocked maternal mRNAs guarantee the accurate response of the oocyte to external stimulation. For example, *mos* mRNA becomes polyadenylated and translated after progesterone stimulation (Mendez and Richter, 2001). Prior to hormonal stimulus, cytoplasmic polyadenylation element (CPE)-containing mRNAs are translationally masked, and have a short poly(A) tail. During meiotic resumption, CPEB is phosphorylated by Aurora A (Mendez et al., 2000), which in turn increases the affinity of CPEB for the cleavage and polyadenylation specificity factor (CPSF). CPSF binds to the AAUAAA sequence and recruits poly(A) polymerase to the end of the mRNA, resulting in polyadenylation of CPE-containing mRNAs, which is coupled with their translation (Mendez and Richter, 2001).

4.1.2. Release from G2 Arrest: Activation of Mos-p42MAPK-p90Rsk Pathway

Mos, the product of the proto-oncogene c-*mos*, is a 39-kDa germ cell-specific Ser/Thr protein kinase that was first identified in cells transformed by Moloney murine sarcoma virus. The Mos protein is not detected in G2-arrested oocytes but starts to be synthesized shortly after progesterone stimulation. This is thought to be due to the phosphorylation of the translational regulators CPEB and Maskin by Aurora A (Mendez et al., 2000; Pascreau et al., 2005) and the stabilization of the Mos protein through the phosphorylation of Ser3 by CDK1/cyclin B and p42MAPK (Nishizawa et al., 1992; Yue and Ferrell, 2006). The level of Mos protein remains high throughout meiosis I and meiosis II, but is rapidly degraded upon fertilization. The absence of Mos protein expression during embryonic development suggests that it has unique functions in meiotic maturation (Nishizawa et al., 1993).

Mos protein functions as a MAPK (mitogen-activated protein kinase) kinase kinase. It activates MAPK kinase MEK1 during oocyte maturation by phosphorylating two conserved residues, Ser218 and Ser222 (Huang et al., 1995; Posada et al., 1993). The only known substrates for MEK1 are ERK (extracellular-signal-regulated kinase)-

type MAPKs. MEK1 is a dual-specificity protein kinase that activates MAP kinase through phosphorylation of Thr183 and Tyr185 within its activation loop (Crews et al., 1992; Crews and Erikson, 1992; Kosako et al., 1993). In *Xenopus* oocytes, only a single ERK-type MAPK is expressed, p42MAPK, also known as ERK1/2. An important downstream target of the Mos-MEK1-p42MAPK pathway during oocyte maturation is the protein kinase p90Rsk (Palmer et al., 1998). In *Xenopus* oocytes, p90Rsk was originally identified as a kinase that can phosphorylate ribosomal protein S6 kinase, and it was shown to be activated during oocyte maturation (Anjum and Blenis, 2008). In G2-arrested oocytes, unphosphorylated and inactive p90Rsk associates with inactive p42MAPK to form a heterodimer, which dissociates during oocyte maturation concomitant with phosphorylation and activation of both kinases (Hsiao et al., 1994). The efficient activation of p90Rsk by p42MAPK requires their interaction through a docking site located at the C-terminal domain of p90Rsk (Gavin and Nebreda, 1999). A possible link between Mos-p42MAPK-p90Rsk pathway and direct activation of pre-MPF by Myt1 has been described (Palmer et al., 1998) and will be discussed below.

4.2. Regulation of Myt1 and Cdc25 in *Xenopus* Oocyte Maturation

During oocyte maturation, activation of pre-MPF correlates with dephosphorylation of CDK1 on Thr14 and Tyr15. Thus, the activation of Cdc25 phosphatase and/or the inhibition of Myt1 kinase should be sufficient to activate pre-MPF, and indeed both events occur upon progesterone treatment with a similar timing to pre-MPF activation. To understand how the balance between Myt1 and Cdc25 is reversed at the meiotic G2/M phase transition, it is essential to analyze the states of Myt1 and Cdc25 after maturation-inducing hormonal signalling, but before CDK1/cyclin B activation.

4.2.1. Regulation of Myt1 Kinase Activity

Two related classes of CDK1 inhibitory kinases have been identified in metazoans, Wee1 and Myt1. Wee1 is a nuclear kinase that phosphorylates CDK1 on Tyr15 (Lee et al., 1994; Mueller et al., 1995a). Myt1 localizes to Golgi and endoplasmic reticulum. Myt1 was identified as a membrane-associated kinase that phosphorylates CDK1 on both Thr14 and Tyr15 (Liu et al., 1997; Mueller et al., 1995b). Interestingly, Myt1 phosphorylation inactivates CDK1-containing cyclin complexes but not complexes containing CDK2, as reported for Wee1 (Booher et al., 1997). In addition,

overexpression in mammalian cells of either kinase-active or kinase-inactive forms of Myt1 causes a delay in the G2 phase of the cell cycle by sequestering CDK1/cyclin B complexes in the cytoplasm (Liu et al., 1999; Wells et al., 1999). Thus, Myt1 can negatively regulate CDK1/cyclin B and inhibit G2/M progression by two means, both of which require the C-terminal domain, Myt1 binds to and sequesters CDK1/cyclin B in the cytoplasm preventing entry into the nucleus, and it phosphorylates CDK1 at Thr14 and Tyr15 thus inhibiting its catalytic activity (Liu et al., 1999; Liu et al., 1997; Mueller et al., 1995b; Wells et al., 1999). These differences in Wee1 and Myt1 protein localization and target site specificity suggest that the metazoan CDK1 inhibitory kinases have evolved distinct cell cycle regulatory functions required at different stages of the cell cycle.

The protein kinase Wee1 is not detectable in G2-arrested *Xenopus* oocytes, although these oocytes contain maternal Wee1 mRNA that starts to be translated later during oocyte maturation (Nakajo et al., 2000). In contrast, Myt1 is present in G2 oocytes, and interfering with its function by the injection of antibodies against Myt1 is sufficient to induce oocyte maturation and CDK1 dephosphorylation (Nakajo et al., 2000), suggesting that Myt1 plays a key role in maintaining the meiotic G2 arrest. Moreover, Myt1 is phosphorylated during oocyte maturation, and the inactivation of Myt1 during M phase correlates with the phosphorylation of its C-terminal non-catalytic region (Liu et al., 1999; Wells et al., 1999).

Depending on the organism, different kinases can phosphorylate Myt1 and may potentially contribute to its regulation. For example, Akt/PKB phosphorylates Ser75 at the N-terminus of starfish Myt1 and downregulates its kinase activity toward CDK1/cyclin B (Okumura et al., 2002). The Mos-p42MAPK-p90Rsk pathway is thought to regulate Myt1 phosphorylation during *Xenopus* oocyte maturation (Palmer et al., 1998; Peter et al., 2002). Mos could directly phosphorylate Myt1 but the effect on Myt1 activity remains unknown (Peter et al., 2002). The p90Rsk kinase has been shown to phosphorylate and inhibit Myt1 *in vitro*, although specific phosphorylation sites are unknown (Fig. 5) (Palmer et al., 1998).

Intriguingly, fresh *Xenopus* oocytes obtained from frogs that have been primed with hormones can also be induced to mature by progesterone in the absence of Mos synthesis and p42MAPK activation, as showed by using Mos morpholino oligonucleotides, the MEK1/2 inhibitor U0126, or the Hsp90 inhibitor Geldanamycin (Dupre et al., 2002; Fisher et al., 1999; Gross et al., 2000; Peter et al., 2002). This

process is also mediated by MPF and involves Myt1 inactivation (Nebreda and Ferby, 2000), indicating that the Mos-p42MAPK-p90Rsk pathway is not essential for CDK1/cyclin B activation and meiotic maturation.

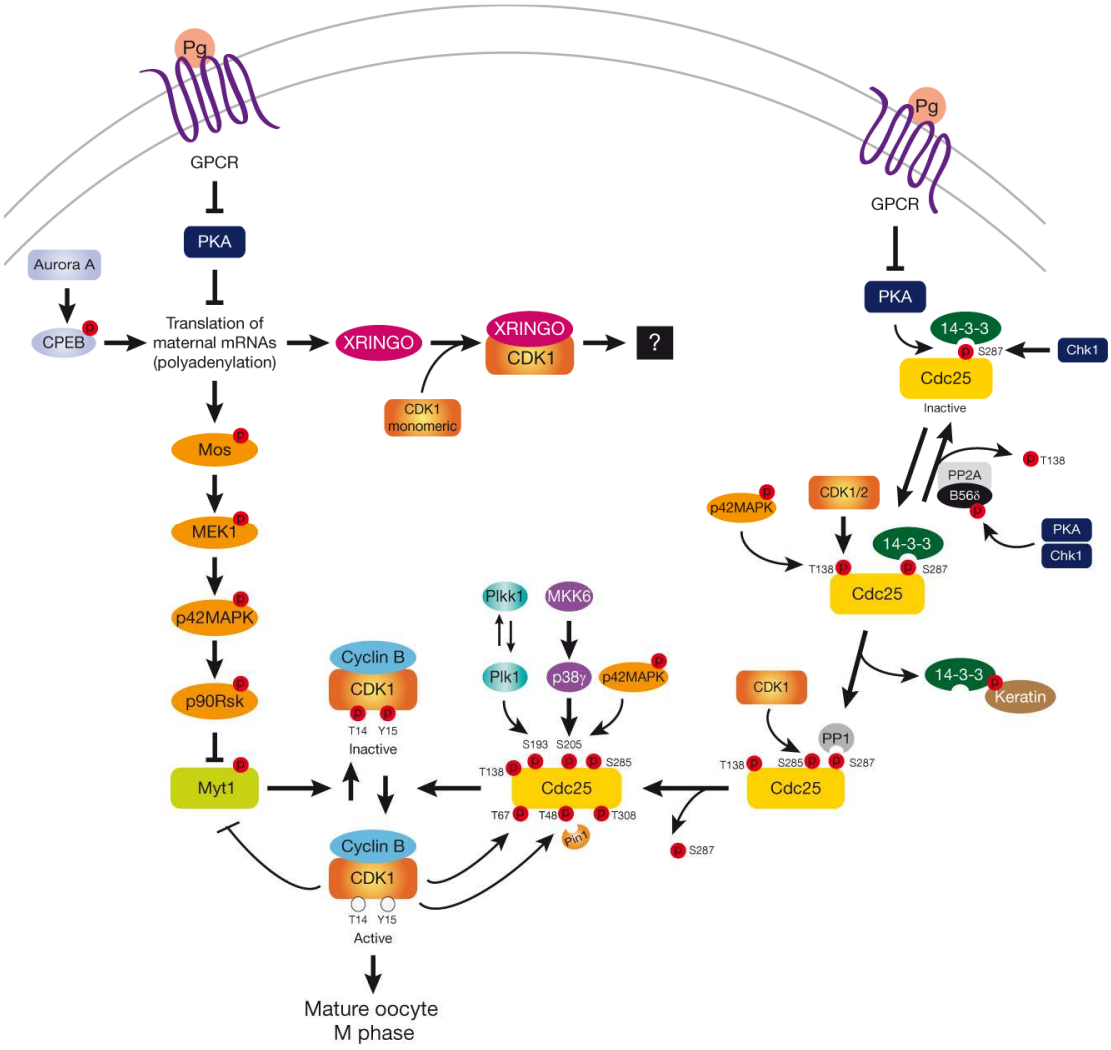

Figure 5 | Signalling Pathways Involved in *Xenopus* Oocyte Meiotic Maturation. Fully grown *Xenopus* oocytes are arrested in a G2-like phase and are induced to enter meiosis I by progesterone (Pg) stimulation in a process called meiotic maturation. Progesterone binding to its GPCR inhibits adenylyl cyclase and decreases the level of cAMP. The resulting decrease in PKA activity leads to the activation of protein synthesis. Aurora A participates in the translational activation via CPEB phosphorylation. Newly synthesized Mos activates p42MAPK-p90Rsk pathway, resulting in the suppression of Myt1. In other pathway, Cdc25 is held inactive by inhibitory phosphorylation at Ser287 and 14-3-3 binding. Likewise, PP2A/B56δ maintains Thr138 in the dephosphorylated state. After progesterone stimulation, Cdc25 is activated in a stepwise fashion. CDK1 or CDK2 and p42MAPK phosphorylate Thr138 which triggers the release of 14-3-3. Phosphorylated keratin intermediate filaments assist in 14-3-3 removal from Cdc25. Exposed Ser287 is then readily dephosphorylated by PP1. *Xenopus* Plk1 (Plx1) and p38γ/p42MAPK phosphorylate Ser193 and Ser205, respectively, inducing the activation of Cdc25 and dephosphorylation of CDK1/cyclin B. These both pathways converge on the initial activation of pre-MPF (CDK1/cyclin B), although the p42MAPK-p90Rsk pathway is not essential. Then CDK1/cyclin B is further activated. In another pathway, newly synthesized XRINGO/Speedy associates with CDK1, but the substrates phosphorylated by CDK1/XRINGO remain unknown.

Hyperphosphorylation of Myt1 has been shown to depend on CDK1 activity in *Xenopus* egg extracts, and purified CDK1/cyclin B can phosphorylate Myt1 *in vitro* (Booher et al., 1997; Inoue and Sagata, 2005; Mueller et al., 1995b). In addition, the hyperphosphorylated form of Myt1 isolated from M phase extracts has reduced kinase activity (Mueller et al., 1995b). These observations have led to the idea of a positive feedback loop in which CDK1 directly phosphorylates and inactivates Myt1, thereby contributing to a rapid rise in CDK1 activity and entry into M phase (Fig. 5) (Booher et al., 1997). However, it is unclear how CDK1 can phosphorylate Myt1 since Myt1 phosphorylates and maintains CDK1 catalytically repressed.

4.2.2. Regulation of Cdc25 Phosphatase Activity

The Cdc25 family of phosphatases is responsible for dephosphorylation of inhibitory Thr and Tyr residues on CDKs in order to promote their activation. Two isoforms (A and C) have been characterized in *Xenopus*. Cdc25C (hereafter referred to as Cdc25) is essential for promoting mitosis, while Cdc25A does not appear to be critical for mitotic entry. To date, CDK/cyclin complexes are the only known substrates for Cdc25 phosphatases.

In G2-arrested oocytes, both PKA activity and the basal, but not checkpoint-dependent, activity of Chk1 negatively regulate Cdc25 by phosphorylating Ser287 (Ser216 in human Cdc25) (Duckworth et al., 2002; Oe et al., 2001), which results in binding of 14-3-3ε and 14-3-3ζ proteins, decreasing Cdc25 catalytic activity and favoring its cytoplasmic sequestration (Kumagai and Dunphy, 1999; Kumagai et al., 1998). When oocyte maturation is initiated by progesterone stimulation, the activation of Cdc25 begins with the phosphorylation of a conserved Thr (Thr138 in *Xenopus*, Thr130 in human) in the N-terminus non-catalytic region of Cdc25 (Margolis et al., 2003). The phosphorylation of Thr138 at the G2/M transition is thought to be required for the release of 14-3-3 from Cdc25 (Fig. 5).

Recently, it was shown that protein phosphatase 2A (PP2A), in association with the B56δ regulatory subunit, actively dephosphorylates Thr138 (Forester et al., 2007; Margolis et al., 2006a). Interestingly, both PKA and Chk1 phosphorylate B56δ, promoting PP2A holoenzyme formation and the activity of PP2A/B56δ towards Thr138, holding Cdc25 inactive (Ahn et al., 2007; Margolis et al., 2006a).

Several kinases have been proposed to phosphorylate Cdc25 on Thr138 during *Xenopus* oocyte maturation, p42MAPK, CDK1, CDK2 and probably Greatwall

kinase (Margolis et al., 2003; Wang et al., 2007; Yu et al., 2006). Once Thr138 becomes phosphorylated, 14-3-3 proteins are released from Cdc25. It is possible that phosphorylation at Thr138 creates a conformational change in the protein, which then decreases 14-3-3´s affinity for Cdc25 (Margolis et al., 2003). Studies in mammalian cells suggest that phosphorylated Thr138 provides a docking site for the binding of the polo-box domain of the polo-like kinase, Plk1 (Elia et al., 2003a; Elia et al., 2003b). This suggests that Plk1 might be involved in the release of 14-3-3 from Cdc25 but this hypothesis has yet to be formally proven. Interestingly, it has been reported that phosphorylated keratin proteins could act as a high affinity sink for binding to 14-3-3 (Ahn et al., 2007; Margolis et al., 2006a). Thus, both Thr138 phosphorylation and the accumulation of phosphorylated keratin proteins promote the release of 14-3-3 proteins from Cdc25.

Once 14-3-3 becomes release from Cdc25, Ser287 is dephosphorylated very quickly and this occurs around the time of entry into M phase of meiosis I (GVBD) (Stanford and Ruderman, 2005). Recently, it was shown that the phosphorylation of Ser285 by CDK1 recruit protein phosphatase 1 (PP1) to Cdc25. PP1 is the enzyme responsible for dephosphorylating Ser287 (Margolis et al., 2003). But, it has remained unclear how CDK1 could phosphorylate Cdc25 on Ser285 since CDK1 remains phosphorylated on Thr14 and Tyr15 and, therefore, inhibited. It has been proposed that following 14-3-3 release from Cdc25, PP1 binds weakly to Cdc25 resulting in inefficient dephosphorylation of Ser287. Cdc25 then acquires a basal catalytic activity, which triggers dephosphorylation of a small pool of pre-MPF. In turn, CDK1/cyclin B partially phosphorylates Cdc25. Although attractive, this hypothesis has never been proven.

Following Ser287 dephosphorylation, Cdc25 becomes phosphorylated on Ser193 and Ser205 by *Xenopus* polo-like kinase, Plx1, and p38γ/p42MAPK, respectively, and therefore, activated (Kumagai and Dunphy, 1996; Nakajima et al., 2003; Perdiguero et al., 2003; Wang et al., 2007). Once activated, Cdc25 dephosphorylates and activates pre-MPF, which triggers the auto-amplification loop resulting in higher MPF activity (Hoffmann et al., 1993).

Additional sites on Cdc25 that are reportedly phosphorylated by CDK1/cyclin B, including Thr48, Thr67 and Thr308, appear to be required for the full activation of Cdc25 (Izumi and Maller, 1993). p42MAPK also phosphorylates Thr48 (Wang et al., 2007). These phosphorylations (Thr48 and Thr67) create Pin1 binding sites, which

either further increase the phosphatase activity or somehow ensures that Cdc25 remains fully active during the rest of the meiotic cell cycle (Fig. 5) (Stukenberg and Kirschner, 2001).

Based on these findings, it appears that activation of Cdc25 occurs at several levels, and these also have lead to the hypothesis that CDK1 forms a direct positive feedback loop with Cdc25, thereby amplifying Cdc25 activation (Hoffmann et al., 1993). However, it is unknown what is the prime kinase that triggers activation of Cdc25, considering that Thr138 phosphorylation is required for the initiation step. In principle, kinases that are involved in the initiation step can be activated prior to CDK1/cyclin B activation, leading to a threshold level of Cdc25 activity. It has been proposed that Plx1 may function as a triggering kinase that directly phosphorylates and activates Cdc25. Nevertheless, Plx1 does not phosphorylate Thr138 and the inhibition of Plx1 by injection of specific antibodies delay, but does not block, both oocyte maturation and Cdc25 activation, suggesting that Plx1 is not the kinase implicated in the process of Cdc25 pre-activation (Karaiskou et al., 1998; Qian et al., 1998).

Interestingly, p42MAPK has recently been shown to be able to phosphorylate Thr138 during *Xenopus* oocyte maturation (Wang et al., 2007). The progesterone treatment of oocytes activates low levels of p42MAPK prior to CDK1 activation and may trigger Cdc25 activation via Thr138 phosphorylation (Wang et al., 2007). However, several studies convincingly shown that the activation of p42MAPK is not necessary for both Cdc25 and progesterone-induced MPF activation in *Xenopus* oocytes (Dupre et al., 2002; Fisher et al., 1999; Gross et al., 2000; Peter et al., 2002), suggesting that other kinases are likely to be implicated in Cdc25 phosphorylation during oocyte maturation.

4.3. *Xenopus* RINGO Triggers Meiotic G2/M Transition

The overexpression of either a kinase-inactive CDK1 mutant (CDK1 K33R) or antibodies against CDK1 inhibit both progesterone-induced oocyte maturation and pre-MPF activation, suggesting that the activation of free CDK1 is required for these processes. This CDK1 mutant has been proposed to exert its negative effect on oocyte maturation by binding and sequestering newly synthesized proteins which normally would bind to and activate free CDK1 in the oocyte (Nebreda et al., 1995). The most likely candidates to activate free CDK1 would be the A- or B-type cyclins,

which are newly synthesized during oocyte maturation. However, the ablation of all the endogenous cyclins (cyclin A, cyclins B1, B2, B4 and B5) does not interfere with progesterone-induced M phase entry, indicating that cyclin synthesis is not required for this process (Hochegger et al., 2001; Kobayashi et al., 1991; Minshull et al., 1991). Moreover, Mos is unable to induce pre-MPF activation if protein synthesis is inhibited, although p42MAPK is normally activated in these conditions (Nebreda and Hunt, 1993; Yew et al., 1992).

What alternative protein could be participating in *Xenopus* oocyte maturation and pre-MPF activation, taking into consideration that new protein synthesis is absolutely required for meiotic resumption? After excluding Mos and cyclins A and B, an interesting candidate for a newly synthesized protein is RINGO (Rapid INducer of G2/M transition in Oocytes) or Speedy (Ferby et al., 1999; Lenormand et al., 1999).

RINGO/Speedy proteins were initially identified as new cell cycle regulators, which exhibited no amino acid sequence homology to cyclins but were able to activate CDK1 and CDK2 independently of cyclin binding (Ferby et al., 1999; Lenormand et al., 1999). Two groups independently cloned *Xenopus* RINGO/Speedy (XRINGO/Speedy) protein based in its ability to induce oocyte maturation (Ferby et al., 1999) or to rescue the sensitivity of the Rad1 *S. pombe* mutant to UV and γ-radiation (Ferby et al., 1999; Lenormand et al., 1999). The two proteins were 98% identical at the amino acid level and both were able to induce oocyte meiotic maturation much faster than progesterone and other meiotic regulators such as the protein kinase Mos (Ferby et al., 1999; Lenormand et al., 1999).

The elimination of endogenous XRINGO/Speedy mRNAs using antisense oligonucleotides delayed progesterone-induced oocyte maturation, suggesting that accumulation of XRINGO/Speedy protein is normally required for this process (Ferby et al., 1999). Similarly, a recent study using porcine RINGO/Speedy A2 has shown accelerated meiotic maturation in porcine oocytes indicating this function may be conserved for the mammalian RINGO/Speedy proteins as well (Kume et al., 2007).

Endogenous XRINGO/Speedy protein accumulates transiently in oocytes upon progesterone stimulation and contributes to meiosis I entry, probably via CDK1 or CDK2 activation (Gutierrez et al., 2006). XRINGO/Speedy is then downregulated soon after meiosis I by the ubiquitin ligase Siah-2, which probably requires phosphorylation of XRINGO on Ser243, and this is necessary for meiotic progression (Gutierrez et al., 2006). Recently, it has been reported that XRINGO/Speedy expression is regulated by

polyadenylation (Padmanabhan and Richter, 2006), and that XRINGO/Speedy translation is necessary for polyadenylation and translation of *mos* mRNA (Kim and Richter, 2007; Padmanabhan and Richter, 2006).

Experiments using a catalytically inactive CDK1 mutant (CDK1 K33R), which inhibits XRINGO-induce oocyte maturation, suggest that XRINGO/Speedy may function by directly activating monomeric CDK1 in *Xenopus* oocytes (Ferby et al., 1999). It has also been shown that recombinant XRINGO/Speedy protein can induce oocyte maturation and MPF activation in Cycloheximide-treated oocytes (Ferby et al., 1999), where the protein synthesis and Mos-p42MAPK-p90Rsk pathway are inhibited. Together, these observations suggest that the function of XRINGO/Speedy is more likely involved in the activation of CDK1 rather than in p42MAPK pathway.

AIM OF THE WORK

The G2/M transition during *Xenopus* oocyte maturation is induced by the steroid hormone progesterone, which triggers a signalling cascade that leads to the activation of CDK1/cyclin B (pre-MPF), the key regulator of M phase in all eukaryotic cells. Cdc25 phosphatase is responsible for the activating dephosphorylation of CDK1 on Thr14 and Tyr15, which is antagonized by the kinase Myt1. In late G2 phase, the balance between Myt1 and Cdc25 activities shifts in favor of CDK1 dephosphorylation, resulting in the activation of CDK1/cyclin B complexes and entry into meiosis. A key unanswered question regarding the meiotic G2/M phase transition is to understand how the balance between opposing Myt1 and Cdc25 activities is reversed to initiate the activation of CDK1/cyclin B.

CDK1 and CDK2 can be activated by non-cyclin proteins like RINGO, which were identified as potent inducers of the G2/M transition in *Xenopus* oocytes. The results discussed above suggest that *Xenopus* RINGO may be an essential protein that needs to be synthesized *de novo* upon progesterone stimulation to initiate the meiotic maturation of oocytes. However, it is unclear how XRINGO triggers the activation of pre-MPF in G2-arrested oocytes. The observation that recombinant XRINGO protein can induce oocyte maturation and MPF activation in Cycloheximide-treated oocytes (Ferby et al., 1999), where the protein synthesis and p42MAPK-p90Rsk pathway are inhibited, suggest that XRINGO could be directly targeting the cell cycle regulators Myt1 or Cdc25 during oocyte maturation.

The aim of this work is to clarity whether Myt1 and Cdc25 are putative CDK/XRINGO substrates in *Xenopus* oocytes. Indeed, we show here that XRINGO-activated CDKs can phosphorylate specific residues in the regulatory domain of Myt1 and Cdc25 proteins.

The finding of relevant substrates and specific amino acids that are selectively phosphorylated by CDK/XRINGO is a key discovery to understand the role of RINGO proteins in cell cycle regulation. An important question that arises is how XRINGO-activated CDKs achieve their substrate specificity. Like cyclins, which contain specific motifs to interact with their substrates, RINGO proteins may have their own unique substrate interaction motifs to target a separate set of substrates under different

conditions. We also show here that in fact, XRINGO and cyclin B use different motifs for substrate recruitment, which, in turn, could facilitate the phosphorylation of different sites in the same CDK substrate.

MATERIAL AND METHODS

1. DNA Cloning

Constructs for expression in *Xenopus* oocytes, FTX5-XRINGO, FTX5-Cdc25-Nt (9-205), FTX5-Myt1-Ct (399-548), FTX5-Myt1-Nt (1-338) and FTX5-Myt1 full-length have been previously described (Ferby et al., 1999; Nebreda et al., 1995; Palmer et al., 1998). Constructs based on FTX5 allow protein expression that can be recognized by Myc antibodies in its N-terminal.

Constructs to express recombinant proteins in *E. coli*, MBP-XRINGO, GST-Cdc25-Nt, GST-Cdc25 full-length, GST-CA-p90Rsk-EE, GST-Myt1-Ct, GST-CDK1 (*Xenopus*) WT and K33R and GST-CDK2 (human) WT, K33R, and T160A have been previously described (Ferby et al., 1999; Nebreda et al., 1995; Palmer et al., 1998). GST-Cdc25 fragments (F1, F2, F3, F4 and F5) and their mutants were provided by Jian Kuang (Wang et al., 2007). His-cyclin A (bovine) (Brown et al., 1995) and GST-Cak1/Civ1 (Brown et al., 1999) were purified from *E. coli*. A polycistronic construct to coexpress GST-CDK1, Cak1/Civ1, and cyclin B1-His in *E. coli* was provided by Yoshimi Tanaka. Recombinant His-cyclin B1 (human) was purified from baculovirus-infected insect cells as described (Kumagai and Dunphy, 1995). Baculovirus-expressed GST-CDK1 (human) was purchased from SignalChem (C22-14G-20).

2. Mutagenesis and Oligonucleotides for Mutagenesis

Cdc25 and Myt1 mutants were prepared using the Quick Change site-directed mutagenesis Kit (Stratagene, Cat. No. 200518-5) and were verified by DNA sequencing. Complementary oligonucleotide pairs (usually 30-45 bp long) were designed containing the desired point mutations in the middle of the primer sequence, had a minimum GC content of 40% and terminated in one or more C or G bases. The primers were extended by PCR using the reagents provided in the Kit under the following conditions: a total volume of 50 µl with 10-50 ng of template plasmid DNA, 1x reaction buffer, 250 nM of each primer, 1 µl dNTP mixture and 2.5 U of *Pfu*Turbo™ DNA polymerase was subjected to 16 cycles of 30 seconds denaturing at 95°C, 1 minute annealing at 55°C and 8 minutes DNA synthesis at 72°C. The PCR reactions were further incubated with 10 U DpnI restriction enzyme for 1 hour at 37°C to digest the parental DNA and directly transformed into 50 µl of *E. coli* XL1-Blue supercompetent cells and plated onto LB-ampicillin (50 µg/ml) agar plates. Resulting colonies were grown in LB broth-ampicillin (10 µg/ml) for plasmid preparation (Qiaprep Spin Miniprep Kit, Qiagen, Cat. No. 27106). Plasmids were subjected to DNA

sequencing to verify the mutation and the fidelity of the whole cDNA sequence. Oligonucleotides for mutagenesis were purchased from Invitrogen. The codons mutated are shown in red.

Name of the Mutant	Oligonucletide Sequence
Myt1 S414A	5'-AGGTCACCTCCCTGTGCTCCTTTTCCTAACCAT-3'
Myt1 S410A + S414A	5'-AGGGCTCTTCCAAGGGCACCTCCCTGTGCTCCT-3'
Myt1 S423A + S424A + S426A + S427A	5'-AACCATCTTGGGGAGGCCGCCTTCTCTAGTGACTGGGATGATGAG-3'
Myt1 S444A	5'-TTTGAGGTACCGCCAGCCCCACTGGCCACTCAC-3'
Myt1 T453A	5'-ACTCACCGAAATCTGGCATACCATGGGCAGGAG-3'
Myt1 S472A + S475A	5'-CTACTCTCAAGGCCGGCACTTGGAGCTACCTCTACCCCTCGC-3'
Myt1 S492A	5'-AGCATGAGAAAGAGGGCTGCCCTGCCTCTAACG-3'
Myt1 S504A	5'-AATGTCAGTCGGATTGCCCAGGATTCTACAGGC-3'
Myt1 S410D	5'-AGGGCTCTTCCAAGGGACCCTCCCTGTTCTCCT-3'
Myt1 S410D + S414D	5'-AGGGACCCTCCCTGTGACCCTTTTCCTAACCAT-3'
Myt1 S444D	5'-TTTGAGGTACCGCCAGACCCACTGGCCACTCAC-3'
Myt1 T453D	5'-ACTCACCGAAATCTGGACTACCATGGGCAGGAG-3'
Myt1 S472D + S475D	5'-CTACTCTCAAGGCCGGACCTTGGAGACACCTCTACCCCTCGC-3'
Myt1 S492D	5'-AGCATGAGAAAGAGGGACGCCCTGCCTCTAACG-3'
Myt1 S504D	5'-AATGTCAGTCGGATTGACCAGGATTCTACAGGC-3'
Myt1 A414S	5'- AGGGCACCTCCCTGTTCTCCTTGTCCTAACCAT-3'
Myt1 A410S + A414S	5'-AGGGCTCTTCCAAGGTCACCTCCCTGTTCTCCT-3'
Myt1 A444S	5'-TTTGAGGTACCGCCAAGCCCACTGGCCACTCAC-3'
Myt1 RNL-AAA	5'-ACCTTATTTCTTCCTGCCGCTGCGCTCGGTATGTTTGAC-3'

3. Isolation of *Xenopus laevis* Oocytes and Induction of Meiotic Maturation

Female *Xenopus laevis* frogs (African Reptile Park, South Africa) were anaesthetized with 0.4% 3-aminobenzoic acid ethyl ester (Sigma, Cat. No. A5040) for 30 minutes at room temperature (RT). The ovaries were removed surgically and stored in mBarth medium (15 mM HEPES, pH 7.6, 88 mM NaCl, 1 mM KCl, 2.4 mM $NaHCO_3$, 0.3 mM $Ca(NO_3)_2$, 0.4 mM $CaCl_2$, 0.8 mM $MgSO_4$, and 10 µg/ml each of Streptomycin and Penicillin-G). In some cases, it was necessary to prime the frogs before removing the ovaries to ensure oocyte maturation. For the priming, frogs were injected with 100 I.U. of pregnant mare serum gonadotropin (Intergonan®; Intervet, Toenisvorst, Germany) 3 days prior to operation.

Meiotic maturation of *Xenopus* oocytes was induced by incubation of manually dissected oocytes with 5 mg/ml (15 µM) of progesterone (Sigma, St Louis, MO. A 5 mg/ml stock solution was prepared in ethanol and stored at -20°C) or by injection with 50 nl of purified MBP-XRINGO protein (1 µg/µl) and scored by the appearance of a white spot at the animal pole of the oocytes, which indicates GVBD and entry meiosis I.

For expression of HA- or Myc-tagged proteins, oocytes were microinjected with 50 nl of *in vitro* transcribed mRNAs (mMessage mMachine kit, Ambion, Austin, TX) and maintained overnight in modified Barth's medium at 18°C before treatment.

Cicloheximide (Sigma), U0126 (Promega) or Roscovitine (Sigma) were added to the oocyte medium to a final concentration of 50 µg/ml, 50 µM and 100 µM, respectively, for 1-2 h before the injection of MBP-XRINGO (1 µg/µl).

4. Preparation of mRNAs for Injection into *Xenopus* Oocytes

To prepare mRNAs for injection into oocytes, cDNAs of interest were cloned into the vector FTX5 (Ferby et al., 1999; Nebreda et al., 1995; Palmer et al., 1998). The FTXs constructs were linearized with either XbaI or XmnI (depending on the presence of internal restriction sites), which cut the FTX-vectors downstream of their poly(A) sequence. Usually, 2 µg DNA (10 µl of a Qiagen DNA mini preparation) was digested for 2 h at 37°C in a total volume of 20 µl using 20 units (U) of the respective enzymes. Four µl of this linearization reaction was directly used to prepare mRNA using the mMESSAGE mMACHINE® T7 Ultra Kit (Ambion, Austin, Tx). In a total volume of 20 µl, 4 µl linearized DNA was incubated for 3 h at 37°C with 2 µl of 10X reaction buffer, 10

µl of NTPs and 2 µl T7 enzyme mix. After RNA synthesis, the plasmid DNA was digested with 2 U of DNase free RNase for 15 minutes at 37°C. Then, the reaction was supplemented with 10 µl of 10% SDS, diluted to 200 µl with RNase-free water, and 18 µl ammonium acetate stop solution was added. The mixture was vigorously vortexed prior to phenol/chloroform extraction and precipitation of the mRNA with 1 volume (200 µl) of isopropanol at -20°C for 30 minutes. The RNA pellet was washed twice with 70% ethanol and dissolved in 50 µl RNase-free water; 3 µl of this mRNA preparation was analyzed on a 1% TAE-agarose gel, and the stock was frozen in aliquots at -70°C.

5. Microinjection of *Xenopus* Oocytes with mRNAs

Xenopus oocytes were microinjected with 50 nl of solutions containing mRNA or purified protein in different concentrations. Control injections for mRNAs were done with water; for proteins, injection of dialysed buffer was used. The standard protocol of mRNA preparation yields mRNA concentrations about 1 µg/µl. These mRNAs were injected diluted into oocytes delivering between 5 and 50 ng of mRNA per oocyte. In general, injection of 5 to 50 ng mRNA leads to sufficient expression of the respective protein albeit the efficiency of translation varies between different mRNAs or even the same mRNA from distinct preparations, independently of the mRNA concentration. Therefore, the correct dilutions needed to be established for each mRNA preparation and experiment.

The injections were done with an IM 300 microinjector (Narishige). The oocytes were put onto a small plastic grid to prevent them from moving during the micromanipulation and injected preferentially at the border between the animal and the vegetal hemisphere as this ensures both expression of the mRNAs and optimal survival of the oocytes. After the injection, the oocytes were transferred quickly into mBarth medium to recover. Oocytes injected with mRNA were left for 14 h at 18°C for protein expression.

6. Preparation of *Xenopus* Oocyte Lysates

For the preparation of lysates, oocytes were homogenized in 10 µl per oocyte of ice-cold H1K buffer (80 mM β-glycerophosphate (pH 7.5), 20 mM EGTA, 15 mM $MgCl_2$, 1 mM DTT, 1 mM AEBSF, 2.5 mM Benzamidine, and 10 µg/µl each of Aprotinin

and Leupeptin) with a thin plastic stick. The lysates were centrifuged at 10,000 g for 10 min, and the cleared supernatants were stored at -70°C.

7. Lambda Phosphatase Treatment

Oocytes lysates (equivalent to one oocyte) were incubated with 250 U of lambda phosphatase (Upstate, 14-405) or phosphatase buffer alone (50 mM HEPES, 0.1 mM EDTA, 2 mM $MnCl_2$, 1 mM DTT) for 60 min at 30°C. Reactions were stopped by the addition of sample buffer and were analyzed by immunoblotting.

8. Immunoblotting, Immunoprecipitation and GST Pull-Down Experiments

Immunoblotting was performed as described (Ferby et al., 1999; Palmer et al., 1998). Briefly, oocyte lysates were separated by SDS-PAGE (sodium dodecyl sulphate-polyacrylamide gel electrophoresis) on a 15% Anderson gel, applying the equivalent of one oocyte per lane. After electrophoresis, the proteins were transferred from the polyacrylamide gels to nitrocellulose membranes (Protran 0.22 µm, Schleicher & Schuell) using a semi-dry blotting apparatus (Hoefer) or wet blotting apparatus (Bio-Rad). The membranes were blocked for 1 h at room temperature in PBS supplemented with 5% non-fat dry milk. The corresponding primary antibodies were usually diluted in PBS supplemented with 1% milk or, in fewer cases, 5% BSA. The membranes were incubated with the primary antibodies overnight at 4°C. After incubation with the first antibodies, the blots were washed three times for 5 min in PBS followed by incubation with the secondary antibodies for 1 h at room temperature. After extensive washing with PBS, secondary antibodies bound to the proteins on the membranes were detected using Odyssey Infrared Imaging System.

The following antibodies were used: CDK1 monoclonal antibody 3E1 (Ferby et al., 1999; Nebreda et al., 1995; Palmer et al., 1998), CDK1 (Santa Cruz Biotechnology, sc-54), CDK2 (Santa Cruz Biotechnology, sc-163), cyclin B2 rabbit antiserum (Hochegger et al., 2001), p42MAPK and Myt1 rabbit antisera (Palmer et al., 1998), Myc monoclonal antibody 9E10 (Santa Cruz Biotechnology, sc-40), HA (Roche, 3F10), His monoclonal antibody (Roche), p90Rsk-1 (Santa Cruz Biotechnology, sc-231), phospho-ERK (Santa Cruz Biotechnology, sc-7383), phospho-Tyr15-CDK1 (Cell Signaling, 9111), phospho-Tyr (Upstate, 05-321X), phospho-Thr160 (Santa Cruz Biotechnology, sc-101656), GST and MBP monoclonal antibodies were provided by

the Monoclonal Antibodies Core Unit (CNIO), phospho-Ser285-Cdc25 was provided by Dmitri Bulavin (Bulavin et al., 2003), phospho-Thr48-Cdc25, phospho-Thr67-Cdc25 and phospho-Thr138-Cdc25 were provided by Sally Kornbluth (Margolis et al., 2006b). For detection, we used Alexa Fluor 680- (Molecular Probes) or Li-Cor IRDye 800- (Rockland) labeled antibodies with the Odyssey Infrared Imaging System (Li-Cor).

Immunoprecipitations were performed as described (Palmer et al., 1998), using 5 µl of anti-Myc or 8 µl of anti-cyclin B2 antibodies and the following IP buffer: 50 mM Tris-HCl (pH 7.5), 150 mM NaCl, 1% (v/v) NP-40, 5 mM EDTA (pH 8.0), 5 mM EGTA (pH 8.0), 20 mM NaF, 0.1 µM PMSF, 0.5 µM Benzamidin, 2 µM Microcystin, 0.1 µM $NaVO_3$ and 10 µg/µl each of Aprotinin and Leupeptin. The immunocomplexes were washed twice with IP buffer and once with H1K buffer and then either used immediately for *in vitro* kinase assay as indicated below or analysed by immunoblotting.

For GST pull-down experiments, 5 µg of the bacterially produced GST fusion proteins were pre-bound to 20 µl of glutathione-Sepharose beads and then incubated in 100-250 µl of oocyte lysates. After 2 h rocking at 4°C, the beads were washed three times with H1K buffer and then analyzed by immunoblotting.

9. Staining with Coomassie Blue

In some cases, proteins were visualized by staining with Coomassie Blue R (Sigma). After SDS-PAGE electrophoresis, gels were stained for 5 minutes and distained until proteins became visible (2 h usually). Afterwards, gels were dried in a gel dryer at 80°C for 45 minutes.

10. Translation of Proteins in Reticulocyte Lysates

In order to verify proper transcription and translation of cDNAs cloned into FTX5 or into other vectors containing the T7 promoter, the TNT® T7 coupled reticulocyte lysate system (Promega, Cat. No. L4610) was used. In this coupled transcription/translation system, linear plasmid DNA is transcribed into RNA followed by translation into protein in a single tube reaction. For testing a plasmid constructs, 1.5 µl of a standard Qiagen plasmid mini preparation (about 200 ng DNA) was incubated in a total volume of 20 µl with 10 µl TNF reticulocyte lysate, 0.8 µl TNT reaction buffer, 0.4 µl amino acid mixture minus methione (1 mM), 0.8 µl Redivue™ Pro-Mix™ L-(^{35}S) *in vitro* cell labelling mix (10 µCi/ml; Amersham Cat. No. AGQ0080),

0.4 µl TNT RNA polymerase (units not given by Promega) and 16U RNasin® ribonuclease inhibitor (40U/µl, Promega Cat. No. N2515) for 90 min at 30°C. Five µl of this reaction were subjected to SDS-PAGE followed by autoradiography of the Coomassie-stained dried gel. Usually, exposure of 16 h was enough to detect distinct signals.

11. Myt1 Kinase Activity Assays

Myc-tagged Myt1 proteins were expressed from FTX5-Myt1 using the TNT® reticulocyte lysate system supplemented with canine pancreatic microsomal membranes as recommended by the supplier (Promega, L4610). We estimated that the concentration of Myt1 in the lysate was about 1 ng/µl by immunoblotting with anti-Myt1 antibodies using GST-Myt1-Ct as a reference. Typically, 20 µl of the Myt1-expressing reticulocyte lysate were diluted in 500 µl of IP buffer and then incubated at 4°C with 7 µl of 9E10 anti-Myc antibody for 3-4 h followed by incubation with 30 µl of protein G sepharose beads (Amersham Biosciences, 17-0618-02) for 1 h. As a control, reticulocyte lysates that do not express Myt1 were also immunoprecipitated. The Myc-Myt1 immunocomplexes bound to the beads were washed three times in IP buffer, twice with H1K buffer, and then incubated in 20 µl of kinase buffer containing 100 µM ATP and 120 ng of recombinant coexpressed CDK1-cyclin B1-Cak1/Civ1. After 30 min at RT, the CDK1/cyclin B1 activity was assayed with 4 µg of histone H1 and 2 µCi of [γ-^{32}P]ATP for 15 min at 30°C. Samples were finally boiled in sample buffer and analyzed by SDS-PAGE and autoradiography.

To determine the effect of XRINGO-activated CDK1 and CDK2 on Myt1 kinase activity, the immunoprecipitated Myc-Myt1 was preincubated with active recombinant CDK1/XRINGO or CDK2/XRINGO for 30-45 min at RT in 40 µl of H1K buffer supplemented with 300 µM ATP and then washed at least three times with H1K buffer before incubation with the substrate CDK1/cyclin B1. The phosphorylation of CDK1 on Tyr15 was studied by incubating the immunoprecipitated Myc-Myt1 in 30 µl of kinase buffer containing 350 µM ATP and 1 µg each of recombinant CDK1-K33R and cyclin B1 or XRINGO for 45–60 min. Samples were analyzed by immunoblotting with phopho-Tyr antibody.

To determine the effect of p90Rsk phosphorylation on Myt1 activity, the Myt1 immunocomplexes were preincubated with recombinant active CA-p90Rsk-EE for 40 min at RT in 30 µl of S6 kinase buffer (50 mM MOPS (pH 7.2), 1 mM DTT, 10 mM

$MgCl_2$, 10 mM *p*-nitrophenylphosphate, 1 mM $NaVO_3$, 10 µg/µl Leupeptin, 10 µg/µl Aprotinin, 100 µM PMSF or AEBSF) supplemented with 350 µM ATP and then washed at least three times with H1K buffer before incubation with the substrate CDK1/cyclin B1.

12. Activation of Recombinant CDK1 and CDK2

Purified bacterially expressed GST-CDK2 or baculovirus-expressed GST-CDK1 (200 or 400 ng) were activated by incubation with GST-Cak1/Civ1 (100-200 ng) followed by the addition of either His-cyclin A or His-cyclin B1 (200 ng), respectively, or by direct incubation with MBP-XRINGO (400 ng) and then used for kinase assays. In contrast, bacterially expressed GST-CDK1 cannot be directly activated *in vitro* by incubation with cyclins or XRINGO proteins and require prior incubation in concentrated extracts. For activation, GST-CDK1 (1.5 µg) was incubated in concentrated *Xenopus* egg extracts (15 µl) for 40 min at RT and then was recovered on glutathione-Sepharose beads (10 µl, Amersham Biosciences, 17-0756-01). After washing three times with IP buffer, the bead-bound GST-CDK1 was incubated with either MBP-XRINGO or His-cyclin B1 (1.5 µg) in kinase buffer and used for kinase assays.

13. Kinase Assays

Histone H1 kinase (H1K) assays were performed as described (Palmer et al., 1998) in a final volume of 12 µl of H1K buffer containing 4 µl of oocyte lysate, 50 µM cold ATP, 2 µCi of [γ-^{32}P]ATP (3000 Ci/mmol), and 4 µg of histone H1 (Sigma, H5505). After 15 min at 30°C, the phosphorylation reactions were terminated by addition of sample buffer and analyzed by SDS-PAGE and autoradiography.

Recombinant protein kinases were assayed for 15-30 min at 30°C in a final volume of 10 µl of kinase buffer (50 mM Tris-HCl (pH 7.5), 10 mM $MgCl_2$, 2 mM DTT, 100-150 µM cold ATP) containing 2 µCi of [γ-^{32}P]ATP and 4 µg of histone H1, 2 µg of GST-Myt1-Ct, 2 µg of GST-Cdc25-Nt, 2 µg of GST-Cdc25 full-length or the indicated amounts of immunoprecipitated Myt1. The reactions were stopped with sample buffer and analyzed by SDS-PAGE and autoradiography.

14. Tryptic Phosphopeptide Mapping of Cdc25 Proteins

Recombinant GST-Cdc25-Nt or GST-Cdc25 full-length (10 µg) were phosphorylated in the presence of [γ-^{32}P]ATP by CDK1/cyclin B or CDK1/XRINGO as described above. [^{32}P]-Cdc25 proteins were subjected to tryptic peptide mapping as recommended by the supplier (C.B.S. Scientific, Cat. No. HTLE-7002). Briefly, samples were resolved by 10% SDS-PAGE, excised from unstained gels, and rehydrated in 50 mM ammonium bicarbonate, pH 7.3-7.6. Cdc25 proteins were then digested with 50 ng of sequencing-grade trypsin (Promega, Cat. No. V5111) at 37°C overnight. The tryptic peptides were separated on thin-layer cellulose plates (EM chemicals) by horizontal electrophoresis at 1,000 V for 30 min in pH 1.9 buffer (2.5% formic acid and 7.8% acetic acid) followed by ascending thin layer chromatography in 32.5% n-butanol, 25% pyridine and 7.5% acetic acid. Following chromatography, the plate was dried and autoradiographed.

15. Analysis of Cdc25 Phosphorylation by Mass Spectrometry

GST-Cdc25-Nt (16 µg) was phosphorylated by CDK1/cyclin B or CDK1/XRINGO for 2 h at 30°C in the presence of 1 mM ATP. Eight µg (160 pmol) of control and phosphorylated GST-Cdc25-Nt per lane were loaded on non-denaturing 12.5% PAGE gels and visualized by Coomassie staining. The bands corresponding to the non-phosphorylated and phosphorylated Cdc25-Nt were excised from the gels and digested with sequencing-grade trypsin or chymotrypsin (Princeton Separations, Adelphia, USA). The peptides were analyzed in the Protein Technology Core Unit at CNIO, using an LTQ linear IT spectrometer (ThermoFinningan, San Jose, CA, USA) equipped with a dynamic nano-ESI source.

16. Recombinant Cdc25 Phosphatase Assays

The catalytic activity of recombinant full-length GST-Cdc25 towards inactive CDK1/cyclin B complexes was assayed using pre-MPF immunoprecipitated from G2-arrested oocytes. Typically, 250 µl of G2-arrested oocytes lysates were diluted in 500 µl of IP buffer and then incubated at 4°C with 8 µl of agarose-conjugated p13^{Suc1} antibody for 3 h (Upstate, Cat. No. 14-132). The p13^{Suc1}-CDK1/cyclin B immunocomplexes were washed three times in IP buffer and twice with phosphatase buffer (40 mM Tris-HCl, pH 8, 300 mM NaCl, 10 mM EDTA, 10 mM DTT).

To determine the effect of cyclin B- and XRINGO-activated CDK1 on Cdc25 phosphatase activity, recombinant GST-Cdc25 (1 µg) bound to glutathione-beads was preincubated with active CDK1/cyclin B or CDK1/XRINGO (250 ng each complex) at 30ºC in 40 µl of H1K buffer supplemented with 300 µM ATP. After 60 min, GST-Cdc25 was recovered and washed at least three times with phosphatase buffer. Bead-bound GST-Cdc25 was incubated with $p13^{Suc1}$-CDK1/cyclin B immunocomplexes during 45 min at 30ºC in phosphatase buffer and then washed at least three times with H1K buffer. Kinase assays were performed with histone H1 (4 µg) and [γ-^{32}P]ATP for 15 min at 30ºC. H1 phosphorylation was visualized by autoradiography.

17. Protein Analysis by Two Dimensional Gels

Recombinant GST-Cdc25-Nt or GST-Myt1-Ct (10 µg) were phosphorylated by CDK2/cyclin A or CDK2/XRINGO in the presence or absence of ATP as described above. The non-phosphorylated and phosphorylated proteins were analyzed by two dimensional gels in the Protein Technology Core Unit at CNIO.

18. Bacterial Expression and Purification of GST, MBP and 6xHis Fusion Proteins

Recombinant GST-, MBP- or 6xHis-fusion proteins were expressed in *Escherichia coli* DE3. For GST fusions, fresh overnight LB-ampicillin (100 µg/ml) cultures were diluted 10-fold with fresh medium and incubated at 37°C until the *A*595 was 0.4-0.5. For protein expression, cultures were incubated for 5 h at 25°C using 0.1 mM isopropyl-β-D-thiogalactopyranoside (IPTG). The cells were harvested, washed with cold phosphate-buffered saline (PBS) and lysed in 50 mM Tris, pH 7.5, 150 mM NaCl, 1 mM EDTA, 1 mM phenylmethylsulfonyl fluoride (PMSF), 1 mM benzamidine, 0.05% NP-40 and 0.5 mg/ml lysozyme, for 30 min at 4°C. After sonication and centrifugation at 10,000 *g* for 20 min, the supernatant was mixed with glutathione-Sepharose (Amersham Biosciences, 17-0756-01) for 90 min at 4°C. Beads were washed in lysis buffer lacking NP-40 and lysozyme, and the GST fusion proteins were eluted with 10 mM glutathione in 50 mM Tris, pH 7.5, 50 mM NaCl, 1 mM dithiothreitol (DTT).

For the purification of MBP fusions, *E. coli* cultures were induced with 0.1 mM IPTG as above. Bacterial pellets were lysed for 20 min at 4°C in 50 mM Tris, pH 8.0, 50 mM NaCl, 5 mM EDTA, 1 mM PMSF and 1 mg/ml lysozyme. The lysates were

sonicated, and 1 mM DTT was added before centrifugation. The supernatants were incubated with amylose beads (New England Biolabs, E8021S) for 90 min at 4°C and the beads were washed with 50 mM Tris, pH 8.0, 50 mM NaCl, 1 mM DTT. The MBP-fused protein was eluted in the same buffer supplemented with 0.1 mM EDTA and 12 mM maltose.

For the purification of 6xHis fusions, the *E. coli* cultures were induced with 0.1 mM IPTG for 5 h at 30°C. The cells were harvested, washed with cold PBS and lysed in 5 mM Imidazole, 500 mM NaCl, 20 mM Tris-HCl pH 7.9, 1 mM PMSF, 1 mM benzamidine and 1 mg/ml lysozyme for 30 min at 4°C. The lysates were sonicated, and 0.1 % NP40 was added before centrifugation. The supernatants were incubated with talon beads (Clontech, 635501) for 90 min at 4°C and the beads were washed with 60 mM Imidazole, 500 mM NaCl, 20 mM Tris-HCl pH 7.9. The 6xHis-fused protein was eluted in the same buffer supplemented with 1M Imidazole.

Fractions containing the purified GST, MBP or histidine fusion proteins were dialysed overnight against 20-50 mM Tris, pH 7.5-8.0, 50 mM NaCl, 0.1 mM EDTA, 0.5 mM DTT, 5% glycerol and stored in aliquots at -70°C. A Coomassie-stained gel with the purified recombinant proteins is shown in Figure 6.

19. Analysis of the Interaction of Purified Recombinant Proteins with Reticulocyte Lysate Translated Proteins

To investigate the interaction between two proteins, one of the proteins was purified as a bacterially expressed recombinant protein tagged with GST, His or MBP, and the other putative binding partner was translated in the TNT® T7 coupled reticulocyte lysate system (Promega, Cat. No. L4610). The putative interaction was tested in a pull-down experiment. Per pull-down reaction, 5 µg of the recombinant protein (the putative binding partner and the tag protein alone as a control) were bound to 20 µl of glutathione sepharose or amylose resin, depending on the tag, by incubating the protein in IP buffer with pre-washed beads for 2 h at 4°C on a rotating wheel, followed by three washes with IP buffer. In parallel, 1.5 µl plasmid mini preparation DNA encoding the other binding partner was translated in a total volume of 20 µl using 10 µl TNT reticulocyte lysate, 0.8 µl TNT reaction buffer, 0.4 µl amino acid mixture minus Methionine (1 mM), 0.8 µl Redivue™ Pro-mix™ L-(^{35}S) *in vitro* cell labelling mix (10 µCi/ml; Amersham Cat. No. AGQ0080), 0.4 µl TNT RNA polymerase (units not given by Promega) and 16 U RNasin® ribonuclease inhibitor (40 U/µl,

Promega, Cat. No. N2515) for 90 min at 30°C. Three µl were removed to analyse the reaction by SDS-PAGE. The remaining volume was filled up to 500 µl with IP buffer and divided into two aliquots. One aliquot was incubated in a total volume of 500 µl with 5 µg of GST or MBP beads corresponding as a control reaction. The other aliquot was incubated with 5 µg of the recombinant protein of interest bound to 20 µl of the corresponding beads for 2-4 h at 4°C on a rotating wheel. The beads were washed three times with 500 µl IP buffer, resuspended in 20 µl 5x sample buffer, boiled for 5 min at 95°C and subjected to SDS-PAGE followed by autoradiography of the Coomassie-stained dried gel.

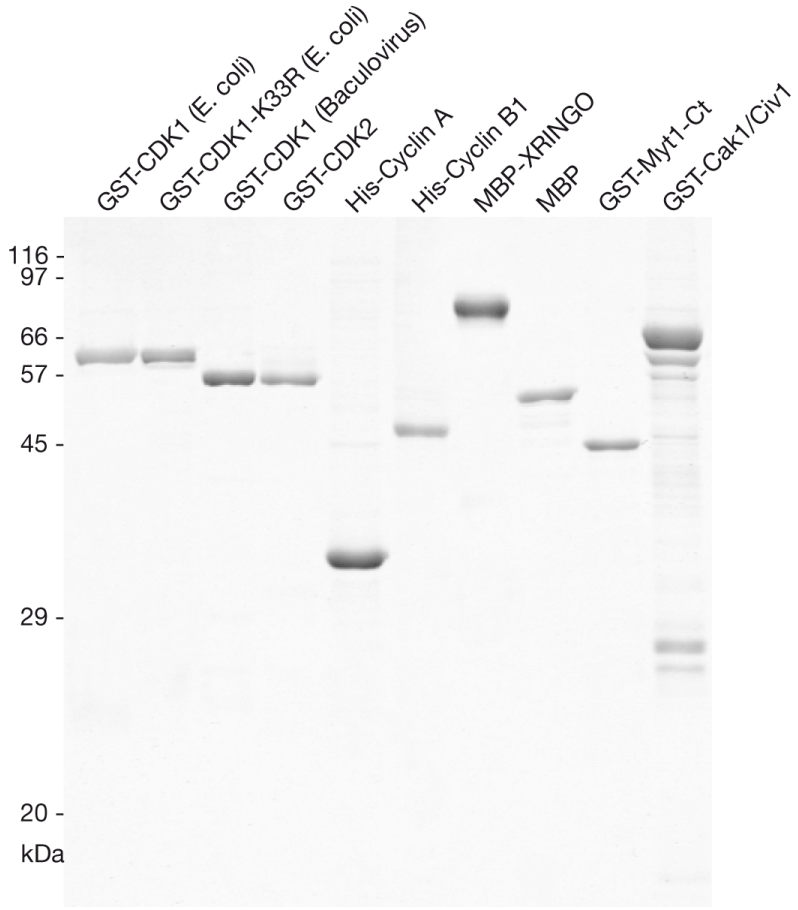

Figure 6 | Purified Recombinant Proteins. Purified recombinant proteins (0.5-1 µg) were analyzed by SDS-PAGE and stained with Coomassie. Molecular weight standards are indicated in kilodaltons (kDa) at the left. GST-CDK1 and GST-CDK1-K33R from *E. coli* and GST-CDK1 from baculovirus-infected insect cells are indicated.

RESULTS

1. Meiotic Inactivation of Myt1 Kinase Activity by Interplay between CDK/XRINGO and p90Rsk

1.1. Characterization of Purified Proteins

The main objective of this work was the identification of substrates phosphorylated by CDK/XRINGO complexes. For that reason it was necessary to get a source of efficient and reproducible *in vitro* kinase activity.

We initiated our work by purifying and characterizing the recombinant CDK1, CDK2, Cak1/Civ1, cyclin A, cyclin B and XRINGO proteins that would be used throughout these studies, as described in Material and Methods. The purity and the integrity of these proteins is show in Figure 6.

As we described in the Introduction, CDKs are catalytically inactive as monomers and their activation requires binding to cyclins. In addition, CDK/cyclin complex requires phosphorylation of a conserved Thr residue located on the activation loop for full activation (Jeffrey et al., 1995). The kinase responsible for this phosphorylation is the CDK-activating kinase, CAK in higher eukaryotes or Cak1/Civ1 in budding yeast (Kaldis et al., 1998). In contrast, CDK/RINGO complexes do not require phosphorylation on the activation loop for CDK activity (Cheng et al., 2005a; Dinarina et al., 2005; Karaiskou et al., 2001b).

We first analyzed the activation of CDK1 and CDK2 by cyclins and XRINGO in the absence or presence of Cak1/Civ1. We confirmed that the yeast CDK-activating kinase Cak1/Civ1 phosphorylates CDK1 and CDK2 on the activation loop, specifically on Thr161 and Thr160, respectively (Fig. 7).

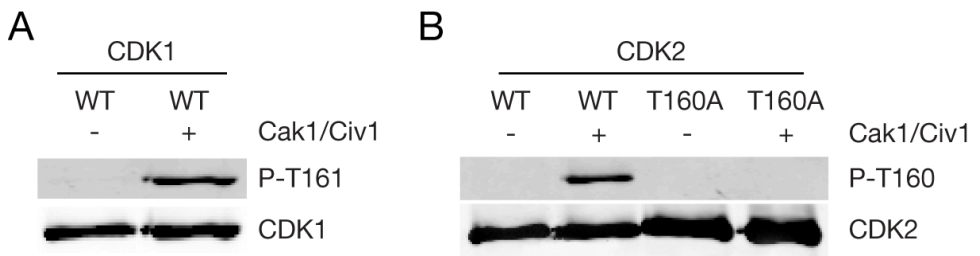

Figure 7 | CDK1 and CDK2 are Phosphorylated by Cak1/Civ1 on the T loop. (A) Baculovirus-expressed GST-CDK1 (200 ng) or (B) bacterially produced GST-CDK2 WT or T160A mutant (200 ng) were incubated with Cak1/Civ1 (200 ng) in the presence of ATP (150 μM) for 10 min at RT. The reaction mixtures were analyzed by immunoblotting using phospho-specific antibodies.

Unphosphorylated CDK1 and CDK2 in complex with cyclin B and cyclin A, respectively, display a low but detectable histone H1 kinase activity (Fig. 8A and 8B), as previously reported (Desai et al., 1992). When both kinases CDK1 and CDK2 were preincubated in the presence of Cak1/Civ1 and ATP, we observed a strong increase in the H1 kinase activity triggered by purified cyclins (Fig. 8A and 8B), confirming the importance of T loop phosphorylation for the kinase activity of CDK/cyclin complexes. In contrast, the recombinant MBP-XRINGO protein activated CDK1 and CDK2 in the presence or absence of Cak1/Civ1 equally well, indicating that phosphorylation in the activation loop is not required for CDK activation by XRINGO (Fig. 8A and 8B). Therefore, we used Cak1/Civ1 phosphorylated CDKs for activation by cyclins and unphosphorylated CDKs for activation by XRINGO in all the following experiments.

We used histone H1 to normalize the kinase activities. We found that CDK/XRINGO complexes require two times more protein activator and kinase protein to reach the same level of histone H1 phosphorylation than the same CDKs activated by cyclins (Fig. 8). These results are in agreement with a previous report showing that CDK/RINGO complexes are less active than CDK/cyclin complexes (Cheng et al., 2005a).

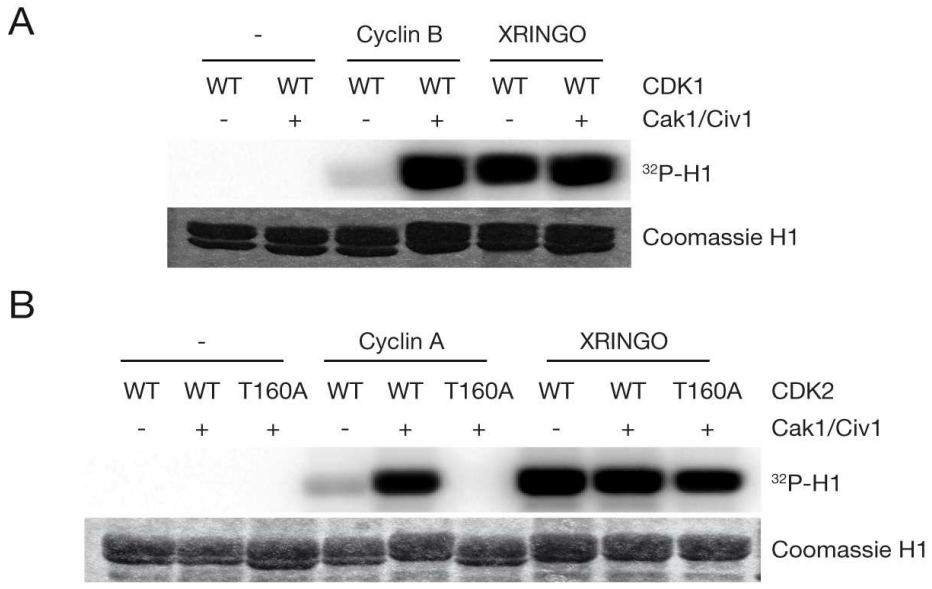

Figure 8 | XRINGO Activates CDK1 and CDK2 Independently of T loop Phosphorylation. (A) Baculovirus-expressed GST-CDK1 (200 or 400 ng) was incubated with cyclin B (200 ng) or MBP-XRINGO (400 ng). (B) Bacterially produced GST-CDK2 WT or T160A mutant (250 or 500 ng) was incubated with cyclin A (250 ng) or MBP-XRINGO (500 ng). Where indicated, CDKs were preincubated with Cak1/Civ1 (200 ng) for 10 min at RT in the presence of 150 μM ATP before adding cyclins or XRINGO. Kinase assays were performed with histone H1 (4 μg) and [γ-^{32}P]ATP for 15 min at 30°C. H1 phosphorylation was visualized by autoradiography.

1.2. CDK/XRINGO Phosphorylates and Inhibits Myt1 Kinase Activity

1.2.1. XRINGO Induces Myt1 Phosphorylation in *Xenopus* Oocytes

CDK/XRINGO Complexes Phosphorylate Myt1 *in vitro*

During progesterone-induced *Xenopus* oocyte maturation, Myt1 undergoes a significant electrophoretic mobility upshift due to hyperphosphorylation (Gross et al., 2000; Palmer et al., 1998; Peter et al., 2002). The C-terminal regulatory domain of Myt1 includes several potential CDK phosphorylation sites, which are likely to participate in the regulation of the catalytic activity of Myt1 (Inoue and Sagata, 2005; Wells et al., 1999).

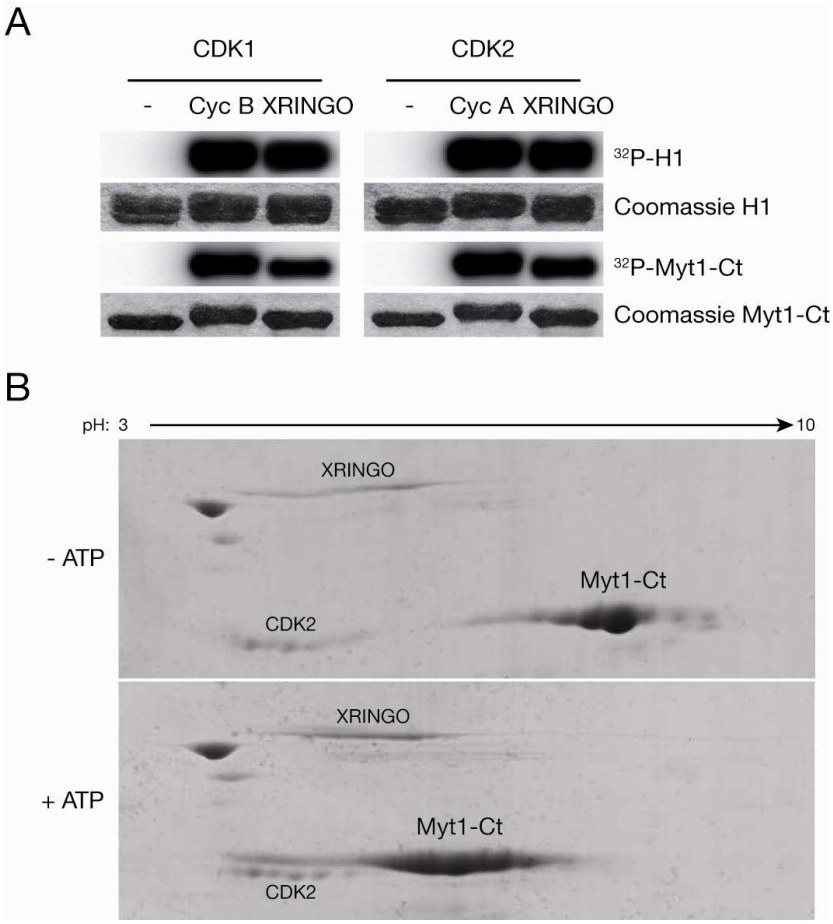

Figure 9 | Phosphorylation of Myt1 by CDK/XRINGO. (A) Baculovirus-expressed GST-CDK1 (200 or 400 ng) was incubated with cyclin B (200 ng) or MBP-XRINGO (400 ng). GST-CDK2 (250 or 500 ng) was incubated with cyclin A (250 ng) or MBP-XRINGO (500 ng). In the case of cyclins, CDKs were preincubated with Cak1/Civ1 (200 ng) for 10 min at RT in the presence of ATP. Kinase assays were performed with histone H1 (4 µg) or Myt1-Ct (2 µg) and [γ-^{32}P]ATP for 15 min at 30°C. Myt1 and H1 phosphorylations were visualized by autoradiography. (B) CDK2/XRINGO complex was prepared as in (A) and kinase assays were performed with GST-Myt1-Ct (10 µg) in the presence or absence of ATP for 15 min at 30°C. Myt1 phosphorylation was visualized by 2D gel. IPG strips (pH 3–10) were used for the IEF and SDS-PAGE 12% for the second dimension.

To test whether the regulatory domain of Myt1 was directly phosphorylated by CDK/XRINGO, we fused the C-terminal residues 399-548 of Myt1 (Myt1-Ct) to glutathione-S-transferase (GST) and the bacterially produced fusion protein was used in *in vitro* kinase assays as described in (Palmer et al., 1998). We found that recombinant CDK1 and CDK2 activated by XRINGO phosphorylated Myt1-Ct as efficiently as CDK1/cyclin B and CDK2/cyclin A, respectively (Fig. 9A). Histone H1 was used to normalize the kinase activities. Moreover, CDK/XRINGO phosphorylation changed the electrophoretic mobility of Myt1 in two dimensional gels, so that several new spots appeared, suggesting that Myt1 was phosphorylated on several residues (Fig. 9B).

XRINGO Induces Myt1 Phosphorylation in Oocytes

Next, we investigated whether XRINGO was able to induce Myt1 phosphorylation in oocytes by injecting mRNA-encoding Myc-tagged Myt1-Ct, and then reinjecting the oocytes with recombinant MBP-XRINGO protein. We observed that the electrophoretic mobility of Myt1, as determined by immunoblotting, was significantly reduced when oocytes entered meiosis I (Fig. 10A), which is in agreement with previous results showing Myt1 hyperphosphorylation in M phase (Inoue and Sagata, 2005; Mueller et al., 1995b). Interestingly, we also detected an electrophoretic mobility upshift of Myt1 only 1 h after injection of XRINGO, at a time when MPF and p42MAPK-p90Rsk pathway were all inactive (Fig. 10A). Furthermore, this early Myt1 mobility upshift correlated with a small increase in the histone H1 kinase (H1K) activity of the total lysates from oocytes injected with XRINGO. In contrast, the histone H1 kinase activity associated with CDK1/cyclin B appears 3 h after XRINGO injection (Fig. 10A). To determine whether the changes in the electrophoretic mobility upshift of Myt1 in *Xenopus* oocytes were due to phosphorylation, lysates from oocytes expressing Myc-tagged Myt1-Ct proteins were treated with λ phosphatase, which efficiently dephosphorylates phospho-Ser, phospho-Thr and phospho-Tyr residues. After treatment with λ phosphatase, we observed that the slower migrating bands disappeared, indicating that the mobility upshifts of Myt1 were indeed due to phosphorylation (Fig. 10B).

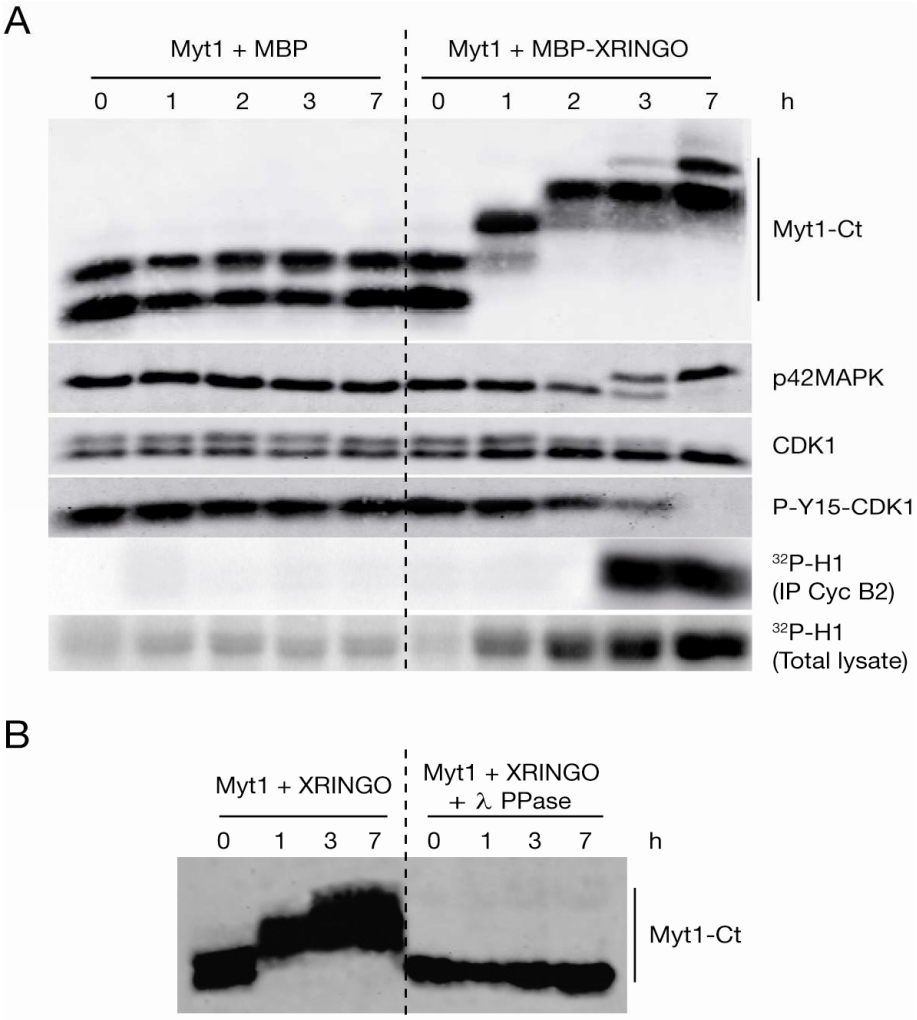

Figure 10 | XRINGO Induces Myt1 Phosphorylation in *Xenopus* Oocytes. (A) *Xenopus* oocytes were injected with Myc-tagged Myt1-Ct mRNA, incubated 14 h at 18°C, and reinjected with MBP or MBP-XRINGO (50 ng). Oocytes were collected at the indicated times after the second injection. H1K activity was assayed using either total lysates (4 µl) or cyclin B2 immunoprecipitates (200 µl of total lysate). Oocyte lysates were also analyzed by immunoblotting. Myt1-Ct was detected with Myc antibody. (B) Oocyte lysates were treated or not with λ phosphatase, as indicated, and analyzed for Myt1 expression by immunoblotting with Myc antibody.

We also analyzed the phosphorylation of Myt1-Ct during progesterone-induced oocyte maturation. We found that the electrophoretic mobility of Myt1-Ct was reduced at early time points, before the p42MAPK-p90Rsk pathway and MPF were activated, and this correlated with the progesterone-induced accumulation of endogenous XRINGO protein in the oocytes (Fig. 11).

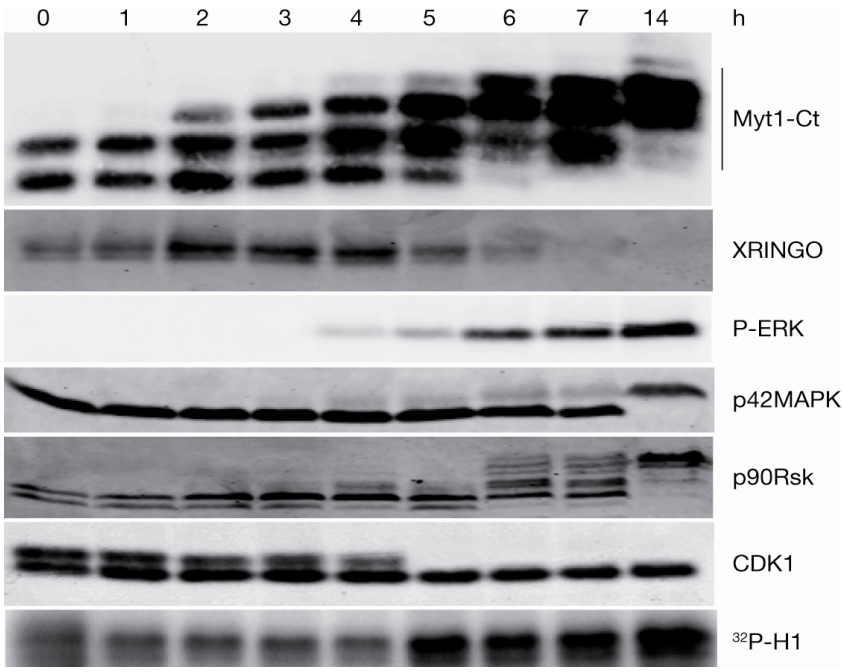

Figure 11 | Myt1 Phosphorylation during Oocyte Maturation. *Xenopus* oocytes from primed frogs were injected with Myc-tagged Myt1-Ct mRNA and 14 h later were incubated at 18°C with progesterone for the indicated times. Oocyte extracts were assayed for H1K activity or analyzed by immunoblotting. Myt1-Ct was detected with Myc antibody.

To test whether Myt1 could be directly phosphorylated by CDK/XRINGO in oocytes, we used the CDK1 and CDK2 inhibitor Roscovitine. We first confirmed that Roscovitine was able to inhibit histone H1 and Myt1-Ct phosphorylations induced by both cyclin B- and XRINGO-activated CDK1 *in vitro* (Fig. 12A). We found that Roscovitine abolished the XRINGO-induced phosphorylation of Myt1-Ct in *Xenopus* oocytes (Fig. 12B). We also observed Myt1 phosphorylation in XRINGO-injected oocytes treated with the protein synthesis inhibitor Cycloheximide (CHX), where the p42MAPK-p90Rsk pathway was inhibited (Fig. 12C). Furthermore, CHX did not affect the ability of XRINGO to induce MPF activation and entry into meiosis I, as expected from previous work (Ferby et al., 1999). Taken together, these results suggest that XRINGO induces the phosphorylation of the regulatory domain of Myt1 in the absence of both new protein synthesis and activation of the p42MAPK pathway; however, this XRINGO-induced phosphorylation requires CDK activity.

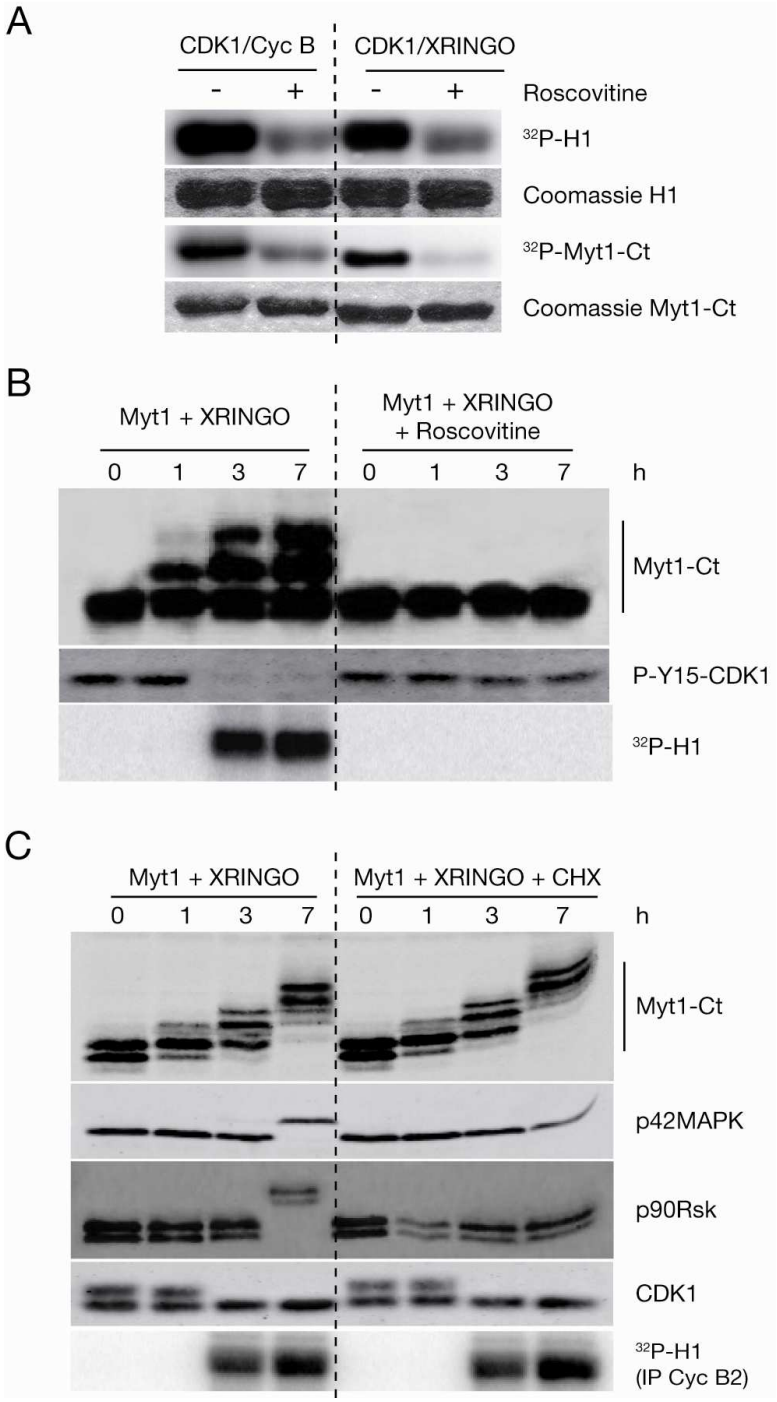

Figure 12 | XRINGO-Induced Phosphorylation of Myt1 Requires CDK Activation. (A) Baculovirus-expressed GST-CDK1 (200 or 400 ng) was incubated with either cyclin B (200 ng) or MBP-XRINGO (400 ng). In the case of cyclin B, CDK1 was preincubated with Cak1/Civ1 for 10 min at RT in the presence of ATP. Roscovitine (10 μM) or DMSO (-) was added 10 min before performing the kinase assays with histone H1 (4 μg) or Myt1-Ct (2 μg). Phosphorylation of Myt1 and H1 was visualized by autoradiography. (B) *Xenopus* oocytes were injected with Myc-tagged Myt1-Ct mRNA and 14 h later were treated or not with Roscovitine (100 μM) for 1 h before being injected with MBP-XRINGO. Oocyte extracts were assayed for H1K phosphorylation and analyzed by immunoblotting with phospho-Tyr15-CDK1 or Myc antibodies. (C) Oocytes were injected with Myc-tagged Myt1-Ct mRNA and incubated for 14 h at 18°C. Next, the oocytes were treated or not with Cycloheximide (CHX) and 1 h later were injected with MBP-XRINGO. Oocyte extracts were analyzed by immunoblotting. Myt1-Ct was detected with Myc antibody. H1K activity was assayed using cyclin B2 immunoprecipitates.

1.2.2. Identification of Myt1 Sites Phosphorylated by CDK/XRINGO

The sequence of *Xenopus* Myt1-Ct contains eight consensus CDK phosphorylation sites (Ser/Thr-Pro) (Fig. 13).

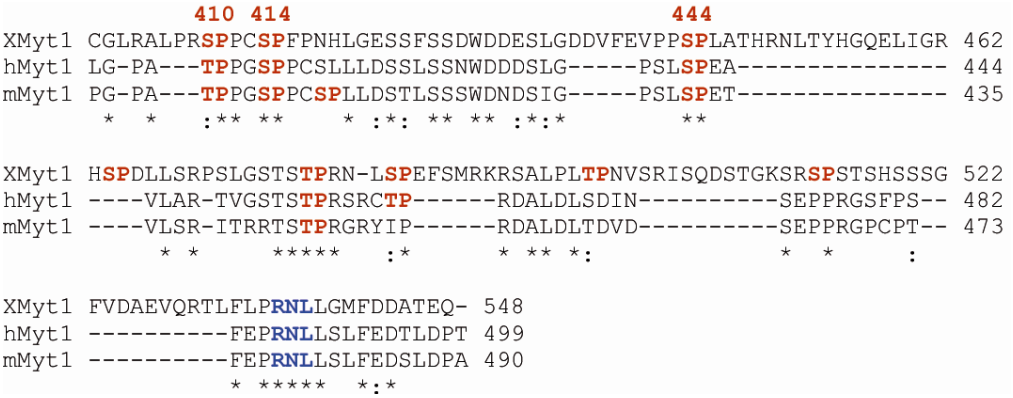

Figure 13 | Sequence Alignment of the C-Terminal Regulatory Domains of *Xenopus*, Human and Mouse Myt1 Proteins. Ser/Thr-Pro motifs are highlighted in red and RXL motif in blue. Asterisks and colons indicate identical and conserved residues, respectively.

To identify which residues of Myt1 were phosphorylated by CDK/XRINGO, we used generic phospho-Ser and phospho-Thr antibodies and we found that Myt1-Ct was phosphorylated by CDK1/XRINGO mainly on Ser residues *in vitro*. In contrast, Myt1-Ct was phosphorylated efficiently on both Ser and Thr residues by CDK1/cyclin B (Fig. 14A). These results suggest that CDK1/cyclin B and CDK1/XRINGO complexes might phosphorylate different sites on the regulatory domain of Myt1. In agreement with this idea, we also observed that XRINGO and cyclin B produce different patterns of electrophoretic mobility upshift of Myt1 in *Xenopus* oocytes, although in both cases the p42MAPK pathway and MPF were activated with similar kinetics (Fig. 14B).

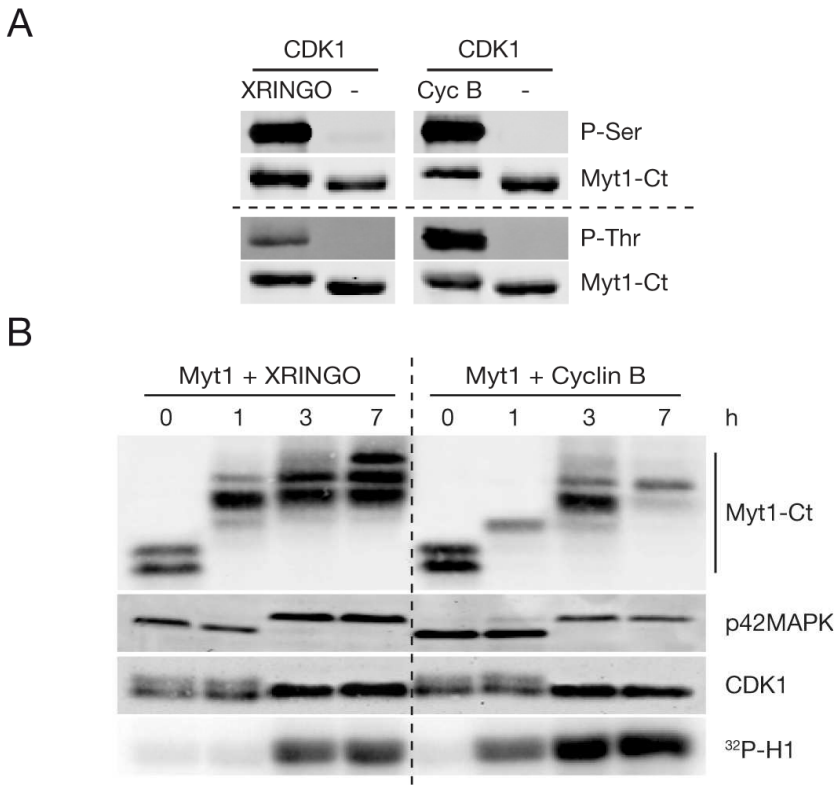

Figure 14 | CDK1/XRINGO and CDK1/Cyclin B Phosphorylate Different Sites on the Regulatory Domain of Myt1. (A) Baculovirus-expressed GST-CDK1 (200 or 400 ng) was incubated with cyclin B (200 ng) or MBP-XRINGO (400 ng). In the case of cyclin B, CDK1 was preincubated with Cak1/Civ1 (200 ng) for 10 min at RT in the presence of ATP. Kinase assays were performed with Myt1-Ct (2 µg) and ATP for 15 min at 30°C. The reaction mixture was analyzed by immunoblotting using phospho-specific antibodies. (B) *Xenopus* oocytes were injected with Myc-tagged Myt1-Ct mRNA, incubated 14 h at 18°C, and reinjected with MBP-XRINGO or His-cyclin B (25 ng). Oocytes were collected at the indicated times after the second injection. Oocyte extracts were assayed for H1K activity or analyzed by immunoblotting. Myt1-Ct was detected with Myc antibody.

To identify the Myt1 residues differentially phosphorylated by CDK/XRINGO, we systematically mutated Ser to Ala residues in the Myt1-Ct region (Fig. 13). We found that a mutant with seven Ser (410, 414, 423, 424, 426, 427 and 444) replaced by Ala (Myt1-7A) was poorly phosphorylated *in vitro* by CDK1/XRINGO (Fig. 15A) and CDK2/XRINGO (Fig. 15B). Surprisingly, both CDK1/cyclin B and CDK2/cyclin A phosphorylated the Myt1-7A mutant with similar efficiency as the WT Myt1 (Fig. 15A and 15B). Consistent with these results, Myt1-7A expressed in oocytes did not display the XRINGO-induced mobility upshift observed in WT Myt1, although the p42MAPK pathway and MPF were active in these oocytes (Fig. 15C).

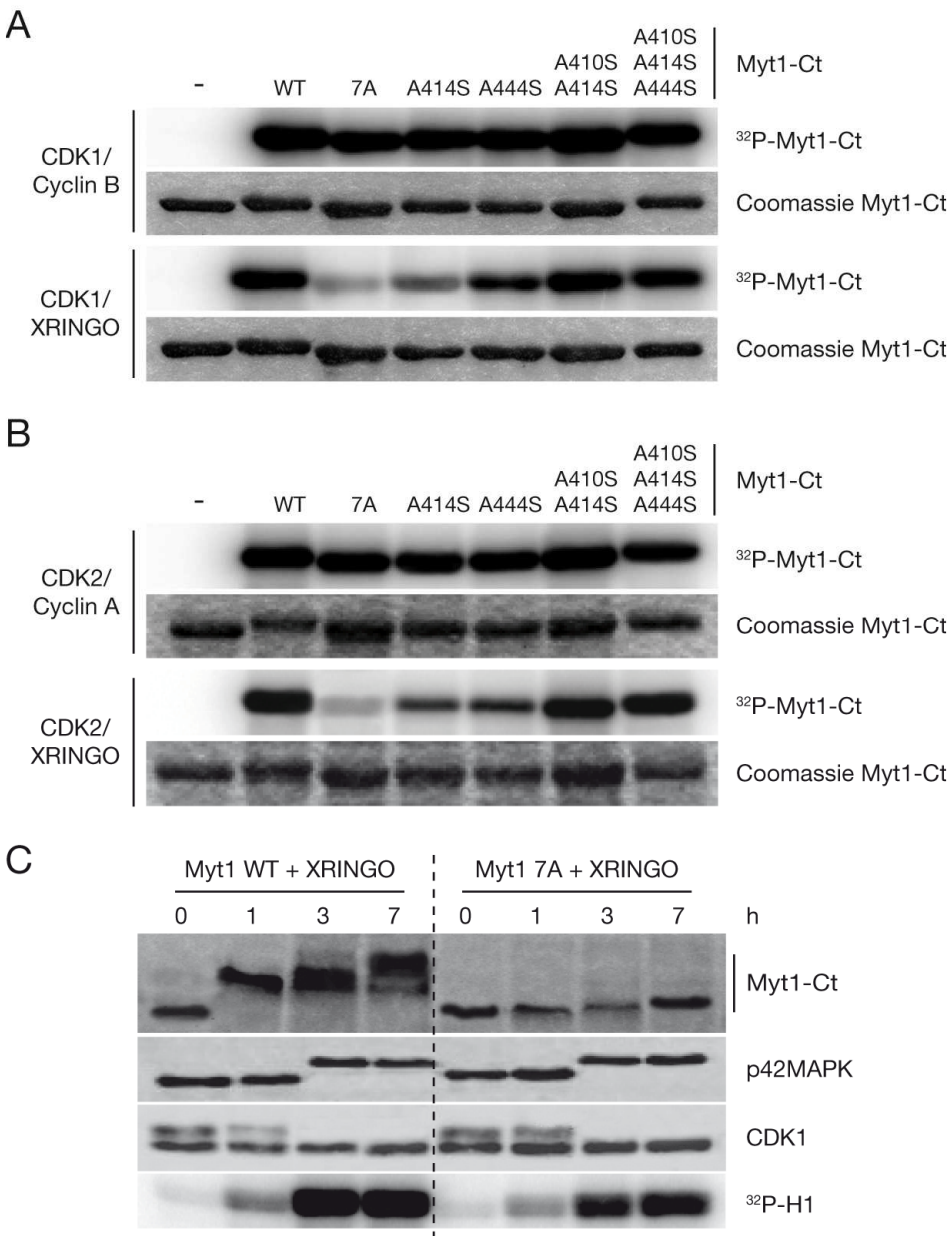

Figure 15 | Identification of Specific CDK/XRINGO Phosphorylation Sites on the Regulatory Domain of Myt1. (A) Baculovirus-expressed GST-CDK1 (200 or 400 ng) was incubated with cyclin B (200 ng) or MBP-XRINGO (400 ng). (B) GST-CDK2 (250 or 500 ng) was incubated with cyclin A (250 ng) or MBP-XRINGO (500 ng). In the case of cyclins, CDK1 and CDK2 were preincubated with Cak1/Civ1 (200 ng) for 10 min at RT in the presence of ATP. WT or mutant GST-Myt1-Ct proteins (2 µg) were then added together with [γ-^{32}P]ATP, and the reactions were incubated for 15 min at 30°C. Myt1 phosphorylation was visualized by autoradiography. (C) *Xenopus* oocytes were injected with GST-Myt1-Ct, either WT or with 7 Ser mutated (Myt1-7A), incubated 30 min, and then reinjected with MBP-XRINGO (50 ng). Oocytes were collected at the indicated times after XRINGO injection. Oocyte lysates were assayed for H1K activity or analyzed by immunoblotting. Myt1-Ct was detected with GST antibody.

The Myt1-7A mutant contained three Ser-Pro consensus sites (410, 414 and 444) changed to Ala that are conserved in the sequence of mouse and human Myt1 proteins (Fig. 13). To test the contribution of these three residues to the phosphorylation of Myt1 by CDK/XRINGO, we reintroduced these Ser in the Myt1-7A mutant and then performed *in vitro* kinase assays. Our results showed that the mutant Ala410Ser, Ala414Ser, Ala444Ser was phosphorylated as efficiently as WT Myt1, suggesting that these three Ser accounted for most of the CDK/XRINGO-induced phosphorylation of Myt1-Ct (Fig. 15A and 15B). To confirm these observations, we performed the complementary experiment mutating Ser410, Ser414 and Ser444 to Ala in WT Myt1-Ct (mutant Myt1-3AP). We observed that these three mutations eliminated about 80% of the phosphorylation by CDK1/XRINGO or CDK2/XRINGO *in vitro* (Fig. 16A). In contrast, the CDK1/cyclin B and CDK2/cyclin A-induced phosphorylations were only reduced by about 30% when comparing the mutant Myt1-3AP with WT Myt1 (Fig. 16A).

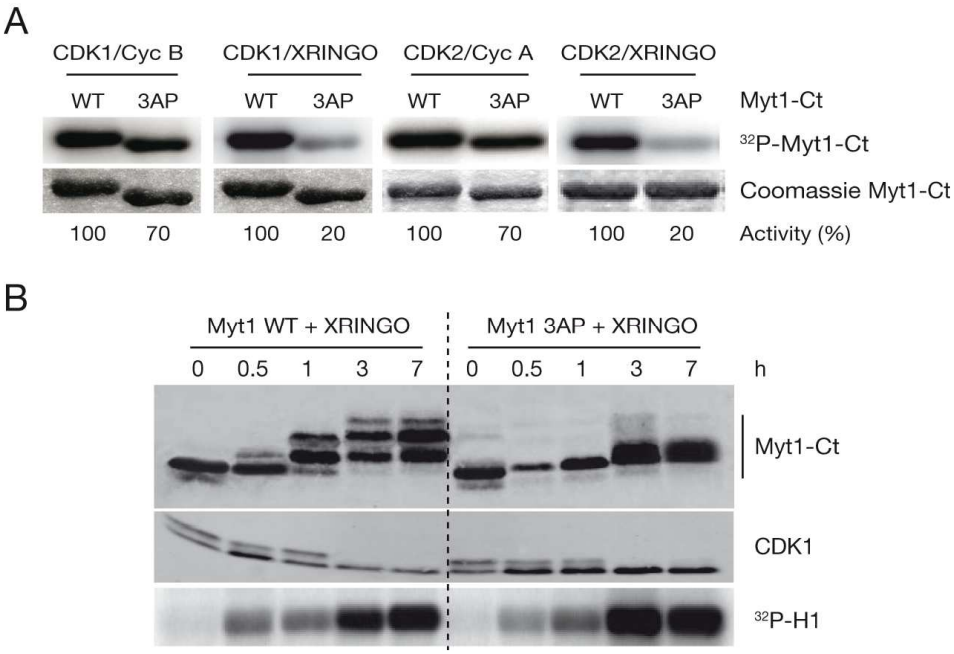

Figure 16 | CDK1/XRINGO and CDK2/XRINGO Phosphorylate Ser410, Ser414 and Ser444 in the Regulatory Domain of Myt1. (A) Baculovirus-expressed GST-CDK1 (200 or 400 ng) was incubated with cyclin B (200 ng) or MBP-XRINGO (400 ng). GST-CDK2 (250 or 500 ng) was incubated with cyclin A (250 ng) or MBP-XRINGO (500 ng). In the case of cyclins, CDK1 and CDK2 were preincubated with Cak1/Civ1 (200 and 250 ng, respectively) for 10 min at RT in the presence of ATP. Kinase assays were performed with WT or mutant 3AP GST-Myt1-Ct (2 µg) in the presence of [γ-^{32}P]ATP for 15 min at 30°C. Myt1 phosphorylation was visualized by autoradiography. (B) *Xenopus* oocytes were injected with Myc-tagged Myt1-Ct, either WT or mutant 3AP, incubated 14 h at 18°C, and reinjected with MBP-XRINGO. Oocytes were collected at the indicated times after XRINGO injection, and lysates were assayed for H1K activity or analyzed by immunoblotting with CDK1 and Myc antibodies.

Moreover, we found that the Myt1-3AP mutant was only partially phosphorylated in XRINGO-injected oocytes (Fig. 16B). In particular, the early Myt1 phosphorylation induced by XRINGO was delayed and reduced and we did not observe the marked upshift of Myt1 at meiosis I entry, in spite of the full activation of both MPF and the p42MAPK pathway (Fig. 16B). These results implicate Ser410, Ser414 and Ser444 in the phosphorylation of Myt1 during M-phase.

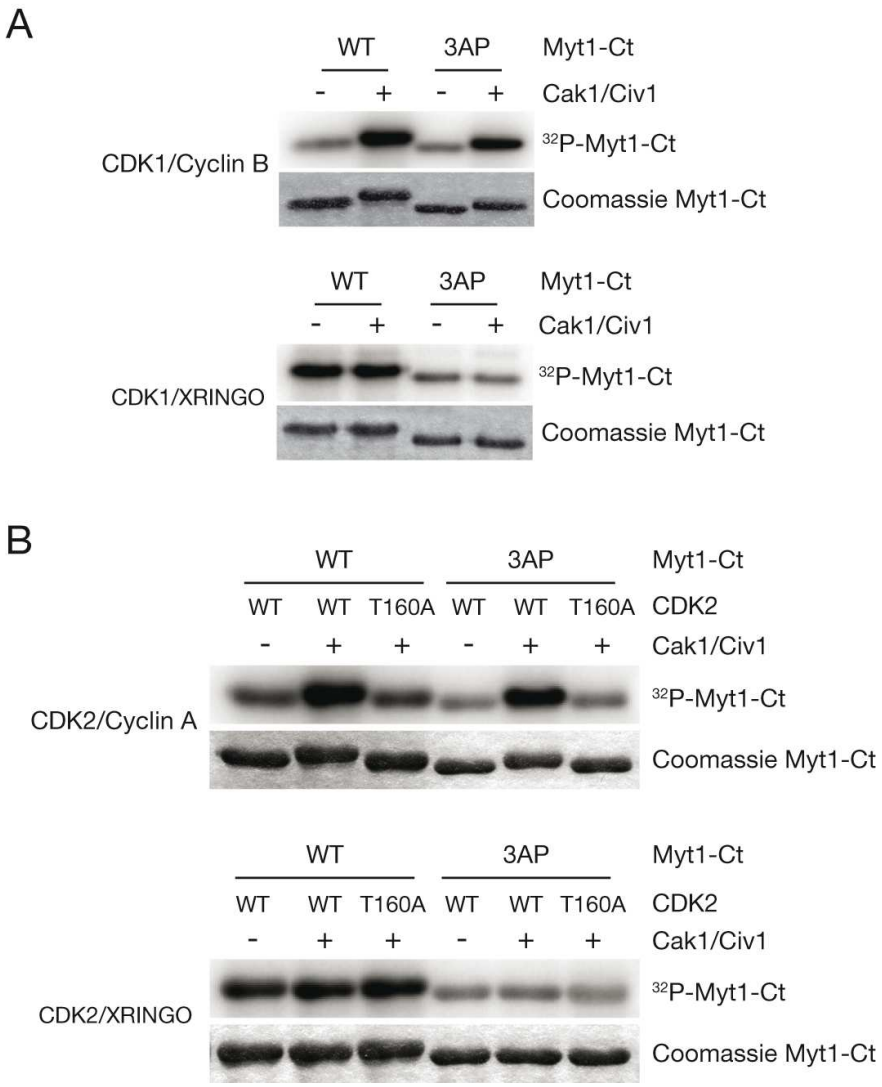

Figure 17 | T loop Phosphorylation Does Not Affect the Activity of CDK/XRINGO on Myt1. (A) Baculovirus-expressed GST-CDK1 (200 or 400 ng) was incubated with cyclin B (200 ng) or MBP-XRINGO (400 ng). (B) GST-CDK2 and GST-CDK2 T160A (250 or 500 ng) were incubated with cyclin A (250 ng) or MBP-XRINGO (500 ng). Where indicated, CDKs were preincubated with Cak1/Civ1 (200 ng) for 10 min at RT in the presence of ATP before adding cyclins or XRINGO. Kinase assays were performed with [γ-^{32}P]ATP for 15 min at 30°C using as a substrate either WT or mutant 3AP GST-Myt1-Ct (2 µg). Myt1-Ct phosphorylation was visualized by autoradiography.

We also determined the effect of T loop phosphorylation on the substrate recognition by CDK/XRINGO complexes. We observed that neither the overall catalytic activity nor the substrate specificity of both CDK1/XRINGO and CDK2/XRINGO on Myt1-Ct were affected by T loop phosphorylation (Fig. 17A and 17B). In contrast, the kinase activity and substrate recognition of CDK/cyclin complexes depended on activating phosphorylation of CDKs (Fig. 17A and 17B).

Taken together, our results suggest that XRINGO in complex with CDK1 or CDK2 can phosphorylate Ser410, Ser414 and Ser444 in the regulatory domain of Myt1. It also appears that XRINGO-activated CDKs may target a different subset of phosphorylation sites in Myt1 than the same CDKs activated by cyclins and that the Myt1 phosphorylation by CDK/XRINGO is dispensable for the T loop phosphorylation.

1.2.3. CDK/XRINGO-Induced Phosphorylation Downregulates Myt1 Kinase Activity

Phosphorylation of Myt1 Affected Its Ability to Inhibit Oocyte Maturation

To understand the biological significance of Myt1 phosphorylation by CDK/XRINGO, we generated a mutant version of full-length Myt1 in which the three Ser-Pro sites (Ser410, Ser414 and Ser444) were changed to either Ala (Myt1-3AP) or Asp (Myt1-3DP).

Overexpression of full-length WT Myt1 in *Xenopus* oocytes (via injection of mRNA) inhibited meiosis I entry induced by either XRINGO or progesterone. Analysis of the biochemical markers showed that the p42MAPK pathway was inactive and CDK1 remained phosphorylated on Thr14/Tyr15 and, therefore, inhibited as shown by kinase assay (Fig. 18A). Previous work has shown that high concentrations of Myt1 are required to inhibit the kinase activity of CDK/XRINGO *in vitro* (Karaiskou et al., 2001b). To test the effect of Myt1 concentration on CDK/XRINGO activity in *Xenopus* oocytes, we expressed different concentrations of ectopic full-length Myt1 in the oocytes. We observed that high concentrations of Myt1 (>17 ng of mRNA per oocyte) strongly inhibited oocyte maturation induced by XRINGO. However, low concentrations (<5 ng) only delayed meiosis I entry (Fig. 18B). These results indicate that Myt1 can inhibit XRINGO-induced oocyte maturation in a dose-dependent manner.

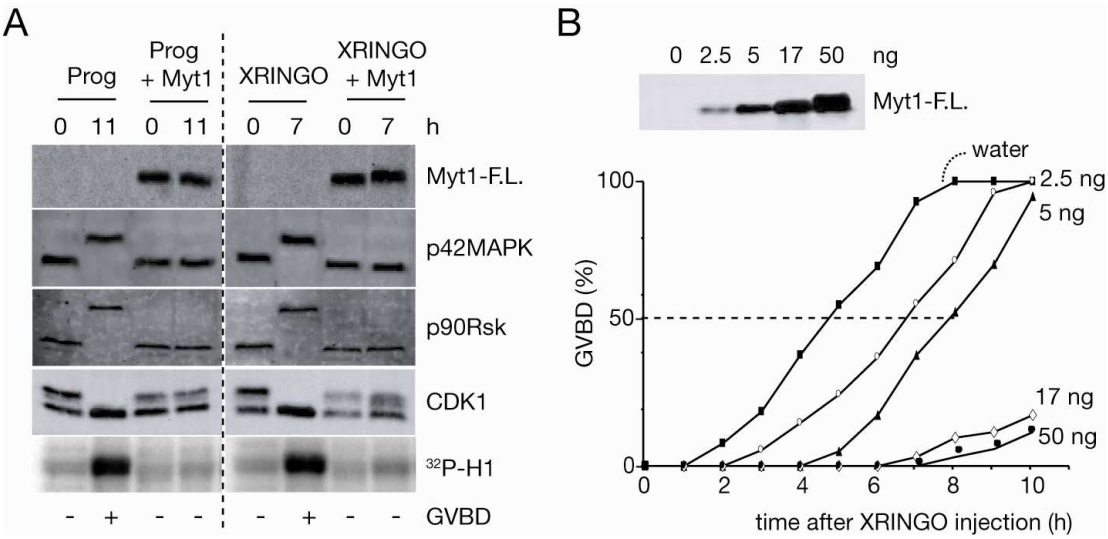

Figure 18 | Overexpression of Full-Length Myt1 in Oocytes Inhibited Meiosis I Entry Induced by both XRINGO and Progesterone. (A) *Xenopus* oocytes were injected with Myc-tagged full-length Myt1 mRNA (50 ng) and incubated 14 h. Next, the oocytes were treated with progesterone or reinjected with MBP-XRINGO (50 ng). Oocyte extracts were assayed for H1K activity or analyzed by immunoblotting. Myt1 was detected with Myc antibody. (B) *Xenopus* oocytes were injected with different concentrations (2.5, 5, 17, and 50 ng) of mRNA-encoding Myc-tagged full-length Myt1 and incubated 14 h at 18°C. The oocytes were reinjected with MBP-XRINGO and GVBD was scored at the indicated times. Lysates from oocytes collected before XRINGO injection were analyzed for Myt1 expression by immunoblotting with Myc antibody.

Next, we asked whether phosphorylation of Myt1 on Ser410, Ser414 and Ser444 affected its ability to inhibit oocyte maturation. For this purpose, we first injected mRNAs to express full-length WT Myt1 or the mutants Myt1-3AP and Myt1-3DP in oocytes and then injected XRINGO (Fig. 19A). As expected, moderate overexpression of WT Myt1 (about 2-fold the endogenous level obtained by injection of 5 ng of mRNA) delayed the kinetics of meiosis I entry induced by XRINGO, and a stronger effect was observed upon expression of the non-phosphorylatable mutant Myt1-3AP (Fig. 19A, left panel). In contrast, oocytes injected with the phospho-mimetic mutant Myt1-3DP entered meiosis I with the same kinetics as the oocytes injected with XRINGO alone, indicating that Myt1-3DP was less efficient at inhibiting XRINGO-induced oocyte maturation (Fig. 19A, left panel). In agreement with these observations, dephosphorylation of the inhibitory Thr14/Tyr15 sites of endogenous CDK1 and activation of CDK1/cyclin B were both slower in the oocytes expressing WT Myt1 or the 3AP mutant than in oocytes expressing Myt1-3DP (Fig. 19A, right panels). Consistent with these results, overexpression of high concentrations of WT Myt1 or the mutant Myt1-3AP (injection of 17 ng of mRNA) strongly inhibited the XRINGO-induced oocyte maturation, whereas the mutant Myt1-3DP only decreased the rate of

meiosis I entry induced by XRINGO (Fig. 19B). Taken together, these results suggest that phosphorylation of these three Ser interferes with the inhibitory role of Myt1 on oocyte maturation.

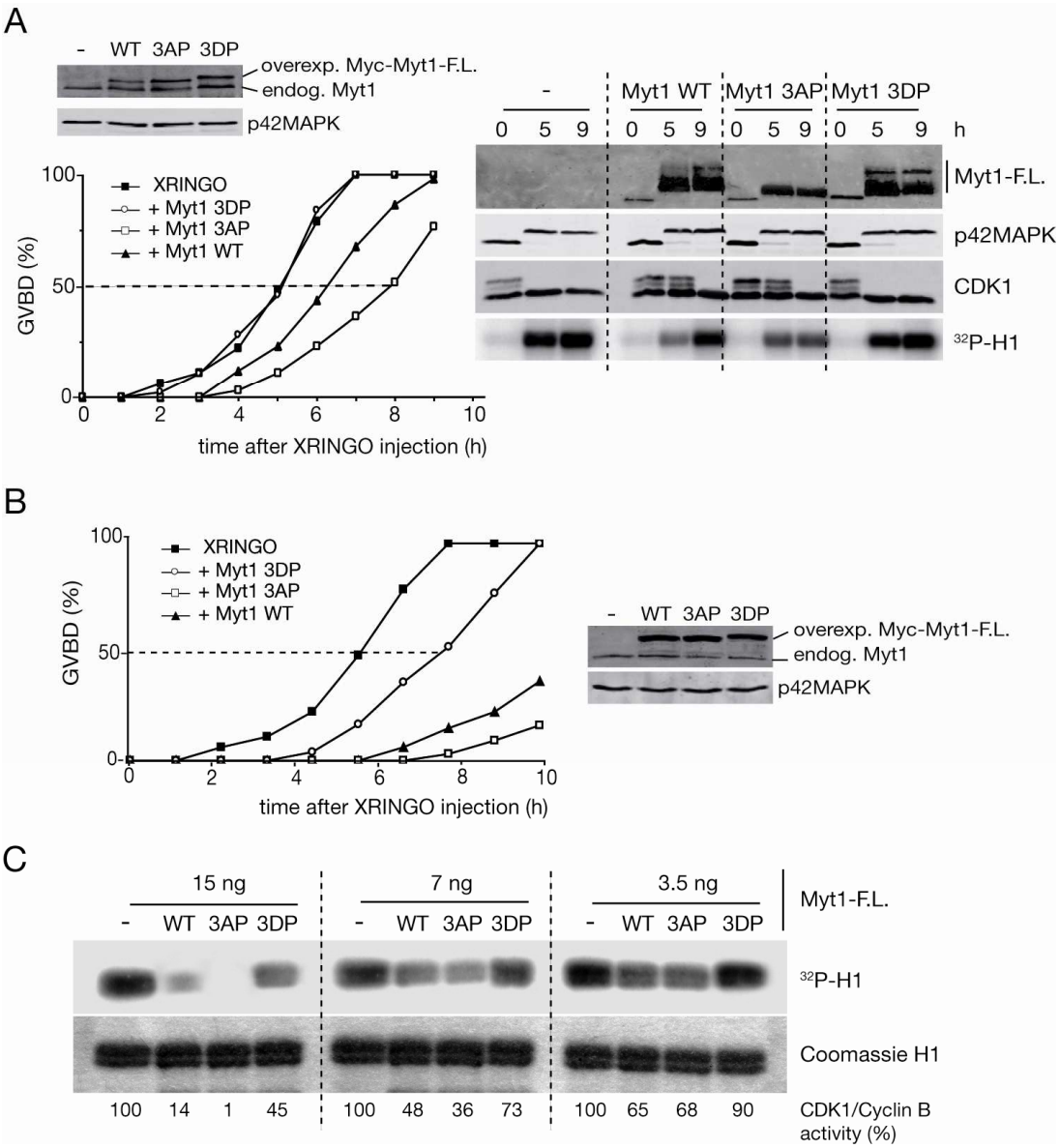

Figure 19 | Reduced Inhibitory Activity of the Myt1-3DP Mutant on XRINGO-Induced Oocyte Maturation and *in vitro*. (A) *Xenopus* oocytes were injected with 5 ng of mRNA-encoding, Myc-tagged full-length Myt1, either WT or the mutants 3AP and 3DP, incubated 14 h at 18°C, and then injected again with MBP-XRINGO. (Left panel) GVBD was scored every h. Lysates from oocytes taken before XRINGO injection were analyzed by immunoblotting with Myt1 and p42MAPK antibodies. (Right panel) Oocytes were collected at the indicated times after XRINGO injection, and the lysates were assayed for H1K activity or analyzed by immunoblotting. Myt1 was detected with Myc antibody. (B) *Xenopus* oocytes were injected with 17 ng of mRNA encoding Myc-tagged full-length Myt1, either WT or the mutants 3AP and 3DP, incubated 14 h at 18°C and then reinjected with MBP-XRINGO. GVBD was scored every h. Lysates from oocytes taken before XRINGO injection were analyzed by immunoblotting with Myt1 and p42MAPK antibodies. (C) Myc-tagged full-length Myt1 (WT or mutants 3AP and 3DP) was expressed in reticulocyte lysates, immunoprecipitated with Myc antibodies, and then incubated with recombinant CDK1-cyclin B1-Cak1/Civ1 (120 ng) for 30 min before performing H1K assays.

To test whether XRINGO-induced phosphorylation could directly inhibit Myt1 kinase activity, we performed *in vitro* kinase assays. First, we incubated different concentrations of reticulocyte-translated full-length WT Myt1 or mutant proteins with recombinant active CDK1/cyclin B for 30 min and then assayed the kinase activity on histone H1. These experiments showed that *in vitro* phosphorylation by WT Myt1 or the mutant Myt1-3AP effectively inhibited the kinase activity of CDK1/cyclin B in a dose-dependent manner (Fig. 19C). In contrast, the mutant Myt1-3DP was less efficient and only partially reduced CDK1/cyclin B activity (about 45%), which was consistent with the reduced ability of this mutant to inhibit XRINGO-induce oocyte maturation (Fig. 19A and 19B). These results suggest that phosphorylation of Ser410, Ser414 and Ser444 regulate the ability of Myt1 to inhibit CDK1/cyclin B kinase activity.

CDK/XRINGO Phosphorylates and Inhibits Myt1 Kinase Activity

Next, we tested whether CDK/XRINGO phosphorylation inhibited Myt1 kinase activity toward CDK1/cyclin B. We preincubated full-length WT Myt1 with different concentrations of recombinant CDK2/XRINGO and found that Myt1 phosphorylation correlated well with the CDK2/XRINGO concentrations (Fig. 20A). Myt1 was then immunoprecipitated (after the preincubation with CDK2/XRINGO) and thoroughly washed to eliminate the possible carryover of CDK2/XRINGO activity (Fig. 20B). The kinase activity of the immunopurified Myt1 was assayed by incubation with CDK1/cyclin B and histone H1. The results showed a direct correlation between increased CDK2/XRINGO concentrations, Myt1 phosphorylation and the reduced ability of Myt1 to inhibit CDK1/cyclin B (Fig. 20C). Importantly, XRINGO bound to catalytically inactive CDK2-K33R neither phosphorylated Myt1 nor inhibited its kinase activity (Fig. 20C), indicating that Myt1 phosphorylation was required for its inhibition by CDK2/XRINGO. To confirm that Myt1 inhibition involved phosphorylation on Ser410, Ser414 and Ser444, we preincubated WT Myt1 and the Myt1-3AP mutant with recombinant CDK2/XRINGO and then immunopurified Myt1 and assayed its kinase activity by incubation with CDK1/cyclin B and histone H1. The results showed that, in contrast to WT Myt1, the ability of Myt1-3AP to inactivate CDK1/cyclin B was not affected by preincubation with CDK2/XRINGO (Fig. 20D).

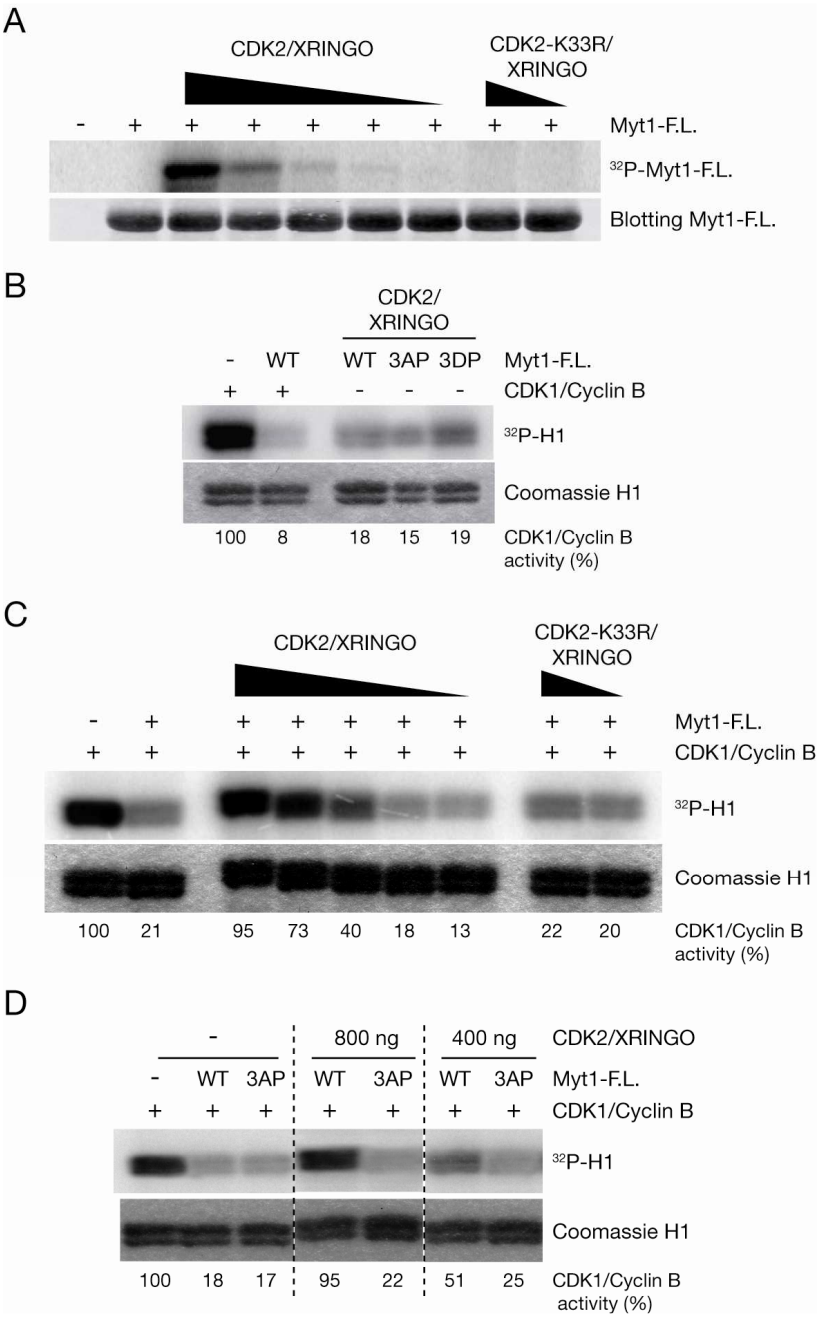

Figure 20 | Phosphorylation and Inhibition of Myt1 by XRINGO-Activated CDK2. (A) Myc-tagged full-length Myt1 was expressed in reticulocyte lysates, immunoprecipitated, and incubated with different concentrations of recombinant CDK2/XRINGO (1000, 500, 250, 125, and 60 ng) or CDK2-K33R/XRINGO (1000 and 500 ng) for 30 min in the presence of [γ-^{32}P]ATP. (B) Myc-tagged full-length Myt1 (WT or mutants 3AP and 3DP) was expressed in reticulocyte lysates, immunoprecipitated and incubated with recombinant CDK2/XRINGO (1 μg) in the presence of ATP. After 30 min, Myt1 was immunoprecipitated and washed extensively. The immunopurified Myt1 was further incubated in the presence or absence of recombinant CDK1-cyclin B1-Cak1/Civ1 (120 ng) for other 30 min before H1K assays were performed. The three right lanes show the controls with immunopurified Myt1 that was directly assayed for H1K activity, in the absence of CDK1/cyclin B1. (C) Myc-tagged full-length Myt1 was expressed in reticulocyte lysates, immunoprecipitated, and incubated with different concentrations of CDK2/XRINGO or CDK2-K33R/XRINGO as in (A). Myt1 was immunopurified and further incubated with recombinant CDK1-cyclin B1-Cak1/Civ1 (120 ng) for 30 min before H1K assays were performed. (D) Myc-tagged full-length Myt1 (WT or mutant 3AP) was expressed in reticulocyte lysates, immunoprecipitated, and incubated with different concentrations of CDK2/XRINGO (800 and 400 ng) in the presence of ATP. After 30 min, the bead-bound Myt1 was immunopurified, washed, and further incubated with CDK1-cyclin B1-Cak1/Civ1 (120 ng) for 30 min before H1K assays were performed.

We then investigated whether XRINGO-activated CDK1 also inhibited Myt1 kinase activity via phosphorylation of these three Ser. For this, WT Myt1 or the mutant Myt1-3AP were preincubated with different concentrations of CDK1/XRINGO. Myt1 was then immunopurified and thoroughly washed before incubation with CDK1/cyclin B to perform H1K assays. As a control, immunopurified Myt1 was also directly incubated with histone H1 (without CDK1/cyclin B) to verify the absence of contaminating CDK1/XRINGO activity from the pre-incubation step. Our results showed that CDK1/XRINGO efficiently inactivated WT Myt1 but had no effect on the mutant Myt1-3AP (Fig. 21A). Moreover, we observed that the inhibition of CDK1/cyclin B activity by WT Myt1 and the mutant Myt1-3AP correlated with their ability to phosphorylate CDK1 on Tyr15. Thus, upon preincubation with CDK1/XRINGO, WT Myt1 failed to catalyze the inhibitory phosphorylation on CDK1 whereas Myt1-3AP was not affected (Fig. 21B). These results clearly demonstrate that XRINGO-activated CDKs can directly phosphorylate and inhibit Myt1 activity.

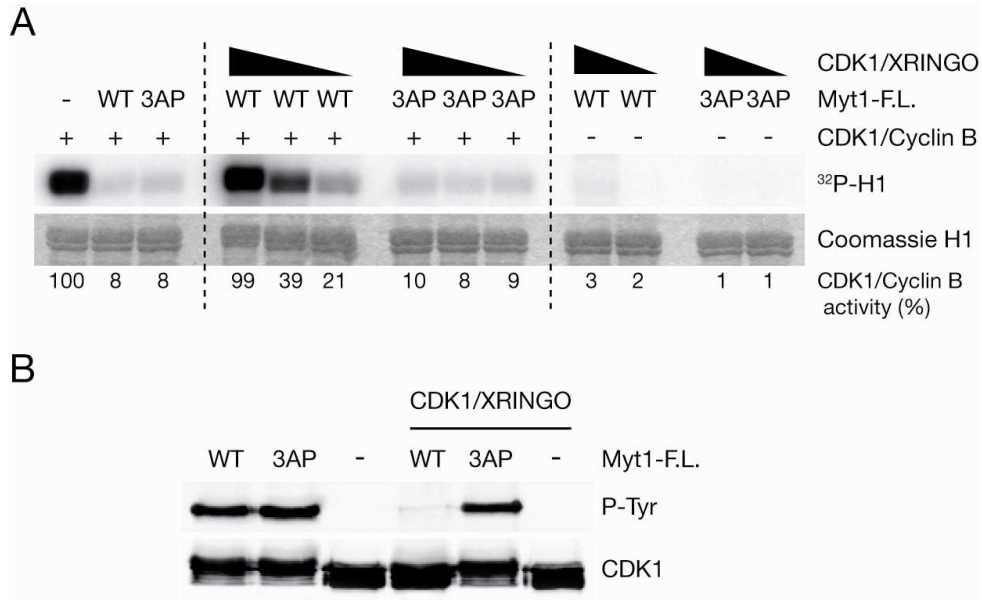

Figure 21 | CDK1/XRINGO Phosphorylates and Inhibits Myt1 Activity. (A) Myc-tagged full-length Myt1 (WT or mutant 3AP) was expressed in reticulocyte lysates, immunoprecipitated, and incubated at 30°C with different concentrations of baculovirus-expressed CDK1 activated with MBP-XRINGO (1200, 600, and 300 ng) in the presence of ATP. After 40 min, Myt1 was immunoprecipitated and washed extensively. The immunopurified Myt1 was further incubated in the presence or absence of CDK1-cyclin B1-Cak1/Civ1 (120 ng) for 30 min before H1K assays were performed. The four right lanes show the controls, to confirm the lack of contaminating CDK1/XRINGO activity from the pre-incubation step. (B) Myc-tagged full-length Myt1 proteins were expressed in reticulocyte lysates, immunoprecipitated, and incubated with CDK1/XRINGO (800 ng) in the presence of ATP (300 µM) at 30°C. After 45 min, Myt1 was immunoprecipitated and washed extensively. The immunopurified Myt1 was further incubated in the presence of bacteria-expressed CDK1-K33R and cyclin B (1 µg) for 45 min in H1K buffer supplemented with fresh ATP (300 µM) at 30°C. The reaction mixture was analyzed by immunoblotting.

We also confirmed that CDK1/XRINGO, but not CDK1/cyclin B, was able to phosphorylate full-length Myt1 *in vitro*. Interestingly, the absence of phosphorylation of Myt1 upon incubation with CDK1/cyclin B, correlated with the phosphorylation of CDK1, which was not observed in the case of XRINGO-activated CDK1 (Fig. 22A, upper panels). As a control, we investigated in parallel the phosphorylation of Myt1-Ct by both complexes and found that CDK1/cyclin B was even more efficient than CDK1/XRINGO at phosphorylating Myt1-Ct *in vitro* (Fig. 22A, lower panels). Moreover, Myt1-Ct was apparently stoichiometrically phosphorylated by both CDK1/cyclin B and CDK1/XRINGO, as determined by the upshift of the phosphorylated proteins, although the electrophoretic mobility was different in both cases, which is consistent with the phosphorylation of different sites (Fig. 22B).

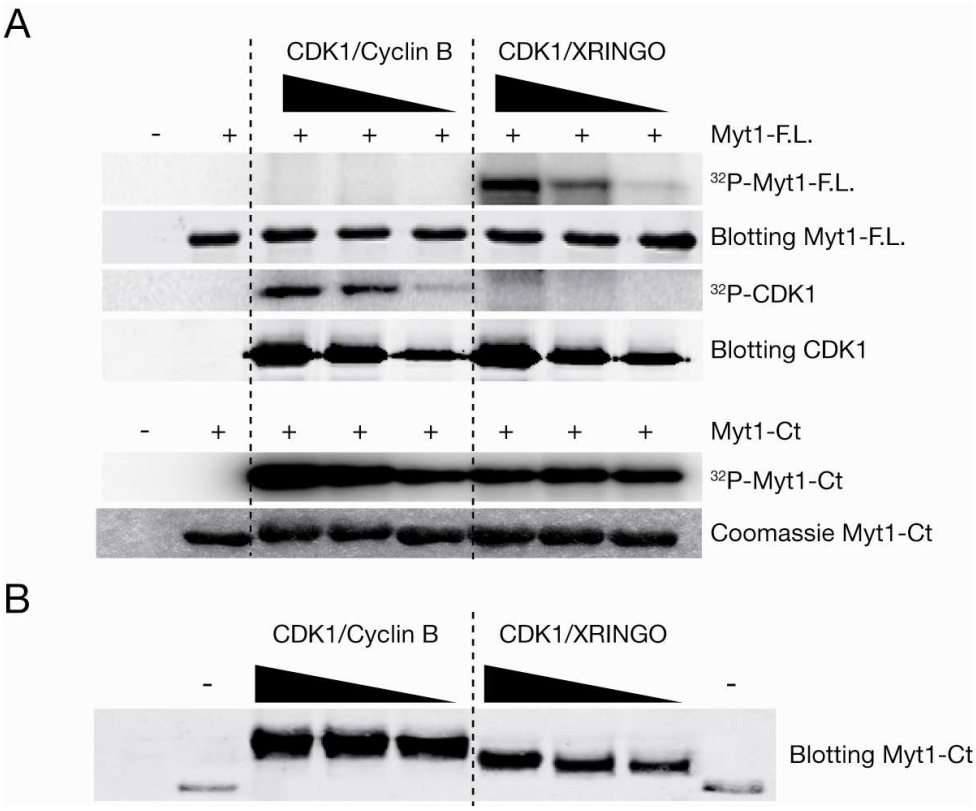

Figure 22 | CDK1/XRINGO, but Not CDK1/Cyclin B, Phosphorylate and Inhibited Myt1. (A) Myc-tagged full-length Myt1 was expressed in reticulocyte lysates, immunoprecipitated, and incubated with different concentrations of baculovirus-expressed CDK1 activated with either cyclin B or MBP-XRINGO (1200, 600, and 300 ng) for 30 min at 30°C in the presence of [γ-^{32}P]ATP. Phosphorylation of Myt1 and CDK1 was visualized by autoradiography. The same samples were analyzed by immunoblotting with CDK1 and Myc antibodies. For the phosphorylation of Myt1-Ct, kinase assays were performed as above but using GST-Myt1-Ct (500 ng) as a substrate. (B) Myc-tagged Myt1-Ct was expressed in reticulocyte lysates, immunoprecipitated (from 20 µl of lysate) and incubated with different concentrations of CDK1 activated with either cyclin B or MBP-XRINGO (1200, 600 and 300 ng) for 30 min at 30°C in the presence of ATP (300 µM). Samples were analysed by immunoblotting with Myt1 antibodies.

Finally, we analyzed whether CDK1 in CDK/XRINGO complex is phosphorylated by Myt1. Interestingly, we observed that Myt1 phosphorylated cyclin B-bound CDK1 on Tyr15 more efficiently than the CDK1 bound to XRINGO (Fig. 23). Taken together, the results indicate that the inhibition of Myt1 activity by CDK1/XRINGO is probably a consequence of two factors: XRINGO-associated CDK1 phosphorylates more efficiently the inhibitory Myt1 sites, but it is also itself less susceptible to phosphorylation by Myt1.

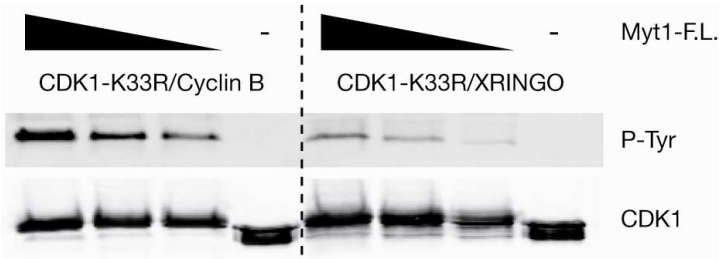

Figure 23 | Myt1 Phosphorylates CDK1/XRINGO with Reduced Efficiency. Myc-tagged full-length Myt1 was expressed in reticulocyte lysates and different amounts of lysate (20, 10 and 5 µl) were immunoprecipitated and incubated with GST-CDK1-K33R in the presence of either cyclin B or MBP-XRINGO (1 µg) and ATP (300 µM) for 45 min at 30°C. Samples were analyzed by immunoblotting.

1.3. Regulation of CDK Substrate Specificity by RINGO Proteins

1.3.1. Myt1-XRINGO Interaction

Previous work has shown that the RXL motif of Myt1 is involved in the binding to human cyclin B (Liu et al., 1999). The sequence RNL is contained within the regulatory domain of *Xenopus* Myt1 at positions 536 to 538 (Fig. 13). To determine whether XRINGO make use of the RXL motif for Myt1 recruitment and phosphorylation, we mutated this sequence to Ala and then made pull down and kinase assays. We first confirmed that the RNL sequence is necessary for the interaction between Myt1-Ct and cyclin B *in vitro* and in oocytes extracts, and it is also required for efficient phosphorylation of Myt1 induced by CDK1/cyclin B (Fig. 24A and 24B). Surprisingly, the mutation of this motif neither affects the binding of Myt1-Ct to XRINGO nor Myt1 phosphorylation by CDK1/XRINGO *in vitro* (Fig. 19A and 19B), suggesting that XRINGO and cyclin B use different motifs for substrate recruitment.

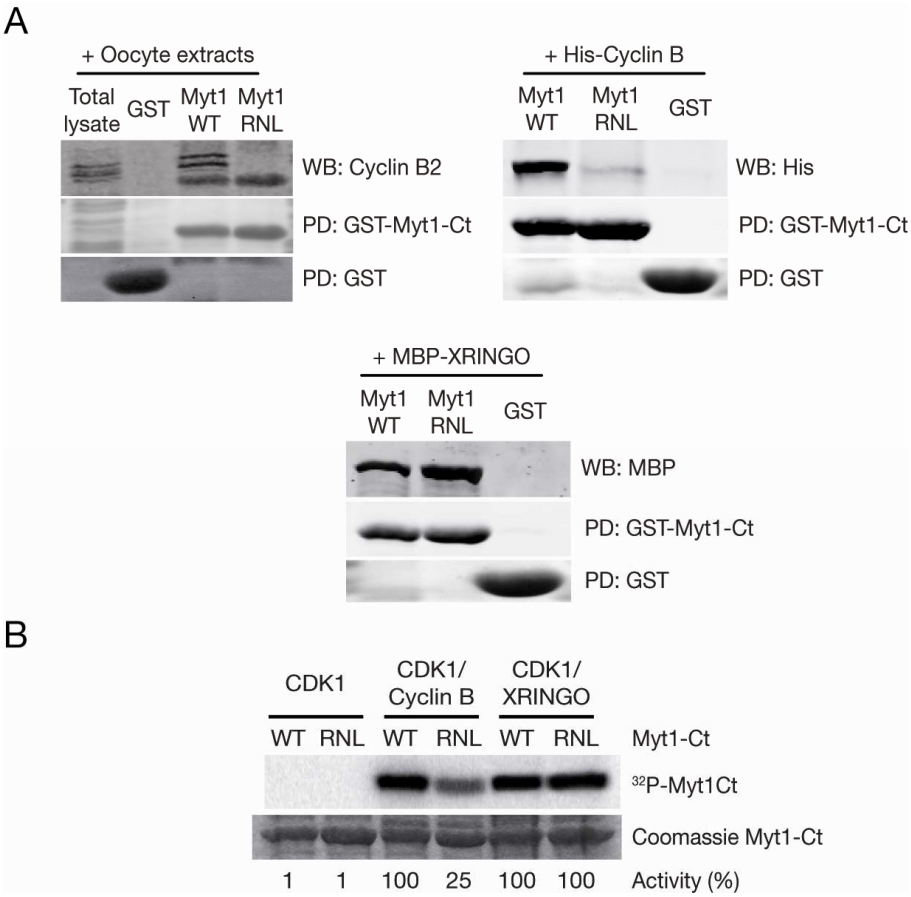

Figure 24 | The RXL Motif Neither Impairs the Myt1-XRINGO Interaction Nor Myt1 Phosphorylation by CDK1/XRINGO. (A) WT or RNL mutant GST-Myt1-Ct (5 µg) were incubated with G2-arrested oocytes lysates during 3 h at 4°C. GST pull-downs were analyzed by immunoblotting with cyclin B2 antibody. WT or mutant RNL GST-Myt1-Ct (5 µg) were incubated with His-cyclin B or MBP-XRINGO (5 µg) during 3 h at 4°C. GST pull-downs were analyzed by immunoblotting with histidine, MBP or GST antibodies. (B) Bacterially produced GST-CDK1 (1.5 µg) was preincubated in concentrated *Xenopus* oocyte extracts, recovered on glutathione-Sepharose beads and then incubated with either cyclin B or MBP-XRINGO (1.5 µg). Kinase assays were performed with WT or mutant RNL GST-Myt1-Ct (2 µg) in the presence of [γ-^{32}P]ATP for 15 min at 30°C. Myt1 phosphorylation was visualized by autoradiography.

To identify the region of Myt1 that interacts with XRINGO, we prepared different fragments of Myt1 as GST-fusion proteins that cover all amino acid sequence of the regulatory domain of Myt1 (Fig. 25A). By pull down assay, we observed that Myc-tagged XRINGO was able to bind recombinant WT Myt1-Ct, containing residues 399-548, but not four C-terminal fragments, namely 6.1, 4.2, 6.1S and 4.2S. Further deletion of the 36 C-terminal residues in WT Myt1-Ct did not reduce Myt1 interaction with XRINGO. Interestingly, this fragment (Myt1-Ct 1.3) does not contain the RNL sequence, confirming that RXL motif of Myt1-Ct is not necessary for binding to XRINGO (Fig. 25B). Further experiments will be required to determine the binding region of XRINGO to Myt1-Ct.

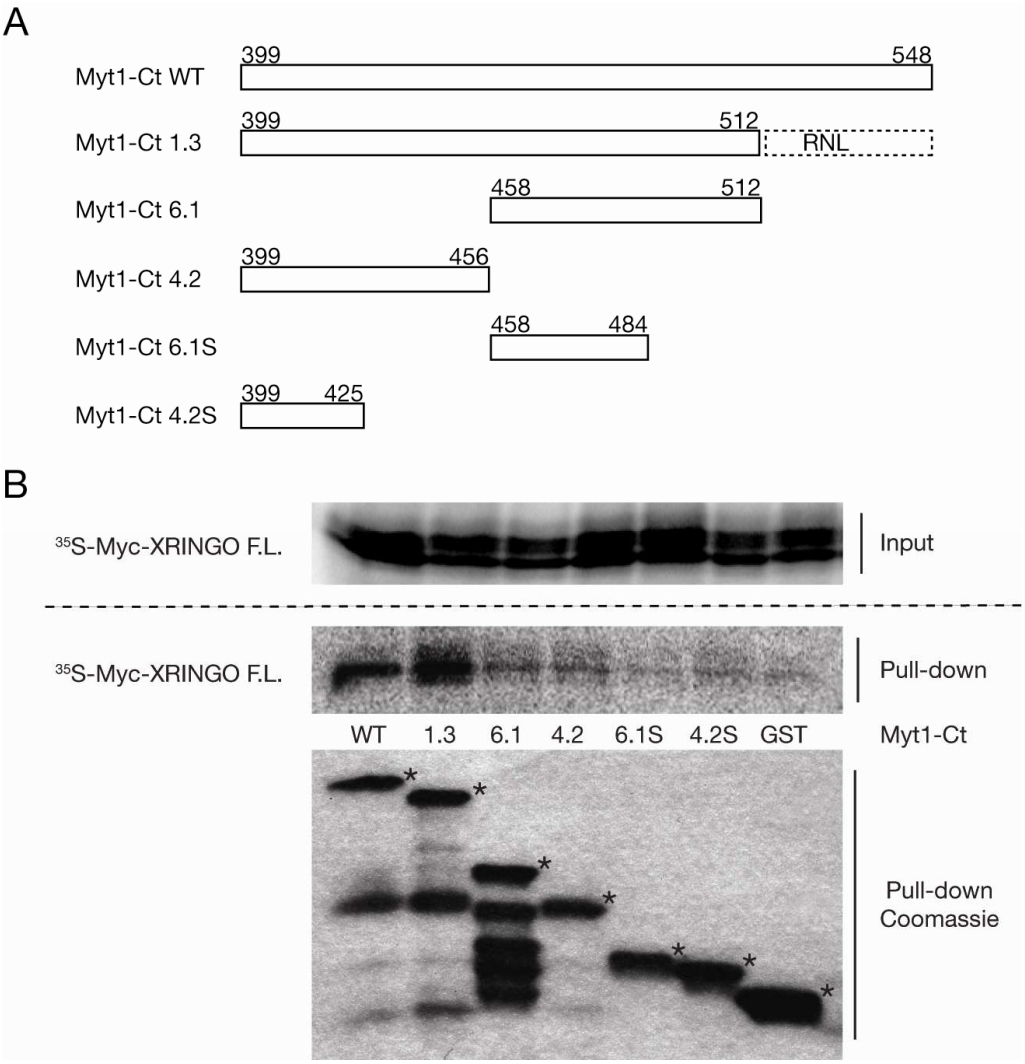

Figure 25 | Mapping the Boundaries of the Myt1-XRINGO Interaction. (A) Diagram of the six Myt1-Ct fragments produced as GST fusion proteins for pull-down assay. (B) ^{35}S-Myc-tagged full-length XRINGO was expressed in reticulocyte lysates and then incubated with GST or GST-tagged Myt1 fragments. XRINGO protein bound to each of the GST-Myt1 proteins was visualized by autoradiography. * indicates protein of interest.

1.4. CDK/XRINGO and p90Rsk Phosphorylate the Regulatory Domain of Myt1 on Different Sites

1.4.1. Identification of Myt1 Sites Phosphorylated by p90Rsk

The protein kinase p90Rsk has been previously shown to interact with and phosphorylate Myt1 and thereby inhibits its kinase activity during oocyte maturation (Palmer et al., 1998). Two Ser that are phosphorylated by CDK/XRINGO (Ser410 and Ser414) belong to the typical p90Rsk phosphorylation motifs (N-terminal Arg residues,

RXRRXS/T) (Anjum and Blenis, 2008). However, there is no evidence that p90Rsk can phosphorylate CDKs consensus sites (Ser/Thr-Pro) (Anjum and Blenis, 2008). Thus, it is possible that p90Rsk and CDK/XRINGO phosphorylate the regulatory domain of Myt1 on different sites. To test this possibility, we used the Myt1-3AP mutant as a substrate in kinase assays. As expected, XRINGO-activated CDK1 and CDK2 did not phosphorylate the Myt1-3AP mutant. Interestingly, we observed that p90Rsk phosphorylates the Myt1-3AP mutant with similar efficiency as WT Myt1 (Fig. 26A).

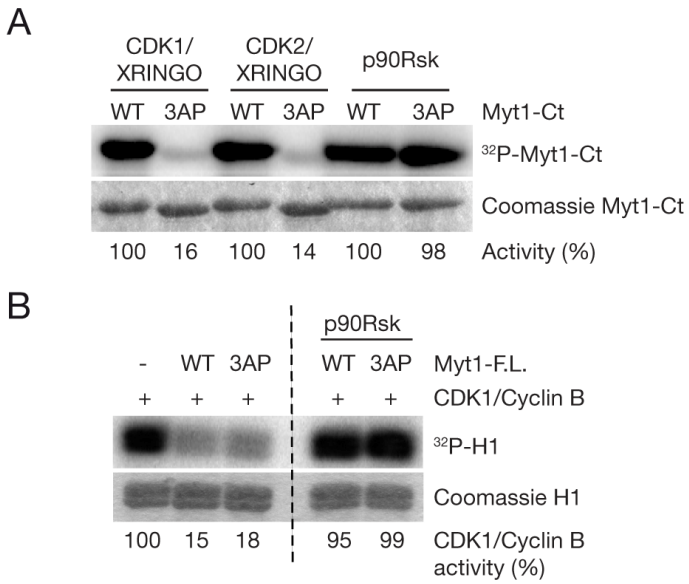

Figure 26 | p90Rsk and CDK1/XRINGO Phosphorylate Different Sites on the Regulatory Domain of Myt1. A) Baculovirus-expressed GST-CDK1 (200 ng) and bacterially produced GST-CDK2 (250 ng) were incubated with MBP-XRINGO (200 and 250 ng, respectively). Kinase assays were performed with CDK/XRINGO complexes or recombinant p90Rsk (300 ng) and WT or mutant 3AP GST-Myt1-Ct (2 µg) in the presence of [γ-^{32}P]ATP for 15 min at 30°C. Myt1 phosphorylation was visualized by autoradiography. (B) Myc-tagged full-length Myt1 (WT or mutant 3AP) was expressed in reticulocyte lysates, immunoprecipitated, and incubated with recombinant p90Rsk (900 ng) in the presence of ATP at 30°C. After 60 min, Myt1 was immunoprecipitated and washed extensively. The immunopurified Myt1 was further incubated in the presence of recombinant CDK1-cyclin B1-Cak1/Civ1 (120 ng) for 30 min before H1K assays were performed.

Next, we tested whether p90Rsk phosphorylation directly inhibited Myt1-3AP mutant kinase activity. For this propose, we first preincubated reticulocyte-translated full-length WT Myt1 or the Myt1-3AP mutant with p90Rsk. Myt1 proteins were then immunoprecipitated and their kinase activity was assayed by incubation with CDK1/cyclin B and histone H1. The results show that Myt1 proteins have less ability to inhibit CDK1/cyclin B activity, indicating that p90Rsk efficiently inactivated both WT Myt1 and the Myt1-3AP mutant (Fig. 26B).

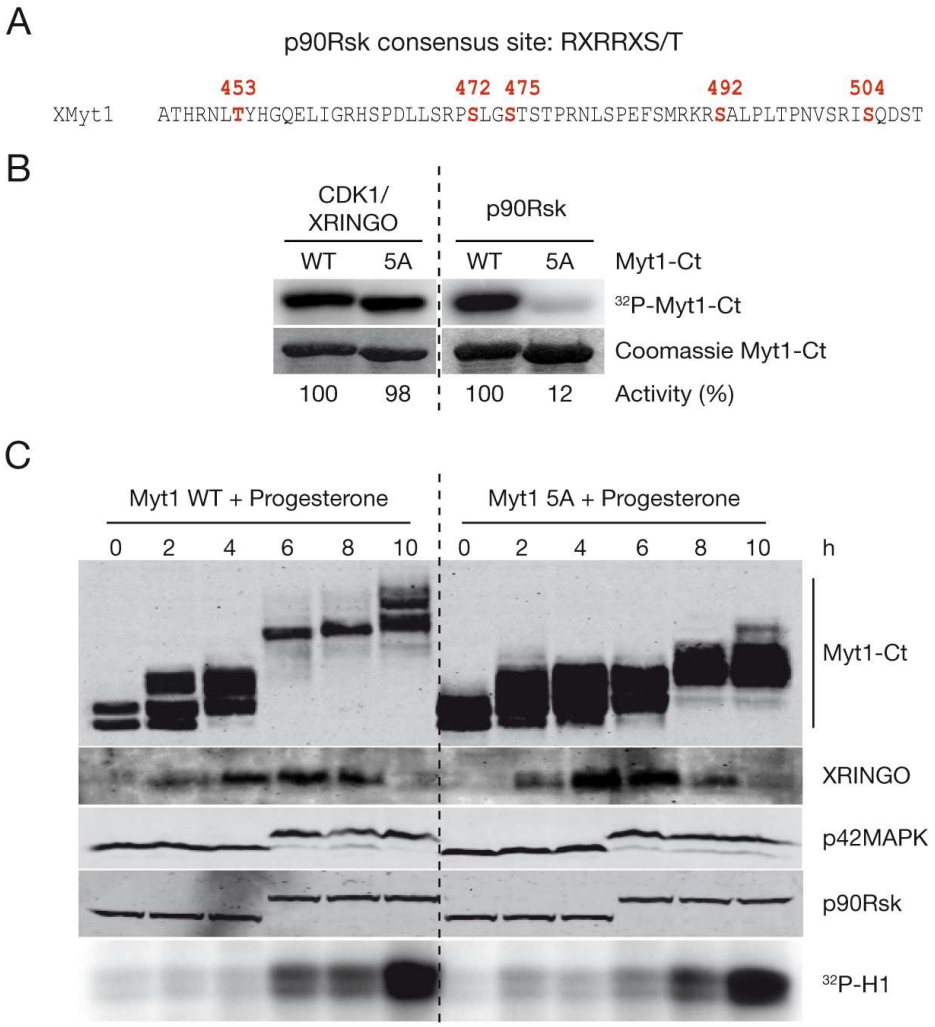

Figure 27 | Identification of Specific p90Rsk Phosphorylation Sites on the Regulatory Domain of Myt1. (A) Sequence of *Xenopus* Myt1-Ct. p90Rsk phosphorylation sites are highlighted in red. (B) Baculovirus-expressed GST-CDK1 (200 ng) was activated with MBP-XRINGO (200 ng). Kinase assays were performed with CDK1/XRINGO or recombinant p90Rsk (300 ng) and WT or mutant 5A GST-Myt1-Ct (2 µg) in the presence of [γ-^{32}P]ATP for 30 min at 30°C. Myt1 phosphorylation was visualized by autoradiography. (C) *Xenopus* oocytes from primed frogs were injected with Myc-tagged Myt1-Ct, either WT or mutant 5A, incubated for 14 h at 18°C, and then stimulated with progesterone. Oocytes were collected at the indicated times after progesterone stimulation, and lysates were assayed for H1K activity or analyzed by immunoblotting. Myt1-Ct was detected with Myc antibody.

To identify which residues of Myt1-Ct were phosphorylated by p90Rsk, we mutated potential p90Rsk consensus sites (RXRRXS/T) (Fig. 27A). We found that a mutant with four Ser (472, 475, 492 and 504) and one Thr (453) replaced by alanines (Myt1-5A) was poorly phosphorylated by p90Rsk *in vitro* (Fig. 27B). Surprisingly, CDK1/XRINGO phosphorylated the Myt1-5A mutant as efficiently as the WT Myt1 (Fig. 27B). Moreover, we found that the Myt1-5A mutant was partially phosphorylated in progesterone-stimulated oocytes (Fig. 27C). In particular, the late Myt1

phosphorylation induced by progesterone was delayed and reduced and we did not observe the marked upshift of Myt1 at meiosis I entry, in spite of the full activation of both MPF and the p42MAPK-p90Rsk pathway (Fig. 27C). Interestingly, the accumulation of endogenous XRINGO protein correlated with Myt1 phosphorylation at early time points. These results implicate Thr453, Ser472, Ser475, Ser492 and Ser504 in the late phosphorylation of Myt1 during M phase.

1.4.2. p90Rsk-Induced Phosphorylation Downregulates Myt1 Activity

To understand the biological significance of Myt1 phosphorylation by p90Rsk, we generated a mutant version of full-length Myt1 in which the five p90Rsk consensus sites (Thr453, Ser472, Ser475, Ser492 and Ser504) were changed to either Ala (Myt1-5A) or Asp (Myt1-5D).

We injected mRNAs to express full-length WT Myt1 or the mutants Myt1-5A and Myt1-5D in oocytes, and then they were stimulated with progesterone (Fig. 28A, left panel). Overexpression of WT Myt1 (about 4-fold the endogenous level obtained by injection of 10 ng of mRNA) delayed the kinetics of meiosis I entry induced by progesterone, and a stronger effect was observed upon expression of the non-phosphorylatable mutant Myt1-5A. In contrast, the oocytes injected with phospho-mimetic mutant Myt1-5D mature with similar kinetics as oocytes stimulated with progesterone, indicating that Myt1-5D was less efficient at inhibiting progesterone-induced oocyte maturation (Fig. 28A, left panel). Consistent with these results, dephosphorylation of the inhibitory Thr14/Tyr15 sites of endogenous CDK1 and activation of CDK1/cyclin B were both slower in the oocytes expressing WT Myt1 or the Myt1-5A mutant than in oocytes expressing Myt1-5D, as shown by kinase assays (Fig. 28A, right panel). Taken together, these results suggest that phosphorylation of these five residues interferes with the inhibitory role of Myt1 on oocyte maturation.

To investigate whether p90Rsk inhibited Myt1 kinase activity, we first confirmed that *in vitro* phosphorylation by WT Myt1 or the mutant Myt1-5A effectively inhibited the kinase activity of CDK1/cyclin B (Fig. 28B). In contrast, the phospho-mimetic mutant Myt1-5D was less efficient and only partially reduced CDK1/cyclin B activity (about 40%), which was consistent with the reduced ability of this mutant to inhibit progesterone-induced oocyte maturation (Fig. 28A). These results suggest that phosphorylation of Thr453, Ser472, Ser475, Ser492 and Ser504 regulates the ability of Myt1 to inhibit CDK1/cyclin B kinase activity.

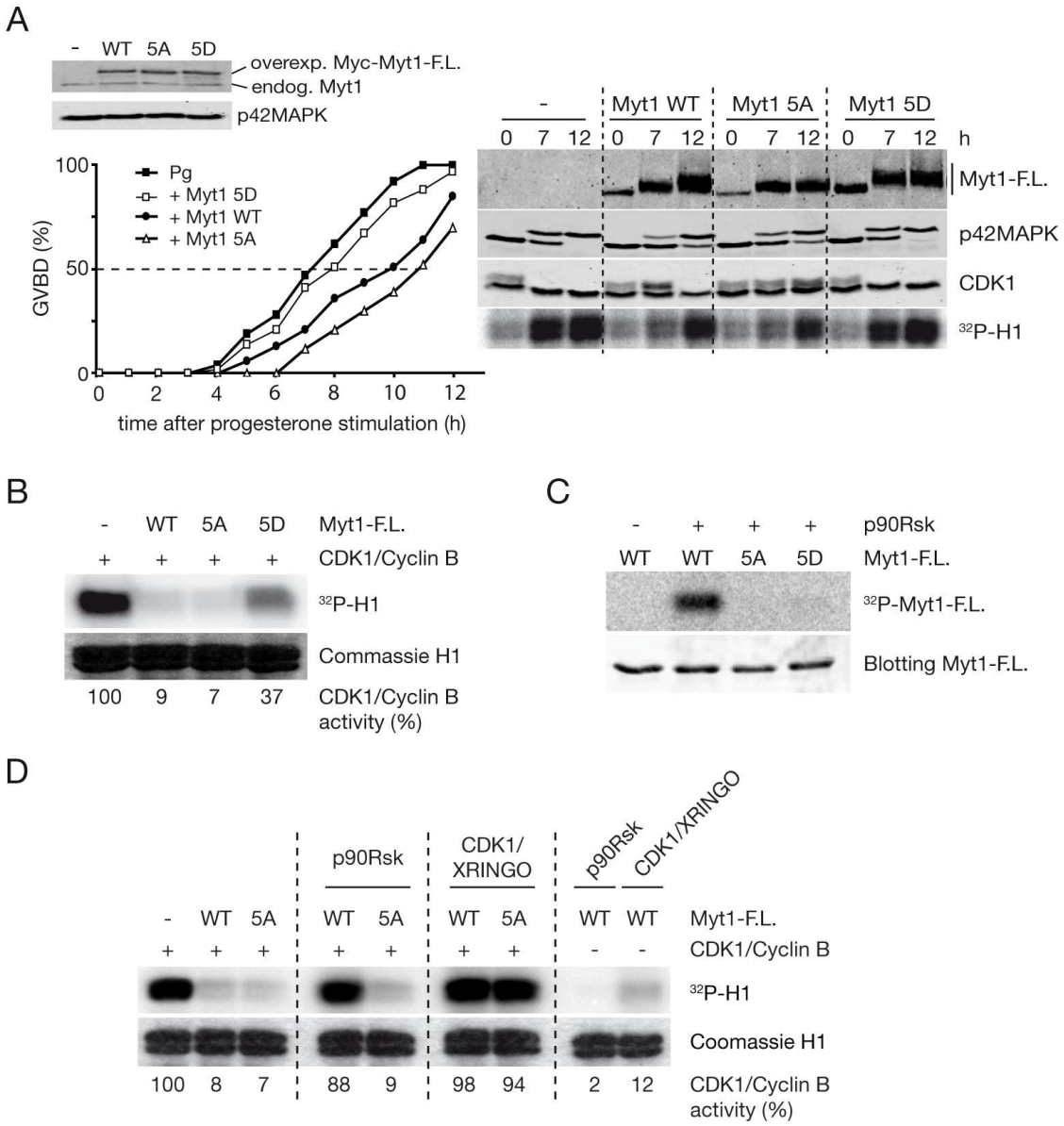

Figure 28 | Phosphorylation and Inhibition of Myt1 by p90Rsk. (A) *Xenopus* oocytes were injected with 10 ng of mRNA-encoding Myc-tagged full-length Myt1, either WT or the mutants 5A and 5D, incubated 14 h at 18°C, and then were stimulated with progesterone. (Left panel) GVBD was scored every h. Lysates from oocytes taken before progesterone stimulation were analyzed by immunoblotting with Myt1 and p42MAPK antibodies. (Right panel) Oocytes were collected at the indicated times after progesterone stimulation, and the lysates were assayed for H1K activity or analyzed by immunoblotting. Myt1 was detected with Myc antibody. (B) Myc-tagged full-length Myt1 (WT or mutants 5A and 5D) was expressed in reticulocyte lysates, immunoprecipitated with Myc antibodies, and then incubated with recombinant CDK1-cyclin B1-Cak1/Civ1 (120 ng) for 30 min before performing H1K assays. (C) Myc-tagged full-length Myt1 proteins were expressed in reticulocyte lysates, immunoprecipitated, and incubated with p90Rsk (900 ng) for 45 min in the presence of [γ-^{32}P]ATP. (D) Myc-tagged full-length Myt1 (WT or mutant 5A) was expressed in reticulocyte lysates, immunoprecipitated, and preincubated with p90Rsk (900 ng) or CDK1/XRINGO (800 ng) in the presence of ATP at 30°C. After 45 min, Myt1 was immunoprecipitated and washed extensively. The immunopurified Myt1 was further incubated in the presence or absence of recombinant CDK1-cyclin B1-Cak1/Civ1 (120 ng) for 30 min at 30°C before H1K assays were performed. The two right lanes show the controls with immunopurified Myt1 that was directly assayed for H1K activity, in the absence of CDK1/cyclin B1, to confirm the lack of contaminating p90Rsk and CDK1/XRINGO activities from the preincubation step.

Next, we tested whether p90Rsk inhibited Myt1 kinase activity via phosphorylation of those residues. To this end, we preincubated full-length WT Myt1 or the mutant Myt1-5A with recombinant p90Rsk and found that WT Myt1, but not the mutant Myt1-5A, was phosphorylated by p90Rsk (Fig. 28C). Myt1 proteins were then immunopurified and thoroughly washed before incubation with CDK1/cyclin B to perform H1K assays. As a control, immunopurified Myt1 was also directly incubated with histone H1 (without CDK1/cyclin B) to verify the absence of contaminating p90Rsk activity from the preincubation step. The results showed a direct correlation between Myt1 phosphorylation induced by p90Rsk and the reduced ability of WT Myt1 to inhibit CDK1/cyclin B (Fig. 28D). However, the ability of Myt1-5A mutant to inactivate CDK1/cyclin B was not affected by the preincubation with p90Rsk (Fig. 28D). We also observed that phosphorylation induced by CDK1/XRINGO directly inhibited Myt1-5A mutant kinase activity (Fig. 28D).

Taken together, these results suggested that p90Rsk and CDK1/XRINGO phosphorylated the regulatory domain of Myt1 on different sites and could represent parallel pathways that lead to Myt1 inactivation.

1.4.3. CDK/XRINGO and p90Rsk Collaborate to Inhibit Myt1

In the previous section, we have shown that Myt1-Ct was phosphorylated at early time points, before p90Rsk was activated, and this correlated with the progesterone-induced accumulation of endogenous XRINGO protein (Fig. 11 and 27C). To determine whether Myt1 phosphorylation induced by CDK/XRINGO affect its binding to p90Rsk, we incubated GST-fused Myt1-Ct either WT or the mutants Myt1-3AP and Myt1-3DP in lysates prepared from G2-arrested oocytes or progesterone-matured oocyte lysates and then made pull down assays to analyze the binding of p90Rsk.

Consistent with previous results (Palmer et al., 1998), we observed that the C-terminal domain of Myt1 associates with the active and hyperphosphorylated p90Rsk present in lysates prepared from progesterone-matured oocytes (Fig. 29, right panel), but not with the inactive and unphosphorylated form of p90Rsk present in G2-arrested oocytes (Fig. 29, left panel). Surprisingly, the non-phosphorylatable mutant Myt1-3AP interacts less efficiently with p90Rsk than WT Myt1 in progesterone-matured oocyte lysates. In agreement with this result, we observed a correlation between the phospho-mimetic mutant Myt1-3DP and the ability of Myt1 to bind more efficiently to

p90Rsk (Fig. 29, right panel). These results suggest that Ser410, Ser414 and Ser444 participate in the interaction between Myt1-Ct and p90Rsk through the formation of a putative docking site motif containing phospho-Ser410, phospho-Ser414 and phospho-Ser444.

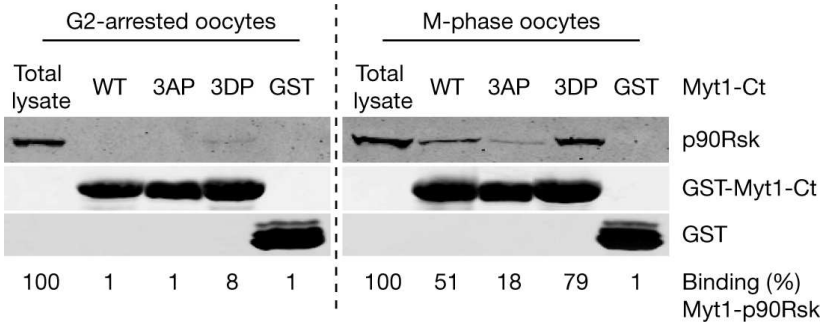

Figure 29 | p90Rsk Binds to Myt1 Pre-Phosphorylated by CDK/XRINGO. *Xenopus* oocytes were incubated or not with progesterone for 12 h. WT or mutants 3AP or 3DP GST-Myt1-Ct (5 µg) were incubated with G2-arrested oocytes or progesterone-mature oocytes during 3 h at 4°C. GST pull-downs were analyzed by immunoblotting with p90Rsk or GST antibodies.

1.4.4. Myt1 Phosphorylation Induced by p90Rsk Disrupt the Myt1-CDK1/Cyclin B Interaction

The question arising is how is it possible that Myt1 phosphorylation induced by p90Rsk impair Myt1 activity toward CDK1/cyclin B. There are two possibilities, Myt1 kinase activity could be affected directly by p90Rsk phosphorylation or alternatively Myt1 phosphorylation induced by p90Rsk impairs Myt1-CDK1/cyclin B interaction.

To test the first possibility, we evaluated the autophosphorylation capacity (Kristjansdottir et al., 2006) of the full-length WT Myt1 or the mutants Myt1-5A and Myt1-5D. We observed that both WT Myt1 and phospho-mimetic mutant Myt1-5D retain their ability to be autophosphorylated, suggesting that p90Rsk phosphorylation does not impair Myt1 kinase activity (Fig. 30A).

Previous work has shown that the C-terminal domain of Myt1 is involved in the recognition and recruitment of its substrate CDK1/cyclin B (Liu et al., 1999; Wells et al., 1999). To determine whether Myt1 phosphorylation by either CDK1/XRINGO or p90Rsk affects its binding to CDK1, we incubated GST-fused Myt1-Ct either WT or the mutants Myt1-3AP, Myt1-3DP, Myt1-5A or Myt1-5D, in lysates prepared from G2-arrested oocytes and then made pull down assays to analyze the binding of endogenous CDK1.

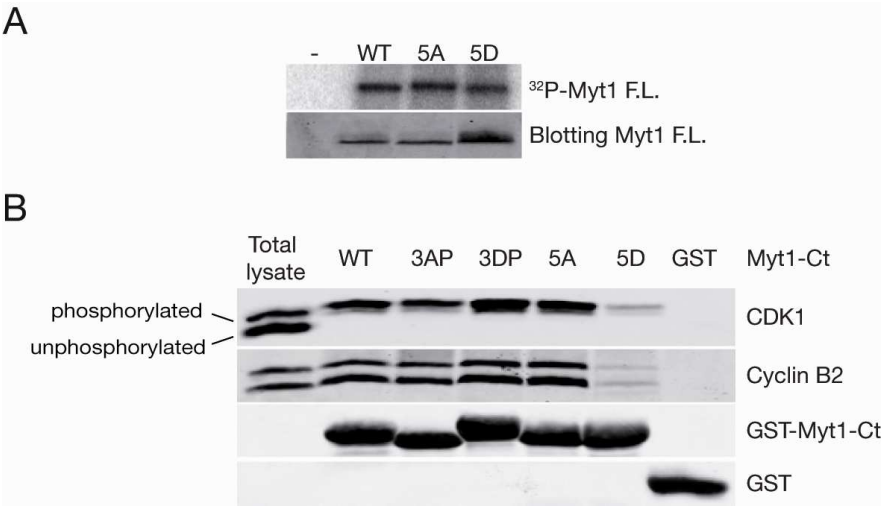

Figure 30 | Reduced Ability of the Myt1-5D Mutant to Bind to CDK1/Cyclin B. (A) Myc-tagged full-length Myt1 (WT or mutants 5A and 5D) was expressed in reticulocyte lysates, immunoprecipitated, and incubated in the presence of [γ-^{32}P]ATP for 2 h at 30°C. Myt1 autophosphorylation was visualized by autoradiography. (B) WT or mutants GST-Myt1-Ct (6 µg) were incubated with G2-arrested oocytes lysates during 3 h at 4°C. GST pull-downs were analyzed by immunoblotting with CDK1, cyclin B2 and GST antibodies.

In this experiment, we found that the majority of the CDK1 associated with Myt1 proteins probably corresponded to the inactive CDK1, phosphorylated on Thr14 and Tyr15 (Fig. 30B). Surprisingly, only the phospho-mimetic mutant Myt1-5D interacted less efficiently with CDK1 than the other Myt1 proteins, suggesting that Thr453, Ser472, Ser475, Ser492 and Ser504 are located in a region that participates in the interaction between Myt1-Ct and CDK1. Previous studies have shown that Myt1 only phosphorylates CDK1 when it is bound to cyclin B (Booher et al., 1997). Consistent with the presence of phosphorylated CDK1 in the GST-Myt1 pull-downs, we confirmed, by immunoblotting analysis, that endogenous cyclin B2 also co-immunoprecipitated with CDK1 in these assays (Fig. 30B).

1.4.5. The C-terminal Domain of Myt1 is Required For Its Biological Activity

To determine whether the C-terminal regulatory domain is required for Myt1 biological activity, we injected oocytes with mRNAs expressing full-length Myt1 or Myt1-ΔC lacking of 210 C-terminal residues, but retains the catalytic domain of Myt1, and then stimulated with progesterone (Fig. 31A). As expected, overexpression of full-length Myt1 delayed the kinetics of meiosis I entry induced by progesterone. However,

the oocytes injected with Myt1-ΔC mature with similar kinetics as oocytes stimulated with progesterone (Fig. 31A).

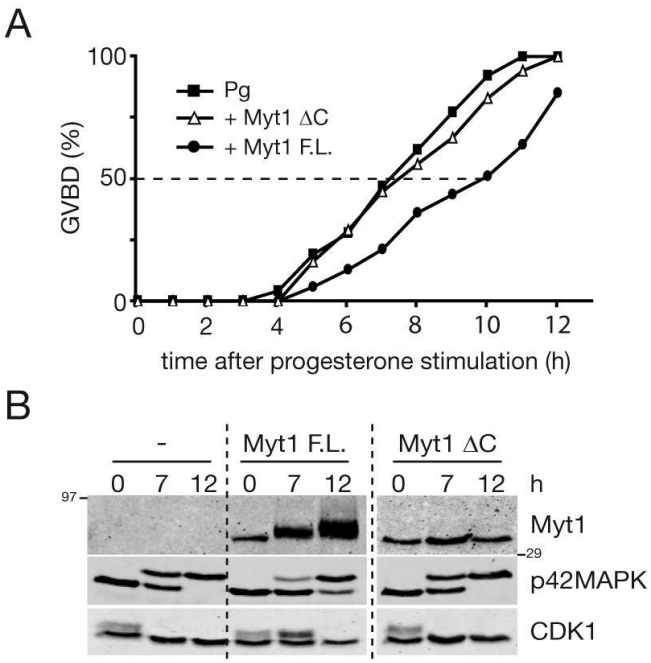

Figure 31 | Myt1 C-terminal domain is required for biological activity. (A) *Xenopus* oocytes were injected with 10 ng of mRNA-encoding Myc-tagged full-length Myt1 or Myt1-ΔC, incubated 14 h at 18°C, and then stimulated with progesterone. GVBD was scored every h. (B) *Xenopus* oocytes were collected at the indicated times after progesterone stimulation, and the lysates were analyzed by immunoblotting. Myt1 was detected with Myc antibody. Molecular weight is indicated in kDa.

Moreover, we found that Myt1-ΔC was not phosphorylated in those oocytes, in spite of the activation of both MPF and the p42MAPK pathway (Fig. 31B). Consistent with these results, dephosphorylation of the inhibitory Thr14/Tyr15 sites of endogenous CDK1 was slower in the oocytes expressing full-length Myt1 than in oocytes expressing Myt1-ΔC (Fig. 31B). Taken together, these results suggest that the C-terminal regulatory domain of Myt1 is necessary for inhibition of *Xenopus* oocyte maturation.

2. CDK/XRINGO Phosphorylates and Regulates Cdc25 Phosphatase Activity

2.1. XRINGO Induces Cdc25 Phosphorylation in *Xenopus* Oocytes

During progesterone-induced *Xenopus* oocyte maturation, Cdc25 undergoes a significant electrophoretic mobility upshift due to hyperphosphorylation (Izumi and Maller, 1993; Kumagai and Dunphy, 1992; Wang et al., 2007). The N-terminal regulatory domain of Cdc25 includes several potential CDK phosphorylation sites, which are known to participate in the regulation of the catalytic activity of Cdc25 (Izumi and Maller, 1993).

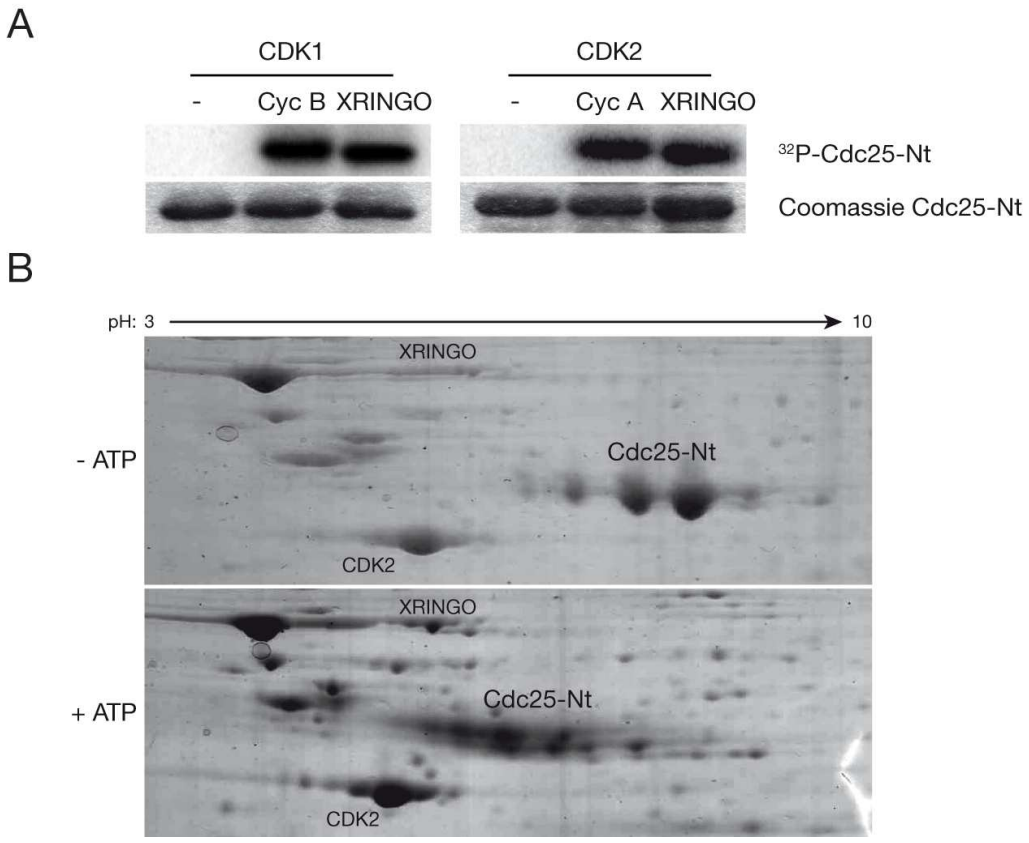

Figure 32 | Phosphorylation of Cdc25 by CDK/XRINGO. (A) Baculovirus-expressed GST-CDK1 (200 or 400 ng) was incubated with cyclin B (200 ng) or MBP-XRINGO (400 ng). GST-CDK2 (250 or 500 ng) was incubated with cyclin A (250 ng) or MBP-XRINGO (500 ng). In the case of cyclins, CDK1 and CDK2 were preincubated with Cak1/Civ1 (200 and 250 ng, respectively) for 10 min at RT in the presence of ATP. Kinase assays were performed with Cdc25-Nt (2 µg) and [γ-^{32}P]ATP for 15 min at 30°C. Cdc25 phosphorylation was visualized by autoradiography. (B) CDK2/XRINGO complex was prepared as in (A). Kinase assays were performed with GST-Cdc25-Nt (10 µg) in the presence or absence of unlabeled ATP for 15 min at 30°C. Cdc25 phosphorylation was visualized by two dimensional gel. IPG strips (pH 3–10) were used for the IEF and SDS-PAGE 12% for the second dimension.

To test whether the regulatory domain of Cdc25 was directly phosphorylated by CDK/XRINGO, we fused the N-terminal residues 9-205 of Cdc25 (Cdc25-Nt) to GST and the bacterially produced fusion protein was used in kinase assays. We observed that recombinant CDK1/XRINGO and CDK2/XRINGO phosphorylated Cdc25-Nt as efficiently as CDK1/cyclin B and CDK2/cyclin A, respectively (Fig. 32A). Moreover, CDK/XRINGO phosphorylation changed the electrophoretic mobility of Cdc25 in two dimensional gels, so that several new spots appeared, suggesting that Cdc25 was phosphorylated on several residues (Fig. 32B).

Next, we investigated whether XRINGO was able to induce Cdc25 phosphorylation in oocytes by injecting mRNA-encoding Myc-tagged Cdc25-Nt and then reinjecting the oocytes with recombinant MBP-XRINGO protein. We observed that the electrophoretic mobility of Cdc25, as determined by immunoprecipitation, was significantly reduced when oocytes entered meiosis I (Fig. 33A), which is in agreement with previous results showing Cdc25 hyperphosphorylation in M phase (Izumi and Maller, 1993; Kumagai and Dunphy, 1992; Wang et al., 2007). Interestingly, we also detected an electrophoretic mobility upshift of Cdc25 only 1 h after injection of XRINGO, at a time when MPF and p42MAPK were all inactive (Fig. 33A).

Recently, it has been published that p42MAPK phosphorylates Cdc25 (Wang et al., 2007). To determine whether XRINGO-induced Cdc25 phosphorylation depends on p42MAPK activity, *Xenopus* oocytes were preincubated with the MEK1/2 inhibitor U0126 and then injected with XRINGO protein. We observed that p42MAPK inhibition delayed but did not inhibit Cdc25 phosphorylation induced by XRINGO (Fig. 33B). These results, together with the presence of Ser/Thr-Pro phosphorylation motifs for CDKs in Cdc25, suggested that Cdc25 could be directly phosphorylated by CDK/XRINGO in oocytes. To test this possibility, we used the CDK1 and CDK2 inhibitor Roscovitine. We found that Roscovitine abolished the XRINGO-induced phosphorylation of Cdc25 in oocytes (Fig. 33C), indicating that XRINGO induces the phosphorylation of the regulatory domain of Cdc25 in the absence of p42MAPK activation but requires CDK kinase activity.

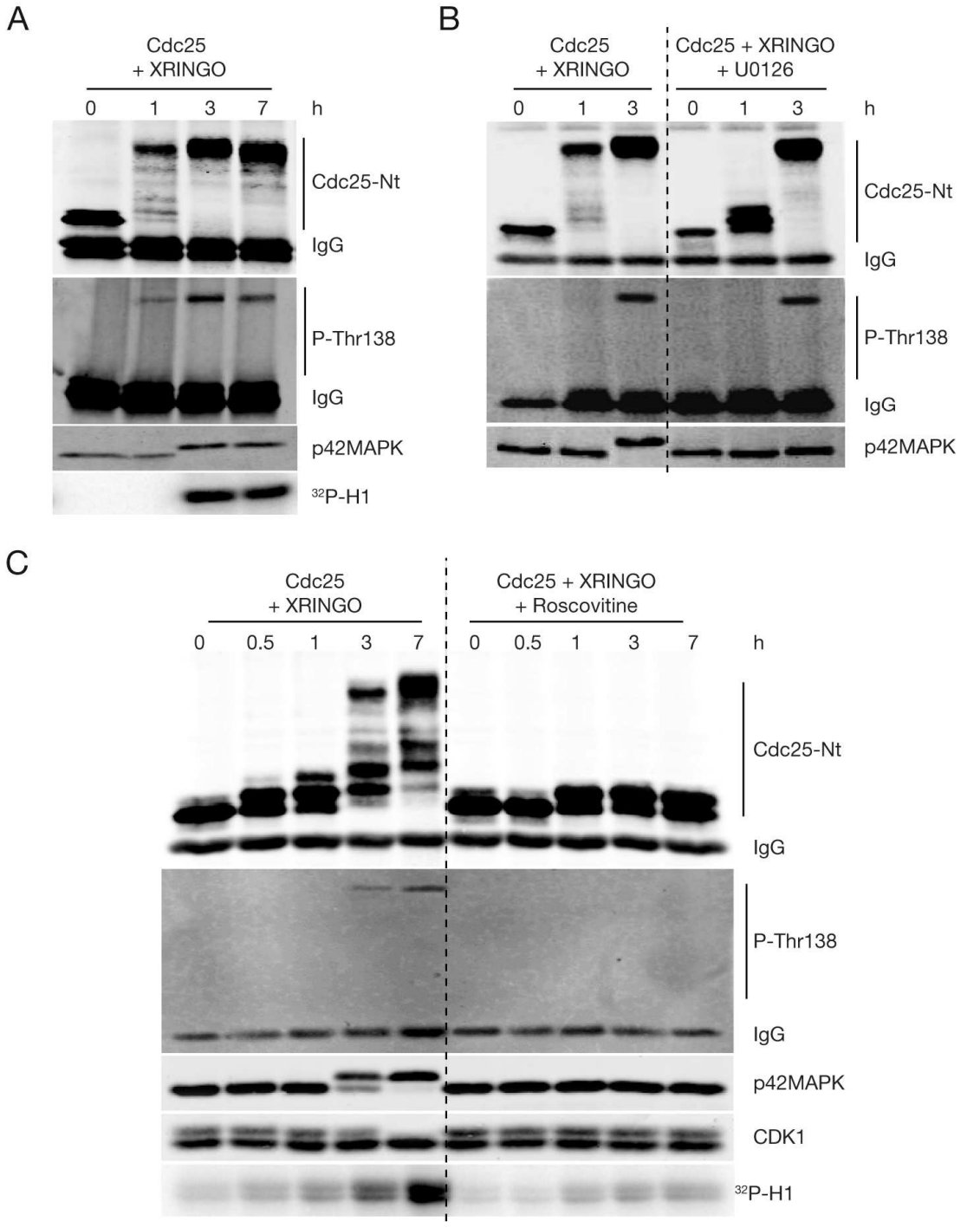

Figure 33 | XRINGO-Induced Phosphorylation of Cdc25 Requires CDK Activation. (A) *Xenopus* oocytes were injected with Myc-tagged Cdc25-Nt mRNA, incubated 14 h at 18°C, and reinjected with MBP-XRINGO (50 ng). Oocytes were collected at the indicated times after the second injection. Oocyte extracts were assayed for H1K phosphorylation or analyzed by immunoblotting. Cdc25-Nt and phospho-Thr138 were detected after immunoprecipitation with Myc and phospho-Thr138 antibodies. (B) *Xenopus* oocytes were injected as in (A), they were treated or not with U0126 and 1 h later they were injected with MBP-XRINGO. Cdc25-Nt and phospho-Thr138 were detected after immunoprecipitation with Myc and phospho-Thr138 antibodies. (C) *Xenopus* oocytes were injected with Myc-tagged Cdc25-Nt mRNA and 14 h later were treated or not with Roscovitine (100 µM) for 2 h before being injected with MBP-XRINGO. Oocyte extracts were assayed for H1K phosphorylation and analyzed by immunoblotting. Cdc25-Nt and phospho-Thr138 were detected after immunoprecipitation with Myc and phospho-Thr138 antibodies.

2.2. Identification of Cdc25 Sites Phosphorylated by CDK/XRINGO

The sequence of *Xenopus* Cdc25-Nt contains 11 consensus CDK phosphorylation sites (Ser/Thr-Pro). To identify which residues of Cdc25 were phosphorylated by CDK/XRINGO, we used mass spectrometry analyses and identified a total of eight phosphorylated residues on the regulatory domain of Cdc25 by CDK1/cyclin B and CDK1/XRINGO (Thr48, Thr67, Thr86, Ser99, Thr112, Thr138, Ser163 and Ser205) (Table 1). However, by means of this technique, we did not observe differences in the phosphorylation sites between CDK/cyclin and CDK/XRINGO complexes.

Table 1

Xenopus Site	Human Site	+/-	Kinase	Function	XRINGO phosphorylation
Thr48		+	CDK1, p42MAPK	Enhances activity and required for CDK1 activation, binds to Pin1	CDK2/XRINGO[1,2]
Thr67		+	CDK1	Required for CDK1 activation, binds to Pin1	CDK1/XRINGO[1,2] CDK2/XRINGO[1,2]
Thr86		?		?	CDK1/XRINGO[1]
Ser99		?		?	CDK1/XRINGO[1]
Thr112		?		?	CDK1/XRINGO[1]
Thr138	Thr130	+	CDK1, p42MAPK	Promotes 14-3-3 release, may create binding site for Plk1	CDK1/XRINGO[1,2] CDK2/XRINGO[1,2]
Ser163		?		?	CDK1/XRINGO[1]
Ser205	Ser168	+/-	p42MAPK, p38γ	Increases activity in *Xenopus* Inhibits activity in mammalian cells	CDK1/XRINGO[1]
Ser251	Ser198	+	Plk1	Promotes nuclear translocation	
Ser285	Ser214	+	CDK1	Promotes PP1-mediated dephosphorylation of Ser287	CDK1/XRINGO[1,2]
Ser287	Ser216	-	PKA, Chk1/2, C-TAK, CAMKII	Binding site for 14-3-3, blocks nuclear import	

Table 1 | Phosphorylated Residues on Cdc25. The effect of phosphorylation at specific residues is listed as activating (+) or inactivating (-). 1- Identified by mass spectrometry, 2- Identified by immunoblotting. ? Indicates unknown function.

To identify the specific XRINGO phosphorylation sites in Cdc25, we used five GST-tagged Cdc25 fragments (namely F1, F2, F3, F4 and F5) that contained residues 9-129, 128-213, 251-353, 371-500, and 499-550 of Cdc25, respectively (Fig. 34A) (Wang et al., 2007), and phosphorylated these fragments with CDK complexes.

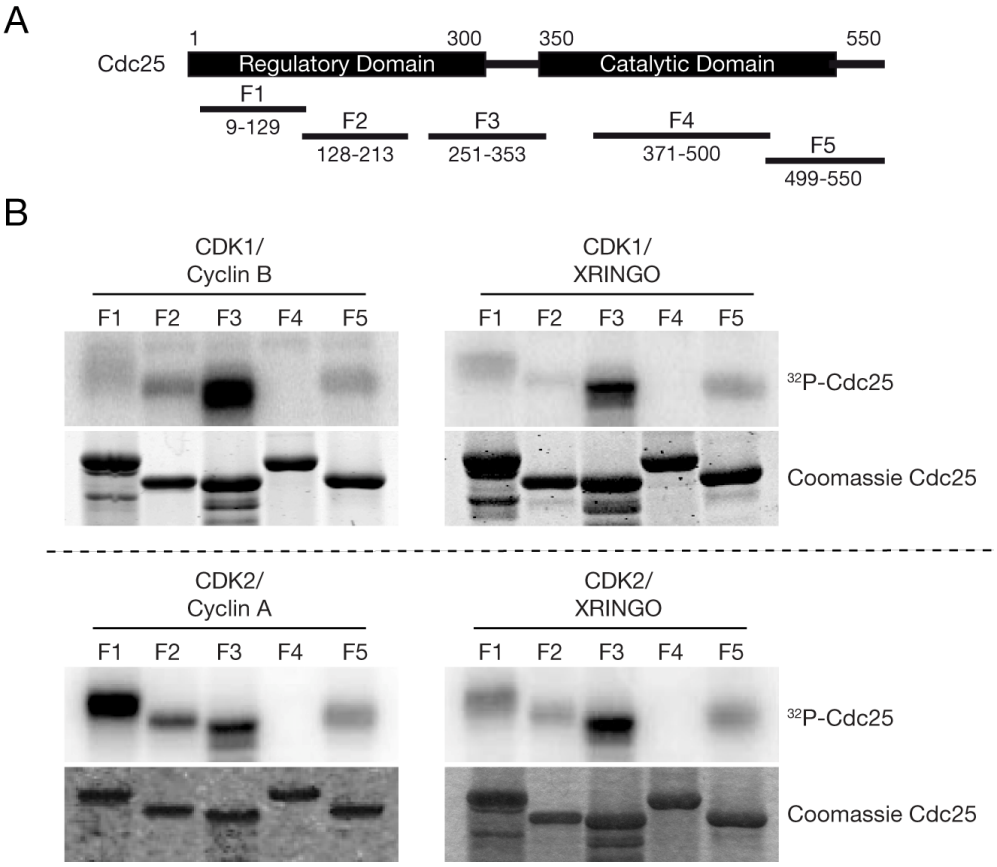

Figure 34 | CDK/Cyclin and CDK/XRINGO Complexes Phosphorylate Similar Cdc25 Fragments. (A) Diagram of the five Myt1-Ct fragments produced as GST fusion proteins for *in vitro* phosphorylation. (B) Bacterially produced GST-CDK1 (1.5 µg) was preincubated in concentrated *Xenopus* oocyte extracts, recovered on glutathione-Sepharose beads and then incubated with either cyclin B or MBP-XRINGO (1.5 µg). GST-CDK2 (250 or 500 ng) was incubated with cyclin A (250 ng) or MBP-XRINGO (500 ng). In the case of cyclin A, CDK2 were preincubated with Cak1/Civ1 (200 and 250 ng, respectively) for 10 min at RT in the presence of ATP. Kinase assays were performed with Cdc25 fragments (2 µg) and [γ-^{32}P]ATP for 15 min at 30°C. Cdc25 phosphorylations were visualized by autoradiography.

We observed that CDK1/cyclin B and CDK1/XRINGO phosphorylated *in vitro* mainly the F3 fragment, which contains three potential sites of phosphorylation: Ser285, Thr308 and Ser321 (Fig. 34B). This result is consistent with the idea that CDK1 phosphorylates Ser285 (Izumi and Maller, 1993). In contrast, CDK2 complexes phosphorylated F1, F2, F3 and F5 fragments, but to different extents (Fig. 34B). We then mutated each of the potential phosphorylation sites in the F3 fragment and

determined the effect on phosphorylation by the relevant kinase. For CDK1 complexes, elimination of most (about 90%) of the F3 phosphorylation required both the Ser285Ala and Thr308Val mutations, whereas the Ser270Ala mutation (a non-consensus CDK site) had no effect (Fig. 35A). Curiously for CDK2 complexes, the Ser270Ala mutation eliminated about 80% of the phosphorylation of F3 (Fig. 35B), whereas the double Ser285Ala and Thr308Val mutation completely eliminated the F3 phosphorylation.

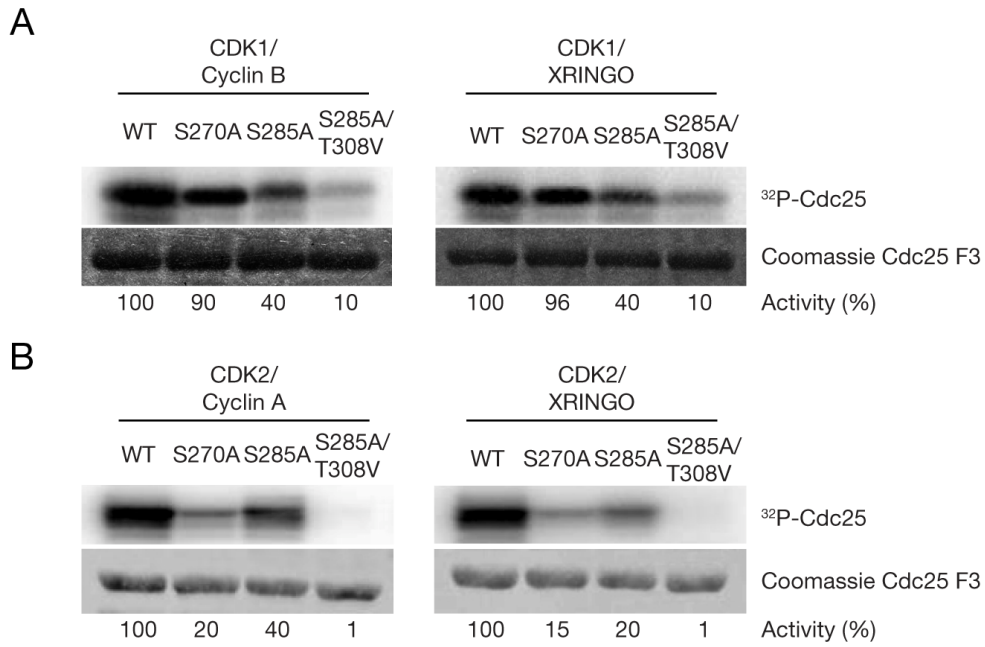

Figure 35 | CDK/Cyclin and CDK/XRINGO Complexes Phosphorylate the Same Cdc25 Sites. (A) Bacterially produced GST-CDK1 (1.5 µg) was preincubated in concentrated *Xenopus* oocyte extracts, recovered on glutathione-Sepharose beads and then incubated with either cyclin B or MBP-XRINGO (1.5 µg). (B) GST-CDK2 (250 or 500 ng) was incubated with cyclin A (250 ng) or MBP-XRINGO (500 ng). In the case of cyclin A, CDK2 were preincubated with Cak1/Civ1 for 10 min at RT in the presence of ATP. Kinase assays were performed with WT or mutants GST-Cdc25 F3 (2 µg) in the presence of [γ-^{32}P]ATP for 15 min at 30°C. Cdc25 phosphorylations were visualized by autoradiography.

To confirm these results, we used antibodies that recognized Cdc25 phosphorylated on specific phospho-Thr48, phospho-Thr67, phospho-Thr138 and phospho-Ser285 residues. Consistent with the above results, CDK1 bound to XRINGO or cyclin B phosphorylate Ser285 to a similar extent. In the case of CDK2, we observed that Ser285 is phosphorylated by CDK2/cyclin A more efficiently than CDK2/XRINGO. However, CDK2/XRINGO phosphorylates Cdc25 mainly on Thr48 (Fig. 36 and Table 1). Thr138 was phosphorylated more efficiently by CDK/cyclin than CDK/XRINGO complexes. Finally, Thr67 is phosphorylated with similar efficiency by

the different CDK complexes. Together, these results indicate that CDK/XRINGO phosphorylates *in vitro* Cdc25 in relevant sites required for its activation.

In agreement with these results, we also found that XRINGO induces Cdc25 phosphorylation on Thr138 during *Xenopus* oocyte maturation (Fig. 33A). Importantly, this XRINGO-induced phosphorylation did not depend on p42MAPK activation but required CDK activity (Fig. 33B and 33C).

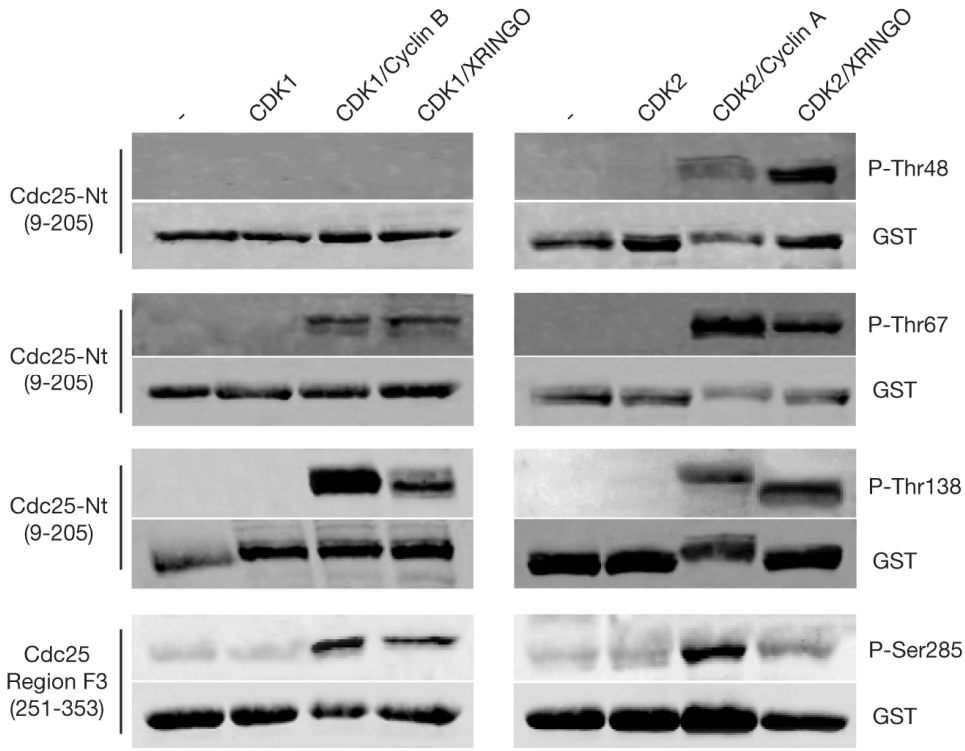

Figure 36 | CDK/XRINGO Phosphorylates Cdc25 in Sites Required for Its Activation. Bacterially produced GST-CDK1 (1.5 µg) was preincubated in concentrated *Xenopus* oocyte extracts, recovered on glutathione-Sepharose beads and then incubated with either cyclin B or MBP-XRINGO (1.5 µg). GST-CDK2 (250 or 500 ng) was incubated with cyclin A (250 ng) or MBP-XRINGO (500 ng). In the case of cyclin A, CDK2 was preincubated with Cak1/Civ1 in the presence of ATP. Kinase assays were performed with GST-Cdc25-Nt or GST-Cdc25 F3 (2 µg) in the presence of ATP for 30 min at 30°C. Cdc25 phosphorylations were detected with antibodies that recognize phosphorylated Thr48, Thr67, Thr138 and Ser285.

Recently, it has been reported that CDK2/cyclin A and CDK2/RINGO A phosphorylate *in vitro* different subsets of sites on all three mammalian Cdc25 isoforms (A, B and C) (Cheng et al., 2005a). To identify which residues of Cdc25 were specifically phosphorylated by CDK/XRINGO we used phosphopeptide mapping. We first confirmed that recombinant full-length GST-Cdc25 was phosphorylated to about the same extent by each CDK1 complex. Since there are multiple potential CDK

phosphorylation sites in *Xenopus* Cdc25 protein, it was not surprising that multiple sites were phosphorylated (Fig. 37).

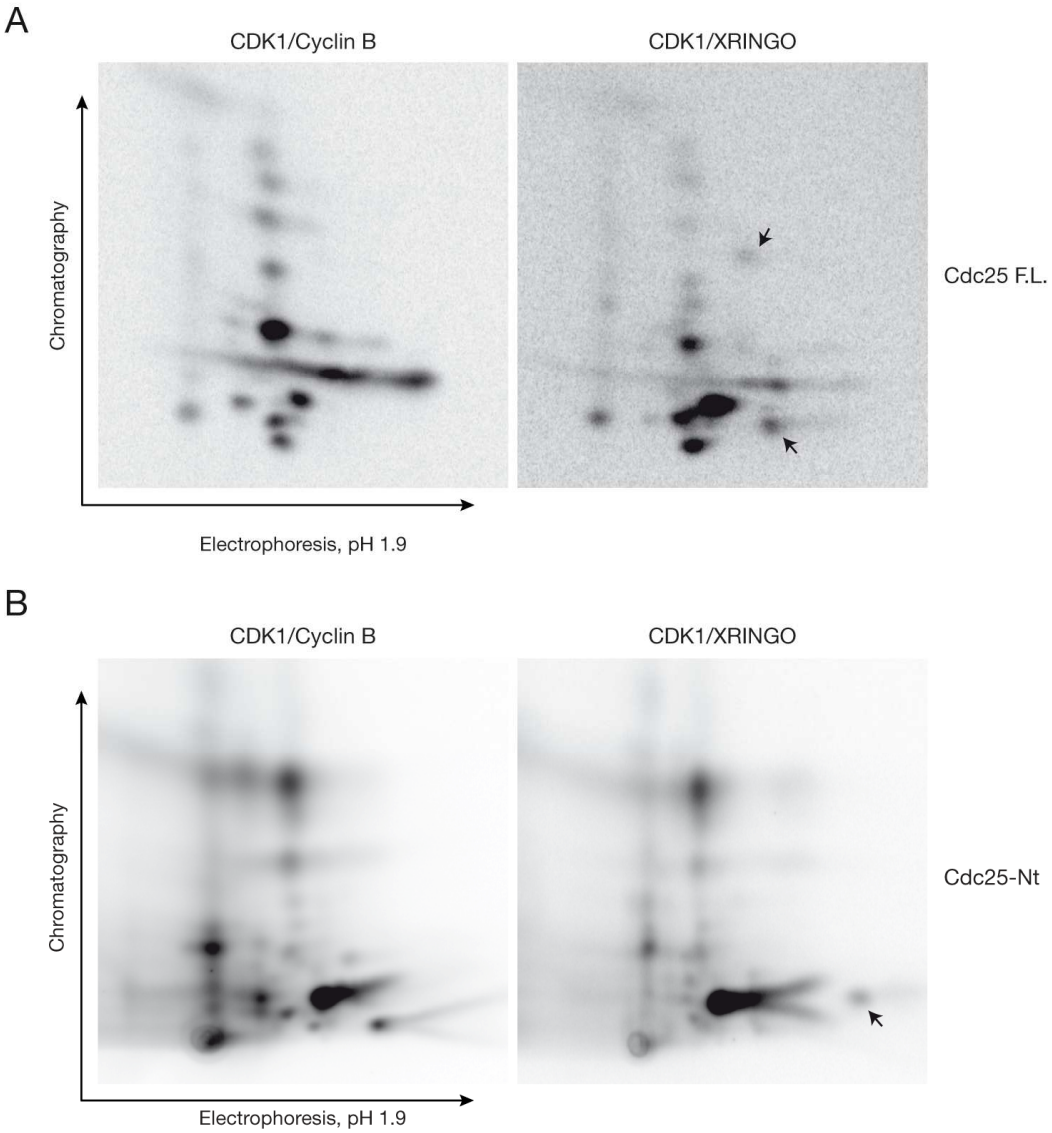

Figure 37 | Tryptic Phosphopeptide Mapping of Cdc25 Proteins. Tryptic phosphopeptide mapping of full-length GST-Cdc25 (A) and GST-Cdc25-Nt (B) phosphorylated by CDK1/cyclin B and CDK1/XRINGO. GST-Cdc25 proteins (10 µg) were phosphorylated by baculovirus-expressed CDK1 activated with cyclin B or MBP-XRINGO (200 ng), separated by 10% SDS-PAGE, extracted, and digested with trypsin. Phosphopeptides were separated on thin layer chromatography plates by horizontal electrophoresis followed by chromatography and were detected by autoradiography. Arrows indicate phosphopeptides unique for CDK1/XRINGO.

By using phosphopeptide mapping, we found that CDK1/cyclin B and CDK1/XRINGO produced distinct phosphopeptide patterns (Fig. 37A). These phosphopeptides could be grouped into two categories. In the first group, we observed phosphopeptides unique to one kinase (i.e. CDK1/cyclin B or

CDK1/XRINGO), indicating a strong influence of the CDK1 partner on phosphorylation specificity. Phosphopeptides in the second group were phosphorylated by both kinases, but to different extents. In particular, we observed that CDK1/XRINGO phosphorylates *in vitro*, at least, two different peptides on full-length Cdc25 than CDK1/cyclin B (Fig. 37A). To identify whether peptides phosphorylated by CDK1/XRINGO are located in the regulatory domain of Cdc25, we performed phosphopeptide mapping in this Cdc25 region. We also observed different phosphopeptide patterns by either CDK1/cyclin B or CDK1/XRINGO (Fig. 37B).

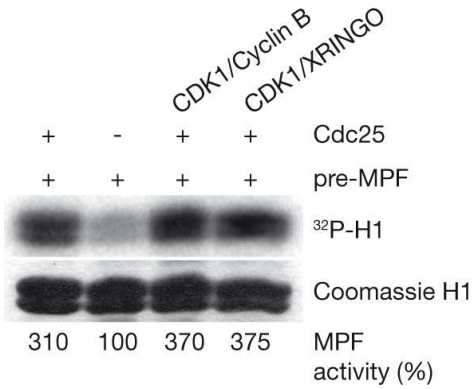

Figure 38 | CDK1/XRINGO-Induced Phosphorylation Activates Cdc25 Phosphatase Activity. Full length GST-Cdc25 (1 µg) bound to beads was preincubated with baculovirus-expressed CDK1 activated with cyclin B or MBP-XRINGO (200 ng) for 60 min at 30°C in the presence of ATP. GST-Cdc25 then was recovered and washed extensively. Cdc25 was incubated with pre-MPF immunoprecipitated from G2-arrested oocytes during 45 min at 30°C in phosphatase buffer. Kinase assays were the performed with histone H1 (4 µg) and [γ-^{32}P]ATP for 15 min at 30°C. H1 phosphorylation was visualized by autoradiography.

Finally, we performed phosphatase assays to test whether XRINGO-induced phosphorylation could directly activate Cdc25 phosphatase activity toward pre-MPF. For this purpose, recombinant full-length GST-Cdc25 was preincubated with CDK1/cyclin B or CDK1/XRINGO. Cdc25 was then recovered by glutathione-beads and thoroughly washed to eliminate the possible carryover of CDK1 activity. The phosphatase activity of Cdc25 was assayed by incubation with pre-MPF immunoprecipitated from G2-arrested oocytes and histone H1. The results showed that Cdc25 dephosphorylates and activates pre-MPF and this activation is increased by pre-phosphorylation by CDK1/cyclin B and CDK1/XRINGO (Fig. 38).

Taken together, these results suggest that CDK1/XRINGO and CDK1/cyclin B have distinct but also partially overlapping sites on Cdc25, some of which are required for Cdc25 activation, e.g. Thr138 and Ser285.

DISCUSSION

1. Interplay Between CDK1/XRINGO and p90Rsk Plays an Important Role in Myt1 Inactivation During Oocyte Maturation

The molecular mechanisms that regulate Myt1 activity during M phase entry are still unsolved. We have identified three Ser-Pro sites (Ser410, Ser414 and Ser444) located in the C-terminal non-catalytic domain of Myt1 whose phosphorylation inhibits Myt1 kinase activity. Importantly, these sites are efficiently phosphorylated by CDK1/XRINGO but not CDK1/cyclin B complexes. Moreover, XRINGO-associated CDK1 is also less susceptible to inhibitory phosphorylation by Myt1 than CDK1/cyclin B complex.

We also have identified five p90Rsk consensus sites (Thr453, Ser472, Ser475, Ser492 and Ser504) located in the C-terminal domain of Myt1 whose phosphorylation by p90Rsk reduces the affinity of Myt1 for CDK1/cyclin B. Moreover, these sites are phosphorylated during progesterone-induced oocyte maturation.

Our findings have uncovered a novel and important role for RINGO proteins in the M phase-associated inactivation of Myt1.

1.1. Regulation of Myt1 Activity by CDK/XRINGO During Oocyte Maturation

The protein kinase Myt1 presents two domains, the N-terminal catalytic domain and the C-terminal regulatory domain. Moreover, there is a 20 residues long hydrophobic domain that is thought to anchor the protein to the endoplasmic reticulum and Golgi membranes (Liu et al., 1999; Liu et al., 1997; Mueller et al., 1995b; Wells et al., 1999). Cyclin B2 also localizes to the Golgi complex (Jackman et al., 1995). It has been proposed that both the kinase domain and the regulatory domain are oriented toward the cytosolic face of these membrane compartments, where Myt1 is able to recruit CDK1/cyclin B through a cyclin B interaction motif (RXL motif) present in its regulatory domain. This, in turn, facilitates that the N-terminal catalytic domain of Myt1 phosphorylates CDK1 (Liu et al., 1999; Liu et al., 1997; Mueller et al., 1995b; Wells et al., 1999).

Myt1-induced phosphorylation of CDK1 on Thr14 and Tyr15 is known to play a key role in the G2 arrest of oocytes by maintaining preformed CDK1/cyclin B complexes inactive (pre-MPF). Although the kinase activity of Myt1 appears to be cell cycle regulated, no changes in intracellular localization or protein levels have been

detected (Liu et al., 1999; Liu et al., 1997; Mueller et al., 1995b; Wells et al., 1999). Myt1 is active in interphase when CDK/cyclins are inhibited and has decreased activity in M phase when CDK/cyclins are activated (Booher et al., 1997). The decrease in activity during M phase has been linked to hyperphosphorylation of Myt1. Although phosphorylation-dependent inactivation of Myt1 kinase activity has been known for several years (Inoue and Sagata, 2005; Kristjansdottir et al., 2006; Liu et al., 1999; Liu et al., 1997; Mueller et al., 1995b; Okumura et al., 2002; Palmer et al., 1998; Wells et al., 1999), little is known about the molecular mechanisms involved in Myt1 inactivation during the G2/M transition.

Previous studies supported the implication of the p42MAPK-activated protein kinase p90Rsk in the phosphorylation and inactivation of Myt1 during *Xenopus* oocyte maturation (Palmer et al., 1998). However, in some cases (see Introduction), progesterone can induce CDK1/cyclin B activation in the absence of detectable p42MAPK activity (Dupre et al., 2002; Fisher et al., 1999; Gross et al., 2000; Peter et al., 2002), suggesting that p90Rsk-independent pathways can also lead to Myt1 inactivation in *Xenopus* oocytes. This is consistent with a previous observation of our laboratory. Palmer et al. (1998) identified two protein kinase activities that can bind to and phosphorylate Myt1. One of them was p90Rsk and the other was dependent on CDK1 activity and could be either CDK1/cyclin B or CDK1/XRINGO complex. Indeed, we here demonstrated that the latter is the responsible complex.

We have found that XRINGO-activated CDK1 and CDK2 can phosphorylate the regulatory domain of Myt1 on specific Ser-Pro sites (Ser410, Ser414 and Ser444), which are poorly targets of the CDK/cyclin complexes. Moreover, these sites are phosphorylated during XRINGO-induced oocyte maturation prior to MPF activation and in a CDK-dependent manner, but independently of new protein synthesis (e.g. Mos) and the p42MAPK-p90Rsk pathway. Finally, phosphorylation of these sites inhibits Myt1 activity both *in vitro* and in oocytes, suggesting that the catalytic activity of Myt1 has been impeded. Thus, our results indicate that CDK/XRINGO is an excellent candidate to trigger Myt1 inactivation during meiosis I entry in *Xenopus* oocytes.

The finding that the Myt1-3AP mutant, which is not phosphorylated by CDK/XRINGO, only delays, instead of blocks, XRINGO-induced oocyte maturation could be explained by the participation of other signalling pathways that converge in the inactivation of Myt1 activity. This might be sufficient to allow some pre-MPF

activation, which, in turn, would trigger the positive feedback loops targeting both Myt1 and Cdc25 (Schmitt and Nebreda, 2002). An alternative, not mutually exclusive explanation, would be that CDK/XRINGO phosphorylates other substrates in the oocyte, such as CPEB (Kim and Richter 2007) or Cdc25 (see below), which could also contribute to the induction of oocyte maturation.

1.2. Regulation of Myt1-CDK1/Cyclin B Interaction by p90Rsk

The finding that the overexpression of the catalytic domain of Myt1 did not inhibit progesterone-induced oocyte maturation, suggested that the C-terminal domain, which contains the RXL motif necessary for binding to cyclin B, is essential for the biological activity of *Xenopus* Myt1. Therefore, Myt1 negatively regulates CDK1/cyclin B by stepwise mechanism, which requires the C-terminal domain: Myt1 binds to and sequesters CDK1/cyclin B in the cytoplasm, which in turn allow the phosphorylation of CDK1 at Thr14 and Tyr15, resulting in the inactivation of its catalytic activity.

Interestingly, Liu et al. (1999) have shown that unphosphorylated Myt1 interacts with CDK1/cyclin B but the hyperphosphorylated form of Myt1 does not associate with CDK1/cyclin B complexes. This observation suggested that the phosphorylation status of Myt1 could define the binding to CDK1/cyclin B. However, the molecular mechanisms involved in the release of CDK1 from Myt1 are not known.

We have observed that the phosphorylation on three Ser residues by CDK/XRINGO (Ser410, Ser414 and Ser444) do not impair the interaction between Myt1 and CDK1/cyclin B. On the other hand, the protein kinase p90Rsk can phosphorylate the C-terminal regulatory domain of Myt1 on different sites than CDK/XRINGO. Moreover, these p90Rsk-specific sites (Thr453, Ser472, Ser475, Ser492 and Ser504) are phosphorylated during progesterone-induced oocyte maturation. Importantly, phosphorylation of these five residues by p42MAPK-activated p90Rsk decreases the affinity of Myt1 for CDK1/cyclin B.

Thus, our results suggest that two mechanisms regulate Myt1 activity, both of which require its C-terminal regulatory domain: the catalytic activity of Myt1 is negatively regulated through the phosphorylation induced by CDK/XRINGO, whereas p90Rsk-induced phosphorylation impairs the binding between Myt1 and pre-MPF.

An important question arising from these results is what would be the initial event in the regulation of Myt1 activity. We have observed that there is indeed a timing

in Myt1 phosphorylation. The C-terminal regulatory domain of Myt1 is phosphorylated at early time points, before the activation of p42MAPK-p90Rsk pathway, and this correlates with the progesterone-induced accumulation of endogenous XRINGO protein. In contrast, late Myt1 phosphorylation correlates with p90Rsk activation. Thus, we think that CDK/XRINGO-induced phosphorylation is the first step in the regulation of Myt1. In agreement with this idea, it has been shown that Myt1 preferentially associates with the active and hyperphosphorylated form of p90Rsk present in mature oocytes (Palmer et al., 1998). Moreover, we have found that early Myt1 phosphorylation induced by CDK/XRINGO increases the interaction between Myt1 and p90Rsk. This, in turn, facilitates p90Rsk-induced phosphorylation of Myt1, resulting in the release of CDK1/cyclin B from Myt1.

Previously, our group evaluated the importance of XRINGO during oocyte maturation using antisense oligonucleotides. Ferby et al. (1999) showed that the elimination of endogenous XRINGO mRNAs strongly delayed progesterone-induced oocyte maturation (about 50%), suggesting that accumulation of XRINGO protein is critically required for the initiation of meiotic maturation. Similar results have been observed in the absence of Mos-p42MAPK-p90Rsk pathway activation (Dupre et al., 2002; Fisher et al., 1999; Gross et al., 2000; Peter et al., 2002). Moreover, the constitutively active form of p90Rsk triggers oocyte maturation (about 40%) in the absence of progesterone stimulation, suggesting that other proteins are required for efficient meiotic maturation (Gross et al., 2001).

We proposed that both proteins, XRINGO and p90Rsk, are required for correct timing entry into meiosis I and MPF activation. We think that progesterone activates more than one pathway to induce meiotic maturation, in case one pathway fails, then progesterone would still be able to trigger CDK1 activation. It is possible that each individual pathway is dispensable, provided that the other one remains functional. We have observed that neither p42MAPK-p90Rsk pathway nor new protein synthesis (e.g. Mos) are required for Myt1 phosphorylation, MPF activation and oocyte maturation induced by injection of XRINGO protein. These results are in agreement with previous results, where the injection of mRNA encoding XRINGO induced meiotic maturation even in oocytes in which the synthesis of Mos and cyclin B was blocked by the antisense oligonucleotides (Haccard and Jessus 2006). Although we did not evaluate the phosphorylation of Myt1 in absence of the XRINGO synthesis, it is possible that progesterone-activated p42MAPK-p90Rsk pathway is able to phosphorylate and

inhibit Myt1 activity. Further experiments will be required to determine whether progesterone is able to induce Myt1 phosphorylation in the absence of both XRINGO synthesis and activation of the p42MAPK-p90Rsk pathway.

2. Regulation of Cdc25 Activity During *Xenopus* Oocyte Maturation

The molecular mechanism by which Cdc25 becomes activated during M phase induction is one of the key unsolved problems in the eukaryotic cell cycle control. It has been proposed that full activation of Cdc25 during *Xenopus* oocyte maturation requires both initiation and amplification steps (Perdiguero and Nebreda, 2004). In principle, kinases that are involved in the initiation step can be activated prior to pre-MPF activation, leading to a threshold level of Cdc25 activity.

Recently, it has been proposed that p42MAPK is the kinase responsible for the initiation of Cdc25 activation during *Xenopus* oocyte maturation (Wang et al., 2007). However, the same authors showed that p42MAPK activation is critically, but not absolutely required for activation of Cdc25. Moreover, inhibition of p42MAPK activity delays, but does not block, progesterone-induced oocyte maturation (Dupre et al., 2002; Fisher et al., 1999; Gross et al., 2000; Peter et al., 2002), and forced activation of p42MAPK does not always induce CDK1 activation (Shibuya et al., 1992). Thus, these observations suggest that progesterone stimulation activates at least one additional kinase that is involved in Cdc25 activation.

In the present study, we have found that XRINGO-activated CDK1 and CDK2 can phosphorylate the regulatory domain of Cdc25 in sites required for its activation. Our results also show that during XRINGO-induced oocyte maturation, Cdc25 is phosphorylated prior to MPF activation and in a CDK-dependent manner, but independently of the p42MAPK activation. Finally, phosphorylation of Cdc25 by CDK1/XRINGO increases its phosphatase activity *in vitro* towards pre-MPF. Thus, CDK/XRINGO complex is an excellent candidate for one of the kinases involved in initiating Cdc25 activation during *Xenopus* oocyte maturation.

The involvement of CDK1/XRINGO in both the initiation and amplification steps of Cdc25 activation can be explained because CDK1/XRINGO phosphorylates Thr138 and Ser285, events required for the release of 14-3-3 from Ccd25 and the recruitment of PP1 to Cdc25, respectively. It is likely that p42MAPK and CDK1/XRINGO may

cause together a precise and robust activation of both Cdc25 and MPF during *Xenopus* oocyte maturation.

Our results also indicate that CDK1/XRINGO and CDK1/cyclin B phosphorylate Cdc25 on different sites. However, the specific XRINGO-phosphorylations are still unknown. Thus, site-directed mutagenesis should be used to validate the importance of these new Cdc25 phosphorylation sites *in vitro* and *in vivo*.

3. Regulation of CDK Substrate Specificity by RINGO Proteins

3.1. T loop Phosphorylation and Its Role in Substrate Recognition

Full activation of CDK1 and CDK2 by cyclins requires the phosphorylation on the T loop of the kinase, which undergoes a conformational change (Russo et al., 1996b). This phosphate group plays a role in substrate recognition by interacting with the P+3 position of substrates (Brown et al., 1999). An important distinctive feature of CDK activation by RINGO proteins is that the T loop phosphorylation is not required for the activity of CDK/RINGO complexes (Karaiskou et al., 2001b; Nebreda, 2006), suggesting that XRINGO should provide a phosphorylation-independent mechanism to tether the T loop in an active conformation similar to that displayed by the active CDK2/cyclin A complex. However, it is unclear whether this T loop phosphorylation is required for substrate recognition. Thus, CDK2 phosphorylation on Thr160 does not appear to significantly change the ability of CDK2/RINGO A to phosphorylate short synthetic peptides (Cheng et al., 2005a), whereas it seems to be required for CDK2/RINGO A to efficiently phosphorylate $p27^{Kip1}$ (McAndrew et al., 2007).

Here, we have shown that the phosphorylation of Myt1 by CDK/XRINGO is not affected by the T loop phosphorylation of the CDK, unlike CDK/cyclin complexes. In fact, our group have also observed that XRINGO proteins mutated in the core region seem to be much more dependent than WT XRINGO on the T loop phosphorylation of the CDK to promote activity towards histone H1 (unpublished data). It therefore appears that the RINGO core is not only important for CDK activation but might also compensate for the lack of T loop phosphorylation in substrate recognition by the CDK/RINGO complex, perhaps by creating a negatively charged environment in the proximity of the ligand binding site. This idea is consistent with the observation that in the full active CDK2/cyclin A complex, the peptide substrate is bound within a region that is mostly negatively charged (Brown et al., 2007).

These observations also suggest that RINGO binding to CDKs should mimic, at least partially, the conformational changes that lead to the displacement of the activation loop (Cheng et al., 2005a). This is similar to the mechanism that has been proposed, on the basis of structural studies, for the activation of CDK5 by p25 (Tarricone et al., 2001). Binding of p25 triggers all conformational changes required for CDK5 activation in the absence of T loop phosphorylation. The observation that some RINGO proteins can also bind to and activate CDK5 supports the idea that RINGO/Speedy proteins might use a similar mechanism for CDK activation as p25 does (Dinarina et al., 2005). Thus, RINGO/Speedy proteins would interact with the activation loop more extensively than cyclins do, without the requirement of phosphorylation to bring the T loop in an active conformation.

An important conclusion of our study is that XRINGO-activated CDK1 and CDK2 phosphorylate Myt1 on different sites as the same CDKs activated by cyclins. Moreover, these phosphorylations have important functional consequences for the regulation of Myt1. Previous work showed that CDK/RINGO complexes can phosphorylate all CDK/cyclin substrates tested *in vitro*. However, studies using degenerate peptides based on the canonical CDK substrate sequence KSPRK indicate a more relaxed requirement for specific amino acids in the position P+2, and P+3 in the case of CDK2 activated by human RINGO A, than for CDK2/cyclin A (Cheng et al., 2005a). Interestingly, the C-terminal regulatory domain of Myt1 contains eight SP/TP sites, but none of them contain the canonical sequence S/TPXK/R. Therefore, the residues at positions P+2 and P+3 of Ser410, Ser414, and Ser444 in Myt1 are not favorable for CDK2/cyclin A substrate binding (Stevenson-Lindert et al., 2003), which might explain why these sites are poorly phosphorylated by CDK/cyclin in comparison with CDK/XRINGO.

3.2. The RXL Motif is not Required for Substrate Recognition by CDK/XRINGO

The interaction between a hydrophobic patch containing the MRAIL sequence that is present on the surface of some cyclins (e.g. α1-helix in cyclin A) and the K/RXL motif found on some CDK substrates (such as Rb, p107, Cdc6, E2F and $p27^{Kip1}$) is thought to play an important role in determining substrate specificity and efficient phosphorylation of substrates by CDK/cyclin complexes (Brown et al., 2007; Loog and Morgan, 2005; Schulman et al., 1998; Stevenson-Lindert et al., 2003). Binding to the

K/RXL motif is important because it increases the local concentration of the substrate in the vicinity of the catalytic site of the CDK, and it is responsible for orientating specific CDK phosphorylation sites within the active site of the CDK to further facilitate their phosphorylation, especially when the phosphorylation site lacks a basic residue at position P+3 (Brown et al., 2007; Cheng et al., 2006; Takeda et al., 2001). We have observed that Myt1 contains a canonical RXL sequence that is necessary for binding to cyclin B and it is also required for efficient Myt1 phosphorylation by CDK1/cyclin B. However, mutation of this motif neither affects the binding of Myt1 to XRINGO nor Myt1 phosphorylation induced by CDK1/XRINGO *in vitro*, suggesting that XRINGO and cyclin B use different motifs for substrate recruitment, which, in turn, would facilitate the phosphorylation of different sites in the same CDK substrate.

Although Myt1 contains an RXL motif necessary for binding to cyclin B, it is unclear why CDK1/cyclin B fails to efficiently phosphorylate Myt1 on Ser410, Ser414 and Ser444. In CDK/cyclin substrates, the K/RXL motif facilitates the phosphorylation of SP/TP sites located at a distance of at least 17-60 residues from the K/RXL motif (Cheng et al., 2006). The three Ser residues identified (410, 414, and 444) are too far from this optimal distance to the RXL motif (residues 536-538) of Myt1 to allow that the recruitment of phosphorylation sites to be effective. In agreement with this idea, Inoue and Sagata (Inoue and Sagata 2005) have shown that Myt1 is phosphorylated efficiently by CDK1/cyclin B on Thr478, a residue that is located around 60 residues from the RXL motif.

Unlike CDK/cyclin complexes, CDK/XRINGO complexes are able to phosphorylate non-canonical sequences without the need of an RXL motif. We think that the differences in the catalytic properties of CDK/cyclin and CDK/RINGO complexes are likely to arise from different binding mechanisms and different dynamic properties of the kinases upon association with different partners.

3.3. CDK1/XRINGO is Less Susceptible to Inhibition by Myt1 than CDK1/Cyclin B

XRINGO-bound CDKs are less susceptible to two mechanisms that negatively regulate the activity of CDK/cyclin complexes: interaction with CKIs (Karaiskou et al., 2001b) and inhibitory phosphorylation on Thr14 and Tyr15. Interestingly, the similarity between XRINGO and other non-cyclin CDK activators also extends to regulators

such as p35, which allows CDK5 to escape inhibition by the Tyr15-specific kinase Wee1 (Poon et al., 1997), and binding to CKIs such as $p27^{Kip1}$ (Lee et al., 1996).

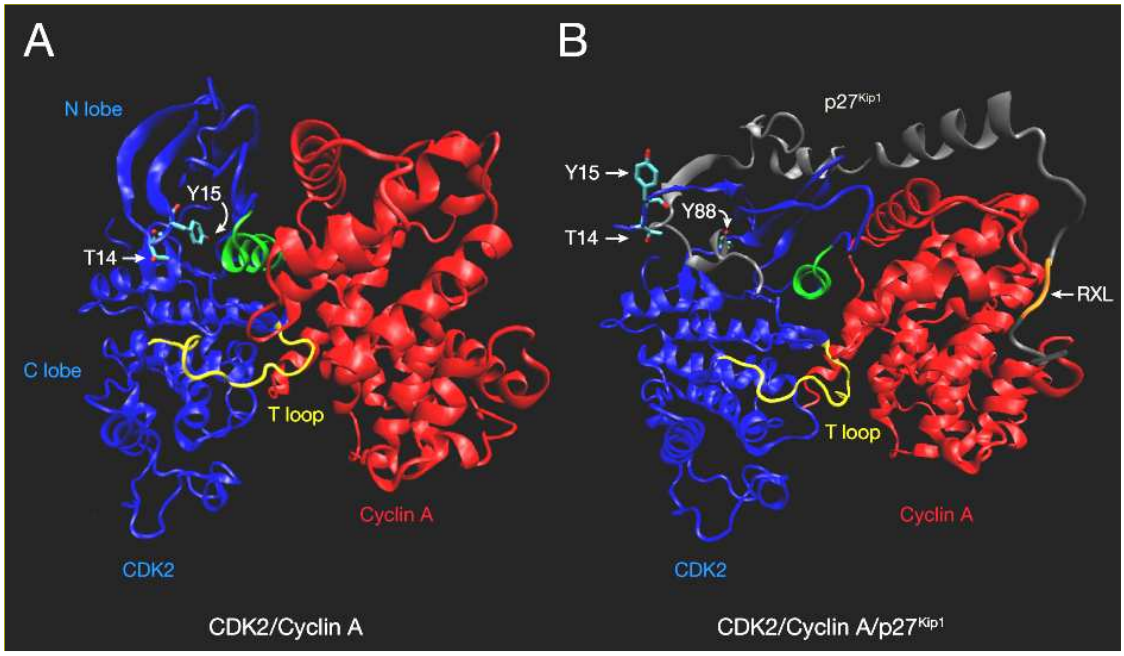

Figure 39 | Crystal Structures of CDK2/cyclin A and CDK2/cyclin A/$p27^{KIP1}$. CDK2/cyclin A (A) and CDK2/cyclin A/$p27^{KIP1}$ (B) complexes are shown. Thr14 and Tyr15 of CDK2 and Tyr88 and RXL motif of $p27^{KIP1}$ are indicated. $p27^{KIP1}$ binds as an extended structure interacting with both cyclin A and CDK2. Binding of $p27^{KIP1}$ to CDK2 is accompanied by extensive structural changes in the N-terminal lobe and catalytic cleft of CDK2 (De Bondt et al., 1993; Jeffrey et al., 1995). For details see text.

We have observed that Myt1 binds to XRINGO, but it is unclear how XRINGO-associated CDK1 is less susceptible to inhibitory phosphorylation by Myt1 than CDK1/cyclin B. The structure of CDK1/cyclin B in complex with the C-terminal domain of Myt1 has not yet been solved. Thus, we do not know how CDK1 is phosphorylated on Thr14 and Tyr15 by the protein kinase Myt1. In the crystal structure of both monomeric CDK2 and CDK2/cyclin A complex, Thr14 and Tyr15 are located deeply into the catalytic cleft of the CDK, and the side chains of both residues are inaccessible to the solvent and thus, to inhibitory phosphorylation (Fig. 39A) (Jeffrey et al., 1995). However, structural studies of the CDK2/cyclin A/$p27^{Kip1}$ complex have shown that $p27^{Kip1}$ is recruited by its RXL motif to cyclin A, and inhibits CDK2 kinase activity by inducing a significant conformational change in the kinase N-terminal β-sheet lobe (Russo et al., 1996a; Russo et al., 1998). In fact, the Tyr88 residue of $p27^{Kip1}$, located 60 residues from the RXL motif, is positioned into the catalytic cleft of

the CDK2. As a consequence of this conformational change, the hydroxyl groups of both Thr14 and Tyr15 of CDK2 are fully exposed to the solvent, making them more accessible to inhibitory phosphorylations (Fig. 39B).

From these observations, we propose that the C-terminal regulatory domain of Myt1 behaves like $p27^{Kip1}$, in such a way that after Myt1-Ct binding to CDK1/cyclin B complex via an RXL motif, CDK1 undergoes a conformational change similar to the one in CDK2 bound to $p27^{Kip1}$ (Fig. 39B). This, in turn, facilitates that the hydroxyl groups of both Thr14 and Tyr15 are accessible to the catalytic domain of Myt1, which then phosphorylates both residues of CDK1. This idea is in agreement with previous results showing that CDK1 binding to cyclin B is required in order to be phosphorylated and inhibited by Myt1, because in the absence of cyclin B, CDK1 is not recruited to Myt1 (Liu et al., 1999; Wells et al., 1999).

An important question that arises from our results is why the CDK1/XRINGO complex is less susceptible to inhibitory phosphorylation by Myt1 than CDK1/cyclin B, in spite of both complexes being capable efficiently to bind to Myt1-Ct. We have shown that XRINGO is not recruited to Myt1 through an RXL motif, as cyclin B does. Thus, the phosphorylation sites of CDK1 (Thr14/Tyr15) would be exposed in a different manner. In agreement with this idea, it has been shown that CDK activation by RINGO proteins is different to cyclin-activated CDKs (Karaiskou et al., 2001b; Nebreda, 2006). Although RINGO proteins bind to a similar region of the CDK as cyclins do (PSTAIRE helix and T loop) (Dinarina et al., 2005), the activation loop conformation adopted by CDK2 upon binding RINGO A appears to differ significantly from that adopted upon cyclin A binding (Cheng et al., 2005a). Moreover, the absence of the MRAIL hydrophobic motif, a typical region in cyclins responsible for K/RXL recruitment, could be also an important factor for the reduced inhibitory efficiency of Myt1 on CDK1/XRINGO complexes.

Our results suggest that CDK1/XRINGO is regulated by a different mechanism to inhibitory phosphorylation by Myt1 than CDK1/cyclin B. First, CDK1/cyclin B is easily phosphorylated and inhibited by Myt1, due to efficient binding of Myt1-Ct to cyclin B through the RXL motif. In contrast, XRINGO-associated CDK1 is not targeted by inhibitory phosphorylation induced by Myt1, and CDK1/XRINGO also phosphorylates more efficiently the inhibitory Myt1 sites, resulting in the inactivation of Myt1 kinase activity.

4. Model for *Xenopus* Oocyte Maturation

We propose the following sequence of events during oocyte maturation. In G2-arrested oocytes, the protein kinase Myt1 is active and Cdc25 phosphatase remains inactive by phosphorylation on Ser287 and 14-3-3 binding. About 90% of the CDK1 present in these oocytes is not associated with cyclins, and only part of the pool of this monomeric CDK1 appears to be already phosphorylated on Thr161 (De Smedt et al., 2002). When G2-arrested oocytes are stimulated with progesterone, XRINGO protein accumulates transiently, probably due to both enhanced mRNA translation (Padmanabhan and Richter 2006) and protein stabilization (Gutierrez et al., 2006). XRINGO protein then binds to both monomeric CDK1 populations, phosphorylated and non-phosphorylated on Thr161, and the CDK1/XRINGO complexes phosphorylate Myt1 on Ser410, Ser414 and Ser444, downregulating its kinase activity towards pre-MPF (Fig. 40). Although XRINGO-CDK1 and -CDK2 can both, in principle, phosphorylate the same Myt1 sites, we favor CDK1 as the initial partner of XRINGO for the triggering events, mainly because G2-arrested oocytes contain a larger pool of monomeric CDK1, whereas CDK2 is almost undetectable at this stage (Rempel et al., 1995).

The same CDK1/XRINGO complexes can also phosphorylate Cdc25 on Thr138, leading to the release of 14-3-3 proteins from Cdc25 (Fig. 40) (Margolis et al., 2006a; Margolis et al., 2003). p42MAPK can also contribute to Thr138 phosphorylation (Wang et al., 2007). CDK1/XRINGO, but not p42MAPK, then phosphorylates Ser285, resulting in the recruitment of PP1 to Cdc25, which in turn dephosphorylates Ser287 (Fig. 40) (Margolis et al., 2003). Cdc25 then acquires a basal level of phosphatase activity, which triggers the dephosphorylation of a pool of pre-MPF. We still do not know if Cdc25 removes the inhibitory phosphorylations when pre-MPF is bound to Myt1 or when it is released from Myt1 (Fig. 40).

The initial pool of MPF could participate in positive feedback loops targeting both Myt1 and Cdc25 that help to trigger entry into meiosis I (Schmitt and Nebreda, 2002). However, there is no evidence that CDK1/cyclin B phosphorylation can inactivate Myt1 (Booher et al., 1997). Thus, any contribution of MPF to Myt1 inactivation is likely mediated at other levels, perhaps by the inhibition of PP1-mediated Myt1 dephosphorylation (Liu et al., 1997; Wang et al., 2004), which should preserve Myt1 inactive.

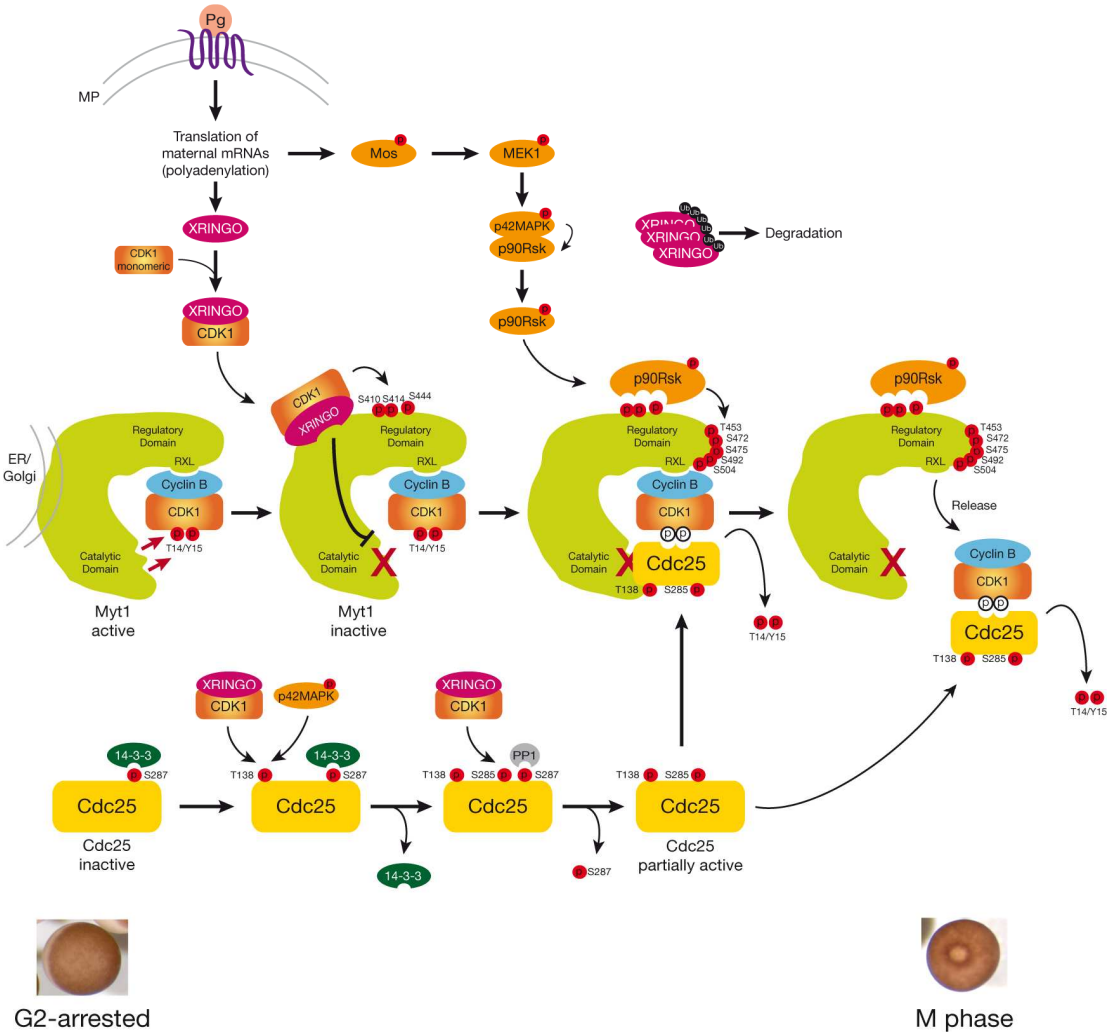

Figure 40 | Mechanism Proposed for Meiotic Oocyte Maturation. See text for explanation.

During this time, the p42MAPK-p90Rsk pathway is fully active and contributes to Myt1 phosphorylation (Palmer et al., 1998). In principle, there is no evidence that p90Rsk can phosphorylate Ser-Pro sites (Anjum and Blenis, 2008). In fact, our results suggest that both p90Rsk and CDK1/XRINGO target Myt1 on different sites. Myt1 phosphorylation on three Ser-Pro sites by CDK1/XRINGO increases the interaction between Myt1 and p90Rsk probably through the formation of a putative docking site for p90Rsk (Fig. 40). Although these phosphorylations are not absolutely required, the three Ser seem to be necessary for Myt1-p90Rsk interaction. Then, p90Rsk phosphorylates five residues on the regulatory domain of Myt1. Once Myt1 becomes phosphorylated, CDK1/cyclin B is released from Myt1. It is possible that phosphorylation at Thr453, Ser472, Ser475, Ser492 and Ser504 by p90Rsk creates a

conformational change in the protein or generates an electrostatic repulsion by a highly negative charge, which then decreases pre-MPF affinity for Myt1 (Fig. 40). Thus, both the p42MAPK-p90Rsk pathway and the CDK1/XRINGO complex would represent parallel pathways that lead to both Myt1 inactivation and Cdc25 activation. It is interesting to note that XRINGO is degraded after GVBD (Gutierrez et al., 2006), but Myt1 is thought to be inactive and hyperphosphorylated (based on its reduced electrophoretic mobility) during the MI to MII transition and MII arrest, suggesting that additional kinases are likely to be implicated in Myt1 phosphorylation during oocyte maturation.

There are kinases that are known to phosphorylate and inactivate Myt1. For example, p90Rsk phosphorylation motif (RXRRXS/T) is also shared by other kinases, such as AKT/PKB, p70S6K1/2 and MSKs (Anjum and Blenis, 2008). Although it is conceivable that the equivalent sites in Myt1 are phosphorylated by AKT/PKB, there is no evidence that AKT/PKB could have a triggering role in *Xenopus* oocyte maturation. However, it does become activated during oocyte maturation and it could therefore participate in Myt1 phosphorylation at some later stage of the meiotic cell cycle (Andersen et al., 2003).

Another candidate would be Plx1, but this kinase neither interacts with nor phosphorylates Myt1 during oocyte maturation. The link between Plx1 and Myt1 appears to be operational only after fertilization, at the M phase of the embryonic cell cycle, excluding Plx1 as one of the kinases responsible for Myt1 inactivation in *Xenopus* oocytes (Inoue and Sagata 2005). Moreover, it seems that the Myt1 phosphorylation induced by p90Rsk inhibits the interaction between Myt1 and Plx1 during oocyte maturation (Inoue and Sagata, 2005).

Although Myt1 is active in G2-arrested oocytes, CDK1/XRINGO is able to phosphorylate efficiently both the inhibitory Myt1 sites and the activating Cdc25 sites because it is less susceptible to inhibitory phosphorylation by Myt1. CDK1/XRINGO bypasses as well the negative regulation by Thr161 phosphatases potentially present in the oocyte, such as PP2C (De Smedt et al., 2002). Thus, the XRINGO-activated CDK1 generated in response to progesterone would not be affected by negative regulators of CDK1 activity present in the oocyte and would be able to trigger the maturation process. Our results also indicate that both the inactivation of Myt1 kinase activity by CDK1/XRINGO-catalyzed phosphorylation, and the release of CDK1/cyclin

B from Myt1 by p90Rsk-induced Myt1 phosphorylation, are very likely to be physiologically relevant for the activation of pre-MPF during oocyte maturation.

5. Myt1 and Its Role in the Mitotic Cell Cycle

Although Myt1 has a pivotal role in gametogenesis in various species, little is known about its functions to regulate mitotic entry during somatic cell cycle in vertebrates.

Overexpression of Myt1 causes a G2/M phase arrest in U2-OS cells (Liu et al., 1999; Wells et al., 1999). Inhibition of Myt1 expression by siRNA in HeLa cells does not change the timing of mitotic entry but rather induces severe defects in the morphology of the Golgi and endoplasmic reticulum (ER), resulting in abnormally condensed Golgi structures and disrupted ER meshwork (Nakajima et al., 2008). These morphology defects are observed after the cells pass through mitosis, suggesting that Myt1 is required for Golgi and ER reassembly during mitotic exit by suppressing CDK1/cyclin B activity, but not for the biogenesis or maintenance of Golgi and ER structures during interphase (Nakajima et al., 2008).

Mitotic Golgi fragmentation in mammalian cells is dependent on CDK1 (Lowe et al., 1998), and Golgi proteins such as GM130, GRASP65, p47, and Rab1 are substrates of CDK1 (Shorter and Warren, 2002). CDK1-mediated phosphorylation of these Golgi proteins is expected to promote mitotic Golgi disassembly. Thus, during telophase, these phosphoproteins must be dephosphorylated for proper Golgi reassembly to occur. Therefore, the active CDK1 would need to be inactivated during telophase to ensure Golgi reassembly (Nakajima et al., 2008). Homologous *Xenopus* RINGO in humans, RINGO A, is expressed in G1/S transition but is downregulated during G2/M phase (Porter et al., 2002). The latter may be important for maintaining Myt1 active, which in turn suppresses CDK1/cyclin B activity at telophase, allowing Golgi and ER reassembly during mitotic exit.

6. RINGO/Speedy Proteins Outline

Together, our results indicate that, when RINGO/Speedy proteins and cyclins mediate the phosphorylation of distinct sites within a substrate (e.g. Myt1), the functional consequences of phosphorylation would be different. Nevertheless, when

the phosphorylation sites overlap (e.g. Cdc25), the outcome would be very similar or identical.

Our observations support the idea that, by providing the CDK with distinct substrate specificity, RINGO/Speedy proteins may be able to regulate specific cell cycle events. For example, in *Xenopus* oocytes, XRINGO can target CDKs to phosphorylate specific sites of Myt1, triggering its inactivation and M phase entry. This physiological role is also facilitated by the reduced susceptibility of CDK/XRINGO complexes to mechanisms that negatively regulate CDK/cyclin activity. Thus, a system employing both cyclins and RINGO/Speedy proteins with specific functional capabilities and subjected to different regulation would result in more efficient and robust mechanisms to orchestrate cell cycle progression.

CONCLUSIONS

1. XRINGO-activated CDK1 and CDK2 phosphorylate the regulatory domain of Myt1 on specific Ser-Pro sites (Ser410, Ser414 and Ser444), which are poorly phosphorylated by CDK/cyclin complexes.

2. Myt1 phosphorylation induced by CDK/XRINGO downregulates Myt1 kinase activity towards pre-MPF *in vitro* and in *Xenopus* oocytes.

3. The residues Ser410, Ser414 and Ser444 of Myt1-Ct are phosphorylated during XRINGO-induced oocyte maturation prior to MPF activation and in a CDK-dependent manner, but independently of new protein synthesis and the p42MAPK-p90Rsk pathway.

4. p90Rsk phosphorylates the C-terminal regulatory domain of Myt1 on different sites than CDK/XRINGO. These sites (Thr453, Ser472, Ser475, Ser492 and Ser504) are phosphorylated during progesterone-induced oocyte maturation.

5. Myt1 phosphorylation induced by p90Rsk decreases the affinity of Myt1 for CDK1/cyclin B complex.

6. XRINGO and cyclin B use different motifs for substrate recruitment, which, in turn, should facilitate the phosphorylation of different sites on the same CDK substrate.

7. XRINGO-activated CDK1 and CDK2 phosphorylate the regulatory domain of Cdc25 in sites required for its activation.

8. During XRINGO-induced oocyte maturation, Cdc25 is phosphorylated prior to MPF activation and in a CDK-dependent manner, but independently of the p42MAPK activation.

9. Phosphorylation of Cdc25 by CDK1/XRINGO increases its phosphatase activity *in vitro* towards pre-MPF.

CONCLUSIONES

1. Las quinasas CDK1 y CDK2 activas por XRINGO fosforilan el dominio regulador de Myt1 en sitios específicos Ser-Pro (Ser410, Ser414 y Ser444), los cuales son débilmente fosforilados por los complejos CDK/ciclinas.

2. La fosforilación de Myt1 mediada por CDK/XRINGO regula de manera negativa la actividad quinasa de Myt1 sobre el complejo pre-MPF tanto *in vitro* como en oocitos de *Xenopus*.

3. Los residuos Ser410, Ser414 y Ser444 de Myt1-Ct se fosforilan durante la maduración de oocitos inducida por XRINGO antes de la activación de MPF y de manera dependiente de la actividad de CDKs, pero independiente de la síntesis de proteínas y de la activación de la ruta p42MAPK-p90Rsk.

4. p90Rsk fosforila el dominio regulador de Myt1 en sitios diferentes a CDK/XRINGO. Estos sitios (Thr453, Ser472, Ser475, Ser492 y Ser504) se fosforilan durante la maduración de oocitos inducida por progesterona.

5. La fosforilación de Myt1 mediada por p90Rsk disminuye la afinidad de Myt1 por el complejo CDK1/ciclina B.

6. XRINGO y ciclina B utilizan diferentes regiones para el reclutamiento de sustratos, las cuales a su vez, deberían facilitar la fosforilación mediada por CDKs de diferentes sitios en los mismos sustratos.

7. Las quinasas CDK1 y CDK2 activas por XRINGO fosforilan el dominio regulador de Cdc25 en sitios requeridos para su activación.

8. Durante la maduración meiótica inducida por XRINGO, Cdc25 se fosforilan antes de la activación de MPF y de manera dependiente de la actividad de CDKs, pero independiente de la activación de p42MAPK.

9. La fosforilación de Cdc25 por CDK1/XRINGO incrementa su actividad fosfatasa *in vitro* sobre el complejo pre-MPF.

BIBLIOGRAPHY

Ahn, J.H., McAvoy, T., Rakhilin, S.V., Nishi, A., Greengard, P., and Nairn, A.C. (2007). Protein kinase A activates protein phosphatase 2A by phosphorylation of the B56delta subunit. Proc Natl Acad Sci U S A *104*, 2979-2984.

Andersen, C.B., Sakaue, H., Nedachi, T., Kovacina, K.S., Clayberger, C., Conti, M., and Roth, R.A. (2003). Protein kinase B/Akt is essential for the insulin- but not progesterone-stimulated resumption of meiosis in Xenopus oocytes. Biochem J *369*, 227-238.

Anjum, R., and Blenis, J. (2008). The RSK family of kinases: emerging roles in cellular signalling. Nat Rev Mol Cell Biol *9*, 747-758.

Atherton-Fessler, S., Parker, L.L., Geahlen, R.L., and Piwnica-Worms, H. (1993). Mechanisms of p34cdc2 regulation. Mol Cell Biol *13*, 1675-1685.

Bloom, J., and Cross, F.R. (2007). Multiple levels of cyclin specificity in cell-cycle control. Nat Rev Mol Cell Biol *8*, 149-160.

Bodart, J.F., Gutierrez, D.V., Nebreda, A.R., Buckner, B.D., Resau, J.R., and Duesbery, N.S. (2002). Characterization of MPF and MAPK activities during meiotic maturation of Xenopus tropicalis oocytes. Dev Biol *245*, 348-361.

Booher, R.N., Holman, P.S., and Fattaey, A. (1997). Human Myt1 is a cell cycle-regulated kinase that inhibits Cdc2 but not Cdk2 activity. J Biol Chem *272*, 22300-22306.

Brown, N.R., Lowe, E.D., Petri, E., Skamnaki, V., Antrobus, R., and Johnson, L.N. (2007). Cyclin B and cyclin A confer different substrate recognition properties on CDK2. Cell Cycle *6*, 1350-1359.

Brown, N.R., Noble, M.E., Endicott, J.A., Garman, E.F., Wakatsuki, S., Mitchell, E., Rasmussen, B., Hunt, T., and Johnson, L.N. (1995). The crystal structure of cyclin A. Structure *3*, 1235-1247.

Brown, N.R., Noble, M.E., Endicott, J.A., and Johnson, L.N. (1999). The structural basis for specificity of substrate and recruitment peptides for cyclin-dependent kinases. Nat Cell Biol *1*, 438-443.

Bulavin, D.V., Higashimoto, Y., Demidenko, Z.N., Meek, S., Graves, P., Phillips, C., Zhao, H., Moody, S.A., Appella, E., Piwnica-Worms, H., and Fornace, A.J., Jr. (2003). Dual phosphorylation controls Cdc25 phosphatases and mitotic entry. Nat Cell Biol *5*, 545-551.

Crews, C.M., Alessandrini, A., and Erikson, R.L. (1992). The primary structure of MEK, a protein kinase that phosphorylates the ERK gene product. Science *258*, 478-480.

Crews, C.M., and Erikson, R.L. (1992). Purification of a murine protein-tyrosine/threonine kinase that phosphorylates and activates the Erk-1 gene product: relationship to the fission yeast byr1 gene product. Proc Natl Acad Sci U S A *89*, 8205-8209.

Cheng, A., Gerry, S., Kaldis, P., and Solomon, M.J. (2005a). Biochemical characterization of Cdk2-Speedy/Ringo A2. BMC Biochemistry *6*, 19.

Cheng, A., Xiong, W., Ferrell, J.E., Jr., and Solomon, M.J. (2005b). Identification and comparative analysis of multiple mammalian Speedy/Ringo proteins. Cell Cycle *4*, 155-165.

Cheng, K.Y., Noble, M.E., Skamnaki, V., Brown, N.R., Lowe, E.D., Kontogiannis, L., Shen, K., Cole, P.A., Siligardi, G., and Johnson, L.N. (2006). The role of the phospho-CDK2/cyclin A recruitment site in substrate recognition. J Biol Chem *281*, 23167-23179.

De Bondt, H.L., Rosenblatt, J., Jancarik, J., Jones, H.D., Morgan, D.O., and Kim, S.H. (1993). Crystal structure of cyclin-dependent kinase 2. Nature *363*, 595-602.

De Smedt, V., Poulhe, R., Cayla, X., Dessauge, F., Karaiskou, A., Jessus, C., and Ozon, R. (2002). Thr-161 phosphorylation of monomeric Cdc2. Regulation by protein phosphatase 2C in Xenopus oocytes. J Biol Chem *277*, 28592-28600.

Deng, J., Lang, S., Wylie, C., and Hammes, S.R. (2008). The Xenopus laevis isoform of G protein-coupled receptor 3 (GPR3) is a constitutively active cell surface receptor that participates in maintaining meiotic arrest in X. laevis oocytes. Mol Endocrinol *22*, 1853-1865.

Desai, D., Gu, Y., and Morgan, D.O. (1992). Activation of human cyclin-dependent kinases in vitro. Mol Biol Cell *3*, 571-582.

Dinarina, A., Perez, L.H., Davila, A., Schwab, M., Hunt, T., and Nebreda, A.R. (2005). Characterization of a new family of cyclin-dependent kinase activators. Biochem J *386*, 349-355.

Duckworth, B.C., Weaver, J.S., and Ruderman, J.V. (2002). G2 arrest in Xenopus oocytes depends on phosphorylation of cdc25 by protein kinase A. Proc Natl Acad Sci U S A *99*, 16794-16799.

Dupre, A., Jessus, C., Ozon, R., and Haccard, O. (2002). Mos is not required for the initiation of meiotic maturation in Xenopus oocytes. EMBO J *21*, 4026-4036.

Ekholm, S.V., and Reed, S.I. (2000). Regulation of G(1) cyclin-dependent kinases in the mammalian cell cycle. Curr Opin Cell Biol *12*, 676-684.

Elia, A.E., Cantley, L.C., and Yaffe, M.B. (2003a). Proteomic screen finds pSer/pThr-binding domain localizing Plk1 to mitotic substrates.[see comment]. Science *299*, 1228-1231.

Elia, A.E., Rellos, P., Haire, L.F., Chao, J.W., Ivins, F.J., Hoepker, K., Mohammad, D., Cantley, L.C., Smerdon, S.J., and Yaffe, M.B. (2003b). The molecular basis for phosphodependent substrate targeting and regulation of Plks by the Polo-box domain. Cell *115*, 83-95.

Endicott, J.A., Nurse, P., and Johnson, L.N. (1994). Mutational analysis supports a structural model for the cell cycle protein kinase p34. Protein Eng *7*, 243-253.

Espinoza, F.H., Farrell, A., Erdjument-Bromage, H., Tempst, P., and Morgan, D.O. (1996). A cyclin-dependent kinase-activating kinase (CAK) in budding yeast unrelated to vertebrate CAK. Science *273*, 1714-1717.

Ferby, I., Blazquez, M., Palmer, A., Eritja, R., and Nebreda, A.R. (1999). A novel p34(cdc2)-binding and activating protein that is necessary and sufficient to trigger G(2)/M progression in Xenopus oocytes. Genes Dev *13*, 2177-2189.

Fisher, D.L., Brassac, T., Galas, S., and Doree, M. (1999). Dissociation of MAP kinase activation and MPF activation in hormone-stimulated maturation of Xenopus oocytes. Development *126*, 4537-4546.

Forester, C.M., Maddox, J., Louis, J.V., Goris, J., and Virshup, D.M. (2007). Control of mitotic exit by PP2A regulation of Cdc25C and Cdk1. Proc Natl Acad Sci U S A *104*, 19867-19872.

Gastwirt, R.F., McAndrew, C.W., and Donoghue, D.J. (2007). Speedy/RINGO regulation of CDKs in cell cycle, checkpoint activation and apoptosis. Cell Cycle *6*, 1188-1193.

Gavin, A.C., and Nebreda, A.R. (1999). A MAP kinase docking site is required for phosphorylation and activation of p90(rsk)/MAPKAP kinase-1. Curr Biol *9*, 281-284.

Gross, S.D., Lewellyn, A.L., and Maller, J.L. (2001). A constitutively active form of the protein kinase p90Rsk1 is sufficient to trigger the G2/M transition in Xenopus oocytes. J Biol Chem *276*, 46099-46103.

Gross, S.D., Schwab, M.S., Taieb, F.E., Lewellyn, A.L., Qian, Y.W., and Maller, J.L. (2000). The critical role of the MAP kinase pathway in meiosis II in Xenopus oocytes is mediated by p90(Rsk). Curr Biol *10*, 430-438.

Gutierrez, G.J., Vogtlin, A., Castro, A., Ferby, I., Salvagiotto, G., Ronai, Z., Lorca, T., and Nebreda, A.R. (2006). Meiotic regulation of the CDK activator RINGO/Speedy by

ubiquitin-proteasome-mediated processing and degradation. Nat Cell Biol *8*, 1084-1094.

Harper, J.V., and Brooks, G. (2005). The mammalian cell cycle: an overview. Methods Mol Biol *296*, 113-153.

Hochegger, H., Klotzbucher, A., Kirk, J., Howell, M., le Guellec, K., Fletcher, K., Duncan, T., Sohail, M., and Hunt, T. (2001). New B-type cyclin synthesis is required between meiosis I and II during Xenopus oocyte maturation. Development *128*, 3795-3807.

Hochegger, H., Takeda, S., and Hunt, T. (2008). Cyclin-dependent kinases and cell-cycle transitions: does one fit all? Nat Rev Mol Cell Biol *9*, 910-916.

Hochwagen, A. (2008). Meiosis. Curr Biol *18*, R641-R645.

Hoffmann, I., Clarke, P.R., Marcote, M.J., Karsenti, E., and Draetta, G. (1993). Phosphorylation and activation of human cdc25-C by cdc2--cyclin B and its involvement in the self-amplification of MPF at mitosis. EMBO J *12*, 53-63.

Hsiao, K.M., Chou, S.Y., Shih, S.J., and Ferrell, J.E., Jr. (1994). Evidence that inactive p42 mitogen-activated protein kinase and inactive Rsk exist as a heterodimer in vivo. Proc Natl Acad Sci U S A *91*, 5480-5484.

Huang, W., Kessler, D.S., and Erikson, R.L. (1995). Biochemical and biological analysis of Mek1 phosphorylation site mutants. Mol Biol Cell *6*, 237-245.

Inoue, D., and Sagata, N. (2005). The Polo-like kinase Plx1 interacts with and inhibits Myt1 after fertilization of Xenopus eggs. EMBO J *24*, 1057-1067.

Izumi, T., and Maller, J.L. (1993). Elimination of cdc2 phosphorylation sites in the cdc25 phosphatase blocks initiation of M-phase. Mol Biol Cell *4*, 1337-1350.

Jackman, M., Firth, M., and Pines, J. (1995). Human cyclins B1 and B2 are localized to strikingly different structures: B1 to microtubules, B2 primarily to the Golgi apparatus. EMBO J *14*, 1646-1654.

Jeffrey, P.D., Russo, A.A., Polyak, K., Gibbs, E., Hurwitz, J., Massague, J., and Pavletich, N.P. (1995). Mechanism of CDK activation revealed by the structure of a cyclinA-CDK2 complex. Nature *376*, 313-320.

Kaldis, P., Russo, A.A., Chou, H.S., Pavletich, N.P., and Solomon, M.J. (1998). Human and yeast cdk-activating kinases (CAKs) display distinct substrate specificities. Mol Biol Cell *9*, 2545-2560.

Kaldis, P., Sutton, A., and Solomon, M.J. (1996). The Cdk-activating kinase (CAK) from budding yeast. Cell *86*, 553-564.

Karaiskou, A., Cayla, X., Haccard, O., Jessus, C., and Ozon, R. (1998). MPF amplification in Xenopus oocyte extracts depends on a two-step activation of cdc25 phosphatase. Exp Cell Res *244*, 491-500.

Karaiskou, A., Dupre, A., Haccard, O., and Jessus, C. (2001a). From progesterone to active Cdc2 in Xenopus oocytes: a puzzling signalling pathway. Biol Cell *93*, 35-46.

Karaiskou, A., Perez, L.H., Ferby, I., Ozon, R., Jessus, C., and Nebreda, A.R. (2001b). Differential regulation of Cdc2 and Cdk2 by RINGO and cyclins. J Biol Chem *276*, 36028-36034.

Kim, J.H., and Richter, J.D. (2007). RINGO/cdk1 and CPEB mediate poly(A) tail stabilization and translational regulation by ePAB. Genes Dev *21*, 2571-2579.

Kobayashi, H., Minshull, J., Ford, C., Golsteyn, R., Poon, R., and Hunt, T. (1991). On the synthesis and destruction of A- and B-type cyclins during oogenesis and meiotic maturation in Xenopus laevis. J Cell Biol *114*, 755-765.

Kosako, H., Nishida, E., and Gotoh, Y. (1993). cDNA cloning of MAP kinase kinase reveals kinase cascade pathways in yeasts to vertebrates. EMBO J *12*, 787-794.

Kristjansdottir, K., and Rudolph, J. (2004). Cdc25 phosphatases and cancer. Chem Biol *11*, 1043-1051.

Kristjansdottir, K., Safi, A., Shah, C., and Rudolph, J. (2006). Autophosphorylation of Ser66 on Xenopus Myt1 is a prerequisite for meiotic inactivation of Myt1. Cell Cycle *5*, 421-427.

Kumagai, A., and Dunphy, W.G. (1992). Regulation of the cdc25 protein during the cell cycle in Xenopus extracts. Cell *70*, 139-151.

Kumagai, A., and Dunphy, W.G. (1995). Control of the Cdc2/cyclin B complex in Xenopus egg extracts arrested at a G2/M checkpoint with DNA synthesis inhibitors. Mol Biol Cell *6*, 199-213.

Kumagai, A., and Dunphy, W.G. (1996). Purification and molecular cloning of Plx1, a Cdc25-regulatory kinase from Xenopus egg extracts. Science *273*, 1377-1380.

Kumagai, A., and Dunphy, W.G. (1999). Binding of 14-3-3 proteins and nuclear export control the intracellular localization of the mitotic inducer Cdc25. Genes Dev *13*, 1067-1072.

Kumagai, A., Yakowec, P.S., and Dunphy, W.G. (1998). 14-3-3 proteins act as negative regulators of the mitotic inducer Cdc25 in Xenopus egg extracts. Mol Biol Cell *9*, 345-354.

Kume, S., Endo, T., Nishimura, Y., Kano, K., and Naito, K. (2007). Porcine SPDYA2 (RINGO A2) stimulates CDC2 activity and accelerates meiotic maturation of porcine oocytes. Biol Reprod *76*, 440-447.

Lee, M.H., Nikolic, M., Baptista, C.A., Lai, E., Tsai, L.H., and Massague, J. (1996). The brain-specific activator p35 allows Cdk5 to escape inhibition by p27Kip1 in neurons. Proc Natl Acad Sci U S A *93*, 3259-3263.

Lee, M.S., Enoch, T., and Piwnica-Worms, H. (1994). mik1+ encodes a tyrosine kinase that phosphorylates p34cdc2 on tyrosine 15. J Biol Chem *269*, 30530-30537.

Lenormand, J.L., Dellinger, R.W., Knudsen, K.E., Subramani, S., and Donoghue, D.J. (1999). Speedy: a novel cell cycle regulator of the G2/M transition. EMBO J *18*, 1869-1877.

Liu, F., Rothblum-Oviatt, C., Ryan, C.E., and Piwnica-Worms, H. (1999). Overproduction of human Myt1 kinase induces a G2 cell cycle delay by interfering with the intracellular trafficking of Cdc2-cyclin B1 complexes. Mol Cell Biol *19*, 5113-5123.

Liu, F., Stanton, J.J., Wu, Z., and Piwnica-Worms, H. (1997). The human Myt1 kinase preferentially phosphorylates Cdc2 on threonine 14 and localizes to the endoplasmic reticulum and Golgi complex. Mol Cell Biol *17*, 571-583.

Loog, M., and Morgan, D.O. (2005). Cyclin specificity in the phosphorylation of cyclin-dependent kinase substrates.[see comment]. Nature *434*, 104-108.

Lowe, M., Rabouille, C., Nakamura, N., Watson, R., Jackman, M., Jamsa, E., Rahman, D., Pappin, D.J., and Warren, G. (1998). Cdc2 kinase directly phosphorylates the cis-Golgi matrix protein GM130 and is required for Golgi fragmentation in mitosis. Cell *94*, 783-793.

Malumbres, M. (2005). Revisiting the "Cdk-centric" view of the mammalian cell cycle. Cell Cycle *4*, 206-210.

Malumbres, M., and Barbacid, M. (2001). To cycle or not to cycle: a critical decision in cancer. Nat Rev Cancer *1*, 222-231.

Malumbres, M., and Barbacid, M. (2005). Mammalian cyclin-dependent kinases. Trends in Biochemical Sciences *30*, 630-641.

Malumbres, M., and Barbacid, M. (2009). Cell cycle, CDKs and cancer: a changing paradigm. Nat Rev Cancer *9*, 153-166.

Margolis, S.S., Perry, J.A., Forester, C.M., Nutt, L.K., Guo, Y., Jardim, M.J., Thomenius, M.J., Freel, C.D., Darbandi, R., Ahn, J.H.*, et al.* (2006a). Role for the

PP2A/B56delta phosphatase in regulating 14-3-3 release from Cdc25 to control mitosis. Cell *127*, 759-773.

Margolis, S.S., Perry, J.A., Weitzel, D.H., Freel, C.D., Yoshida, M., Haystead, T.A., and Kornbluth, S. (2006b). A role for PP1 in the Cdc2/Cyclin B-mediated positive feedback activation of Cdc25. Mol Biol Cell *17*, 1779-1789.

Margolis, S.S., Walsh, S., Weiser, D.C., Yoshida, M., Shenolikar, S., and Kornbluth, S. (2003). PP1 control of M phase entry exerted through 14-3-3-regulated Cdc25 dephosphorylation. EMBO J *22*, 5734-5745.

Marston, A.L., and Amon, A. (2004). Meiosis: cell-cycle controls shuffle and deal. Nat Rev Mol Cell Biol *5*, 983-997.

McAndrew, C.W., Gastwirt, R.F., Meyer, A.N., Porter, L.A., and Donoghue, D.J. (2007). Spy1 enhances phosphorylation and degradation of the cell cycle inhibitor p27. Cell Cycle *6*, 1937-1945.

Mendez, R., Hake, L.E., Andresson, T., Littlepage, L.E., Ruderman, J.V., and Richter, J.D. (2000). Phosphorylation of CPE binding factor by Eg2 regulates translation of c-mos mRNA. Nature *404*, 302-307.

Mendez, R., and Richter, J.D. (2001). Translational control by CPEB: a means to the end. Nat Rev Mol Cell Biol *2*, 521-529.

Minshull, J., Murray, A., Colman, A., and Hunt, T. (1991). Xenopus oocyte maturation does not require new cyclin synthesis. J Cell Biol *114*, 767-772.

Mueller, P.R., Coleman, T.R., and Dunphy, W.G. (1995a). Cell cycle regulation of a Xenopus Wee1-like kinase. Mol Biol Cell *6*, 119-134.

Mueller, P.R., Coleman, T.R., Kumagai, A., and Dunphy, W.G. (1995b). Myt1: a membrane-associated inhibitory kinase that phosphorylates Cdc2 on both threonine-14 and tyrosine-15. Science *270*, 86-90.

Murray, A.W. (2004). Recycling the cell cycle: cyclins revisited. Cell *116*, 221-234.

Nakajima, H., Toyoshima-Morimoto, F., Taniguchi, E., and Nishida, E. (2003). Identification of a consensus motif for Plk (Polo-like kinase) phosphorylation reveals Myt1 as a Plk1 substrate. J Biol Chem *278*, 25277-25280.

Nakajima, H., Yonemura, S., Murata, M., Nakamura, N., Piwnica-Worms, H., and Nishida, E. (2008). Myt1 protein kinase is essential for Golgi and ER assembly during mitotic exit. J Cell Biol *181*, 89-103.

Nakajo, N., Yoshitome, S., Iwashita, J., Iida, M., Uto, K., Ueno, S., Okamoto, K., and Sagata, N. (2000). Absence of Wee1 ensures the meiotic cell cycle in Xenopus oocytes. Genes Dev *14*, 328-338.

Nebreda, A.R. (2006). CDK activation by non-cyclin proteins. Curr Opin Cell Biol *18*, 192-198.

Nebreda, A.R., and Ferby, I. (2000). Regulation of the meiotic cell cycle in oocytes. Curr Opin Cell Biol *12*, 666-675.

Nebreda, A.R., Gannon, J.V., and Hunt, T. (1995). Newly synthesized protein(s) must associate with p34cdc2 to activate MAP kinase and MPF during progesterone-induced maturation of Xenopus oocytes. EMBO J *14*, 5597-5607.

Nebreda, A.R., and Hunt, T. (1993). The c-mos proto-oncogene protein kinase turns on and maintains the activity of MAP kinase, but not MPF, in cell-free extracts of Xenopus oocytes and eggs. EMBO J *12*, 1979-1986.

Nishizawa, M., Furuno, N., Okazaki, K., Tanaka, H., Ogawa, Y., and Sagata, N. (1993). Degradation of Mos by the N-terminal proline (Pro2)-dependent ubiquitin pathway on fertilization of Xenopus eggs: possible significance of natural selection for Pro2 in Mos. EMBO J *12*, 4021-4027.

Nishizawa, M., Okazaki, K., Furuno, N., Watanabe, N., and Sagata, N. (1992). The 'second-codon rule' and autophosphorylation govern the stability and activity of Mos during the meiotic cell cycle in Xenopus oocytes. EMBO J *11*, 2433-2446.

Nurse, P. (2000). A long twentieth century of the cell cycle and beyond. Cell *100*, 71-78.

Oe, T., Nakajo, N., Katsuragi, Y., Okazaki, K., and Sagata, N. (2001). Cytoplasmic occurrence of the Chk1/Cdc25 pathway and regulation of Chk1 in Xenopus oocytes. Dev Biol *229*, 250-261.

Okumura, E., Fukuhara, T., Yoshida, H., Hanada Si, S., Kozutsumi, R., Mori, M., Tachibana, K., and Kishimoto, T. (2002). Akt inhibits Myt1 in the signalling pathway that leads to meiotic G2/M-phase transition. Nat Cell Biol *4*, 111-116.

Olashaw, N., and Pledger, W.J. (2002). Paradigms of growth control: relation to Cdk activation. Science's Stke [Electronic Resource]: Signal Transduction Knowledge Environment *2002*, RE7.

Padmanabhan, K., and Richter, J.D. (2006). Regulated Pumilio-2 binding controls RINGO/Spy mRNA translation and CPEB activation.[see comment]. Genes Dev *20*, 199-209.

Palmer, A., Gavin, A.C., and Nebreda, A.R. (1998). A link between MAP kinase and p34(cdc2)/cyclin B during oocyte maturation: p90(rsk) phosphorylates and inactivates the p34(cdc2) inhibitory kinase Myt1.[erratum appears in EMBO J 1999 Feb 15;18(4):1092]. EMBO J *17*, 5037-5047.

Pascreau, G., Delcros, J.G., Cremet, J.Y., Prigent, C., and Arlot-Bonnemains, Y. (2005). Phosphorylation of maskin by Aurora-A participates in the control of sequential protein synthesis during Xenopus laevis oocyte maturation. J Biol Chem *280*, 13415-13423.

Pavletich, N.P. (1999). Mechanisms of cyclin-dependent kinase regulation: structures of Cdks, their cyclin activators, and Cip and INK4 inhibitors. J Mol Biol *287*, 821-828.

Perdiguero, E., and Nebreda, A.R. (2004). Regulation of Cdc25C activity during the meiotic G2/M transition. Cell Cycle *3*, 733-737.

Perdiguero, E., Pillaire, M.J., Bodart, J.F., Hennersdorf, F., Frodin, M., Duesbery, N.S., Alonso, G., and Nebreda, A.R. (2003). Xp38gamma/SAPK3 promotes meiotic G(2)/M transition in Xenopus oocytes and activates Cdc25C. EMBO J *22*, 5746-5756.

Peter, M., Labbe, J.C., Doree, M., and Mandart, E. (2002). A new role for Mos in Xenopus oocyte maturation: targeting Myt1 independently of MAPK. Development *129*, 2129-2139.

Philpott, A., and Yew, P.R. (2008). The Xenopus cell cycle: an overview. Mol Biotechnol *39*, 9-19.

Poon, R.Y., Lew, J., and Hunter, T. (1997). Identification of functional domains in the neuronal Cdk5 activator protein. J Biol Chem *272*, 5703-5708.

Porter, L.A., Dellinger, R.W., Tynan, J.A., Barnes, E.A., Kong, M., Lenormand, J.L., and Donoghue, D.J. (2002). Human Speedy: a novel cell cycle regulator that enhances proliferation through activation of Cdk2. J Cell Biol *157*, 357-366.

Porter, L.A., Kong-Beltran, M., and Donoghue, D.J. (2003). Spy1 interacts with p27Kip1 to allow G1/S progression. Mol Biol Cell *14*, 3664-3674.

Posada, J., Yew, N., Ahn, N.G., Vande Woude, G.F., and Cooper, J.A. (1993). Mos stimulates MAP kinase in Xenopus oocytes and activates a MAP kinase kinase in vitro. Mol Cell Biol *13*, 2546-2553.

Qian, Y.W., Erikson, E., Li, C., and Maller, J.L. (1998). Activated polo-like kinase Plx1 is required at multiple points during mitosis in Xenopus laevis. Mol Cell Biol *18*, 4262-4271.

Radzio-Andzelm, E., Lew, J., and Taylor, S. (1995). Bound to activate: conformational consequences of cyclin binding to CDK2. Structure *3*, 1135-1141.

Rempel, R.E., Sleight, S.B., and Maller, J.L. (1995). Maternal Xenopus Cdk2-cyclin E complexes function during meiotic and early embryonic cell cycles that lack a G1 phase. J Biol Chem *270*, 6843-6855.

Russo, A.A., Jeffrey, P.D., Patten, A.K., Massague, J., and Pavletich, N.P. (1996a). Crystal structure of the p27Kip1 cyclin-dependent-kinase inhibitor bound to the cyclin A-Cdk2 complex. Nature *382*, 325-331.

Russo, A.A., Jeffrey, P.D., and Pavletich, N.P. (1996b). Structural basis of cyclin-dependent kinase activation by phosphorylation. Nat Struct Biol *3*, 696-700.

Russo, A.A., Tong, L., Lee, J.O., Jeffrey, P.D., and Pavletich, N.P. (1998). Structural basis for inhibition of the cyclin-dependent kinase Cdk6 by the tumour suppressor p16INK4a. Nature *395*, 237-243.

Schmitt, A., and Nebreda, A.R. (2002). Signalling pathways in oocyte meiotic maturation. J Cell Sci *115*, 2457-2459.

Schulman, B.A., Lindstrom, D.L., and Harlow, E. (1998). Substrate recruitment to cyclin-dependent kinase 2 by a multipurpose docking site on cyclin A. Proc Natl Acad Sci U S A *95*, 10453-10458.

Sherr, C.J., and Roberts, J.M. (2004). Living with or without cyclins and cyclin-dependent kinases. Genes Dev *18*, 2699-2711.

Shibuya, E.K. (2003). G2 cell cycle arrest--a direct link between PKA and Cdc25C.[comment]. Cell Cycle *2*, 39-41.

Shibuya, E.K., Polverino, A.J., Chang, E., Wigler, M., and Ruderman, J.V. (1992). Oncogenic ras triggers the activation of 42-kDa mitogen-activated protein kinase in extracts of quiescent Xenopus oocytes. Proc Natl Acad Sci U S A *89*, 9831-9835.

Shorter, J., and Warren, G. (2002). Golgi architecture and inheritance. Annu Rev Cell Dev Biol *18*, 379-420.

Smith, L.D., Xu, W.L., and Varnold, R.L. (1991). Oogenesis and oocyte isolation. Methods Cell Biol *36*, 45-60.

Stanford, J.S., and Ruderman, J.V. (2005). Changes in regulatory phosphorylation of Cdc25C Ser287 and Wee1 Ser549 during normal cell cycle progression and checkpoint arrests. Mol Biol Cell *16*, 5749-5760.

Stevenson-Lindert, L.M., Fowler, P., and Lew, J. (2003). Substrate specificity of CDK2-cyclin A. What is optimal? J Biol Chem *278*, 50956-50960.

Stukenberg, P.T., and Kirschner, M.W. (2001). Pin1 acts catalytically to promote a conformational change in Cdc25. Mol Cell *7*, 1071-1083.

Takeda, D.Y., Wohlschlegel, J.A., and Dutta, A. (2001). A bipartite substrate recognition motif for cyclin-dependent kinases. J Biol Chem *276*, 1993-1997.

Tarricone, C., Dhavan, R., Peng, J., Areces, L.B., Tsai, L.H., and Musacchio, A. (2001). Structure and regulation of the CDK5-p25(nck5a) complex. Mol Cell *8*, 657-669.

Tyson, J.J., and Novak, B. (2008). Temporal organization of the cell cycle. Curr Biol *18*, R759-R768.

Wang, R., He, G., Nelman-Gonzalez, M., Ashorn, C.L., Gallick, G.E., Stukenberg, P.T., Kirschner, M.W., and Kuang, J. (2007). Regulation of Cdc25C by ERK-MAP kinases during the G2/M transition. Cell *128*, 1119-1132.

Wang, X., Swain, J.E., Bollen, M., Liu, X.T., Ohl, D.A., and Smith, G.D. (2004). Endogenous regulators of protein phosphatase-1 during mouse oocyte development and meiosis. Reproduction *128*, 493-502.

Wells, N.J., Watanabe, N., Tokusumi, T., Jiang, W., Verdecia, M.A., and Hunter, T. (1999). The C-terminal domain of the Cdc2 inhibitory kinase Myt1 interacts with Cdc2 complexes and is required for inhibition of G(2)/M progression. J Cell Sci *112*, 3361-3371.

Yew, N., Mellini, M.L., and Vande Woude, G.F. (1992). Meiotic initiation by the mos protein in Xenopus. Nature *355*, 649-652.

Yu, J., Zhao, Y., Li, Z., Galas, S., and Goldberg, M.L. (2006). Greatwall kinase participates in the Cdc2 autoregulatory loop in Xenopus egg extracts. Mol Cell *22*, 83-91.

Yue, J., and Ferrell, J.E., Jr. (2006). Mechanistic studies of the mitotic activation of Mos. Mol Cell Biol *26*, 5300-5309.

Zhu, Y., Bond, J., and Thomas, P. (2003a). Identification, classification, and partial characterization of genes in humans and other vertebrates homologous to a fish membrane progestin receptor. Proc Natl Acad Sci U S A *100*, 2237-2242.

Zhu, Y., Rice, C.D., Pang, Y., Pace, M., and Thomas, P. (2003b). Cloning, expression, and characterization of a membrane progestin receptor and evidence it is an intermediary in meiotic maturation of fish oocytes. Proc Natl Acad Sci U S A *100*, 2231-2236.

APPENDIX

Molecular Cell
Article

Meiotic Inactivation of *Xenopus* Myt1 by CDK/XRINGO, but Not CDK/Cyclin, via Site-Specific Phosphorylation

E. Josué Ruiz,[1] Tim Hunt,[2] and Angel R. Nebreda[1,*]
[1]CNIO (Spanish National Cancer Center), Melchor Fernández Almagro 3, 28029 Madrid, Spain
[2]Cancer Research UK, London Research Institute, Clare Hall Laboratories, South Mimms, Hertfordshire EN6 3LD, UK
*Correspondence: anebreda@cnio.es
DOI 10.1016/j.molcel.2008.08.029

SUMMARY

Cell-cycle progression is regulated by cyclin-dependent kinases (CDKs). CDK1 and CDK2 can be also activated by noncyclin proteins named RINGO/Speedy, which were identified as inducers of the G2/M transition in *Xenopus* oocytes. However, it is unclear how XRINGO triggers M phase entry in oocytes. We show here that XRINGO-activated CDKs can phosphorylate specific residues in the regulatory domain of Myt1, a Wee1 family kinase that plays a key role in the G2 arrest of oocytes. We have identified three Ser that are major phosphoacceptor sites for CDK/XRINGO but are poorly phosphorylated by CDK/cyclin. Phosphorylation of these Ser inhibits Myt1 activity, whereas their mutation makes Myt1 resistant to inhibition by CDK/XRINGO. Our results demonstrate that XRINGO-activated CDKs have different substrate specificity than the CDK/cyclin complexes. We also describe a mechanism of Myt1 regulation based on site-specific phosphorylation, which is likely to mediate the induction of G2/M transition in oocytes by XRINGO.

INTRODUCTION

The coordinated regulation of protein kinases and phosphatases plays an important role in cell-cycle transitions. The meiotic maturation of *Xenopus* oocytes is an excellent system to study the mechanisms that regulate M phase entry and progression. Fully grown *Xenopus* oocytes are arrested in a G2-like phase, at prophase in the G2/M boundary of the first meiotic division, and are induced to enter meiosis I by progesterone stimulation in a process called meiotic maturation. A key enzymatic activity that regulates the G2/M transition in eukaryotic cells is the maturation-promoting factor (MPF), a complex of the Ser/Thr protein kinase CDK1 with a B-type cyclin. In G2-arrested *Xenopus* oocytes, the majority of CDK1 is thought to be monomeric, and some of it might be phosphorylated on the T loop (Thr161) (De Smedt et al., 2002), but a small fraction of the CDK1 (~10%) is associated with cyclins B2 and B5 and phosphorylated on Thr161. These preformed CDK1/cyclin B complexes, referred to as pre-MPF, are maintained inactive by phosphorylation of CDK1 on Thr14 and Tyr15. The inhibitory phosphorylations are catalyzed by the Wee1 family of protein kinases (Mueller et al., 1995a, 1995b), whereas dephosphorylation of these residues, which is required to activate CDK1/cyclin B and promote entry into M phase, is catalyzed by the Cdc25 phosphatases (Kumagai and Dunphy, 1992). In late G2 phase, the balance between Wee1 and Cdc25 activities shifts in favor of CDK1 dephosphorylation, resulting in the activation of CDK1/cyclin B complexes and entry into meiosis. However, the initial triggering events that reverse the dominance of Wee1 over Cdc25 activity in late G2 phase and lead to CDK1/cyclin B activation are poorly characterized.

In metazoans, the Wee1 family consists of Wee1, a nuclear kinase that phosphorylates CDK1 on Tyr15 (Lee et al., 1994), and Myt1, a membrane-associated kinase that phosphorylates CDK1 on both Thr14 and Tyr15 (Liu et al., 1997; Mueller et al., 1995b). Phosphorylation by either Wee1 or Myt1 can efficiently inhibit CDK1, but Wee1 protein is not detectable in G2-arrested *Xenopus* oocytes. These oocytes contain maternal Wee1 mRNA that starts to be translated later during oocyte maturation (Nakajo et al., 2000). In contrast, Myt1 is present in G2 oocytes, and interfering with its function by the injection of antibodies is sufficient to induce oocyte maturation (Nakajo et al., 2000), suggesting that Myt1 plays a key role in maintaining the meiotic G2 arrest. Moreover, Myt1 is phosphorylated during oocyte maturation, and the inactivation of Myt1 during M phase correlates with the phosphorylation of its C-terminal noncatalytic region (Liu et al., 1999; Wells et al., 1999).

Several kinases can phosphorylate Myt1 and may potentially contribute to its regulation. For example, Akt/PKB phosphorylates Ser75 at the N terminus of starfish Myt1 and downregulates its activity (Okumura et al., 2002). In addition, the Mos-p42MAPK-p90Rsk pathway is thought to regulate Myt1 phosphorylation during *Xenopus* oocyte maturation (Palmer et al., 1998; Peter et al., 2002), and p90Rsk has been shown to inhibit Myt1 in vitro, although specific phosphorylation sites were not identified (Palmer et al., 1998). Intriguingly, fresh *Xenopus* oocytes obtained from frogs that have been primed with hormones can also be induced to mature by progesterone in the absence of Mos synthesis and p42MAPK activation, as showed by using Mos morpholino oligonucleotides, the MEK1/2 inhibitor U0126, or the Hsp90 inhibitor Geldanamycin (Dupre et al., 2002; Fisher et al., 1999; Gross et al., 2000; Peter et al., 2002). This process is also mediated by MPF and involves Myt1 inactivation (reviewed by Nebreda and Ferby [2000]).

Hyperphosphorylation of Myt1 has been shown to depend on CDK1 activity in *Xenopus* egg extracts, and purified CDK1/cyclin B can phosphorylate Myt1 in vitro (Booher et al., 1997; Inoue and Sagata, 2005; Mueller et al., 1995b). In addition, the hyperphosphorylated form of Myt1 isolated from M phase extracts has reduced kinase activity (Mueller et al., 1995b). These observations have led to the idea of a positive feedback loop in which CDK1 directly phosphorylates and inactivates Myt1, thereby contributing to a rapid rise in CDK1 activity and entry into M phase (Booher et al., 1997).

RINGO/Speedy proteins can activate some CDKs but do not share sequence homology with cyclins (Cheng et al., 2005b; Dinarina et al., 2005; Nebreda, 2006). *Xenopus* RINGO/Speedy (XRINGO) was originally identified for its ability to potently induce G2/M transition in *Xenopus* oocytes (Ferby et al., 1999; Lenormand et al., 1999). Further work showed that endogenous XRINGO accumulates transiently in oocytes upon progesterone stimulation and contributes to meiosis I entry, probably via CDK1 or CDK2 activation. XRINGO is then downregulated soon after meiosis I, and this is important for meiotic progression (Gutierrez et al., 2006). However, it is unknown how XRINGO triggers the activation of pre-MPF in G2 oocytes. The observation that recombinant XRINGO can induce oocyte maturation and MPF activation in Cycloheximide (CHX)-treated oocytes (Ferby et al., 1999) suggests that XRINGO could be directly targeting the cell-cycle regulators Myt1 or Cdc25 during oocyte maturation. Here, we show that XRINGO-activated CDK1 and CDK2 can phosphorylate different residues of Myt1 than the equivalent CDK/cyclin complexes. We also identified three Ser-Pro sites whose phosphorylation by CDK/XRINGO inhibits Myt1 activity. These results support an important role for XRINGO in Myt1 regulation during the G2/M transition.

RESULTS

XRINGO Induces Myt1 Phosphorylation in Oocytes

During progesterone-induced *Xenopus* oocyte maturation, Myt1 undergoes a significant electrophoretic mobility upshift due to hyperphosphorylation (Gross et al., 2000; Palmer et al., 1998; Peter et al., 2002). The regulatory domain of Myt1 includes several potential CDK phosphorylation sites, which are likely to participate in the regulation of the catalytic activity of Myt1 (Inoue and Sagata, 2005; Wells et al., 1999).

To test whether the regulatory domain of Myt1 was directly phosphorylated by CDK/XRINGO, we fused the C-terminal residues 399–548 of Myt1 (Myt1-Ct) to glutathione S-transferase (GST) and used the bacterially produced fusion protein in kinase assays (Palmer et al., 1998). We found that recombinant CDK1 and CDK2 activated by XRINGO phosphorylated Myt1-Ct as efficiently as CDK1/cyclin B and CDK2/cyclin A, respectively (Figure 1A). Histone H1 was used to normalize the kinase activities. We also found that T loop phosphorylation did not affect the ability of CDK1/XRINGO and CDK2/XRINGO to phosphorylate Myt1-Ct, whereas the activity of CDK/cyclin complexes on Myt1-Ct required T loop phosphorylation (Figure S1 available online). Moreover, CDK/XRINGO phosphorylation changed the electrophoretic mobility of Myt1 in 2D gels so that several new spots appeared, suggesting that Myt1 was phosphorylated on several residues (data not shown).

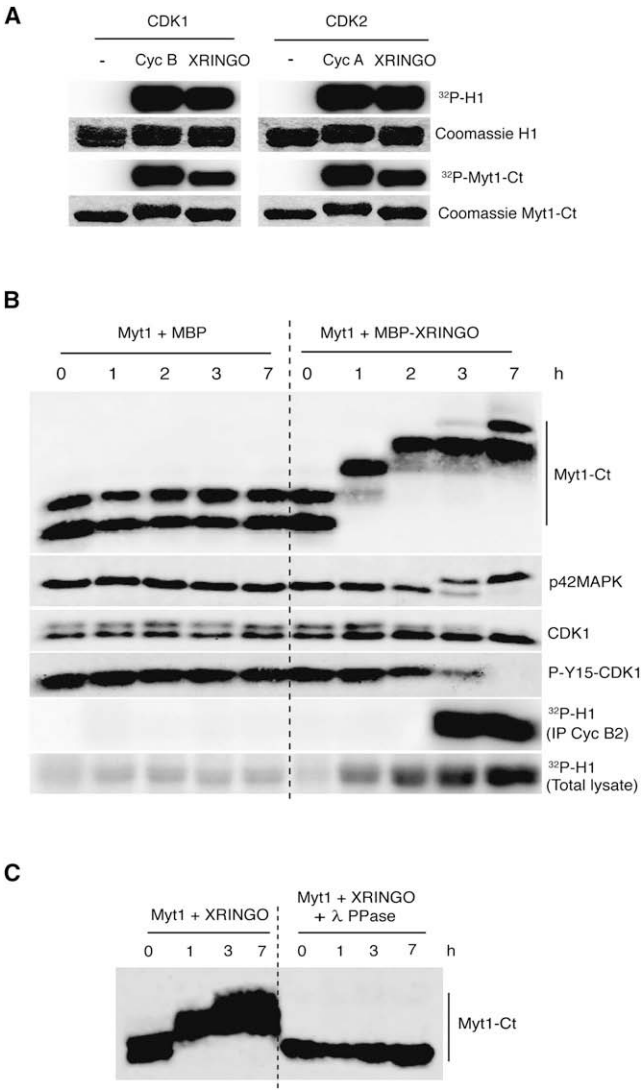

Figure 1. Phosphorylation of Myt1 by CDK/XRINGO

(A) Baculovirus-expressed GST-CDK1 (200 ng) was incubated with cyclin B (200 ng) or MBP-XRINGO (400 ng). GST-CDK2 (250 ng) was incubated with cyclin A (250 ng) or MBP-XRINGO (500 ng). In the case of cyclins, GST-CDK1 and GST-CDK2 were preincubated with Cak1/Civ1 (200 and 250 ng, respectively) for 10 min at RT in the presence of ATP. Kinase assays were performed with histone H1 (4 μg) or Myt1-Ct (2 μg) and [γ-^{32}P]ATP for 15 min at 30°C. Myt1 and H1 phosphorylation was visualized by autoradiography.

(B) *Xenopus* oocytes were injected with Myc-tagged Myt1-Ct mRNA, incubated 14 hr, and reinjected with MBP or MBP-XRINGO (50 ng). Oocytes were collected at the indicated times after the second injection. H1K activity was assayed using either total lysates (4 μl) or cyclin B2 immunoprecipitates (200 μl of total lysate). Oocyte lysates were also analyzed by immunoblotting. Myt1-Ct was detected with Myc antibody.

(C) Oocyte lysates were treated or not with λ phosphatase, as indicated, and analyzed by immunoblotting with Myc antibody.

Next, we investigated whether XRINGO was able to induce Myt1 phosphorylation in oocytes by injecting mRNA-encoding,

Myc-tagged Myt1-Ct and then reinjecting the oocytes with recombinant maltose-binding protein (MBP)-XRINGO. We observed that the electrophoretic mobility of Myt1-Ct, as determined by immunoblotting, was significantly reduced when oocytes entered meiosis I (Figure 1B), which is in agreement with previous results showing Myt1 hyperphosphorylation in M phase (Inoue and Sagata, 2005; Mueller et al., 1995b). Interestingly, we also detected an electrophoretic mobility upshift of Myt1 only 1 hr after injection of XRINGO, at a time when MPF, p42MAPK, and p90Rsk were all inactive (Figure 1B). Furthermore, this early Myt1 mobility upshift correlated with a small increase in the histone H1 kinase (H1K) activity of the total lysates from oocytes injected with XRINGO. We confirmed that the Myt1 upshift was due to phosphorylation by treating the oocyte lysates with λ phosphatase, which resulted in the disappearance of the slower migrating bands (Figure 1C). Finally, we analyzed the phosphorylation of Myt1-Ct during progesterone-induced oocyte maturation. We found that the electrophoretic mobility of Myt1-Ct was reduced at early time points, before the p42MAPK-p90Rsk pathway and MPF were activated, and this correlated with the progesterone-induced accumulation of endogenous XRINGO protein in the oocytes (Figure 2).

The above results, together with the presence of Ser/Thr-Pro phosphorylation motifs for CDKs in Myt1 and its phosphorylation in oocytes that enter meiosis I in the presence of the MEK1/2 inhibitor U0126 (Gross et al., 2000), suggested that Myt1 could be directly phosphorylated by CDK/XRINGO in oocytes. To test this possibility, we used the CDK1 and CDK2 inhibitor Roscovitine, which we confirmed was able to inhibit XRINGO-activated CDKs (Figure 3A). We found that Roscovitine abolished the XRINGO-induced phosphorylation of Myt1-Ct in oocytes (Figure 3B). In agreement with the idea that CDK/XRINGO phosphorylated Myt1 directly, we also observed Myt1 phosphorylation in XRINGO-injected oocytes treated with the protein synthesis inhibitor CHX, where the p42MAPK-p90Rsk pathway was inhibited (Figure 3C). Furthermore, as expected from previous work (Ferby et al., 1999), CHX did not affect the ability of XRINGO to induce MPF activation and entry into meiosis I. Taken together, these results indicate that XRINGO induces the phosphorylation of the regulatory domain of Myt1 in the absence of both new protein synthesis and activation of the p42MAPK pathway; however, this XRINGO-induced phosphorylation requires CDK activity.

Identification of Myt1 Sites Phosphorylated by CDK/XRINGO

The sequence of *Xenopus* Myt1-Ct contains eight consensus CDK phosphorylation sites (Ser/Thr-Pro) (Figure S2). By using generic phospho-Ser and phospho-Thr antibodies, we found that Myt1-Ct was phosphorylated by CDK/XRINGO mainly on Ser residues in vitro. Furthermore, CDK1/XRINGO, but not CDK1/cyclin B, phosphorylated a fragment of Myt1-Ct that contained residues 399–454 (data not shown). Therefore, we systematically mutated Ser to Ala residues in this Myt1-Ct region. We found that a mutant with seven Ser (410, 414, 423, 424, 426, 427, and 444) replaced by Ala (Myt1-7A) was poorly phosphorylated in vitro by CDK1/XRINGO (Figure 4A) and CDK2/XRINGO (Figure S3). Surprisingly, both CDK1/cyclin B and

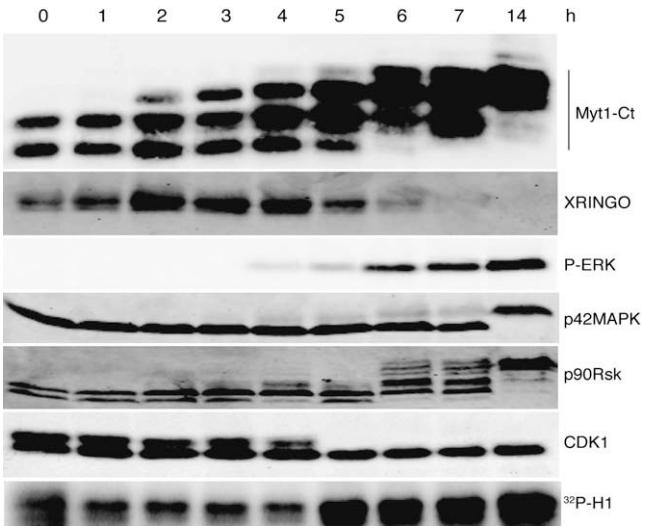

Figure 2. Myt1 Phosphorylation during Oocyte Maturation

Xenopus oocytes from primed frogs were injected with Myc-tagged Myt1-Ct mRNA and 14 hr later were incubated with progesterone for the indicated times. Oocyte extracts were assayed for H1K activity or analyzed by immunoblotting. Myt1-Ct was detected with Myc antibody.

CDK2/cyclin A phosphorylated the Myt1-7A mutant with similar efficiency as the WT Myt1 (Figures 4A and S3). Consistent with these results, Myt1-7A expressed in oocytes did not display the XRINGO-induced mobility upshift observed in WT Myt1, although the p42MAPK pathway and MPF were active in these oocytes (Figure 4B).

The Myt1-7A mutant contained three Ser-Pro consensus sites (410, 414, and 444) changed to Ala. To test the contribution of these three residues to the phosphorylation of Myt1 by CDK/XRINGO, we reintroduced these Ser in the Myt1-7A mutant and then performed in vitro kinase assays. Our results showed that the mutant Ala410Ser, Ala414Ser, Ala444Ser was phosphorylated as efficiently as WT Myt1, suggesting that these three Ser accounted for most of the CDK/XRINGO-induced phosphorylation of Myt1-Ct (Figures 4A and S3). To confirm these observations, we performed the complementary experiment and mutated Ser410, Ser414, and Ser444 to Ala in WT Myt1-Ct (mutant Myt1-3AP). These three mutations eliminated about 80% of the phosphorylation by CDK1/XRINGO or CDK2/XRINGO in vitro. In contrast, the CDK1/cyclin B and CDK2/cyclin A-induced phosphorylations were only reduced by about 30% when comparing the mutant Myt1-3AP with WT Myt1 (Figure 4C). T loop phosphorylation did not change the substrate specificity of CDK/XRINGO complexes on Myt1-Ct (Figure S1).

We also found that Myt1-3AP was only partially phosphorylated in XRINGO-injected oocytes (Figure 4D). In particular, the early Myt1 phosphorylation induced by XRINGO was delayed and reduced, and we did not observe the marked upshift of Myt1 at meiosis I entry, in spite of the full activation of both MPF and the p42MAPK pathway. These results implicate Ser410, Ser414, and Ser444 in the phosphorylation of Myt1 during M phase.

Taken together, our results suggest that XRINGO in complex with CDK1 or CDK2 can phosphorylate Ser410, Ser414, and

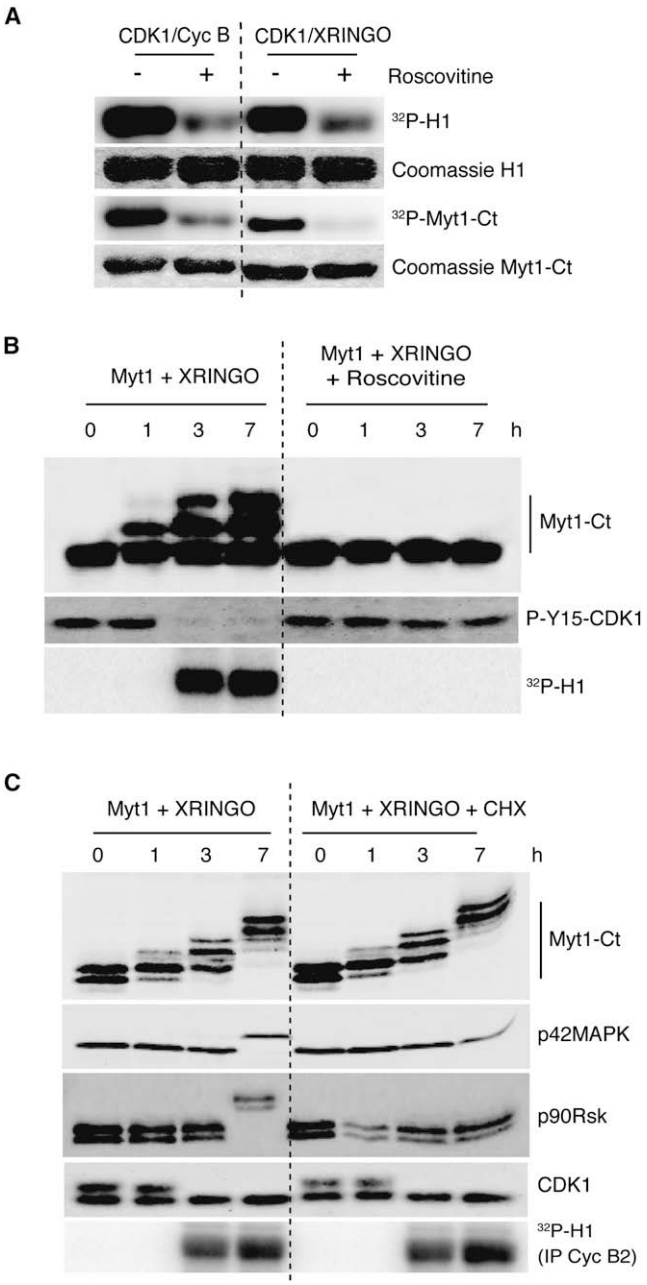

Figure 3. XRINGO-Induced Phosphorylation of Myt1 Requires CDK Activation

(A) Baculovirus-expressed GST-CDK1 (200 ng) was incubated with either cyclin B (200 ng) or MBP-XRINGO (400 ng). In the case of cyclin B, GST-CDK1 was preincubated with Cak1/Civ1 (200 ng) for 10 min at RT in the presence of ATP. Roscovitine (10 μM) or DMSO (–) were added 10 min before performing the kinase assays with histone H1 (4 μg) or Myt1-Ct (2 μg). Phosphorylation of Myt1 and H1 was visualized by autoradiography.

(B) *Xenopus* oocytes were injected with Myc-tagged Myt1-Ct mRNA and 14 hr later were treated or not with Roscovitine (100 μM) for 1 hr before being injected with MBP-XRINGO. Oocyte extracts were assayed for H1K and analyzed by immunoblotting with phospho-Tyr15-CDK1 or Myc antibodies.

(C) *Xenopus* oocytes were injected with Myc-tagged Myt1-Ct mRNA and incubated for 14 hr. Next, the oocytes were treated or not with CHX and 1 hr later were injected with MBP-XRINGO. Oocyte extracts were analyzed by immunoblotting. Myt1-Ct was detected with Myc antibody. H1K activity was assayed using cyclin B2 immunoprecipitates.

Ser444 in the regulatory domain of Myt1. It also appears that XRINGO-activated CDKs may target a different subset of phosphorylation sites in Myt1 than the same CDKs activated by cyclins.

XRINGO-Induced Phosphorylation Downregulates Myt1 Kinase Activity

To understand the biological significance of Myt1 phosphorylation by CDK/XRINGO, we generated a mutant version of full-length Myt1 in which the three Ser-Pro sites (Ser410, Ser414, and Ser444) were changed to either Ala (Myt1-3AP) or Asp (Myt1-3DP).

Overexpression of full-length WT Myt1 in *Xenopus* oocytes (via injection of mRNA) inhibited meiosis I entry induced by either XRINGO or progesterone. Analysis of the biochemical markers showed that the p42MAPK pathway was inactive and CDK1 remained phosphorylated on Thr14/Tyr15 and, therefore, inhibited (Figure 5A). Previous work has shown that high concentrations of Myt1 are required to inhibit the kinase activity of CDK/XRINGO in vitro (Karaiskou et al., 2001). To test the effect of Myt1 concentration on CDK/XRINGO activity in *Xenopus* oocytes, we expressed different amounts of ectopic full-length Myt1 in the oocytes. We observed that high concentrations of Myt1 (>17 ng of mRNA per oocyte) strongly inhibited oocyte maturation induced by XRINGO. However, low concentrations (<5 ng) only delayed meiosis I entry (Figure 5B). These results indicate that Myt1 can inhibit XRINGO-induced oocyte maturation in a dose-dependent manner.

Next, we asked whether phosphorylation of Myt1 on Ser410, Ser414, and Ser444 affected its ability to inhibit oocyte maturation. For this purpose, we first injected mRNAs to express full-length WT Myt1 or the mutants Myt1-3AP and Myt1-3DP in oocytes and then injected XRINGO (Figure 5C). As expected, moderated overexpression of WT Myt1 (about 2-fold the endogenous level obtained by injection of 5 ng of mRNA) delayed the kinetics of meiosis I entry induced by XRINGO, and a stronger effect was observed upon expression of the nonphosphorylatable mutant Myt1-3AP. In contrast, oocytes injected with the phosphomimetic mutant Myt1-3DP entered meiosis I with the same kinetics as the oocytes injected with XRINGO alone, indicating that Myt1-3DP was less efficient at inhibiting XRINGO-induced oocyte maturation (Figure 5C, left panel). In agreement with these observations, dephosphorylation of the inhibitory Thr14/Tyr15 sites of endogenous CDK1 and activation of CDK1/cyclin B were both slower in the oocytes expressing WT Myt1 or the Myt1-3AP mutant than in oocytes expressing Myt1-3DP (Figure 5C, right panel). Consistent with these results, overexpression of high concentrations of WT Myt1 or the mutant Myt1-3AP (injection of 17 ng of mRNA) strongly inhibited the XRINGO-induced oocyte maturation, whereas the mutant Myt1-3DP only decreased the rate of meiosis I entry induced by XRINGO (Figure S4). Taken together, these results suggest that phosphorylation of these three Ser interferes with the inhibitory role of Myt1 on oocyte maturation.

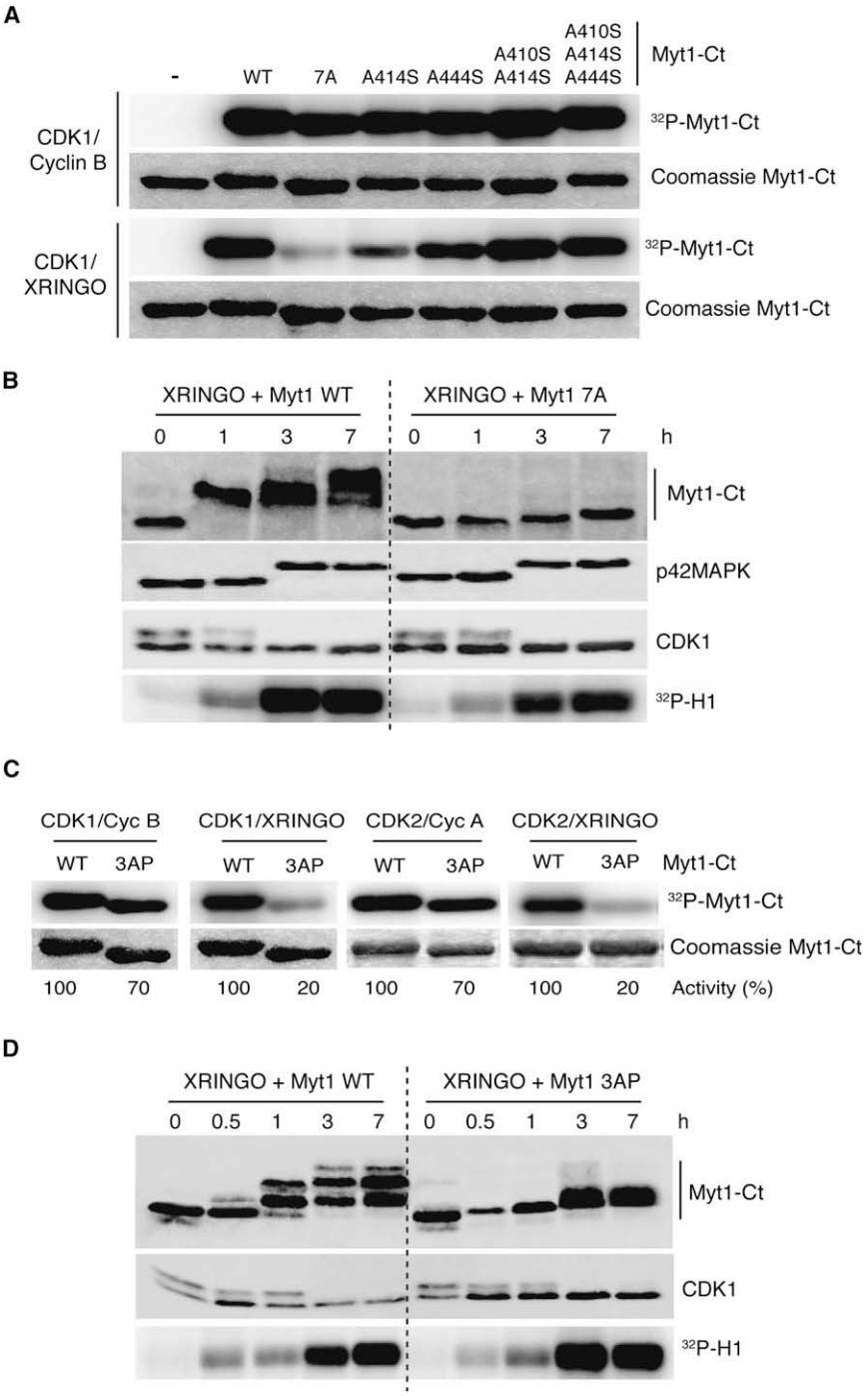

Figure 4. Identification of Specific CDK/XRINGO Phosphorylation Sites on the Regulatory Domain of Myt1

(A) Baculovirus-expressed GST-CDK1 (200 ng) was incubated with cyclin B (200 ng) or MBP-XRINGO (400 ng). In the case of cyclin B, GST-CDK1 was preincubated with Cak1/Civ1 (200 ng) for 10 min at RT in the presence of ATP. WT or mutant GST-Myt1-Ct proteins (2 μg) were then added together with [γ-^{32}P]ATP, and the reactions were incubated for 15 min at 30°C. Myt1 phosphorylation was visualized by autoradiography.

(B) *Xenopus* oocytes were injected with GST-Myt1-Ct, either WT or with 7 Ser mutated (7A), incubated 30 min, and then reinjected with MBP-XRINGO (50 ng). Oocytes were collected at the indicated times after XRINGO injection. Oocyte lysates were assayed for H1K activity or analyzed by immunoblotting. Myt1-Ct was detected with GST antibody.

(C) CDK1 and CDK2 complexes were prepared as in Figure 1A. Kinase assays were performed with WT or mutant 3AP GST-Myt1-Ct (2 μg) in the presence of [γ-^{32}P]ATP for 15 min at 30°C. Myt1 phosphorylation was visualized by autoradiography.

(D) *Xenopus* oocytes were injected with Myc-tagged Myt1-Ct, either WT or mutant 3AP, incubated 14 hr, and reinjected with MBP-XRINGO. Oocytes were collected at the indicated times after XRINGO injection, and lysates were assayed for H1K activity or analyzed by immunoblotting with CDK1 and Myc antibodies.

To test whether XRINGO-induced phosphorylation could directly inhibit Myt1 kinase activity, we performed in vitro kinase assays. First, we incubated different concentrations of reticulocyte-translated full-length WT Myt1 or mutant proteins with recombinant active CDK1/cyclin B for 30 min and then assayed the kinase activity on histone H1. These experiments showed that in vitro phosphorylation by WT Myt1 or the mutant Myt1-3AP effectively inhibited the kinase activity of CDK1/cyclin B in a dose-dependent manner (Figure 6A). In contrast, the mutant Myt1-3DP was less efficient and only partially reduced CDK1/cyclin B activity (about 45%), which was consistent with the reduced ability of this mutant to inhibit XRINGO-induced oocyte maturation (Figure 5C). These results suggest that phosphorylation of Ser410, Ser414, and Ser444 regulates Myt1's ability to inhibit CDK1/cyclin B kinase activity.

Next, we tested whether CDK/XRINGO phosphorylation directly inhibited Myt1 kinase activity. We preincubated full-length WT Myt1 with different concentrations of recombinant CDK2/XRINGO and found that Myt1 phosphorylation correlated well with the CDK2/XRINGO concentrations (Figure 6B). Myt1 was then immunoprecipitated (after the preincubation with CDK2/XRINGO) and thoroughly washed to eliminate the possible carryover of CDK2/XRINGO activity (Figure S5). The kinase activity of the immunopurified Myt1 was assayed by incubation with CDK1/cyclin B and histone H1. The results showed a direct correlation between increased CDK2/XRINGO concentrations, Myt1 phosphorylation, and the reduced ability of Myt1 to inhibit CDK1/cyclin B (Figure 6C).

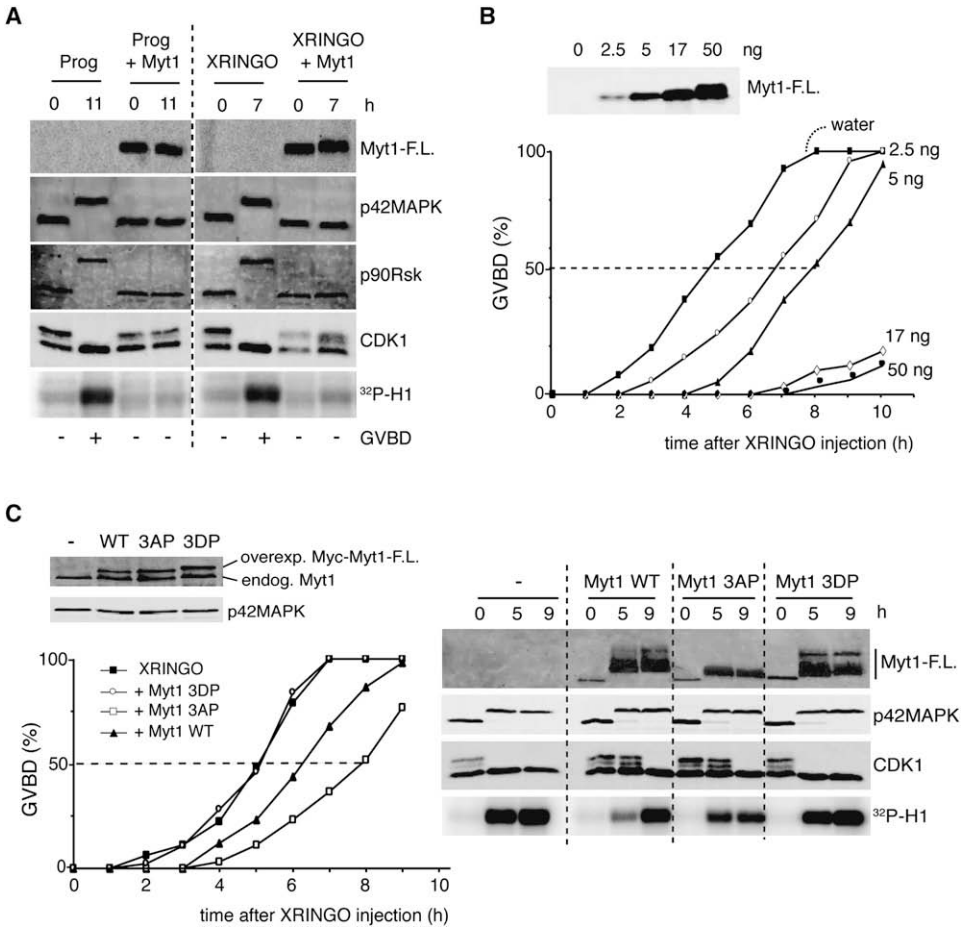

Figure 5. Reduced Inhibitory Activity of the Myt1-3DP Mutant on XRINGO-Induced Oocyte Maturation

(A) *Xenopus* oocytes were injected with Myc-tagged full-length Myt1 mRNA (50 ng) and incubated 14 hr. Next, the oocytes were treated with progesterone or injected with MBP-XRINGO (50 ng). Oocyte extracts were assayed for H1K activity or analyzed by immunoblotting. Myt1 was detected with Myc antibody.

(B) *Xenopus* oocytes were injected with different concentrations (2.5, 5, 17, and 50 ng) of mRNA-encoding, Myc-tagged full-length Myt1 and incubated 14 hr. The oocytes were reinjected with MBP-XRINGO, and GVBD was scored at the indicated times. Lysates from oocytes collected before XRINGO injection were analyzed by immunoblotting with Myc antibody.

(C) *Xenopus* oocytes were injected with 5 ng of mRNA-encoding, Myc-tagged full-length Myt1, either WT or the mutants 3AP and 3DP, incubated 14 hr, and then injected again with MBP-XRINGO. (Left panel) GVBD was scored every hr. Lysates from oocytes taken before XRINGO injection were analyzed by immunoblotting with Myt1 and p42MAPK antibodies. (Right panel) Oocytes were collected at the indicated times after XRINGO injection, and the lysates were assayed for H1K activity or analyzed by immunoblotting. Myt1 was detected with Myc antibody.

Importantly, XRINGO bound to catalytically inactive CDK2-K33R neither phosphorylated Myt1 nor inhibited its kinase activity (Figures 6B and 6C), indicating that Myt1 phosphorylation was required for its inhibition by CDK2/XRINGO.

To confirm that Myt1 inhibition involved phosphorylation on Ser410, Ser414, and Ser444, we preincubated WT Myt1 and the Myt1-3AP mutant with recombinant CDK2/XRINGO and then immunopurified Myt1 and assayed its kinase activity by incubation with CDK1/cyclin B and histone H1. The results showed that, in contrast to WT Myt1, the ability of Myt1-3AP to inactivate CDK1/cyclin B was not affected by preincubation with CDK2/XRINGO (Figure 6D).

We then investigated whether XRINGO-activated CDK1 also inhibited Myt1 kinase activity via phosphorylation of these three Ser. For this, WT Myt1 or the mutant Myt1-3AP were preincubated with different concentrations of CDK1/XRINGO. Myt1 was then immunopurified and thoroughly washed before incubation with CDK1/cyclin B to perform H1K assays. As a control, immunopurified Myt1 was also directly incubated with histone H1 (without CDK1/cyclin B) to verify the absence of contaminating CDK1/XRINGO activity from the preincubation step. Our results showed that CDK1/XRINGO efficiently inactivated WT Myt1 but had no effect on the mutant Myt1-3AP (Figure 7A). Moreover, we observed that the inhibition of CDK1/cyclin B activity by WT Myt1 and the mutant Myt1-3AP correlated with their ability to phosphorylate CDK1 on Tyr15. Thus, upon preincubation with CDK1/XRINGO, WT Myt1 failed to catalyze the inhibitory phosphorylation of CDK1, whereas Myt1-3AP was not

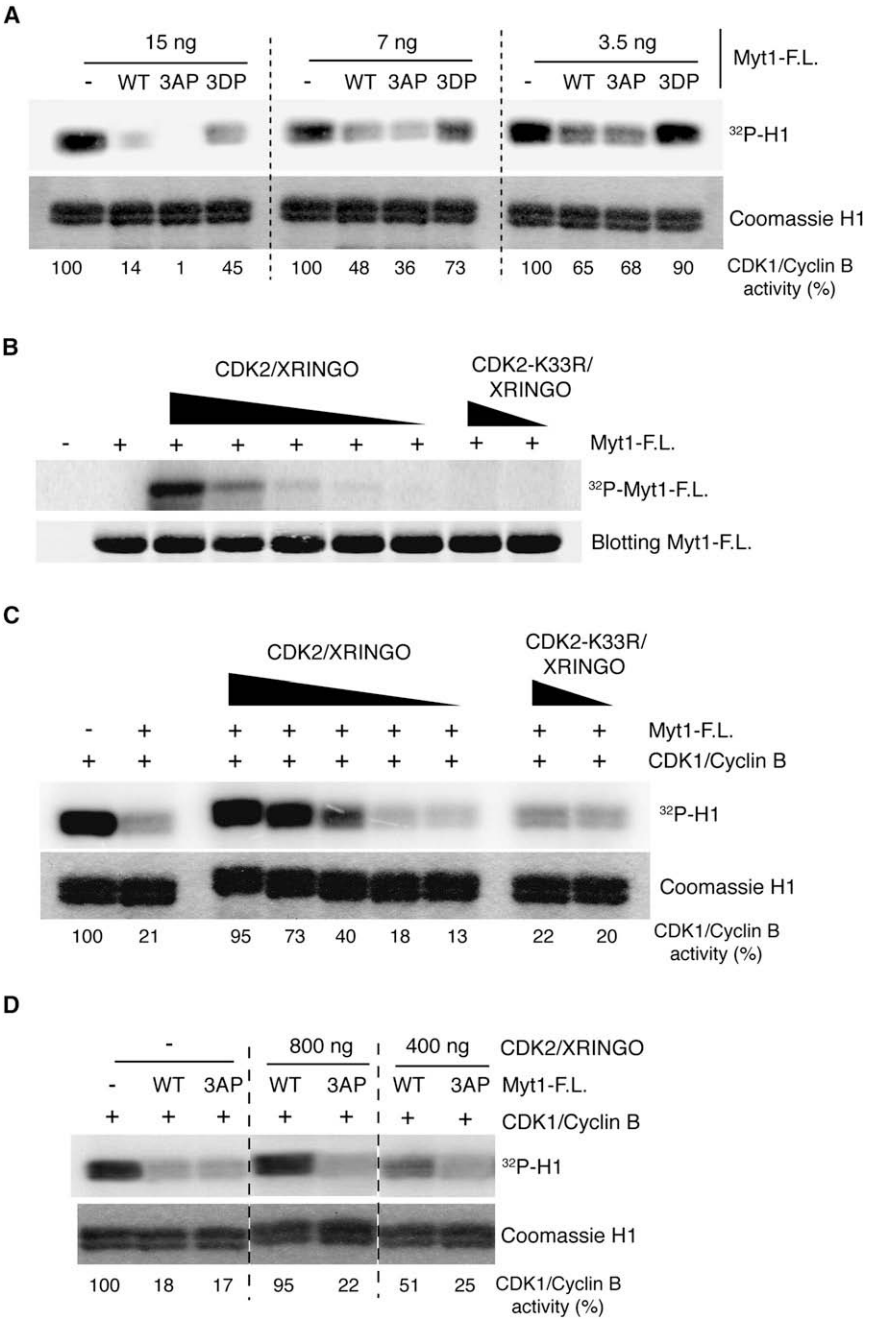

Figure 6. Phosphorylation and Inhibition of Myt1 by XRINGO-Activated CDK2

(A) Myc-tagged full-length Myt1 (WT or mutants 3AP and 3DP) was expressed in reticulocyte lysates, immunoprecipitated with Myc antibodies, and then incubated with recombinant CDK1-cyclin B1-Cak1/Civ1 (120 ng) for 30 min before performing H1K assays.

(B) Myc-tagged full-length Myt1 was expressed in reticulocyte lysates, immunoprecipitated (20 μl of lysate), and incubated with different concentrations of recombinant CDK2/XRINGO (1000, 500, 250, 125, and 60 ng) or CDK2-K33R/XRINGO (1000 and 500 ng) for 30 min in the presence of [γ-^{32}P]ATP.

(C) Myc-tagged full-length Myt1 was expressed in reticulocyte lysates, immunoprecipitated, and incubated with different concentrations of recombinant CDK2/XRINGO or CDK2-K33R/XRINGO as in (B). Myt1 was immunopurified and further incubated with recombinant CDK1-cyclin B1-Cak1/Civ1 (120 ng) for 30 min before H1K assays were performed.

(D) Myc-tagged full-length Myt1 (WT or mutant 3AP) was expressed in reticulocyte lysates, immunoprecipitated, and incubated with different concentrations of CDK2/XRINGO (800 and 400 ng) in the presence of ATP. After 30 min, the bead-bound Myt1 was immunopurified, washed, and further incubated with recombinant CDK1-cyclin B1-Cak1/Civ1 (120 ng) for 30 min before H1K assays were performed.

affected (Figure 7B). These results demonstrate that XRINGO-activated CDKs can directly phosphorylate and inhibit Myt1.

We confirmed that CDK1/XRINGO, but not CDK1/cyclin B, was able to phosphorylate full-length Myt1 in vitro. Interestingly, the lack of phosphorylation of Myt1 upon incubation with CDK1/cyclin B correlated with the phosphorylation of CDK1, which was not observed in the case of XRINGO-activated CDK1 (Figure 7C, upper panels). As a control, we investigated in parallel the phosphorylation of Myt1-Ct by both complexes and found that CDK1/cyclin B was even more efficient than CDK1/XRINGO at phosphorylating Myt1-Ct in vitro (Figure 7C, lower panels). Moreover, Myt1-Ct was apparently stoichiometrically phosphorylated by both CDK1/cyclin B and CDK1/XRINGO, as determined by the upshift of the phosphorylated proteins, although the electrophoretic mobility was different in both cases, which is consistent with the phosphorylation of different sites (Figure S6). Finally, we observed that Myt1 phosphorylated cyclin B-bound CDK1 on Tyr15 more efficiently than the CDK1 bound to XRINGO (Figure S7). Taken together, the results indicate that the inhibition of Myt1 activity by CDK1/XRINGO is probably a consequence of two factors: XRINGO-associated CDK1 phosphorylates more efficiently the inhibitory Myt1 sites, but it is also less susceptible to phosphorylation by Myt1.

DISCUSSION

We have shown that phosphorylation of three Ser in the C-terminal noncatalytic domain of Myt1 inhibits its kinase activity. These sites are efficiently phosphorylated by CDK/XRINGO, but not CDK/cyclin complexes, supporting an important role for RINGO proteins in the M phase-associated inactivation of Myt1.

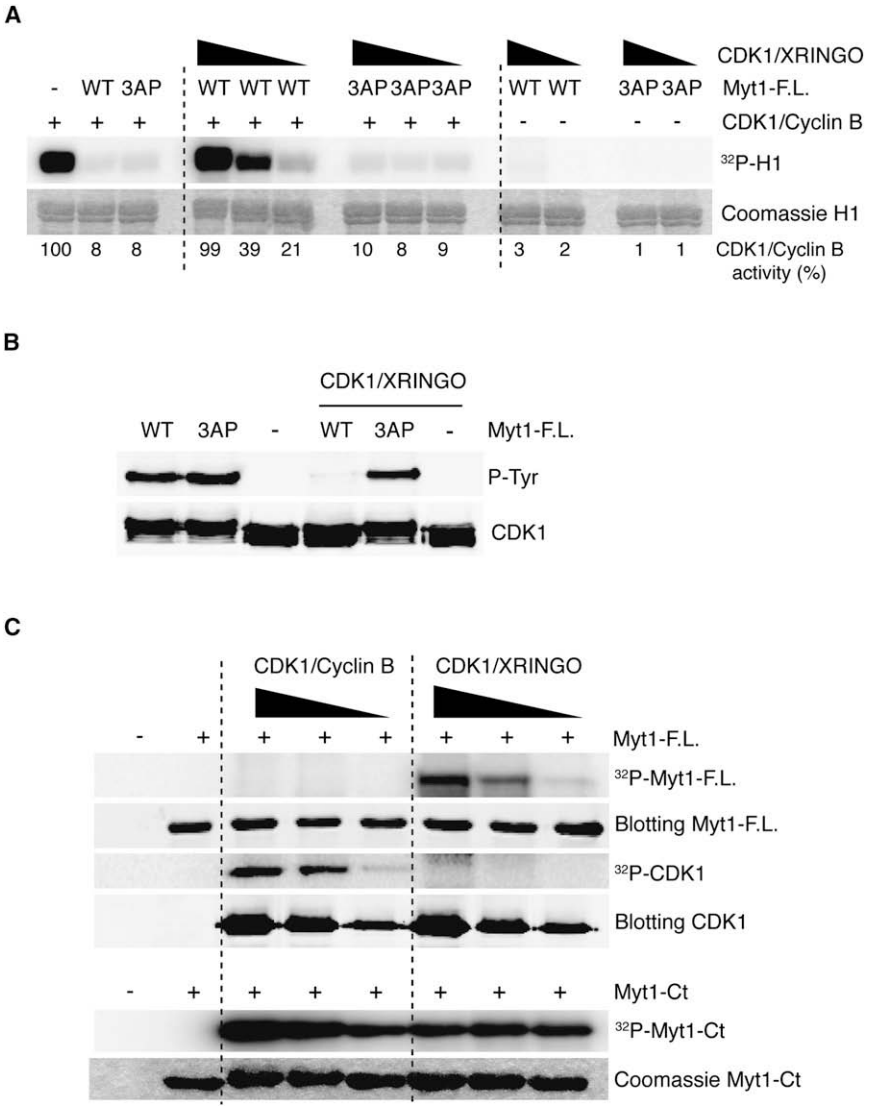

Figure 7. Phosphorylation and Inhibition of Myt1 by CDK1/XRINGO, but Not CDK1/Cyclin B

(A) Myc-tagged full-length Myt1 (WT or mutant 3AP) was expressed in reticulocyte lysates, immunoprecipitated, and incubated with different concentrations of baculovirus-expressed CDK1 activated with MBP-XRINGO (1200, 600, and 300 ng) in the presence of ATP. After 40 min, Myt1 was immunoprecipitated and washed extensively. The immunopurified Myt1 was further incubated in the presence or absence of recombinant CDK1-cyclin B1-Cak1/Civ1 (120 ng) for 30 min before H1K assays were performed. The four right lanes show the controls with immunopurified Myt1 that was directly assayed for H1K activity, in the absence of CDK1/cyclin B1, to confirm the lack of contaminating CDK1/XRINGO activity from the preincubation step.

(B) Myc-tagged full-length Myt1 (WT or mutant 3AP) was expressed in reticulocyte lysates, immunoprecipitated, and incubated with GST-CDK1 activated with MBP-XRINGO (800 ng) in the presence of ATP (300 μM) at 30°C. After 45 min, Myt1 was immunoprecipitated and washed extensively. The immunopurified Myt1 was further incubated in the presence of bacteria-expressed CDK1-K33R and cyclin B (1 μg) for 45 min in H1K buffer supplemented with fresh ATP (300 μM) at 30°C. The reaction mixture was analyzed by immunoblotting.

(C) Myc-tagged full-length Myt1 was expressed in reticulocyte lysates, immunoprecipitated, and incubated with different concentrations of GST-CDK1 activated with either cyclin B or MBP-XRINGO (1200, 600, and 300 ng) for 30 min at 30°C in the presence of [γ-^{32}P]ATP. Phosphorylation of Myt1 and CDK1 was visualized by autoradiography. The same samples were analyzed by immunoblotting with CDK1 and Myc antibodies. For the phosphorylation of Myt1-Ct, kinase assays were performed as above but using GST-Myt1-Ct (500 ng) as a substrate.

Regulation of Myt1 Activity during Oocyte Maturation

Myt1-induced phosphorylation of CDK1 is known to play a key role in the G2 arrest of oocytes by maintaining preformed CDK1/cyclin B complexes inactive. Previous work has shown that Myt1 kinase activity can be regulated by phosphorylation (Inoue and Sagata, 2005; Kristjansdottir et al., 2006; Okumura et al., 2002; Palmer et al., 1998; Wells et al., 1999), but little is known about the molecular mechanisms involved in Myt1 inactivation during the G2/M transition.

The p42MAPK-activated protein kinase p90Rsk has been proposed to phosphorylate and inactivate Myt1 during *Xenopus* oocytes maturation (Palmer et al., 1998). However, in some cases (see Introduction), progesterone can induce CDK1/cyclin B activation in the absence of detectable p42MAPK activity (Dupre et al., 2002; Fisher et al., 1999; Gross et al., 2000; Peter et al., 2002), suggesting that p90Rsk-independent pathways can also lead to Myt1 inactivation in *Xenopus* oocytes. We have found that XRINGO-activated CDK1 and CDK2 can phosphorylate Myt1 on specific sites, which are poorly phosphorylated by CDK/cyclin. Moreover, these sites are phosphorylated during XRINGO-induced oocyte maturation prior to MPF activation and in a CDK-dependent manner, but independently of the p42MAPK-p90Rsk pathway. Finally, phosphorylation of these sites inhibits Myt1 activity in vitro and in oocytes. Thus, CDK/XRINGO is an excellent candidate to trigger Myt1 inactivation during meiosis I entry in *Xenopus* oocytes.

The finding that the Myt1-3AP mutant, which is poorly phosphorylated by CDK/XRINGO, only delays, instead of blocks, XRINGO-induced oocyte maturation could be explained by the inactivation of endogenous Myt1 by CDK/XRINGO. This might be sufficient to allow some pre-MPF activation, which, in turn, would trigger the positive feedback loops targeting both Myt1 and Cdc25 (Schmitt and Nebreda, 2002). An alternative, not mutually exclusive, explanation would be that CDK/XRINGO phosphorylates other substrates in the oocyte, such as Cdc25 (Cheng et al., 2005a) or CPEB (Kim and

Richter, 2007), which could also contribute to the induction of maturation.

We propose the following sequence of events during oocyte maturation. When G2-arrested oocytes are stimulated with progesterone, XRINGO protein accumulates transiently, probably due to both enhanced mRNA translation (Padmanabhan and Richter, 2006) and protein stabilization (Gutierrez et al., 2006). XRINGO protein then binds to monomeric CDK1, and the CDK1/XRINGO complexes phosphorylate Myt1, downregulating its kinase activity toward pre-MPF and allowing the generation of a pool of active MPF. Although XRINGO-CDK1 and -CDK2 can both, in principle, phosphorylate the same Myt1 sites, we favor CDK1 as the initial partner of XRINGO for the triggering events, mainly because G2-arrested oocytes contain a large pool of monomeric CDK1, whereas CDK2 is almost undetectable at this stage (Rempel et al., 1995). The initial pool of MPF could participate in positive feedback loops that help to trigger entry into meiosis I (Schmitt and Nebreda, 2002). During this time, the p42MAPK-p90Rsk pathway is fully active and probably contributes to Myt1 phosphorylation (Palmer et al., 1998). How the p90Rsk pathway and CDK/XRINGO interplay in Myt1 phosphorylation is unclear. We think it likely that both kinases will target different Myt1 sites, as the three Ser that are phosphorylated by CDK/XRINGO do not contain N-terminal Arg residues, which conform the typical p90Rsk phosphorylation motifs. Thus, p90Rsk and CDK/XRINGO could represent parallel pathways that lead to Myt1 inactivation. It is interesting to note that XRINGO is degraded after GVBD (Gutierrez et al., 2006), but Myt1 is thought to be inactive and hyperphosphorylated during the MI to MII transition and MII arrest, suggesting that additional kinases (e.g., p90Rsk) are likely to be implicated in Myt1 phosphorylation during oocyte maturation.

Among the other kinases that are known to phosphorylate Myt1, Akt can also downregulate Myt1 activity in vitro (Okumura et al., 2002). However, there is no evidence for a triggering role of Akt in *Xenopus* oocytes, although it does become activated during oocyte maturation (Andersen et al., 2003). Another candidate would be Plx1, but this kinase neither interacts with nor phosphorylates Myt1 during oocyte maturation. The link between Plx1 and Myt1 appears to be operational only after fertilization, at the M phase of the embryonic cell cycle, excluding Plx1 as one of the kinases responsible for Myt1 inactivation in *Xenopus* oocytes (Inoue and Sagata, 2005). Our results, therefore, indicate that the inhibition of Myt1 by CDK/XRINGO-catalyzed phosphorylation is very likely to be of physiological relevance for the activation of pre-MPF during oocyte maturation.

Regulation of CDK Substrate Specificity by RINGO Proteins

An important conclusion of our study is that XRINGO-activated CDK1 and CDK2 phosphorylate Myt1 on different sites than the same CDKs activated by cyclins. Moreover, these phosphorylations have important functional consequences for the regulation of Myt1. Previous work showed that CDK/RINGO complexes can phosphorylate all CDK/cyclin substrates tested in vitro. However, studies using degenerate peptides based on the canonical CDK substrate sequence KSPRK indicate a more relaxed requirement for specific amino acids in the position P+2, and P+3 in the case of CDK2, activated by human RINGO A than for CDK2/cyclin A (Cheng et al., 2005a). Interestingly, the residues at positions P+2 and P+3 of Ser410, Ser414, and Ser444 in Myt1 are not favorable for CDK2/cyclin A substrate binding (Stevenson-Lindert et al., 2003), which might explain why these sites are poorly phosphorylated by CDK/cyclin in comparison with CDK/XRINGO. In agreement with previous reports (Cheng et al., 2005a; Karaiskou et al., 2001), we also found that the phosphorylation of Myt1 by CDK/XRINGO is not affected by T loop phosphorylation of the CDK, unlike CDK/cyclin complexes.

The K/RXL motif found on some CDK substrates is thought to play an important role in determining specificity, as well as the efficient phosphorylation of substrates, by CDK/cyclin complexes (Brown et al., 2007; Loog and Morgan, 2005; Schulman et al., 1998; Stevenson-Lindert et al., 2003). Myt1 contains an RNL sequence that is necessary for binding to cyclin B (Liu et al., 1999), but mutation of this motif neither affects the binding of Myt1 to XRINGO nor Myt1 phosphorylation by CDK/XRINGO in vitro (data not shown), suggesting that XRINGO and cyclin B use different motifs for substrate recruitment, which, in turn, could facilitate the phosphorylation of different sites in the same CDK substrate.

Our observations support the idea that, by providing the CDK with different substrate specificity, RINGO proteins may be able to regulate specific cell-cycle events. For example, in *Xenopus* oocytes, XRINGO can target CDKs to phosphorylate specific sites of Myt1, triggering its inactivation and M phase entry. The triggering role is also facilitated by the reduced susceptibility of CDK/XRINGO complexes to mechanisms that negatively regulate CDK/cyclin activity. Thus, a system employing both cyclins and RINGO proteins with specific functional capabilities can result in more efficient and robust mechanisms to orchestrate cell-cycle progression.

EXPERIMENTAL PROCEDURES

DNA Cloning

Constructs based on FTX5 to express XRINGO, Myt1-Ct, and Myt1 full-length in *Xenopus* oocytes and constructs to express MBP-XRINGO, GST-Myt1-Ct, GST-CDK1 (*Xenopus*) K33R and GST-CDK2 (human) WT, K33R, and T160A in *E. coli* have been previously described (Ferby et al., 1999; Nebreda et al., 1995; Palmer et al., 1998). His-cyclin A (bovine) (Brown et al., 1995) and GST-Cak1/Civ1 (Brown et al., 1999) were purified from *E. coli*. A polycistronic construct to coexpress GST-CDK1, Cak1/Civ1, and cyclin B1-His in *E. coli* was provided by Yoshimi Tanaka. Recombinant His-cyclin B1 (human) was purified from baculovirus-infected insect cells as described (Kumagai and Dunphy, 1995). Baculovirus-expressed GST-CDK1 (human) was purchased from SignalChem (C22-14G-20). A Coomassie-stained gel with the purified recombinant proteins is shown in Figure S8.

Myt1 mutants were prepared using the Quick Change site-directed mutagenesis kit (Stratagene) and were verified by DNA sequencing.

Oocyte Maturation and mRNA Expression

Meiotic maturation of *Xenopus* oocytes was induced by incubation of manually dissected oocytes with 5 μg/ml (15 μM) of progesterone (Sigma, St Louis, MO) or by injection with 50 nl of purified MBP-XRINGO protein (1 mg/ml) and scored by the appearance of a white spot at the animal pole of the oocytes, which indicates GVBD and meiosis I entry. For expression of Myc-tagged proteins, oocytes were microinjected with 50 nl of in vitro transcribed mRNAs (mMessage mMachine kit, Ambion, Austin, TX) and maintained overnight in modified

Barth's medium at 18°C before progesterone treatment. For the preparation of lysates, oocytes were homogenized in 10 μl per oocyte of ice-cold H1K buffer (80 mM β-glycerophosphate (pH 7.5), 20 mM EGTA, 15 mM $MgCl_2$, 1 mM DTT, 1 mM AEBSF, 2.5 mM Benzamidine, and 10 μg/ml each of Aprotinin and Leupeptin). The lysates were centrifuged at 10,000 g for 10 min, and the cleared supernatants were stored at −70°C.

CHX (Sigma) and Roscovitine (Sigma) were added to the oocyte medium to a final concentration of 50 μg/ml and 100 μM, respectively, for 60 min before the injection of MBP-XRINGO.

Phosphatase Treatment

Oocytes lysates (equivalent to one oocyte) were incubated with 250 U of λ phosphatase (Upstate, 14-405) or phosphatase buffer alone (50 mM HEPES, 0.1 mM EDTA, 2 mM $MnCl_2$, 1mM DTT) for 60 min at 30°C. Reactions were stopped by the addition of sample buffer and were analyzed by immunoblotting.

Immunoblotting and Immunoprecipitation

Immunoblotting was performed as described (Palmer et al., 1998). The following antibodies were used: CDK1 monoclonal antibody 3E1 (Nebreda et al., 1995), cyclin B2 rabbit antiserum (Hochegger et al., 2001), p42MAPK and Myt1 rabbit antisera (Palmer et al., 1998), p90Rsk-1 (Santa Cruz Biotechnology, sc-231), phospho-ERK (Santa Cruz Biotechnology, sc-7383), phospho-Tyr15-CDK1 (Cell Signaling, 9111), phospho-Tyr (Upstate, 05-321X), and Myc monoclonal antibody 9E10 (Santa Cruz Biotechnology, sc-40). For detection, we used Alexa Fluor 680- (Molecular Probes) or Li-Cor IRDye 800- (Rockland) labeled antibodies with the Odyssey Infrared Imaging System (Li-Cor).

Immunoprecipitations were performed as described (Palmer et al., 1998), using 5 μl of anti-Myc or 8 μl of anticyclin B2 antibodies and the following IP buffer: 50 mM Tris-HCl (pH 7.5), 150 mM NaCl, 1% (v/v) NP-40, 5 mM EDTA (pH 8.0), 5 mM EGTA (pH 8.0), 20 mM NaF, 0.1 μM PMSF, 0.5 μM Benzamidin, 1 μg/μl Leupeptin, 1 μg/μl Aprotinin, 2 μM Microcystin, and 0.1 μM $NaVO_3$.

Myt1 Kinase Activity Assays

Myc-tagged Myt1 proteins were expressed from FTX5-Myt1 using the TNT reticulocyte lysate system supplemented with canine pancreatic microsomal membranes as recommended by the supplier (Promega, L4610). We estimated that the concentration of Myt1 in the lysate was about 1 ng/μl by immunoblotting with anti-Myt1 antibodies using GST-Myt1-Ct as a reference. Typically, 20 μl of the Myt1-expressing reticulocyte lysate were diluted in 500 μl of IP buffer and then incubated at 4°C with 7 μl of 9E10 anti-Myc antibody for 3–4 hr followed by incubation with 30 μl of protein G sepharose beads (Amersham Biosciences, 17-0618-02) for 1 hr. As a control, reticulocyte lysates that do not express Myt1 were also immunoprecipitated. The bead-bound Myc-Myt1 immunocomplexes were washed three times in IP buffer, twice with H1K buffer, and then incubated in 20 μl of kinase buffer containing 100 μM ATP and 120 ng of recombinant coexpressed CDK1-cyclin B1-Cak1/Civ1. After 30 min at RT, the CDK1/cyclin B1 activity was assayed with 4 μg of histone H1 and 2 μCi of [γ-^{32}P]ATP for 15 min at 30°C. Samples were finally boiled in sample buffer and analyzed by SDS-PAGE and autoradiography.

To determine the effect of XRINGO-activated CDK1 and CDK2 on Myt1 kinase activity, the immunoprecipitated Myc-Myt1 was preincubated with active recombinant CDK1/XRINGO or CDK2/XRINGO for 30–45 min at RT in 40 μl of H1K buffer supplemented with 300 μM ATP and then washed at least three times with H1K buffer before incubation with the CDK1/cyclin B1 substrate.

The phosphorylation of CDK1 on Tyr15 was assayed by incubating the immunoprecipitated Myc-Myt1 in 30 μl of kinase buffer containing 350 μM ATP and 1 μg each of recombinant CDK1-K33R and cyclin B1 for 45–60 min. Samples were evaluated by immunoblotting with phopho-Tyr antibody.

Activation of Recombinant CDK1 and CDK2

Purified bacterially expressed GST-CDK2 or baculovirus-expressed GST-CDK1 were activated by incubation with GST-Cak1/Civ1 followed by the addition of either His-cyclin A or His-cyclin B1, respectively, or by direct incubation with MBP-XRINGO and then used for kinase assays.

Kinase Assays

H1K assays were performed as described (Palmer et al., 1998) in a final volume of 12 μl of H1K buffer containing 4 μl of oocyte lysate, 50 μM cold ATP, 2 μCi of [γ-^{32}P]ATP (3000 Ci/mmol), and 4 μg of histone H1 (Sigma, H5505). After 15 min at 30°C, the phosphorylation reactions were terminated by addition of sample buffer and analyzed by SDS-PAGE and autoradiography.

Recombinant protein kinases were assayed for 15–30 min at 30°C in a final volume of 10 μl of kinase buffer (50 mM Tris-HCl (pH 7.5), 10 mM $MgCl_2$, 2 mM DTT, 100–150 μM cold ATP) containing 2 μCi of [γ-^{32}P]ATP and 4 μg of histone H1, 2 μg of GST-Myt1-Ct, or the indicated amounts of immunoprecipitated Myt1. The reactions were stopped with sample buffer and analyzed by SDS-PAGE and autoradiography.

Bacterial Expression and Purification of Recombinant Proteins

Recombinant GST- and MBP-fusion proteins were purified from *E. coli* as described (Palmer et al., 1998). His-tagged cyclin A was purified from *E. coli* as described (Brown et al., 1995) but incubating the sonicated lysate supernatant with talon beads (Clontech, 635501) for 90 min at 4°C. The beads were washed with 60 mM Imidazole, 500 mM NaCl, and 20 mM Tris-HCl (pH 7.9), and His-cyclin A was eluted in the same buffer supplemented with 1 M Imidazole. Fractions containing the purified recombinant proteins were dialyzed overnight against 20–50 mM Tris (pH 7.5–8.0), 50 mM NaCl, 0.1 mM EDTA, 0.5 mM DTT, and 5% glycerol and stored in aliquots at −70°C.

SUPPLEMENTAL DATA

The Supplemental Data include eight figures and can be found with this article online at http://www.molecule.org/supplemental/S1097-2765(08)00659-X.

ACKNOWLEDGMENTS

We thank Margaret Jones and Amparo Palmer for early contributions to this project. This work was funded by grant BFU2004-03566 from the Spanish Ministerio de Educación y Ciencia (MEC) and by ISCIII-RETIC RD06/0020/0083. E.J.R. was supported by an MEC predoctoral fellowship and CONACYT (Mexico).

Received: April 4, 2008
Revised: July 11, 2008
Accepted: August 14, 2008
Published: October 23, 2008

REFERENCES

Andersen, C.B., Sakaue, H., Nedachi, T., Kovacina, K.S., Clayberger, C., Conti, M., and Roth, R.A. (2003). Protein kinase B/Akt is essential for the insulin- but not progesterone-stimulated resumption of meiosis in Xenopus oocytes. Biochem. J. *369*, 227–238.

Booher, R.N., Holman, P.S., and Fattaey, A. (1997). Human Myt1 is a cell cycle-regulated kinase that inhibits Cdc2 but not Cdk2 activity. J. Biol. Chem. *272*, 22300–22306.

Brown, N.R., Noble, M.E., Endicott, J.A., Garman, E.F., Wakatsuki, S., Mitchell, E., Rasmussen, B., Hunt, T., and Johnson, L.N. (1995). The crystal structure of cyclin A. Structure *3*, 1235–1247.

Brown, N.R., Noble, M.E., Endicott, J.A., and Johnson, L.N. (1999). The structural basis for specificity of substrate and recruitment peptides for cyclin-dependent kinases. Nat. Cell Biol. *1*, 438–443.

Brown, N.R., Lowe, E.D., Petri, E., Skamnaki, V., Antrobus, R., and Johnson, L.N. (2007). Cyclin B and cyclin A confer different substrate recognition properties on CDK2. Cell Cycle *6*, 1350–1359.

Cheng, A., Gerry, S., Kaldis, P., and Solomon, M.J. (2005a). Biochemical characterization of Cdk2-Speedy/Ringo A2. BMC Biochem. *6*, 19.

Cheng, A., Xiong, W., Ferrell, J.E., Jr., and Solomon, M.J. (2005b). Identification and comparative analysis of multiple mammalian Speedy/Ringo proteins. Cell Cycle *4*, 155–165.

De Smedt, V., Poulhe, R., Cayla, X., Dessauge, F., Karaiskou, A., Jessus, C., and Ozon, R. (2002). Thr-161 phosphorylation of monomeric Cdc2. Regulation by protein phosphatase 2C in Xenopus oocytes. J. Biol. Chem. *277*, 28592–28600.

Dinarina, A., Perez, L.H., Davila, A., Schwab, M., Hunt, T., and Nebreda, A.R. (2005). Characterization of a new family of cyclin-dependent kinase activators. Biochem. J. *386*, 349–355.

Dupre, A., Jessus, C., Ozon, R., and Haccard, O. (2002). Mos is not required for the initiation of meiotic maturation in Xenopus oocytes. EMBO J. *21*, 4026–4036.

Ferby, I., Blazquez, M., Palmer, A., Eritja, R., and Nebreda, A.R. (1999). A novel p34(cdc2)-binding and activating protein that is necessary and sufficient to trigger G(2)/M progression in Xenopus oocytes. Genes Dev. *13*, 2177–2189.

Fisher, D.L., Brassac, T., Galas, S., and Doree, M. (1999). Dissociation of MAP kinase activation and MPF activation in hormone-stimulated maturation of Xenopus oocytes. Development *126*, 4537–4546.

Gross, S.D., Schwab, M.S., Taieb, F.E., Lewellyn, A.L., Qian, Y.W., and Maller, J.L. (2000). The critical role of the MAP kinase pathway in meiosis II in Xenopus oocytes is mediated by p90(Rsk). Curr. Biol. *10*, 430–438.

Gutierrez, G.J., Vogtlin, A., Castro, A., Ferby, I., Salvagiotto, G., Ronai, Z., Lorca, T., and Nebreda, A.R. (2006). Meiotic regulation of the CDK activator RINGO/Speedy by ubiquitin-proteasome-mediated processing and degradation. Nat. Cell Biol. *8*, 1084–1094.

Hochegger, H., Klotzbucher, A., Kirk, J., Howell, M., le Guellec, K., Fletcher, K., Duncan, T., Sohail, M., and Hunt, T. (2001). New B-type cyclin synthesis is required between meiosis I and II during Xenopus oocyte maturation. Development *128*, 3795–3807.

Inoue, D., and Sagata, N. (2005). The Polo-like kinase Plx1 interacts with and inhibits Myt1 after fertilization of Xenopus eggs. EMBO J. *24*, 1057–1067.

Karaiskou, A., Perez, L.H., Ferby, I., Ozon, R., Jessus, C., and Nebreda, A.R. (2001). Differential regulation of Cdc2 and Cdk2 by RINGO and cyclins. J. Biol. Chem. *276*, 36028–36034.

Kim, J.H., and Richter, J.D. (2007). RINGO/cdk1 and CPEB mediate poly(A) tail stabilization and translational regulation by ePAB. Genes Dev. *21*, 2571–2579.

Kristjansdottir, K., Safi, A., Shah, C., and Rudolph, J. (2006). Autophosphorylation of Ser66 on Xenopus Myt1 is a prerequisite for meiotic inactivation of Myt1. Cell Cycle *5*, 421–427.

Kumagai, A., and Dunphy, W.G. (1992). Regulation of the cdc25 protein during the cell cycle in Xenopus extracts. Cell *70*, 139–151.

Kumagai, A., and Dunphy, W.G. (1995). Control of the Cdc2/cyclin B complex in Xenopus egg extracts arrested at a G2/M checkpoint with DNA synthesis inhibitors. Mol. Biol. Cell *6*, 199–213.

Lee, M.S., Enoch, T., and Piwnica-Worms, H. (1994). mik1+ encodes a tyrosine kinase that phosphorylates p34cdc2 on tyrosine 15. J. Biol. Chem. *269*, 30530–30537.

Lenormand, J.L., Dellinger, R.W., Knudsen, K.E., Subramani, S., and Donoghue, D.J. (1999). Speedy: a novel cell cycle regulator of the G2/M transition. EMBO J. *18*, 1869–1877.

Liu, F., Stanton, J.J., Wu, Z., and Piwnica-Worms, H. (1997). The human Myt1 kinase preferentially phosphorylates Cdc2 on threonine 14 and localizes to the endoplasmic reticulum and Golgi complex. Mol. Cell. Biol. *17*, 571–583.

Liu, F., Rothblum-Oviatt, C., Ryan, C.E., and Piwnica-Worms, H. (1999). Overproduction of human Myt1 kinase induces a G2 cell cycle delay by interfering with the intracellular trafficking of Cdc2-cyclin B1 complexes. Mol. Cell. Biol. *19*, 5113–5123.

Loog, M., and Morgan, D.O. (2005). Cyclin specificity in the phosphorylation of cyclin-dependent kinase substrates. Nature *434*, 104–108.

Mueller, P.R., Coleman, T.R., and Dunphy, W.G. (1995a). Cell cycle regulation of a Xenopus Wee1-like kinase. Mol. Biol. Cell *6*, 119–134.

Mueller, P.R., Coleman, T.R., Kumagai, A., and Dunphy, W.G. (1995b). Myt1: a membrane-associated inhibitory kinase that phosphorylates Cdc2 on both threonine-14 and tyrosine-15. Science *270*, 86–90.

Nakajo, N., Yoshitome, S., Iwashita, J., Iida, M., Uto, K., Ueno, S., Okamoto, K., and Sagata, N. (2000). Absence of Wee1 ensures the meiotic cell cycle in Xenopus oocytes. Genes Dev. *14*, 328–338.

Nebreda, A.R. (2006). CDK activation by non-cyclin proteins. Curr. Opin. Cell Biol. *18*, 192–198.

Nebreda, A.R., and Ferby, I. (2000). Regulation of the meiotic cell cycle in oocytes. Curr. Opin. Cell Biol. *12*, 666–675.

Nebreda, A.R., Gannon, J.V., and Hunt, T. (1995). Newly synthesized protein(s) must associate with p34cdc2 to activate MAP kinase and MPF during progesterone-induced maturation of Xenopus oocytes. EMBO J. *14*, 5597–5607.

Okumura, E., Fukuhara, T., Yoshida, H., Hanada Si, S., Kozutsumi, R., Mori, M., Tachibana, K., and Kishimoto, T. (2002). Akt inhibits Myt1 in the signalling pathway that leads to meiotic G2/M-phase transition. Nat. Cell Biol. *4*, 111–116.

Padmanabhan, K., and Richter, J.D. (2006). Regulated Pumilio-2 binding controls RINGO/Spy mRNA translation and CPEB activation. Genes Dev. *20*, 199–209.

Palmer, A., Gavin, A.C., and Nebreda, A.R. (1998). A link between MAP kinase and p34(cdc2)/cyclin B during oocyte maturation: p90(rsk) phosphorylates and inactivates the p34(cdc2) inhibitory kinase Myt1. EMBO J. *17*, 5037–5047.

Peter, M., Labbe, J.C., Doree, M., and Mandart, E. (2002). A new role for Mos in Xenopus oocyte maturation: targeting Myt1 independently of MAPK. Development *129*, 2129–2139.

Rempel, R.E., Sleight, S.B., and Maller, J.L. (1995). Maternal Xenopus Cdk2-cyclin E complexes function during meiotic and early embryonic cell cycles that lack a G1 phase. J. Biol. Chem. *270*, 6843–6855.

Schmitt, A., and Nebreda, A.R. (2002). Signalling pathways in oocyte meiotic maturation. J. Cell Sci. *115*, 2457–2459.

Schulman, B.A., Lindstrom, D.L., and Harlow, E. (1998). Substrate recruitment to cyclin-dependent kinase 2 by a multipurpose docking site on cyclin A. Proc. Natl. Acad. Sci. USA *95*, 10453–10458.

Stevenson-Lindert, L.M., Fowler, P., and Lew, J. (2003). Substrate specificity of CDK2-cyclin A. What is optimal? J. Biol. Chem. *278*, 50956–50960.

Wells, N.J., Watanabe, N., Tokusumi, T., Jiang, W., Verdecia, M.A., and Hunter, T. (1999). The C-terminal domain of the Cdc2 inhibitory kinase Myt1 interacts with Cdc2 complexes and is required for inhibition of G(2)/M progression. J. Cell Sci. *112*, 3361–3371.

Mechanism for the Inactivation of the CDK1/Cyclin B

Inhibitory Kinase Myt1 by p90Rsk

E. Josué Ruiz, Marçal Vilar and Angel R. Nebreda.

CNIO (Spanish National Cancer Center), Melchor Fernández Almagro 3, 28029

Madrid, Spain.

Summary

Xenopus oocyte meiotic maturation requires the activation of CDK1/cyclin B complexes (MPF) [1, 2]. MPF is activated by phosphorylation at Thr161 on the CDK1 but remains inactive due to the inhibitory phosphorylation at Thr14 and Tyr15 mediated by the protein kinase Myt1 in G2-arrested oocytes. This suggests an important role for the inhibitory kinase Myt1 in regulating the G2/M transition during oocyte maturation. Previously we have shown that p90Rsk binds and phosphorylates the C-terminal regulatory domain of Myt1 [3]. Here we characterize in detail the mechanism by which p90Rsk phosphorylation on Myt1 inhibit its activity on MPF. We have identified four serine and one threonine residues on Myt1 as targets of phosphorylation by p90Rsk. Phosphorylation of these five residues inhibits Myt1 activity *in vitro*. Importantly, these residues are phosphorylated during progesterone-induced oocyte maturation, and their mutation to alanine makes Myt1 resistant to the inhibition by p90Rsk both *in vitro* and in oocytes. Moreover, we show that the phosphorylation on the Myt1 C-terminal domain by CDK1/XRINGO complex creates a putative docking site on Myt1 that targets p90Rsk to Myt1, where p90Rsk posterior phosphorylation on those five residues on Myt1, decreases the affinity of Myt1 for CDK1/cyclin B. A model where the CDK1/XRINGO complex and p42MAPK-p90Rsk pathway cooperate to regulate and inactivate Myt1 activity in the G2/M transition in *Xenopus* oocytes is described.

Results and Discussion

The molecular mechanisms that regulate Myt1 activity during M phase entry are still unsolved. The protein kinase Myt1 consist of two domains, the N-terminal catalytic domain and the C-terminal regulatory domain. Moreover, there is a 20 residues long hydrophobic domain that is thought to anchor the protein to the endoplasmic reticulum and Golgi membranes [4-6] (**Fig. 1A**). To determine whether the C-terminal domain is required for Myt1 biological activity, we injected oocytes with mRNAs encoding Myc-tagged full-length Myt1 or Myt1-ΔC lacking the 210 C-terminal residues, but retains the catalytic domain of Myt1, and we stimulated the oocytes with progesterone. As expected, overexpression of full-length Myt1 delay the kinetics of meiosis I entry induced by progesterone (**Fig. 1B**). However, the oocytes injected with Myt1-ΔC mature with similar kinetics as oocytes stimulated with progesterone (**Fig. 1B**). Moreover, we found that Myt1-ΔC was not phosphorylated in those oocytes, in spite of the activation of both MPF and the p42MAPK pathway (**Fig. 1C**). Consistent with these results, dephosphorylation of the inhibitory Thr14/Tyr15 sites of endogenous CDK1 was slower in the oocytes expressing full-length Myt1 than in oocytes expressing Myt1-ΔC (**Fig. 1C**). Taken together, these results suggest that the C-terminal regulatory domain of Myt1 is necessary for inhibition of *Xenopus* oocyte maturation.

Previously, we identified three Ser-Pro sites (Ser410, Ser414 and Ser444) located in the C-terminal non-catalytic domain of Myt1 whose phosphorylation inhibits Myt1 kinase activity [7]. Importantly, these sites are efficiently phosphorylated by CDK1/XRINGO, but not by CDK1/cyclin B complexes. We observed that the Myt1-3AP mutant, which is not phosphorylated by CDK1/XRINGO, only delays, instead of blocks, XRINGO-induced oocyte maturation [7]. This could be explained by the participation of other signalling pathways that converge in the inactivation of Myt1 activity. This might be sufficient to allow some pre-MPF activation, which, in turn, would trigger the positive feedback loops targeting both Myt1 and Cdc25 [8].

The p42MAPK-activated p90Rsk has been previously shown to interact with and phosphorylate Myt1 and thereby inhibits its activity during oocyte maturation [3]. Two Ser that are phosphorylated by CDK1/XRINGO (Ser410 and Ser414) belong to

the typical p90Rsk phosphorylation motifs (N-terminal Arg residues, RXRRXS/T) [9]. However, there is no evidence that p90Rsk can phosphorylate CDKs consensus sites (Ser/Thr-Pro) [9]. Thus, it is possible that p90Rsk and CDK1/XRINGO phosphorylate the regulatory domain of Myt1 on different sites. To test this possibility, we used the Myt1-3AP mutant as a substrate in kinase assays. As expected, XRINGO-activated CDK1 and CDK2 did not phosphorylate the Myt1-3AP mutant. We observed, instead, that p90Rsk phosphorylates the Myt1-3AP mutant with similar efficiency as WT Myt1 (**Fig. 2A**).

Next, we asked whether p90Rsk phosphorylation directly inhibited Myt1-3AP mutant kinase activity. For this propose, we first preincubated reticulocyte-translated full-length WT Myt1 or the Myt1-3AP mutant with p90Rsk. Myt1 proteins were then immunoprecipitated and their kinase activity was assayed by incubation with CDK1/cyclin B and histone H1. The results show that Myt1 proteins have less ability to inhibit CDK1/cyclin B activity, indicating that p90Rsk efficiently inactivated both WT Myt1 and the Myt1-3AP mutant (**Fig. 2B**). To identify which residues of Myt1-Ct were phosphorylated by p90Rsk, we mutated potential p90Rsk consensus sites (RXRRXS/T) (**Fig. S1**). We found that a mutant with four Ser (472, 475, 492 and 504) and one Thr (453) replaced to Ala (Myt1-5A) was poorly phosphorylated by p90Rsk *in vitro* (**Fig. 2C**). In contrast, CDK1/XRINGO phosphorylated the Myt1-5A mutant as efficiently as the WT Myt1 (**Fig. 2C**). Moreover, we found that the Myt1-5A mutant was partially phosphorylated in progesterone-stimulated oocytes (**Fig. 2D**). In particular, the late Myt1 phosphorylation induced by progesterone was delayed and reduced and we did not observe the marked upshift of Myt1 at meiosis I entry, in spite of the full activation of both MPF and the p42MAPK-p90Rsk pathway (**Fig. 2D**). Interestingly, the accumulation of endogenous XRINGO protein correlated with Myt1 phosphorylation at early time points. These results implicate Thr453, Ser472, Ser475, Ser492 and Ser504 in the late phosphorylation of Myt1 during M phase.

To understand the biological significance of Myt1 phosphorylation by p90Rsk, we generated a mutant version of full-length Myt1 in which the five p90Rsk consensus sites (Thr453, Ser472, Ser475, Ser492 and Ser504) were changed to either Ala (Myt1-5A) or to the phospho-mimetic Asp (Myt1-5D) (**Fig. 3**). We injected mRNAs to express full-length WT Myt1 or the mutants Myt1-5A and Myt1-5D in oocytes, and then they were stimulated with progesterone (**Fig. 3A, left panel**).

Overexpression of WT Myt1 (about 4-fold the endogenous level obtained by injection of 10 ng of mRNA) delayed the kinetics of meiosis I entry induced by progesterone, and a stronger effect was observed upon expression of the non-phosphorylatable mutant Myt1-5A. In contrast, the oocytes injected with mutant Myt1-5D mature with similar kinetics as oocytes stimulated with progesterone, indicating that Myt1-5D was less efficient at inhibiting progesterone-induced oocyte maturation (**Fig. 3A**, **left panel**). Consistent with these results, dephosphorylation of the inhibitory Thr14/Tyr15 sites of endogenous CDK1 and activation of CDK1/cyclin B were both slower in the oocytes expressing WT Myt1 or the Myt1-5A mutant than in oocytes expressing Myt1-5D, as shown by kinase assays (**Fig. 3A**, **right panel**). Taken together, these results suggest that phosphorylation of these five residues interferes with the inhibitory role of Myt1 on oocyte maturation.

To investigate whether p90Rsk inhibited Myt1 kinase activity, we first confirmed that *in vitro* phosphorylation by WT Myt1 or the mutant Myt1-5A effectively inhibited the kinase activity of CDK1/cyclin B (**Fig. 3B**). In contrast, the phospho-mimetic mutant Myt1-5D was less efficient and only partially reduced CDK1/cyclin B activity (about 40%), which was consistent with the reduced ability of this mutant to inhibit progesterone-induced oocyte maturation (**Fig. 3A**). These results suggest that phosphorylation of Thr453, Ser472, Ser475, Ser492 and Ser504 regulates the ability of Myt1 to inhibit CDK1/cyclin B kinase activity. Next, we tested whether p90Rsk inhibited Myt1 activity via phosphorylation of those residues. To this end, we preincubated full-length WT Myt1 or the mutant Myt1-5A with recombinant p90Rsk and found that WT Myt1, but not the mutant Myt1-5A, was phosphorylated by p90Rsk (**Fig. 3C**). Myt1 proteins were then immunopurified and thoroughly washed before incubation with CDK1/cyclin B to perform histone H1 kinase assays. As a control, immunopurified Myt1 was also directly incubated with histone H1 (without CDK1/cyclin B) to verify the absence of contaminating p90Rsk activity from the preincubation step. The results showed a direct correlation between Myt1 phosphorylation induced by p90Rsk and the reduced ability of WT Myt1 to inhibit CDK1/cyclin B (**Fig. 3D**). However, the ability of Myt1-5A mutant to inactivate CDK1/cyclin B was not affected by the preincubation with p90Rsk (**Fig. 3D**). We also observed that phosphorylation induced by CDK1/XRINGO directly inhibited Myt1-5A mutant kinase activity (**Fig. 3D**). Taken together, these results suggest that

p90Rsk and CDK1/XRINGO phosphorylate the regulatory domain of Myt1 on different sites and could represent parallel pathways that lead to Myt1 inactivation.

Our results also show that Myt1-Ct was phosphorylated at early time points, before p90Rsk was activated, and this correlated with the progesterone-induced accumulation of endogenous XRINGO protein (**Fig. 2C**) [7]. To determine whether Myt1 phosphorylation induced by CDK1/XRINGO affect its binding to p90Rsk, we incubated GST-fused Myt1-Ct either WT or the mutants Myt1-3AP and phospho-mimetic Myt1-3DP [7] in lysates prepared from G2-arrested oocytes or progesterone-matured oocyte lysates and then made pull down assays to analyze the binding of p90Rsk. We observed that the C-terminal domain of Myt1 associates with the active and hyperphosphorylated p90Rsk present in lysates prepared from progesterone-matured oocytes (**Fig. 4A**), but not with the inactive and unphosphorylated form of p90Rsk present in G2-arrested oocytes (**Fig. 4A**), consistent with previous results [3]. Surprisingly, the non-phosphorylatable mutant Myt1-3AP interacts less efficiently with p90Rsk than WT Myt1 in progesterone-matured oocyte lysates. In agreement with this result, we observed a correlation between the phospho-mimetic mutant Myt1-3DP and the ability of Myt1 to bind more efficiently to p90Rsk (**Fig. 4A**). These results suggest that Ser410, Ser414 and Ser444 participate in the interaction between Myt1-Ct and p90Rsk through the formation of a putative docking site motif containing phospho-Ser410, phospho-Ser414 and phospho-Ser444. The question that arises is how is it possible that Myt1 phosphorylation induced by p90Rsk impair Myt1 activity toward CDK1/cyclin B. There are two possibilities, Myt1 kinase activity could be affected directly by p90Rsk phosphorylation or alternatively Myt1 phosphorylation induced by p90Rsk impairs Myt1-CDK1/cyclin B interaction. To test the first possibility, we evaluated the autophosphorylation capacity of the full-length WT Myt1 or the mutants Myt1-5A and Myt1-5D [10]. We observed that both WT Myt1 and phospho-mimetic mutant Myt1-5D retain their ability to be autophosphorylated, suggesting that p90Rsk phosphorylation does not impair Myt1 kinase activity (**Fig. S2**). Previous work has shown that the C-terminal domain of Myt1 is involved in the recognition and recruitment of its substrate CDK1/cyclin B, through an RXL motif that targets cyclin B [5, 6]. To determine whether Myt1 phosphorylation by either CDK1/XRINGO or p90Rsk affects its binding to CDK1, we incubated GST-fused Myt1-Ct either WT or the mutants Myt1-3AP, Myt1-3DP,

Myt1-5A or Myt1-5D, in lysates prepared from G2-arrested oocytes and then made pull down assays to analyze the binding of endogenous CDK1. We found that the majority of the CDK1 associated with Myt1 proteins correspond to the inactive CDK1, phosphorylated on Thr14 and Tyr15 (**Fig. 4B**). Surprisingly, only the phospho-mimetic mutant Myt1-5D interacted much less efficiently with CDK1 than the other Myt1 proteins, suggesting that Thr453, Ser472, Ser475, Ser492 and Ser504 are located in a region that participates in the interaction between Myt1-Ct and CDK1. Previous studies have shown that Myt1 only phosphorylates CDK1 when it is bound to cyclin B [11]. Consistent with the presence of phosphorylated CDK1 in the GST-Myt1 pull-downs, we confirmed, by immunoblotting analysis, that endogenous cyclin B2 also co-immunoprecipitated with CDK1 in these assays (**Fig. 4B**). These results are in agreement with Liu et al. [5] that showed that unphosphorylated Myt1 interacts with CDK1/cyclin B but the hyperphosphorylated form of Myt1 does not associate with CDK1/cyclin B complexes, suggesting that the phosphorylation status of Myt1 could define the binding to CDK1/cyclin B.

Conclusions

We have observed that the phosphorylation on three Ser residues by CDK/XRINGO (Ser410, Ser414 and Ser444) do not impair the interaction between Myt1 and CDK1/cyclin B. On the other hand, the protein kinase p90Rsk can phosphorylate the C-terminal regulatory domain of Myt1 on different sites than CDK/XRINGO. Moreover, these p90Rsk-specific sites (Thr453, Ser472, Ser475, Ser492 and Ser504) are phosphorylated during progesterone-induced oocyte maturation. Importantly, phosphorylation of these five residues by p42MAPK-activated p90Rsk decreases the affinity of Myt1 for CDK1/cyclin B.

The finding that the overexpression of the catalytic domain of Myt1 did not inhibit progesterone-induced oocyte maturation, suggested that the C-terminal domain, which contains the RXL motif necessary for binding to cyclin B, is essential for the biological activity of *Xenopus* Myt1 in a similar way as demonstrated with mammalian Myt1 [5-6]. Therefore, Myt1 negatively regulates CDK1/cyclin B by a stepwise mechanism, which requires the C-terminal domain: Myt1 binds to and sequesters CDK1/cyclin B, which in turn allows the phosphorylation of CDK1 at Thr14 and Tyr15, resulting in the inactivation of its catalytic activity. We propose a

model where, during progesterone-induced meiotic maturation, two mechanisms converge on the regulation of Myt1 kinase activity, both of which require its C-terminal regulatory domain: the catalytic activity of Myt1 is negatively regulated through the phosphorylation induced by CDK/XRINGO [7], whereas p90Rsk-induced phosphorylation promotes the release of CDK1/cyclin B from Myt1 (**Fig. 4C**). Our model suggest that both proteins, XRINGO and p90Rsk, are required for correct timing entry into meiosis I and MPF activation. We think that progesterone activates more than one pathway to induce meiotic maturation, in case one pathway fails, then progesterone would still be able to trigger CDK1 activation. It is possible that each individual pathway is dispensable, provided that the other one remains functional.

Experimental procedures

Oocyte maturation and mRNA expression

Meiotic maturation of *Xenopus* oocytes was induced by incubation of manually dissected oocytes with 5 μg/ml (15 μM) of progesterone (Sigma, St Louis, MO) and scored by the appearance of a white spot at the animal pole of the oocytes, which indicates GVBD and meiosis I entry. For expression of Myc-tagged proteins, oocytes were microinjected with 50 nl of in vitro transcribed mRNAs (mMessage mMachine kit, Ambion, Austin, TX) and maintained overnight in modified Barth's medium at 18°C before progesterone treatment. For the preparation of lysates, oocytes were homogenized in 10 μl per oocyte of ice-cold H1K buffer (80 mM b-glycerophosphate, pH 7.5, 20 mM EGTA, 15 mM $MgCl_2$, 1 mM DTT, 1 mM AEBSF, 2.5 mM Benzamidine, and 10 μg/ml each of Aprotinin and Leupeptin). The lysates were centrifuged at 10,000 *g* for 10 min and the cleared supernatants were stored at –70°C.

Myt1 kinase activity assays

Myc-tagged Myt1 proteins were expressed from FTX5-Myt1 using the TNT reticulocyte lysate system supplemented with canine pancreatic microsomal membranes as recommended by the supplier (Promega, L4610). We estimated that the concentration of Myt1 in the lysate was about 1 ng/μl, by immunoblotting with anti-Myt1 antibodies using GST-Myt1-Ct as a reference. Typically, 20 μl of the Myt1-expressing reticulocyte lysate were diluted in 500 μl of IP buffer and then incubated

at 4°C with 7 µl of 9E10 anti-Myc antibody for 3-4 h followed by incubation with 30 ml of protein G sepharose beads (Amersham Biosciences, 17-0618-02) for 1 h. As a control, reticulocyte lysates that do not express Myt1 were immunoprecipitated with the 9E10 antibody. The bead-bound myc-Myt1 immunocomplexes were washed three times in IP buffer, twice with H1K buffer and then incubated in 20 µl of kinase buffer containing 100 µM ATP and 120 ng of recombinant co-expressed CDK1-cyclin B1-Cak1/Civ1. After 30 min at RT, the CDK1/cyclin B1 activity was assayed with 4 µg of histone H1 and 2 µCi of [γ-^{32}P]ATP for 15 min at 30ºC. Samples were finally boiled in sample buffer and analyzed by SDS-PAGE and autoradiography. To determine the effect of XRINGO-activated CDK1 on Myt1 kinase activity, the immunoprecipitated Myc-Myt1 was pre-incubated with active recombinant CDK1/XRINGO for 30-45 min at RT in 40 µl of H1K buffer supplemented with 300 µM ATP and then washed at least three times with H1K buffer before incubation with the CDK1/cyclin B1 substrate. To determine the effect of p90Rsk phosphorylation on Myt1 activity, the Myt1 immunocomplexes were preincubated with recombinant active CA-p90Rsk-EE for 40 min at RT in 30 µl of S6 kinase buffer (50 mM MOPS (pH 7.2), 1 mM DTT, 10 mM $MgCl_2$, 10 mM *p*-nitrophenylphosphate, 1 mM $NaVO_3$, 10 µg/µl Leupeptin, 10 µg/µl Aprotinin, 100 µM PMSF or AEBSF) supplemented with 350 µM ATP and then washed at least three times with H1K buffer before incubation with the substrate CDK1/cyclin B1.

Acknowledgments

We thank Margaret Jones and Amparo Palmer for early contributions to this project.

References

1. Nebreda, A.R., and Ferby, I. (2000). Regulation of the meiotic cell cycle in oocytes. Current Opinion in Cell Biology *12*, 666-675.
2. Philpott, A., and Yew, P.R. (2008). The Xenopus cell cycle: an overview. Mol Biotechnol *39*, 9-19.
3. Palmer, A., Gavin, A.C., and Nebreda, A.R. (1998). A link between MAP kinase and p34(cdc2)/cyclin B during oocyte maturation: p90(rsk)

phosphorylates and inactivates the p34(cdc2) inhibitory kinase Myt1.[erratum appears in EMBO J 1999 Feb 15;18(4):1092]. EMBO Journal *17*, 5037-5047.

4. Liu, F., Stanton, J.J., Wu, Z., and Piwnica-Worms, H. (1997). The human Myt1 kinase preferentially phosphorylates Cdc2 on threonine 14 and localizes to the endoplasmic reticulum and Golgi complex. Molecular & Cellular Biology *17*, 571-583.
5. Liu, F., Rothblum-Oviatt, C., Ryan, C.E., and Piwnica-Worms, H. (1999). Overproduction of human Myt1 kinase induces a G2 cell cycle delay by interfering with the intracellular trafficking of Cdc2-cyclin B1 complexes. Molecular & Cellular Biology *19*, 5113-5123.
6. Wells, N.J., Watanabe, N., Tokusumi, T., Jiang, W., Verdecia, M.A., and Hunter, T. (1999). The C-terminal domain of the Cdc2 inhibitory kinase Myt1 interacts with Cdc2 complexes and is required for inhibition of G(2)/M progression. Journal of Cell Science *112*, 3361-3371.
7. Ruiz, E.J., Hunt, T., and Nebreda, A.R. (2008). Meiotic inactivation of Xenopus Myt1 by CDK/XRINGO, but not CDK/cyclin, via site-specific phosphorylation. Mol Cell *32*, 210-220.
8. Schmitt, A., and Nebreda, A.R. (2002). Signalling pathways in oocyte meiotic maturation. J Cell Sci *115*, 2457-2459.
9. Anjum, R., and Blenis, J. (2008). The RSK family of kinases: emerging roles in cellular signalling. Nat Rev Mol Cell Biol *9*, 747-758.
10. Kristjansdottir, K., Safi, A., Shah, C., and Rudolph, J. (2006). Autophosphorylation of Ser66 on Xenopus Myt1 is a prerequisite for meiotic inactivation of Myt1. Cell Cycle *5*, 421-427.
11. Booher, R.N., Holman, P.S., and Fattaey, A. (1997). Human Myt1 is a cell cycle-regulated kinase that inhibits Cdc2 but not Cdk2 activity. Journal of Biological Chemistry *272*, 22300-22306.
12. Ferby, I., Blazquez, M., Palmer, A., Eritja, R., and Nebreda, A.R. (1999). A novel p34(cdc2)-binding and activating protein that is necessary and sufficient to trigger G(2)/M progression in Xenopus oocytes. Genes & Development *13*, 2177-2189.
13. Nebreda, A.R., Gannon, J.V., and Hunt, T. (1995). Newly synthesized protein(s) must associate with p34cdc2 to activate MAP kinase and MPF

during progesterone-induced maturation of Xenopus oocytes. EMBO J *14*, 5597-5607.

14. Brown, N.R., Noble, M.E., Endicott, J.A., Garman, E.F., Wakatsuki, S., Mitchell, E., Rasmussen, B., Hunt, T., and Johnson, L.N. (1995). The crystal structure of cyclin A.[see comment]. Structure *3*, 1235-1247.
15. Brown, N.R., Noble, M.E., Endicott, J.A., and Johnson, L.N. (1999). The structural basis for specificity of substrate and recruitment peptides for cyclin-dependent kinases. Nature Cell Biology *1*, 438-443.
16. Kumagai, A., and Dunphy, W.G. (1995). Control of the Cdc2/cyclin B complex in Xenopus egg extracts arrested at a G2/M checkpoint with DNA synthesis inhibitors. Molecular Biology of the Cell *6*, 199-213.
17. Hochegger, H., Klotzbucher, A., Kirk, J., Howell, M., le Guellec, K., Fletcher, K., Duncan, T., Sohail, M., and Hunt, T. (2001). New B-type cyclin synthesis is required between meiosis I and II during Xenopus oocyte maturation. Development *128*, 3795-3807.

Figure Legends

Figure 1. Myt1 C-terminal domain is required for biological activity. (A) Diagrammatic representation of the protein kinase Myt1. MA represents the membrane anchor region. (B) *Xenopus* oocytes were injected with 10 ng of mRNA-encoding Myc-tagged full-length Myt1 or Myt1-ΔC, incubated 14 h at 18°C, and then stimulated with progesterone. GVBD was scored every h. (C) *Xenopus* oocytes were collected at the indicated times after progesterone stimulation, and the lysates were analyzed by immunoblotting. Myt1 was detected with Myc antibody. Molecular weight is indicated in kDa.

Figure 2. **Identification of Specific p90Rsk Phosphorylation Sites on the Regulatory Domain of Myt1.** (A) Baculovirus-expressed GST-CDK1 (200 ng) and bacterially produced GST-CDK2 (250 ng) were incubated with MBP-XRINGO (200 and 250 ng, respectively). Kinase assays were performed with CDK/XRINGO complexes or recombinant p90Rsk (300 ng) and WT or mutant 3AP GST-Myt1-Ct (2 μg) in the presence of [γ-^{32}P]ATP for 15 min at 30°C. Myt1 phosphorylation was visualized by autoradiography**.** (B) Myc-tagged full-length Myt1 (WT or mutant 3AP)

was expressed in reticulocyte lysates, immunoprecipitated, and incubated with recombinant p90Rsk (900 ng) in the presence of ATP at 30°C. After 60 min, Myt1 was immunoprecipitated and washed extensively. The immunopurified Myt1 was further incubated in the presence of recombinant CDK1-cyclin B1-Cak1/Civ1 (120 ng) for 30 min before H1K assays were performed. (C) Baculovirus-expressed GST-CDK1 (200 ng) was activated with MBP-XRINGO (200 ng). Kinase assays were performed with CDK1/XRINGO or recombinant p90Rsk (300 ng) and WT or mutant 5A GST-Myt1-Ct (2 μg) in the presence of [γ-^{32}P]ATP for 30 min at 30°C. Myt1 phosphorylation was visualized by autoradiography. (D) *Xenopus* oocytes from primed frogs were injected with Myc-tagged Myt1-Ct, either WT or mutant 5A, incubated for 14 h at 18°C, and then stimulated with progesterone. Oocytes were collected at the indicated times after progesterone stimulation, and lysates were assayed for H1K activity or analyzed by immunoblotting. Myt1-Ct was detected with Myc antibody.

Figure 3. Phosphorylation and Inhibition of Myt1 Activity by p90Rsk. (A) *Xenopus* oocytes were injected with 10 ng of mRNA-encoding Myc-tagged full-length Myt1, either WT or the mutants 5A and 5D, incubated 14 h at 18°C, and then were stimulated with progesterone. (Left panel) GVBD was scored every h. Lysates from oocytes taken before progesterone stimulation were analyzed by immunoblotting with Myt1 and p42MAPK antibodies. (Right panel) Oocytes were collected at the indicated times after progesterone stimulation, and the lysates were assayed for H1K activity or analyzed by immunoblotting. Myt1 was detected with Myc antibody. (B) Myc-tagged full-length Myt1 (WT or mutants 5A and 5D) was expressed in reticulocyte lysates, immunoprecipitated with Myc antibodies, and then incubated with recombinant CDK1-cyclin B1-Cak1/Civ1 (120 ng) for 30 min before performing H1K assays. (C) Myc-tagged full-length Myt1 proteins were expressed in reticulocyte lysates, immunoprecipitated, and incubated with p90Rsk (900 ng) for 45 min in the presence of [γ-^{32}P]ATP. (D) Myc-tagged full-length Myt1 (WT or mutant 5A) was expressed in reticulocyte lysates, immunoprecipitated, and preincubated with p90Rsk (900 ng) or CDK1/XRINGO (800 ng) in the presence of ATP at 30°C. After 45 min, Myt1 was immunoprecipitated and washed extensively. The immunopurified Myt1 was further incubated in the presence or absence of recombinant CDK1-cyclin B1-Cak1/Civ1 (120 ng) for 30 min at 30°C before H1K assays were performed. The two

right lanes show the controls with immunopurified Myt1 that was directly assayed for H1K activity, in the absence of CDK1/cyclin B1, to confirm the lack of contaminating p90Rsk and CDK1/XRINGO activities from the preincubation step.

Figure 4. Reduced Ability of the Myt1-5D Mutant to Bind to CDK1/Cyclin B. (A) *Xenopus* oocytes were incubated or not with progesterone for 12 h. WT or mutants 3AP or 3DP GST-Myt1-Ct (5 µg) were incubated with G2-arrested oocytes or progesterone-mature oocytes during 3 h at 4°C. GST pull-downs were analyzed by immunoblotting with p90Rsk or GST antibodies. (B) WT or mutants GST-Myt1-Ct (6 µg) were incubated with G2-arrested oocytes lysates during 3 h at 4°C. GST pull-downs were analyzed by immunoblotting with CDK1, cyclin B2 and GST antibodies. (C) Model of the protein interactions proposed between CDK1/XRINGO, Myt1, CDK1/cyclin B and p90Rsk (see text). KD, kinase domain of Myt1; Ct, C-terminal domain of Myt1.

Supplementary Figure 1. (A) Sequence of *Xenopus* Myt1-Ct. p90Rsk phosphorylation sites are highlighted in bold. (B) Kinase assays were performed with recombinant p90Rsk (300 ng) and WT or mutants GST-Myt1-Ct (2 µg) in the presence of [γ-^{32}P]ATP for 30 min at 30°C. Myt1 phosphorylation was visualized by autoradiography. Myt1-Ct-2A: S472A+S475A; Myt1-Ct-3A: S472A+S475A+S492A; Myt1-Ct-4A: S472A+S475A+S492A+S504A.

Supplementary Figure 2. Myc-tagged full-length Myt1 (WT or mutants 5A and 5D) was expressed in reticulocyte lysates, immunoprecipitated, and incubated in the presence of [γ-^{32}P]ATP for 2 h at 30°C. Myt1 autophosphorylation was visualized by autoradiography.

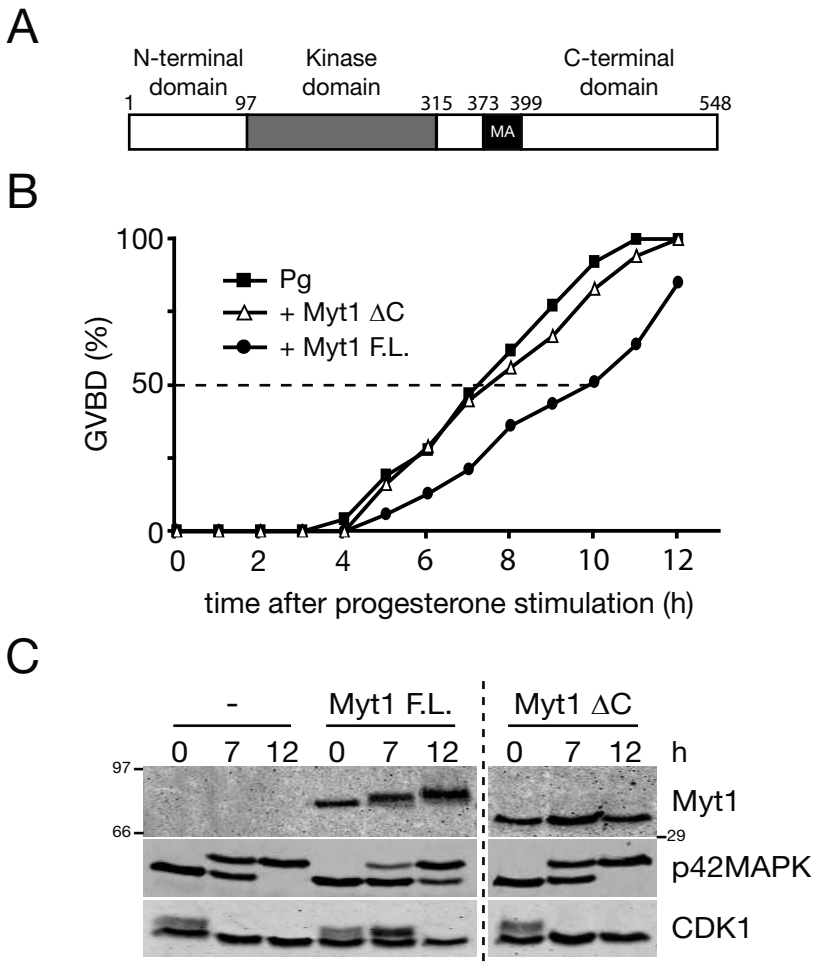

Ruiz et al., Figure 1

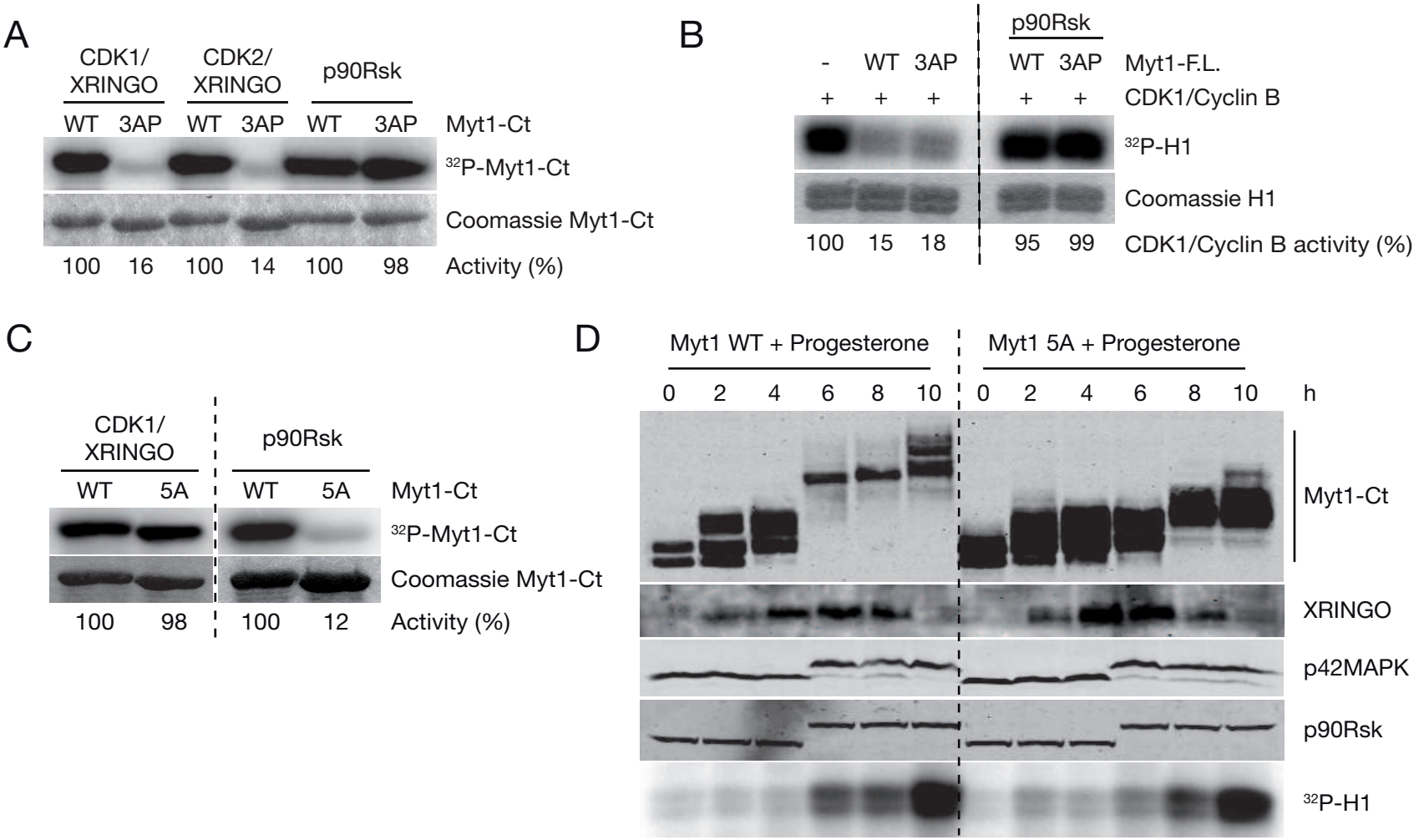

Ruiz et al., Figure 2

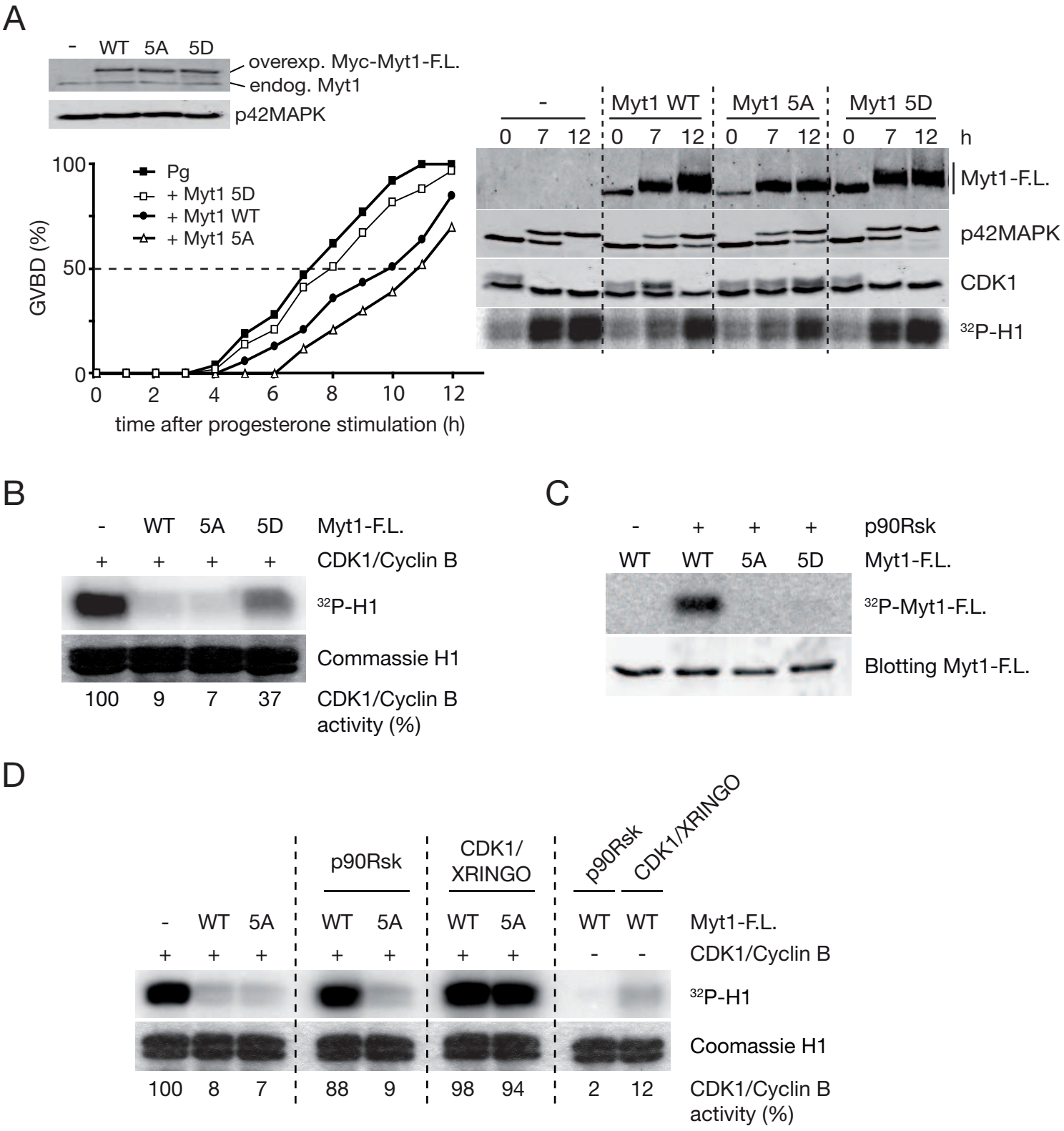

Ruiz et al., Figure 3

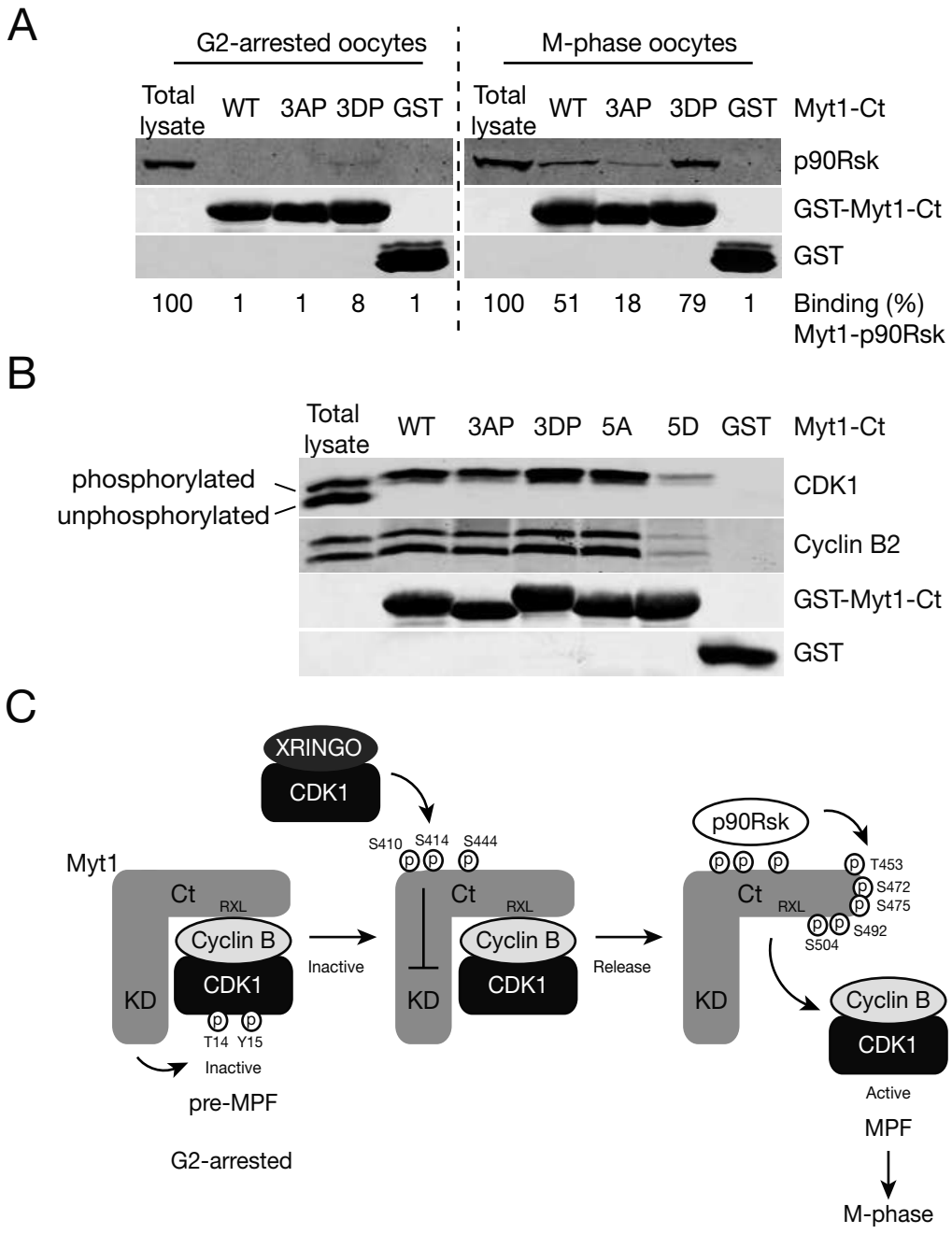

Ruiz et al., Figure 4